

MONITORING DEFORESTATION IN HUAMBO PROVINCE USING DETECTION TECHNOLOGIES AND GEOGRAPHIC
INFORMATION SYSTEMS (2002-2015)



SPATIAL DYNAMIC AND QUANTIFICATION OF DEFORESTATION AND
DEGRADATION IN MIOMBO FOREST OF HUAMBO PROVINCE (ANGOLA)
DURING THE PERIOD 2002-2015



TECHNICAL ASSISTANCE BY

SPONSORED BY THE



Federal Ministry
of Education
and Research

Technical Work Team

Guillermo Palacios Rodríguez. IDAF

Miguel A. Lara Gómez. IDAF

Alba Márquez Torres. IDAF

José Luis Vaca Vidal. IDAF

David Ariza Mateos. UCO

Scientific Monitoring

Rafael M^a Navarro Cerrillo. UCO

Virgínia Lacerda Quartin. UJES



Center for Applied Research in
Agro- Forestry Development - IDAF
Spin-off of the University of Córdoba



University of Córdoba
Evaluation and Restoration of Agricultural and
Forest Systems Research Group - ERSF



Faculty of Agricultural Sciences
University José Eduardo dos Santos – UJES

© SASSCAL Project 2015

All rights reserved

Photographs: Pedro Quartin (cover), Virgínia Lacerda, Miguel A. Lara, Guillermo Palacios (back cover).

Reference:

Palacios, G.; Lara-Gomez, M.; Márquez, A.; Vaca, J.L.; Ariza, D.; Lacerda, V.; Navarro-Cerrillo, R.M. (2015). *Spatial Dynamic and Quantification of Deforestation and Degradation in Miombo Forest of Huambo Province (Angola) during the period 2002-2015*. SASSCAL Project Proceedings. Huambo, Angola. 182 pp.

Table of contents

Executive Summary	1
1. Introduction	3
1.1. Physical environment	4
1.2. Climate	4
1.3. Soil	5
1.4. Ecological features	5
1.5. Rural household	6
1.6. Study Area	7
1.7. Threats	8
1.8. Functions and importance	10
1.9. Summary	12
2. Objectives	14
3. Preparatory activities	15
3.1. Image acquisition	19
3.1.1. Landsat Image selection	20
3.1.2. Preprocessing process	27
3.2. Work Field	29
4. Deforestation study in miombo forest of Huambo	32
4.1. Methodology	33
4.1.1. Classify the image mosaic with Minimum Distance algorithm	34
4.1.2. Elaborating vegetation indices (NDVI)	37
4.2. Results and discussion	39
4.2.1. Initial situation	39
4.2.2. Evaluation of cover change between 2002-2015	40
4.2.3. Distribution of deforestation by type of landcover	44
4.2.4. Distribution of deforestation by type of landcover and municipality	45
5. Degradation study in Miombo forest of Huambo	52
5.1. Methodology	54
5.1.1. Minimum Distance Classification Landcover	55
5.1.2. Quality control and reclassification classification by NDVI	55
5.2. Results and discussion	56
5.2.1. Initial situation	56
5.2.2. Degradation in Huambo province	57
5.2.3. Degradation by municipality	59
6. Conclusion	63
7. Bibliography	65
Annexes	70

Index of Figures

Fig. 1 Distribution of miombo woodlands. Source: While 1983	3
Fig. 2 Changes in temperature and rainfall Source: Climate change knowledge portal	4
Fig. 3 Human population inhabiting the miombo.	6
Fig. 4 Huambo localization; Source: Cabral, 2009.	8
Fig. 5 Advance of the agricultural frontier. Source: Google Earth	9
Fig. 6 Traditional farming practices in Huambo. Source: IDAF Consulting	10
Fig. 7 Miombo regeneration area as potential CO ₂ sink. IDAF Consulting	12
Fig. 8 Camera pigeon	15
Fig. 9 Aerial photographer during World War I, and a French air field	16
Fig. 10 Landsat 1 image in 29-august-1973 (USGS)	16
Fig. 11 Evolution of Landsat satellite and future prospects (Landst webpage)	17
Fig. 12 Demand of Landsat images from January 2007 to January 2013 (Landsat webpage)	18
Fig. 13 Landsat data uses (Landsat webpage)	18
Fig. 14 Standard workflow of image preprocessing	20
Fig. 15 Data used to drive the model. a) Miombo forest in the dry season b) Photosynthetically Active Radiation and Leaf Area Index monthly dynamics. c) Miombo forest in the wet season (Photograph by Brian Huntley).....	21
Fig. 16 Four Landsat image were needed to complete the whole study area. (USGS webpage)	21
Fig. 17 Differences between spectral resolution of Landsat 7 and Landsat 8	22
Fig. 18 Worldwide Reference System-2. Angola is in the red circle.....	24
Fig. 19 SLC Failure	24
Fig. 20 Complete Landsat 7 scene showing affected vs. unaffected area.	25
Fig. 21 Atmospheric effects influencing the measurement of reflected solar energy. Attenuated sunlight and skylight (E) is reflected from a terrain element having reflectance p . The attenuated radiance reflected from the terrain element (pET/π) combines with the path radiance (L_p) to form the total radiance (L_{tot}) recorded by the sensor.....	28
Fig. 22 Mosaic example	29
Fig. 23 Scheme of inventory plots.....	30
Fig. 24 Examples of reflectance of water, soil and vegetation in different wavelengths in different channels of Landsat ETM+.....	32
Fig. 25 Spectral signature of vegetation.....	32
Fig. 26 Workflow of classification process	33
Fig. 27 Supervised Classification Diagram	34
Fig. 28 Steps in Supervised classification.....	34
Fig. 29 Maximum likelihood classification. Source: Centre for Geo-information of Wageningen University and Research Centre, 1999	35
Fig. 30 Example of Minimum Distance Classifiers between spectral band 3 and 4. Source: Centre for Geo- information of Wageningen University and Research Centre, 1999.....	36
Fig. 31 Difference between NDVI index in March, 2004 (a) and September, 2004 (b) in Angola, Africa. (NASA, 2004)	38

Fig. 32 a) Differences in reflected light between a healthy and unhealthy leaf and b) Change in spectral reflectance for a portion of the electromagnetic spectrum for healthy sugar beet plant and one under water stress	38
Fig. 33 Example about the difference between NDVI in forest and NDVI in bare soil in the same area	39
Fig. 34 Rate of miombo forest in Huambo province	40
Fig. 35 Rate of Deforestation since 2002 on the context of Forest/No-forest land cover in the province of Huambo.....	41
Fig. 36 a) Distribution of deforestation in Huambo (Angola), b) Detailed map of increased cover in miombo since 2002 c) Detailed map of miombo cover loss	42
Fig. 37 Example of the most deforested area. a) Between 2001-2013, b) Between 2005-2013. Source: Google Earth.....	43
Fig. 38 Transformation from non-forest landcover to miombo cover, between 2005-2014. Source: Google Earth.....	44
Fig. 39 Percentage of Gain/Loss miombo forest in Huambo Province from 2002.....	44
Fig. 40 Change of land cover from miombo to non-forest (percentage in negative) and change of land cover from non-forest to miombo (percentage in positive) since 2002	46
Fig. 41 Background of current cover of miombo by type of landcover and municipality.....	46
Fig. 42 Distribution of gain in miombo cover since 2002.....	47
Fig. 43 Distribution in hectares the loss of miombo cover by municipality	49
Fig. 44 Rate of loss in miombo cover by municipality	49
Fig. 45 Evolution of degraded forest. (P. Sist et al., 2015).....	52
Fig. 46 Common degrading activities in forest	53
Fig. 47 Degradation drivers for each continent	53
Fig. 48 Uses of miombo for the basic survival of the population	54
Fig. 49 Workflow of the degradation	55
Fig. 50 Detect biomass by passive remote sensing	56
Fig. 51 Miombo Woodlands. (A) Diversity of tree species; (B) Close up <i>Brachystegia bohemii</i> ; (C) Regrowing area; (D) Recently burned area. Source: Tropical Research Institute, Portugal.....	57
Fig. 52 Distribution of miombo NDVI.....	57
Fig. 53 Degradation's rate of miombo in 2015	58
Fig. 54 Map of degradation in Huambo's Province	59
Fig. 55 Distribution of degradation by municipality.....	60
Fig. 56 Degradation by type and municipality in all miombo cover.....	61

Index of Tables

Table 1 Objectives by stages and section.....	14
Table 2 Differences between Landsat 7 ETM+ and Landsat 8 OLI.....	22
Table 3 List of USGS images used to develop the project.....	26
Table 4 Coordinates of tracts and inventory plots.....	30
Table 5 The overall accuracy method and Kappa hat classification between two different algorithm of classification.....	37
Table 6 Percentage of gain, loss and no change of miombo forest in 2015.....	40
Table 7 Detail of how it changed the landcover of miombo since 2002 to 2015	45
Table 8 a) Gain in cover of miombo between 2002 and 2015 in hectares, b) Rate of gain since 2002 c) Percentage of miombo cover in 2015.....	47
Table 9 a) Loss in cover of miombo between 2002 and 2015 in hectares, b) Rate of loss since 2002 c) Percentage of loss in miombo cover (2015).....	50
Table 10 Rate of miombo degradation.....	58
Table 11 Data of degradation by municipality and percentage in miombo cover and the province of Huambo.....	61

Executive Summary

This work is one of the expected results of SASSCAL's (Southern African Science Service Centre for Climate Change and Adaptive and Land Management), as part of the Task 137: **MONITORING DEFORESTATION IN HUAMBO PROVINCE USING DETECTION TECHNOLOGIES AND GEOGRAPHIC INFORMATION SYSTEMS (2002-2015)**, and it was funded by the German Federal Ministry of Education and Research (BMBF). This Task is being coordinated by the Professor Virgínia Lacerda Quartin from the Faculty of Agronomy of the University José Eduardo Dos Santos (Huambo, Angola).

SASSCAL is a joint initiative of Angola, Botswana, Namibia, South Africa and Zambia, funded by the German Federal Ministry of Education and Research (BMBF) to improve the regional capacities for knowledge-based decision making and to provide regional scientific services to address future trends of global climate change, risks & vulnerability of societies and ecosystems, as well as the management of natural resources and ecosystem services.

The content of this work is original and it describes the current rates of deforestation and degradation of the Miombo ecosystem, the forest surface recovered in the province of Huambo, as well as in the eleven municipalities since 2002 to 2015.

The Centre for Applied Research in Forestry Development (IDAF) of the University of Cordoba (Spain) was responsible for the technical assistance and the technical training of Angolan technicians at MSc level on the Applied Geomatics for Natural Resources Management Course

The information obtained provides the awareness of the real situation of the forest resources in the Huambo province to policy makers,, being the first step to to prevent the progressive degradation and deforestation, through the promotion of measures to reverse the current situation.

Regarding the results obtained, the Working Group of Task 137 stresses the importance to continue working for the creation of natural reserves for protection of forest resources in the province of Huambo, and the whole country. This also has the purpose of improving the status of national forest resources, ensuring conservation of the ecosystems biodiversity, contributing to the protection of soil and water cycle and, consequently, mitigating the global effect of climate change , particularly in Angola where extreme droughts and floods, cause very serious human and material consequences.

Acknowledgements:

The working group of Task 137 would like to thank the German Federal Ministry of Education and Research (BMBF) for the financial support of the project; the General, Scientific and Financial SASSCAL Coordinators, Mr. Manfred Finckh, Mr. Norbert Jürgens and Mr. Ingo Homburg, for their contributions and continuous support; Mr. Jörg Helmschrot and Mrs. Marion Stelmes for their technical support; the National SASSCAL Coordinator, Mr. Chipilica Barbosa for his suggestions; the technical team of The Centre for Applied Research in Forestry Development (IDAF) of the University of Cordoba (Spain) for the technical assistance; and all the persons and institutions involved in this work.

The Coordinator of Task 137 SASSCAL Project,

Mrs. Virgínia Lacerda Quartin

1. Introduction

The miombo is one of the most important ecosystems in southern Africa Cone, covering outstanding areas of Angola, Mozambique, Tanzania, Zimbabwe, Zambia and the Democratic Republic of Congo, an area of approximately 270 million hectares (Frost in Campbell, 1996) (Fig, 1). Is the most extensive seasonal tropical woodland and dry forest formation in Africa. This type of ecosystem is made up of mosaics of dry forests and wooded savannas, characterized by a high diversity of flora and fauna (Ryan et al., 2011), average productivity and high social value in terms of wood fuel, construction materials, pasture, food and medicinal plants (MINADERP, 2010). In addition, miombo woodlands play an important role in the fixation of atmospheric CO₂, because in normal conditions they are able to fix up to 110 mg C/ha, between plant biomass and soils (Ryan et al., 2011).



Fig. 1 Distribution of miombo woodlands. Source: While 1983

The Angolan Mopane Woodlands ecoregion Stretches from southwestern Angola into northern Namibia, between 15 ° S and 21 ° S latitude. It lies inland of the Namib escarpment, but mostly to the west of the Zambezian Baikiaea Woodlands. The large salt pan, the Etosha Pan, but falls within this ecoregion is considered its own, the Etosha Pan Halophytics. WWF considers this region as critical in the future scenario of global change. This category determines that this region has been scientifically identified by the WWF as:

- Being home to irreplaceable and Threatened Biodiversity, or
- Representing an opportunity to retain the largest and most representative of their ecosystem intact.

1.1. Physical environment

Mature undisturbed miombo is usually formed by a closed deciduous forest, generally in areas geologically ancient and nutrient-poor soils (Campbell, 1996). The main biophysical factors in the formation of these ecosystems are high solar radiation and temperature throughout the year, plus an annual seasonal climate variation that causes vertical gradients of soil moisture (Perez and Sicard, 2003). The climate of the areas of miombo distribution is characterized by long dry seasons, which can last 7-8 months. The most typical miombo soils are poor soils with a high concentration of aluminium and acidic leachate often shallow and stony (Desanker and Prentice, 1994).

In the last hundred years there has been a change in the dynamics of temperature (Fig, 2) increasing by just over half a degree of temperature recorded. On the other hand, the average annual rainfall has increased across the board if you look at the Angolan country. Fundamentally a notable increase of precipitation in the months of January, March and December is observed (Climate Change Knowledge Portal 2015).

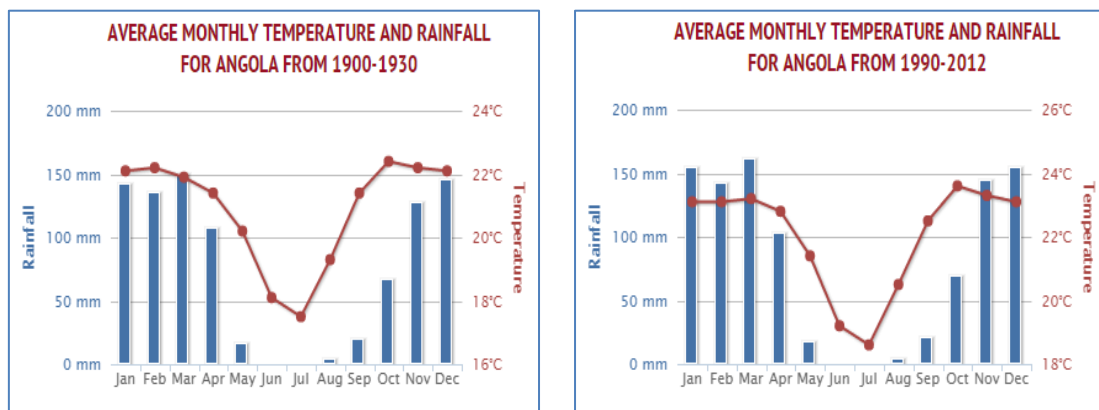


Fig. 2 Changes in temperature and rainfall Source: Climate change knowledge portal

1.2. Climate

Miombo woodland is situated within the southern sub-humid tropical zone of Africa. About two-thirds of the region falls within the Köppen Cw climate class, indicating a warm climate with a dry winter; the rest falls into the Aw (hot climate with dry winter – 26% of 62 sites) and BSh (hot dry steppe – 8%) climate classes. The 10-90% percentiles for mean annual precipitation and mean annual temperature are 710-1365 mm and 18.0-23.1°C, respectively. Coefficients of variation in annual rainfall are less than 30%. More than 95% of annual rainfall occurs during a single 5-7 month wet season. A few sites in northern Tanzania and north eastern Angola have two wet seasons; these and some sites in south-eastern Mozambique receive >5% of their annual rainfall during the dry months. The ratio of annual precipitation to evapotranspiration varies from 0.5 to 1.1 (Frost in Campbell, 1996).

1.3. Soil

Miombo woodland soils are typically acid, have low cation exchange capacities (CEC), and are low in nitrogen, exchangeable cations (total exchangeable bases: TEB) and extractable phosphorus. Soils derived from Precambrian metavolcanics, metacarbonates and some biotite-rich gneisses have a marginally higher base status, as shown by the occasional high values for individual cations and phosphorus. Organic matter levels are generally low, except under densely wooded vegetation. Nevertheless, organic matter contributes substantially to cation exchange capacity in these soils (Frost in Campbell 1996).

The miombo is divided into wet miombo and dry miombo. The dry miombo is represented in southern Malawi, Zimbabwe and Mozambique, in areas with rainfall lower than 1000 mm/year. In these ecosystems, plant diversity is very high. Meanwhile, the wet miombo appears in areas with an annual rainfall greater than 1000 mm/year in parts of western Angola, northern Zambia, Tanzania and southeast of central Malawi (Frost in Campbell, 1996). The origin of these differences is unclear: geomorphic evolution of the landscape; soil factors, particularly moisture and soil nutrients; the effects of fire; and the historical and present land use along with other human factors are involved (Chidumayo, 1987a).

1.4. Ecological features

Miombo comprising forests are finally dominated by savanna at the end of its range of formations. Mature forests, relatively unchanged, have a layer comprising 10-20 m tall with a canopy of trees, mostly wide, pinnate leaves. At ground level a shrub layer of broadleaf discontinuous, and often sparse but continuous layer and herbaceous, small reeds, grasses herbs C4 heliophytic appears. The biomass of large mammals is very low, and is dominated by large-sized species.

The miombo generally has a structure with 2 or 3 layers. The inferior strata, generally composed of shrubs, trees and regeneration oppressed youth in the tops of the highest trees and a dominant upper layer trees. This natural formation is distinguished from other African savanna, woodland and forest formations by the dominance of tree species in the family Fabaceae, subfamily Caesalpinioideae mainly by species of the genera *Brachystegia*, *Julbernardia* and *Isoberlinia* (Campbell et al., 1996). The diversity of canopy tree species is low, overall, although the species richness of the plant is high. Several authors have contrasted the differences in structure between mature miombo and regrowth in different places (Chidumayo, 2002 Luoga et al., 2002).

Plant density varies between 1500 and 4000 plants per hectare, while the density of trees over 2 m height varies between 380 and 400 trees per hectare. The average height of adult trees is around 10-20 m, and its basal area varies depending on the annual rainfall, temperature and evapotranspiration, although in general, the authors are between 7-19 m² (Chidumayo, 1987b).

The average volume varies between 14-59 m³ per hectare in the dry miombo and between 41-100 m³ per hectare in the dry miombo (Frost in Campbell, 1996).

1.5. Rural household

Generally speaking, the human population inhabiting the miombo is relatively low with respect to other areas of African savanna that are in a similar climate range, but this situation is now in a progressive change. This data also leads to relatively low livestock pressure. They are multiple and complex reasons for these data, but partly due to a relationship between climate, soil, geology, production and quality of plant diseases as well as present.

Campbell and others authors estimate a population of 40 million people by the year 1990 in areas occupied by agricultural or wooded area, with a data of 15 million urban dwellers dependent on these systems on wood, charcoal and energy sources. In addition to these uses, forests are providers of other services for people who depend on them. The material goods are not of great value, especially to cover and serve the spiritual needs of people. Certain trees and groves are kept by communities with unique cultural value. These populations keep sacred groves associated with spirits of the dead, or rituals for rain, which is hosting purposes, put through regions occupied by forests and miombo formations.



Fig. 3 Human population inhabiting the Miombo.

Household studies have documented the importance of miombo to rural households. The studies show that poor rural households are vitally dependent on miombo woodlands because of their role as a safety net, not that poor rural households are becoming rich by tapping into markets for miombo products. Among these households, miombo is providing for a very substantial proportion of total household consumption. This proportion increases significantly in households that encounter serious income shocks because of illness or environmental stress. The household studies show that miombo woodland resources are a critical element of the rural household economy and contribute significantly to mitigating the impacts of poverty. If these

resources are lost as a result of deforestation or other proximate causes, the need for alternative safety nets is likely to place further large burdens on public service delivery institutions, already poorly equipped to handle the problem of rural poverty. Spatial analysis (for example, in Malawi and Mozambique) confirms the statistical correlation between areas with extensive miombo cover and areas with high poverty rates (Dewes et al., 2011).

1.6. Study Area

The situation on the Angolan side of the ecoregion is less encouraging. The 30-year civil war in Angola has had a devastating impact on conservation in the area. Protected areas are open to poachers, timber harvesting, human settlement and agriculture. Few, if any, viable populations of larger mammals have survived and populations of lion, black rhino and giraffe have been reduced to the threshold of local extinction. The situation is similar outside of the protected areas, and over-exploitation of wildlife and other natural resources is commonplace. On the positive side, the Angolan government has recently established a State Secretariat for the Environment and has begun training demobilized soldiers as park wardens. Angola is also a signatory to the Convention on Biological Diversity (Dean, 2000).

In Angola, the miombo woodlands are one of the most relevant, taking about 45% of the total forest area, being dispersed over wide areas of the country including the provinces of Huila, Kuando Kubango, Moxico, Bié, Huambo, Malanje, Benguela and Kwanza Sul. It's about a coverage in ecological forests rich in biodiversity, with about 8,500 plant species of which about 54% are endemic (Shackleton, 2007). The climate is humid mesothermal with dry winters and hot summers with maximum annual average temperatures below 20 ° C. The wet season runs from October to April being the dry season between May and September (Delgado and Pukkala, 2011). These forests have been and are a strongly disturbed ecosystem. It present a strong contrast to physiognomic level, structural and biomass, most of its surface in contact with humans, with respect to the few existing mature formations (Davies et al., 2010).

Although there are not many studies focusing on the characterization of the miombo in Angola (Cabral et al, 2012;. Sanfillipo, 2013), recent studies in this regard in two provinces representative of miombo show that presents a very heterogeneous composition, being of average between 11 and 18 species (Ngangula, 2015), among which *Albizia antunesiana*, *Anisophyllea bohemii*, *Bobgunnia madagascariensis*, *Brachystegia bohemii*, *Brachystegia longuiflora*, *Brachystegia spiciformis*, *Hymenocarida acida*, *Monote spp*, *Ochna schweinfurthiana*, *Parinari curatelifolia*, *Pericopsis angolensis*, *Psorospermum febrifugum*, *Pterocarpus angolensis*, *Randia Kuhnian F. Hoffm. Schum.* (*Rothmannia engleriana*.) *Syzygium guineense* and *Terminalia Brachistema*. The density found in these works is around 2000 individuals ha⁻¹ for adult individuals while the regeneration density varies greatly humidity and canopy cover, with data ranging from 1900 to 8000 individuals ha⁻¹ (Dovala, 2015). These data also do generally agree with the literature for miombo species, which appear density data

between 1000-4100 individual per ha-1 (Campbell, 1996; Ribeiro et al., 2002; Banda et al., 2006; Backéus et al., 2006). In relation to the total biomass found, the data of these studies are also similar to those found in the specific literature of miombo in other areas, (Frost in Campbell, 1996; Malimbwi et al., 1994), with a total biomass between 96.75 and 131 Ton ha-1 (Dovala, 2015) and compared to the volume also exists enough uniformity with the data found both outside Angola with a volume of 117 m3 ha-1 found in Zambia (Chidumayo, 1988), as in Angola data between 66.91 m3 ha-1 (Sanfilipo, 2013) and 111.85 m3 ha-1 (Elias, 2014) and 91.93 m3 ha-1 (Dovala, 2015).

Huambo is a province of central Angola with an area of about 29,827 km2 and is divided into 11 municipalities: Huambo, Caála, Ekunha, Longonjo, Ukuma, Bailundo, Tchinjenje, Mungo, Katchiungo, Tchicala Tcholoanga and Londuimbali. (Fig. 4).

It is located in a central plateau, where mountains reach higher elevations. Môco Mountain, in Londuimbali municipality, with 2620 meters, is the highest peak in the province and in Angola. In these central mountains rise most of the rivers of Angola, many of which drain to the Atlantic Ocean, like Cuanza and Cunene. The dominant genera in miombo floristic formation is constituted by *Brachystegia* spp., *Combretum* spp. and *Julbernardia* spp., whereas in savannas or deforested areas dominant species are Graminae dominated by *Hyparrhenia* spp. and *Andropogon* spp.. In badly drained areas vegetation found is constituted by hydrophilic formations dominated by high permanent Graminae, while in those permanently under water, Ciperaceae is the dominant vegetation (Cabral, 2009).



Fig. 4 Huambo localization; Source: Cabral, 2009.

1.7. Threats

The main factors of deforestation in Angola miombo are the advance of the agricultural frontier and to a lesser extent some farming practices and fires (Fig, 5). Once the armed conflict ended in 2002, began the return of a large part of the population that had migrated to the big cities to rural areas, thereby restoring ancient extensive farming practices. This trend is gradually accelerating landscape with the expansion of cattle ranching took (Cabral et al., 2010). The most common practice of shifting cultivation in Angola involves cutting of woody vegetation at ground level, burning the remains on the plowed area, and hoe cultivation for a period of 3-5 years to deplete nutrients soil and lowering the yield (Fig, 6). After the abandonment of agricultural area, begin to appear rapidly colonizing species, forming thickets with time, but until 10-20 years, does not begin to be competition between woody species, and the first steps of the formation of a mature forest. In an early stage of development, the grass growth is very strong, and therefore the continuity of the fires and the result of these, are devastating. Studies show that the use and management practices of forests are largely responsible for the availability of resources (Arnold and Dewees 1995; Campbell et al., 2002), suggesting maintaining sustainable harvest limits and provide an additional support for these practices (Shackleton, 2007).



Fig. 5 Advance of the agricultural frontier. Source: Google Earth

The conversion of miombo woodlands to short-duration croplands has two global consequences. The first is a release of carbon from the soil and biomass into the atmosphere. If half of the carbon in the top 30 cm of soil and all the carbon in woody biomass is released in half of the existing miombo extent in the next thirty years. The second consequence is a change in energy exchange at the land surface (increased reflectance of solar radiation and decreased surface roughness) which, if extensive enough, could result in increased atmospheric stability and a decrease in the formation of rain-generating convective storms (Scholes in Campbell, 1996).



Fig. 6 Traditional farming practices in Huambo. Source: IDAF Consulting

Other process that contributes to deforestation of miombo is the exploration of wood for use as fuel energy. In a country where about 70% of the population has no access to utility power, and other energy sources are still being developed (renewable energy) or the access for the population, especially for rural areas, is difficult (gas); energy from biomass is the main source of domestic energy. For miombo, there are also deep-rooted cultural factors in the population, that make any paradigm shift in terms of forest management is a complicated challenge. The whole process of coal production from exploration wood, as production itself, is developed in a traditional way, with virtually no management, and with a very low profitability. On the other hand demographic and socioeconomic factors, are leading to an increase in coal production to meet the growing population, mainly settled in big cities, which increasing require this resource. In fact, although no quantified data by the institutions, the percentage of wood biomass used for rural populations is negligible in relation to that which is exported to urban areas, basically using residual coal of poor quality that cannot be sold or mostly firewood. All this makes the process of deforestation linked to the production of energy from biomass is growing fast in recent years, the availability of forest land is diminishing, and is further from the people, and that cannot be guaranteed a process of natural regeneration of forest resources to ensure the near future.

The greenhouse effect is likely to increase the mean temperature of the miombo region by 1-2°C in the next century, which by itself is not expected to alter the ecology or distribution of the woodlands significantly. Future trends in rainfall, which could have a profound effect, are not yet reliably predictable (Intergovernmental Panel on Climate Change 2013).

1.8. Functions and importance

Miombo forests play an increasing role in the complex systems of rural land use, integrating the management of trees with crops and livestock production so as to contribute significantly to mitigating the impacts of rural poverty (Deweese et al., 2011). However, various factors related to socioeconomic situation in the country, threatening the proper management of forest resources, so that in recent years the problem of deforestation, agroforestry linked to unsustainable practices and the emergence of recurrent wildfires. Despite the existence of extensive literature

justifying the introduction of silvicultural systems management in the miombo forests, there are hardly any reports on the successful implementation of these practices in community forests are those which comprise the largest area in the region miombo. Conventional techniques and principles of forestry have much to offer to improve the practices of current resource extraction, although the implementation of these is given the complex social structure, and multiple use systems that exist in the regions of miombo (Shackleton and Clarke, 2007).

Other authors (Campbell et al., 2007), have rightly identified the benefits and opportunities of miombo such as global markets capture CO² at the level of local economy in terms of energy, medicinal plants, wild meat, lumber, or other products (Fig, 7). Some of these barriers are difficult to remove, such as low potential productivity of forest ecosystems, while others require changes in policies and practices. But other barriers can be easily removed with sustainable forest management, which will provide a future framework for environmental conservation to increase the costs of habitat destruction.

Many markets are growing locally. In the last decade, medicinal plants are being used by the cities, like other products originating in the forest. Several authors like Lowore (2006), give these forests the title of "safety net" as they can provide resources and commercial goods in a scenario where food resources are exhausted. From a local perspective least, this ecosystem provides a range of services such as maintenance of watersheds and flood protection, maintenance of soil fertility and carbon storage (Davies et al., 2010). Recent research suggests that a number of these products have potential for domestication and the provision of goods and services with market value, thus increasing household incomes of local communities (Akinifessi et al., 2006).

The importance of these forest resources and their contribution to food security of populations, is something widely reported in both the scientific works (Cabral et al., 2010), and institutional documents themselves, including specific sections to ensure the pillars Basic food security availability, access, use and stability of supply (FAO, 2011). Both the most relevant level to forest policy ("National Policy on Forests, Fauna and Areas Conservação Selvagem" (2009)) as the strategic documents in the field (National Strategy Segurança-ENSAN powerup and Nutrition" (2009)) support that despite that "Angola has sufficient forest resources to ensure food security" needs to be improved resource management ethos through silvicultural practices to ensure better quality sustainable forest production, continuous production and increasing production of goods and services increased spatial and temporal diversity". In this sense, improve miombo forest management is a key in the current context, in which the resources are exploited in an unsustainable manner, improving institutional capacity for oversight and management, but also including rural communities throughout the management process, a more participatory and equitable manner.



Fig. 7 Miombo regeneration area as potential CO₂ sink. IDAF Consulting

1.9. Summary

Currently, we are in an important scenario for fight recovery miombo. Advances in GIS systems give us a basic tool to support sustainable management of forests and ecosystems and can anticipate and plan future actions to avoid deforestation and degradation processes. As Ana Cabral and his colleagues reported in his 2009 paper, new extraction processes with the city's population growth and new settlements have been identified, resulting in new fuel wood removals in the proximity of the new paved roads. However in the beginning of the 2000s, losses miombo forest in the region of Huambo find a balance with regeneration, and a relative decrease in the extent of Savanna-Woodland.

At the institutional level, adjustments are also needed to improve the management of forest resources, implementing existing policies, enhancing the capacity of forest managers and increasing control.

In recent years, the Angolan government is making an effort to adapt its policies to the environmental reality and existing international environmental policies, with the signing of major international agreements (Kyoto Protocol in 2007), and approving documents national as the "National Policy on Forests, Fauna and Areas Conservação Selvagem" in 2009, the "National Plan Adaptação (NAPA)" and other specific strategic documents such as the "National Strategy for Food and Nutrition Security" level or the " National Strategy and Repovoamento povoamento Florestal ". Despite these efforts, many improvements are needed in the development of sustainable forest management.

On one side, we see that in Angola there is little technical capacity to forest level. Although in recent years it has been implemented degree in Forest Engineering, few professionals trained sector, there are no vocational studies formed in recent years in the country, so that existing have an outdated training, the result of past cooperation programs at the end of the armed conflict. Joined this need for training of professionals, they are also fundamental environmental

awareness programs and training of civil society, thus ensuring ownership by rural people of good management practices.

Furthermore, the updating of environmental legislation is necessary, ensuring compliance with it. Although there is a document of National Forest Policy, legislation that articulates this strategic document is outdated, and it is unknown both by professionals, such as rural, latest forest resource managers population. Also, the forest-level control is another of the weaknesses in the existing forest management in the miombo in Angola, and in general, in all ecosystems. There is a lack of technical control, the means to those technical and training.

We can summarize that a good forest management, silvicultural programs that include processes profitable and sustainable extraction, can guarantee its own conservation, alternative uses of avoiding more intensive and aggressive land uses, which usually result in irreversible processes of deforestation. These programs have to include rural communities living in the miombo, it is necessary for resource users to become key players in all these processes research and development (Sayer and Campbell, 2004). The control of the resources of local communities requires commitment to a basic monitoring of holdings and the supply and use of these, and when necessary, to make adjustments and regulations necessary to meet the needs of local users, but sustainably (Shackleton and Clarke, 2007).

2. Objectives

The overall objective of this project was to study the degradation and deforestation in miombo forests located in the province of Huambo (Angola) during the period from 2002 to 2015. This general objective is developed through the following specific objectives:

1. Spatial and temporal analysis of deforestation in the province in Huambo from 2002 to 2015
2. Current analysis of the distribution and degradation levels in miombo forest in the province of Huambo.

These specific objectives were developed with a methodology that combines remote sensing and field information through three stages:

Stage 1: At this stage the preparatory activities were performed, mainly downloading images and field work, developed in section 3

Stage 2: The object of this stage is the activities planned in the study of deforestation, developed in section 4

Stage 3: The object of this stage is the analysis of the level of degradation of the miombo forest, which is developed in section 5

Table 1 Objectives by stages and section

Specific Objective	Stage	Section
Preparatory activities	Stage 1	Section 3
Analysis of deforestation	Stage 2	Section 4
Analysis of degradation	Stage 3	Section 5

3. Preparatory activities

Remote sensing has been with us for longer than you may think. In the 1600s, Galileo used optical enhancements to survey celestial bodies. (He also used his optical equipment to observe merchant ships arriving in harbour, capitalizing on this information to modify his investment strategies to anticipate changes in the rapidly fluctuating prices of the local commodity markets.) French balloonist and photographer Gaspard Felix Tournachon attempted (without great success) to perform land surveys in 1859 using photos taken from tethered balloons. Similar technologies were used for the next four years by the Union forces in the USA civil war, also with unsatisfactory results.

In the 1880s, Arthur Batut in Labruguiere, France affixed cameras to kites. His apparatus included an altimeter which encoded the altitude onto the film so the scale of his images could be determined. The camera shutter was triggered by a slow burning fuse, and his mechanism released a red flag when the shutter had been tripped. For all this, Batut is considered the father of kite aerial photography, a technique that persists in modern times. At least one modern preserve manager has a hobbyist interest in attaching cameras to kites for remote sensing applications, but this is still in a novelty stage of development.

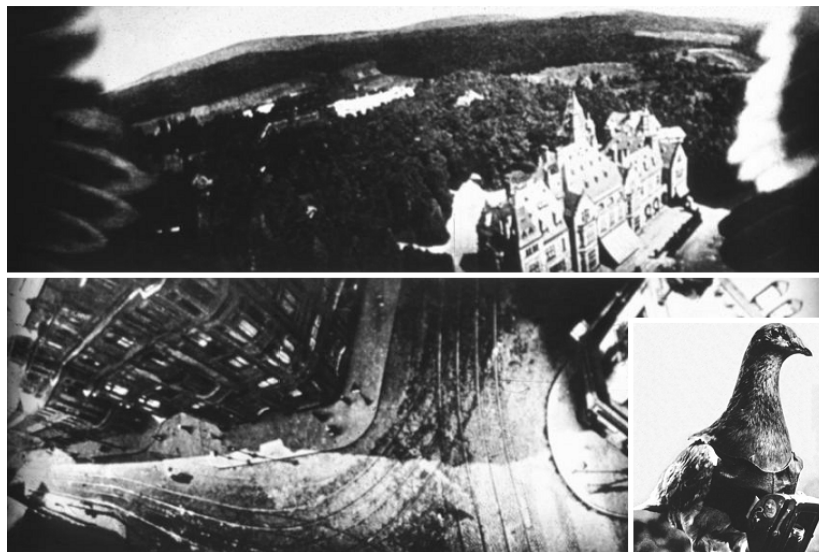


Fig. 8 Camera pigeon

By 1903, camera miniaturization had become so advanced the cameras could be attached to pigeons (Fig. 8). The most famous avian photographers were the Bavarian Pigeon Corps. The cameras had a mass of 70 g, and took photographs every 30 seconds. While their images (that sometimes included wingtips in the frame) were of limited use, the birds looked great in uniforms.

Military applications of remote sensing continued during World War I (Fig. 9), and World War II. Remote sensing changed the course of world history when, during the 1962 Cuban missile crisis, U-2 spy craft detected the installation of intermediate range nuclear missiles in Cuba.

In 1956-1958, W.M. Stinton discovered absorption features in his spectra of Mars that appeared to be consistent with chlorophyll. This was an interesting application of vegetation remote sensing. However, these observations were later explained as resulting from an absorption band due to deuterated water.

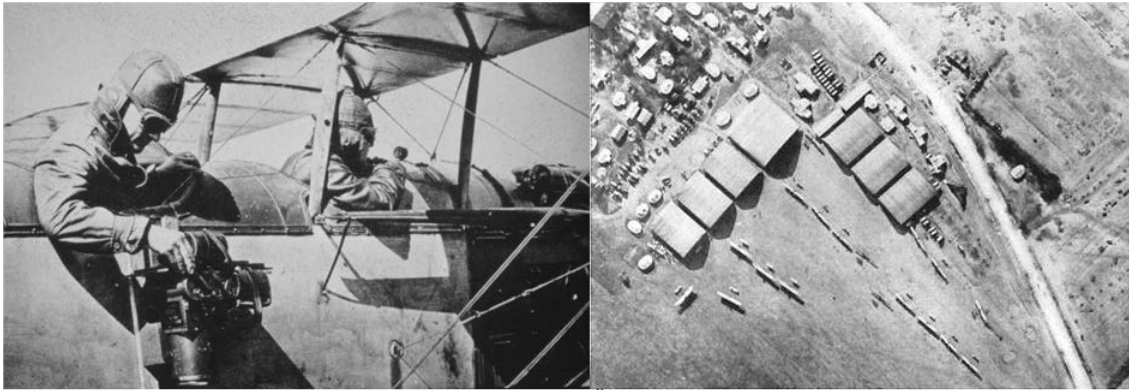


Fig. 9 Aerial photographer during World War I, and a French air field

At 1972 began a new era in remote sensing and environmental management with the launch of Landsat1 (Fig. 10). Such satellites had the ability to take data regularly and with a synoptic view, giving the ability to detect temporal global information, identifying and mapping the changes in the forest.

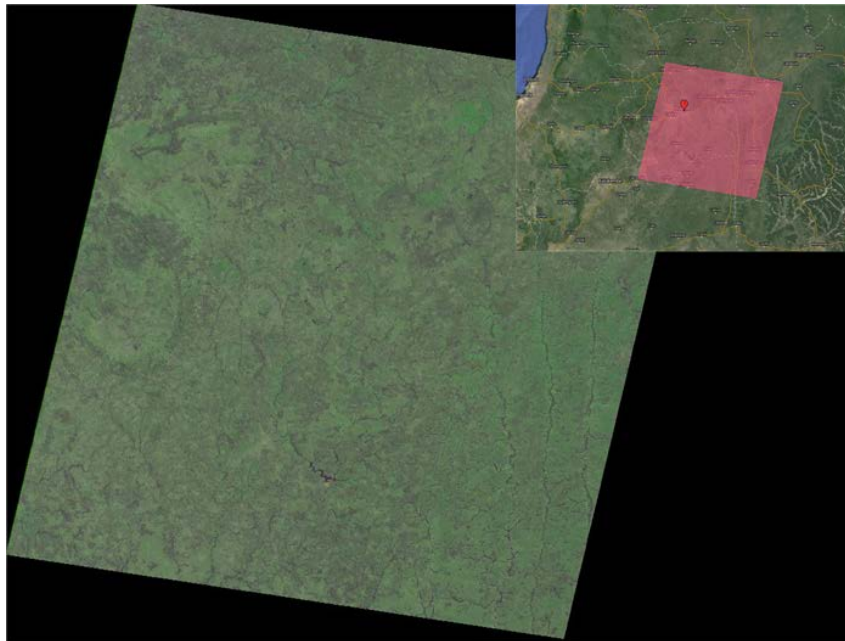


Fig. 10 Landsat 1 image in 29-august-1973. Source: USGS

Aldrich (Aldrich, 1975) predicted in 1975 that "Even low-resolution data from the Landsat MSS scanner, if combined and enhanced, will disclose 80 to 90% of the exchanges of land use between forest and non-forest categories. In addition, such data will show 25 to 90% of the less distinct disturbances in the forest, depending on the category". Digital change detection essentially comprises the quantification of temporal phenomena from multidata imagery that is most commonly acquired by satellite-based multispectral sensors.

The program has run continuously since 1972, so scientists have more than four decades of information in their hand to track changes in land use over time. The launches of Landsat 2, Landsat 3, and Landsat 4 followed in 1975, 1978, and 1982, respectively. When Landsat 5 was launched in 1984, no one could have predicted that the satellite would continue to deliver high quality, global data of Earth's land surfaces for 28 years and 10 months, formally established a new Guinness World Record for "longest-operating Earth observation satellite". Landsat 6 failed to achieve orbit in 1993. Landsat 7 successfully launched in 1999 and, along with Landsat 8, which launched in 2013, continues to provide daily global data. Landsat 9 is tentatively planned to launch in 2023 (Fig.11).

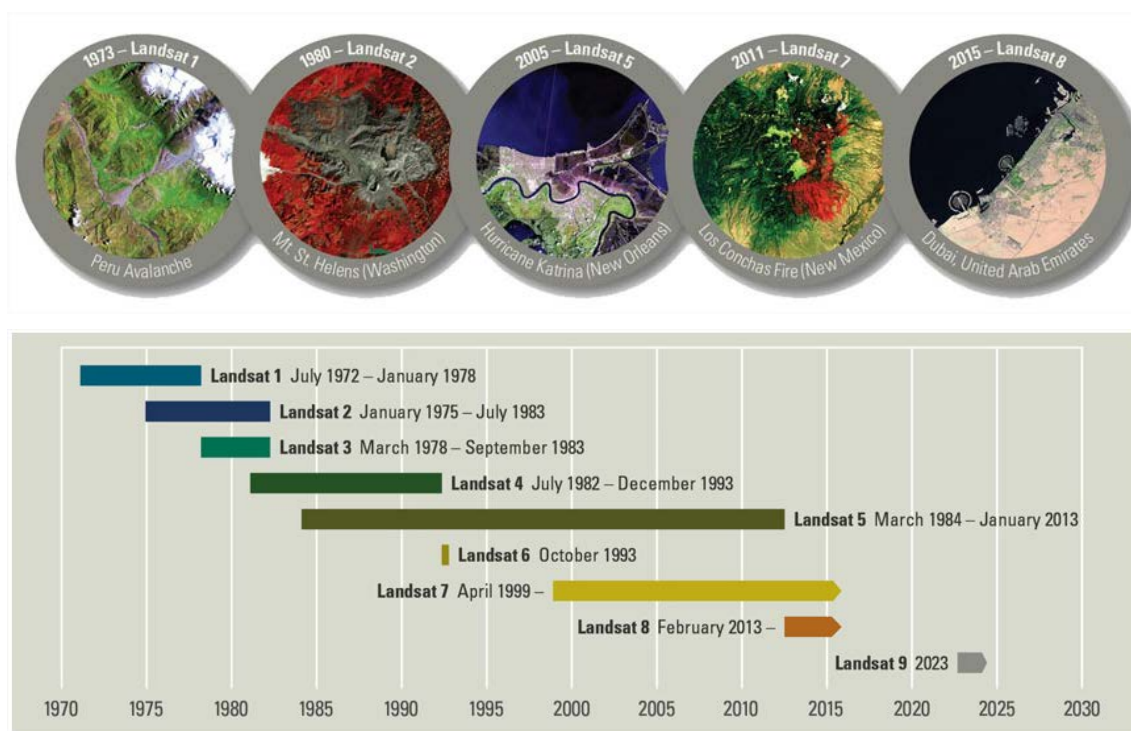


Fig. 11 Evolution of Landsat satellite and future prospects. Source: Landst webpage

Month by month increase the demand of Landsat data. As it can see in the figure below (Fig, 12), the number of images delivered from Landsat satellites series to governments, academics, non-governmental organizations and other institutions from October 2007 to June 2013. The line show the number of scenes crawls along the bottom of the X-axis until Oct. 1, 2008. Then, it is passing the 1-million mark in less than a year. The last data point (June 10, 2013) is just

below of the 12 million scene mark. In 2001, the best year for Landsat image sales, an average of 53 scenes were purchased a day. Today, that figure stands around 5,700 scenes a day.

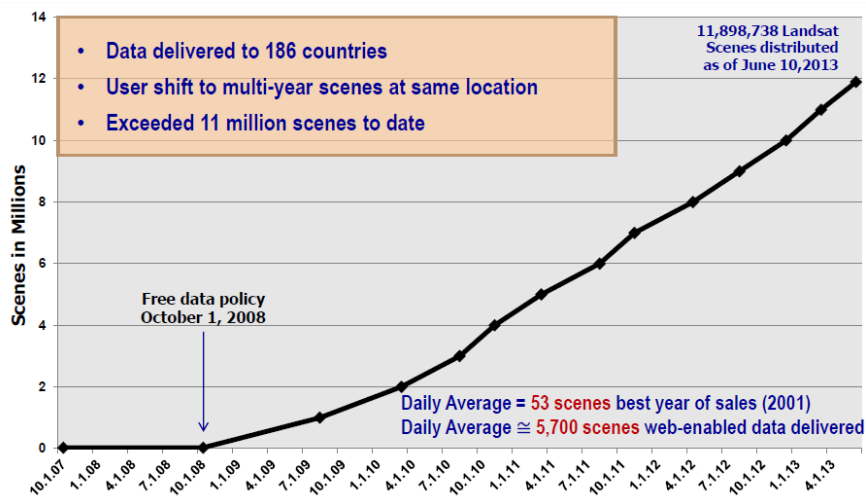


Fig. 12 Demand of Landsat images from January 2007 to January 2013. Source: Landsat webpage

Nowadays, Landsat is used to the field of agriculture, forestry and range resources, land use and mapping, geology, hydrology, coastal resources and environmental monitoring. The graph below (Fig, 13) shows the top ten Landsat data uses from October 1, 2014 through September 30, 2015.

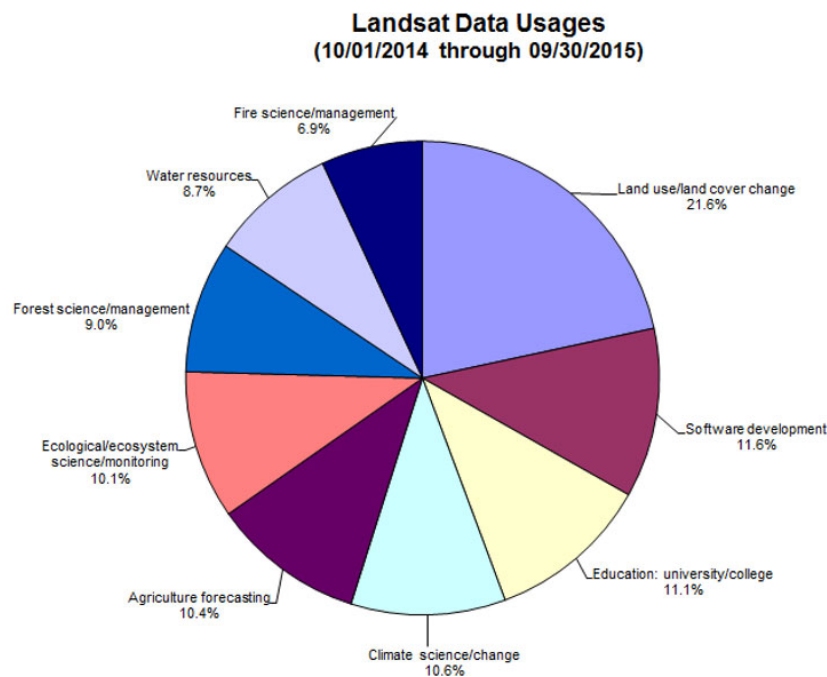


Fig. 13 Landsat data uses. Source:Landsat webpage

The need to mosaic images requires a high amount of data for each year, therefore the cost of commercial satellites images could be unaffordable; that is another reason to prefer Landsat data.

3.1. Image acquisition

The appropriate selection of imagery acquisition dates is as crucial to the change detection method as is the choice of the sensor(s), change categories, and change detection algorithms. The problem has two dimensions: the calendar acquisition dates and the change interval length (temporal resolution).

Lund (1983) (Lund, 1983) very appropriately stated that the forest manager's ability to successfully detect and identify change depends on four crucial factors:

1. The kind of information sought and the priori knowledge of the anticipated alteration or movement
2. The stationary resource base against which change is sought
3. The selection of the method and the tools to detect and label, through repeated observations, the alteration or movement.
4. The follow-up analysis to ensure that all other factors were indeed held constant.

The proper understanding about nature of the change and the principles that enable its detection and categorization, usually encompass more sophistication than the simple detection of the change event itself.

The developed methodology requires the following steps (Fig. 14):

1. Landsat Image selection;
2. Preprocessing process:
 - 2.1. Georeferencing images in order to assign spatial coordinates;
 - 2.2. Creating masks of clouds and shadows, and applying those mask to the Landsat bands in order to exclude pixels belonging to clouds or shadows from LC classification;
 - 2.3. Converting the multispectral bands (1, 2, 3, 4, 5 and 7) from DN to reflectance, applying atmospheric correction;
 - 2.4. Mosaicking temporally different images, in order to obtain a cloud-free and gap-free image

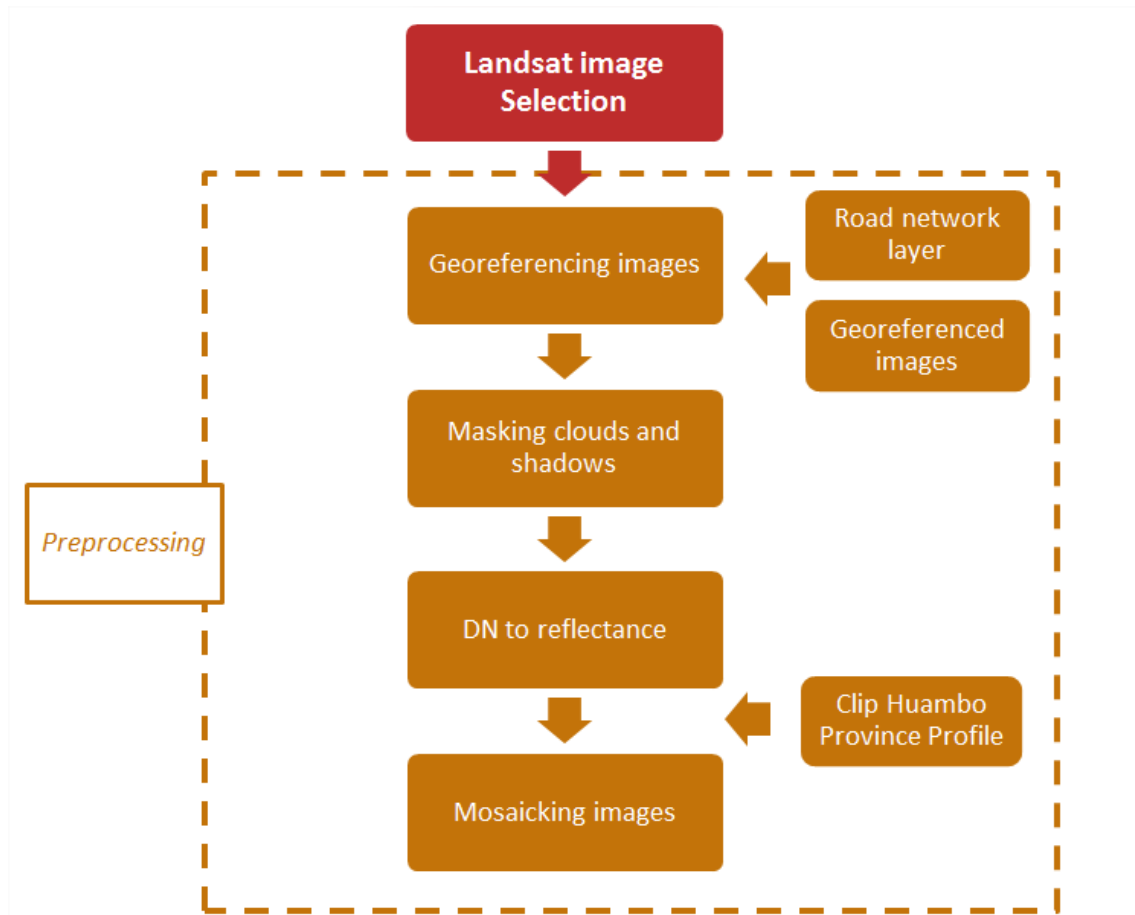


Fig. 14 Standard workflow of image preprocessing

3.1.1.Landsat Image selection

During the dry season, when the miombo forest still has leaf but the grassland are dry, 4 Landsat satellite images were acquired per year to cover the whole study area. In the figure below you can see how the dry season (May to October) photosynthetic activity decreases as they dry grasslands. The figure below (Fig, 15) it can see how the dry season (May to October) photosynthetic activity decreases because of grasslands are going dry. August has been considered most appropriate month because the miombo forest has not lost its leaf yet.

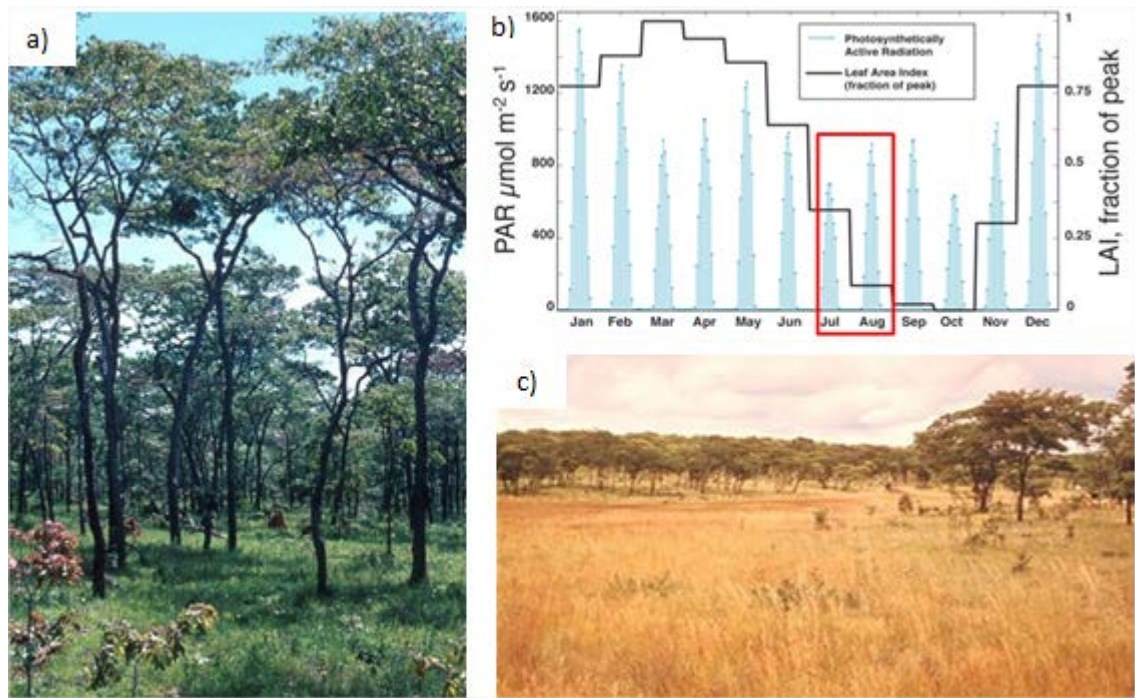


Fig. 15 Data used to drive the model. a) Miombo forest in the dry season b) Photosynthetically Active Radiation and Leaf Area Index monthly dynamics. c) Miombo forest in the wet season (Photograph by Brian Huntley)

Four Landsat satellite images have been collected for each studied year (Fig. 16) during the dry season to complete the province of Huambo (Angola)



Fig. 16 Four Landsat image were needed to complete the whole study area. (USGS webpage)

To cover the temporary space required, in this study Landsat 7 ETM+ (between 2002-2012) and Landsat 8 OLI (2013-2014-2015) were considered. These two satellites have some different sensors characteristics that have been shown in the table below (Table 2).

Table 2 Differences between Landsat 7 ETM+ and Landsat 8 OLI

Landsat 7			Landsat 8		
Band	Bandwidth (μm)	Spatial Resolution (m)	Band	Bandwidth (μm)	Spatial Resolution (m)
			B1. Coastal	0.43 – 0.45	30
B1. Blue	0.45 – 0.52	30	B2. Blue	0.45 – 0.51	30
B2. Green	0.52 – 0.60	30	B3. Green	0.53 – 0.59	30
B3. Red	0.63 – 0.69	30	B4. Red	0.64 – 0.67	30
B4. NIR	0.77 - 0.90	30	B5. NIR	0.85 – 0.88	30
B5. SWIR 1	1.55 – 1.75	30	B6. SWIR 1	1.57 – 1.65	30
B7. SWIR 2	2.09 – 0.35	30	B7. SWIR 2	2.11 – 2.29	30
B8. Pan	0.52 – 0.90	15	B8. Pan	0.50 – 0.68	15
			B9. Cirrus	1.36 – 1.28	30
B6. TIR	10.40 – 12.50	30/60	B10. TIRS 1	10.6 – 11.19	100
			B11. TIRS 2	11.5 – 12.51	100

Every image has different multispectral bands with spatial resolution from 15 to 30m (Landsat 8 has some additional bands), and image size at ground is 170km north-south by 183km east-west (NASA, 2015). Also, the bandwidth between Landsat 7 and 8 is different as shows Figure 17.

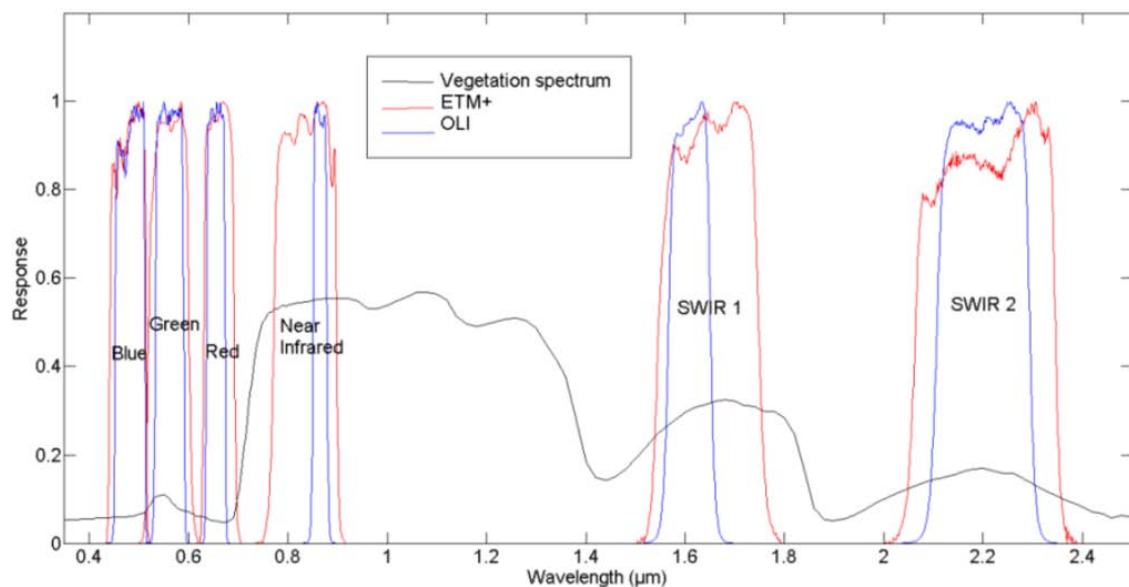


Fig. 17 Differences between spectral resolution of Landsat 7 and Landsat 8

Such differences may have an effect on land cover classification because the impacts on vegetation spectrum change depending on the band. For more details about Landsat 7 ETM+ and Landsat 8 OLI it can see *Annex II. Remote Sensing*

Landsat images are provided for free by the USGS. The USGS is a “science organization that provides impartial information on the health of our ecosystems and environment, the natural hazards that threaten us, the natural resources we rely on, the impacts of climate and land-use change, and the core science systems that help us provide timely, relevant, and useable information” (USGS, 2016). It made available over internet the archive of images acquired since 1984. In the developed methodology were used the reflected solar energy bands, excluding the thermal band, because in this range it is possible to identify materials by their spectral response, using unsupervised classification.

A workflow has been designed for the preprocessing of Landsat data, correcting for atmospheric effects, masking clouds and their shadows in a semiautomatic way, and processing data.

Landsat imagery is distributed by USGS at no charge, indeed it said: “there are no restrictions on Landsat data downloaded from USGS EROS, and it can be used or redistributed as desired. However, a statement of the data source when citing, copying, or reprinting USGS Landsat data or images is requested”. Data of Huambo province can be downloaded free for registered users.

Downloaded imagery is composed of a .tif file for each Landsat band, and an MTL.txt file which contains metadata information.

Images are already georeferenced in WGS84 datum and UTM projection in a north up (map) orientation, and are of Level 1 of the Product Generation System.

It is possible to order for free the processing of images that are present in the USGS on-line archive, but not available for download; depending on the USGS queue for processing, images are generally processed in 1 to 3 days, and an e-mail confirm the process conclusion. In this study the image classification process was based on the semi-automatic Maximum Likelihood (ML) algorithm, which allows for the identification of LC classes; the algorithm is based on training area collected over the image, which define the spectral signatures of classes.

It is necessary to know the situation of the province of Huambo in the WRS (Worldwide Reference System) in order to download Landsat images (Fig. 18). The WRS is “a global notation system for Landsat data. It enables a user to inquire about satellite imagery over any portion of the world by specifying a nominal scene centre designated by PATH and ROW numbers. The WRS has proven valuable for the cataloguing, referencing, and day-to-day use of imagery transmitted from the Landsat sensors”. Landsat 7 and 8 images are referred to the WRS-2 (Worldwide Reference System – 2). Huambo province is in path 180-181 and row 68-69.

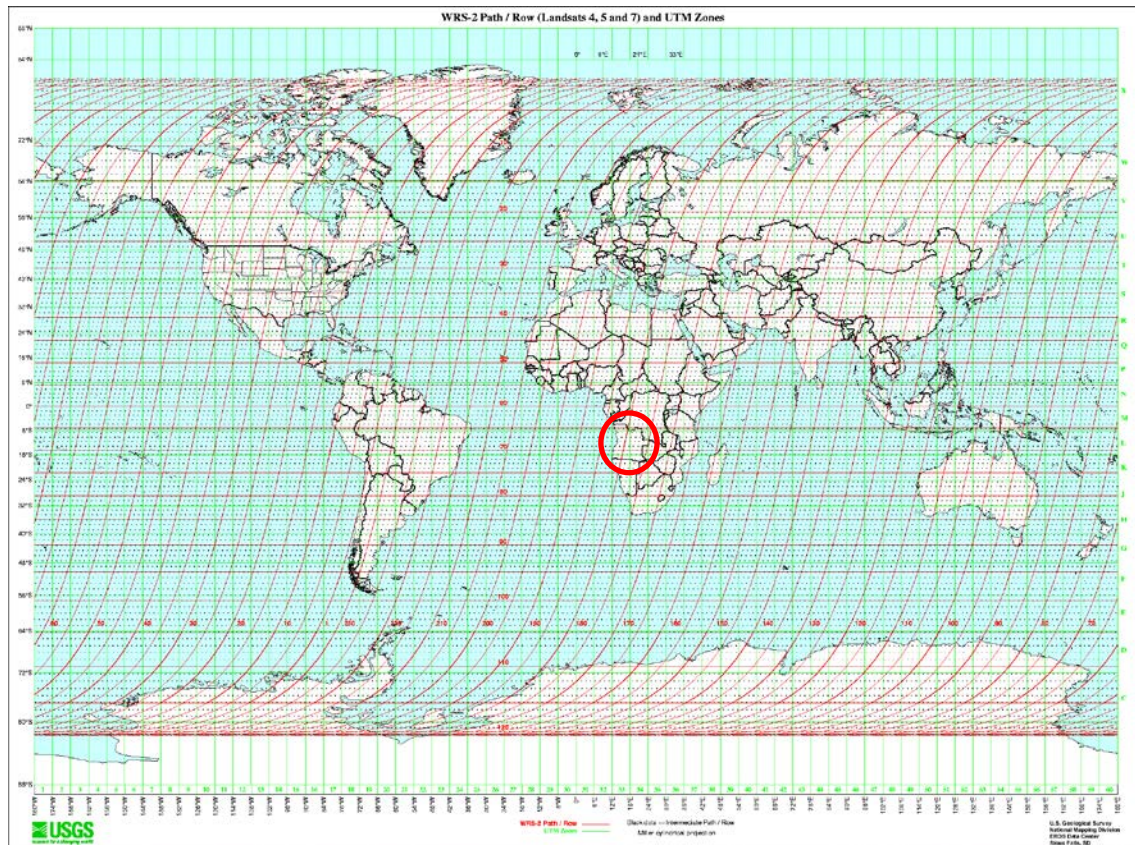


Fig. 18 Worldwide Reference System-2. Angola is in the red circle.

Not all of the 56 Landsat images (four images by year) had been available. The reason is that Landsat 7 images, which were acquired after 2003, are affected by a technical problem causing SLCoff gaps along the image, with stripes of null data; moreover USGS has stopped acquiring Landsat 5 from 2011/11/18 due to electronic problems. USGS explain:

“On May 31, 2003, the Scan Line Corrector (SLC), which compensates for the forward motion of Landsat 7, failed. Subsequent efforts to recover the SLC were not successful, and the failure appears to be permanent. Without an operating SLC, the Enhanced Thematic Mapper Plus (ETM+) line of sight now traces a zig-zag pattern along the satellite ground track (Figure 19). As a result, imaged area is duplicated, with width that increases toward the scene edge.

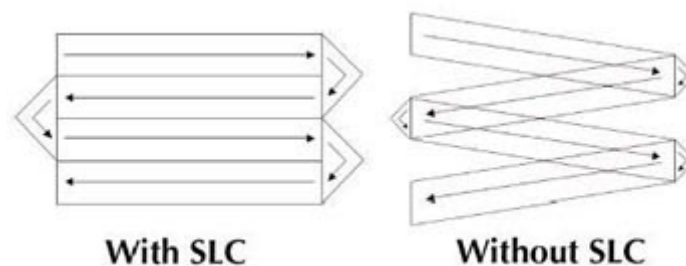


Fig. 19 SLC Failure

The Landsat 7 ETM+ is still capable of acquiring useful image data with the SLC turned off, particularly within the central part of any given scene. The Landsat 7 ETM+ therefore continues to acquire image data in the "SLC-off" mode. All Landsat 7 SLC-off data are of the same high radiometric and geometric quality as data collected prior to the SLC failure.

The SLC-off effects are most pronounced along the edge of the scene and gradually diminish toward the center of the scene (Figure 20). The middle of the scene, approximately 22 kilometers wide on a Level 1 (L1G, L1Gt, L1T) product, contains very little duplication or data loss, and this region of each image is very similar in quality to previous ("SLC-on") Landsat 7 image data.

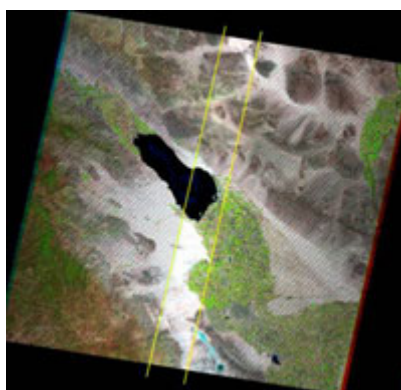


Fig. 20 Complete Landsat 7 scene showing affected vs. unaffected area.

An estimated 22 percent of any given scene is lost because of the SLC failure. The maximum width of the data gaps along the edge of the image would be equivalent to one full scan line, or approximately 390 to 450 meters. The precise location of the missing scan lines will vary from scene to scene."

A review was made and concludes that to replace the missing Landsat images had to consider the following items:

1. Project is about landcover changes therefore we must make a classification where the spectral information is essential
2. Study area have a big area (provincial level), hence highly accurate spatial information is not of utmost importance.
3. It is necessary a satellite with a period of low return because the study is a temporal sequence.

It was selected MODIS because falls under the definition of principal items. Preprocessing process of MODIS images were the same of Landsat. For more information about MODIS, it can see *Annex II. Remote Sensing*

The final list of selected images was downloaded from USGS archive, as shows Table 3.

Table 3 List of USGS images used to develop the project

Year	Number of image (path/row)	Name of the image	Date of the image	Type of Landsat Satellite
2002	1 (181/68)	LE71810682002228EDC00	16-AUG-02	Landsat 7
	2 (181/69)	LE71810692002228JSA00	16-AUG-02	
	3 (180/68)	LE71800682002221EDC00	09-AUG-02	
	4 (180/69)	LE71800692002221EDC00	09-AUG-02	
2003	Coordinates WGS84 -15.0415, 15.5743	MOD13Q1.A2002225.h19v10.005	13-AUG-02	MODIS
2004	1 (181/68)	LE71810682004218ASN01	05-AUG-04	Landsat 7/ MODIS
	2 (181/69)	LE71810692004218ASN01	05-AUG-04	
	Coordinates WGS84 -15.0415, 15.5743	MOD13Q1.A2004225.h19v10.005	12-AUG-04	
2005	1 (181/68)	LE71810682005220ASN00	08-AUG-05	Landsat 7
	2 (181/69)	LE71810692005220ASN00	08-AUG-05	
	3 (180/68)	LE71800682005229ASN00	17-AUG-05	
	4 (180/69)	LE71800692005229ASN00	17-AUG-05	
2006	1 (181/68)	LE71810682006223ASN00	11-AUG-06	Landsat 7/ MODIS
	2 (181/69)	LE71810692006223ASN00	11-AUG-06	
	Coordinates WGS84 -15.0415, 15.5743	MOD13Q1.A2006225.h19v10.005	13-AUG-06	
2007	Coordinates WGS84 -15.0415, 15.5743	MOD13Q1.A2007225.h19v10.005	13-AUG-07	MODIS
2008	Coordinates WGS84 -15.0415, 15.5743	MOD13Q1.A2008225.h19v10.005	12-AUG-08	MODIS
2009	1 (181/68)	LE71810682007226ASN00	14-AUG-07	Landsat 7/MODIS
	2 (181/69)	LE71810692007226ASN00	14-AUG-07	
	Coordinates WGS84 -15.0415, 15.5743	MOD13Q1.A2009225.h19v10.005	13-AUG-09	
2010	Coordinates WGS84 -15.0415, 15.5743	MOD13Q1.A2010225.h19v10.005	13-AUG-10	MODIS
2011	1 (181/68)	LE71810682011221ASN00	09-AUG-11	Landsat 7/ MODIS
	2 (181/69)	LE71810692011221ASN00	09-AUG-11	
	Coordinates WGS84 -15.0415, 15.5743	MOD13Q1.A2011225.h19v10.005	13-AUG-11	
2012	Coordinates WGS84 -15.0209, 15.584	MOD13Q1.A2012225.h19v10.005	12-AUG-12	Landsat 7/ MODIS

	3 (180/68)	LE71800682012217ASN01	04-AUG-12	
	4 (180/69)	LE71800692012217ASN00	04-AUG-12	
2013	1 (181/68)	LC81810682013218LGN00	06-AUG-13	Landsat 8
	2 (181/69)	LC81810692013218LGN00	06-AUG-13	
	3 (180/68)	LC81800682013227LGN00	15-AUG-13	
	4 (180/69)	LC81800692013227LGN00	15-AUG-13	
2014	1 (181/68)	LC81810682014221LGN00	09-AUG-14	Landsat 8
	2 (181/69)	LC81810692014221LGN00	09-AUG-14	
	3 (180/68)	LC81800682014230LGN00	18-AUG-14	
	4 (180/69)	LC81800692014230LGN00	18-AUG-14	
2015	1 (181/68)	LC81810682015224LGN00	12-AUG-15	Landsat 8
	2 (181/69)	LC81810692015224LGN00	12-AUG-15	
	3 (180/68)	LC81800682015217LGN00	05-AUG-15	
	4 (180/69)	LC81800692015217LGN00	05-AUG-15	

3.1.2.Preprocessing process

a) Georeferencing images in order to assign spatial coordinates

The geographical correction of Landsat images acquired through the USGS can be classified as the Standard Terrain Correction (Level 1T, the most accurate), the Systematic Terrain Correction (Level 1GT), or the Systematic Correction (Level 1G) with lower precision.

Depending on the processing type, georeferencing is not always required. In the specific case of this study, multiple control points had been using road network shapefile and georeferenced images. It was verified that using metadata associated with each image (MLT.txt file) and the absence of clouds in the area of interest, georeferencing of USGS was accepted.

b) Creating masks of clouds and shadows

When there are clouds or shadows on Landsat images it has to apply a mask to the Landsat bands in order to exclude pixels belonging to clouds or shadows from LC classification. In this project was not necessary because it was the dry season and there were no clouds.

c) Converting the multispectral bands from DN to reflectance

The radiance and brightness are affected by atmosphere as show Figure 21. First, it attenuates (reduces) the energy illuminating a ground object (and being reflected from the object) at particular wavelengths, thus decreasing the radiance that can be measured. Second, the atmosphere acts as a reflector itself, adding a scattered, extraneous path radiance to the signal detected by the sensor which is unrelated to the properties of the surface.

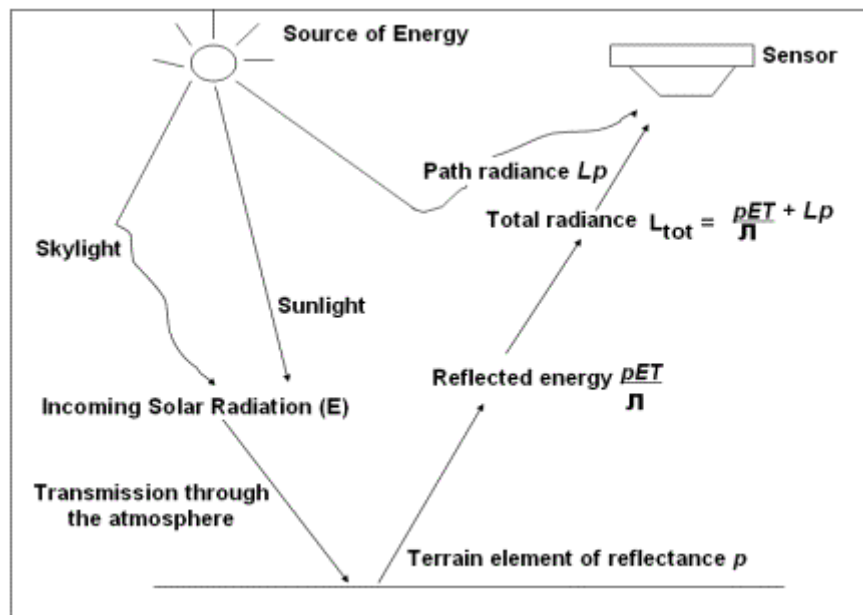


Fig. 21 Atmospheric effects influencing the measurement of reflected solar energy. Attenuated sunlight and skylight (E) is reflected from a terrain element having reflectance p . The attenuated radiance reflected from the terrain element (pET/π) combines with the path radiance (L_p) to form the total radiance (L_{tot}) recorded by the sensor

The Landsat 7 ETM+ sensors capture reflected solar energy, convert these data to radiance, and then rescale this data into an 8-bit digital number (DN) with a range between 0 and 255. It was possible to manually convert these DNs to ToA (Top of Atmosphere) Reflectance using a two-step process. The first step had been converted the DNs to radiance values using the bias and gain values specific to the individual scene it was working with. The second step converted the radiance data to ToA reflectance.

The Landsat 8 OLI sensor is more sensitive so these data are recycled into 16-bit DNs with a range from 0 and 65536. Also these data had been converted to reflectance, rather than radiance, so that DNs can be manually converted to Reflectance in a single step.

Specific software with specific algorithm of atmospheric correction was used to overcome these difficulties.

d) Mosaic images

Mosaicking is the seamless joining or stitching of adjacent imagery (Fig. 22). Joining Landsat imagery that was collected along the same satellite path is not the most difficult part. The main advantage is that the atmosphere is continuous between one image to the next.

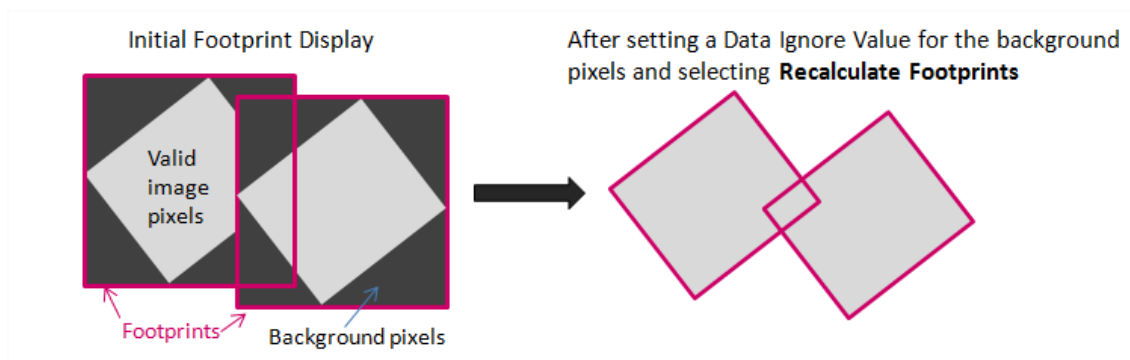


Fig. 22 Mosaic example

However, when it is joining adjacent imagery from different paths, it can pass some days. As such, there is a need to adjust the radiometric differences between the images in an effort to make the join appear seamless. Mosaicking is not a perfectly clean process: it often requires additional image processing to remove some of the 'noise' near the stitch. Once created the mosaic, cut according to the limit of Huambo province.

3.2. Work Field

In this service was combined the information obtained from field work with information from the Remote Sensing techniques. This allowed analysing an extension unapproachable by traditional sampling methods, obtaining results of great spatial accuracy. The field work consisted in carrying out a forest characterization through recognition transect, supported with forest inventory plots.

General status of trees was characterized applying with a five degrees scale. This characterisation was realised although for the trunk and treetop. Finally, was analysed the sanitary status and the origin of the disease or pest.

The forest inventory was realised using the FAO method to define the inventory plots, with adaptations. A tract is a square of 1 km x 1 km. The coordinates of the south-west corner of the tracts correspond to those of the points selected in the systematic sampling frame. Each tract contains four field plots. The plots are rectangles measuring 20 m wide and 250 m long. They start at each corner of an inner 500 m square (same centre as the tract centre) and are numbered clockwise from 1 to 4. Also, three circular subplots with a radius of 3.99 m are delimited within each plot. They correspond to a different level of data collection. These subplots serve to measure tree regeneration ($Dbh < 10$ cm) (FAO, 2009). The scheme is shown below (Fig.23).

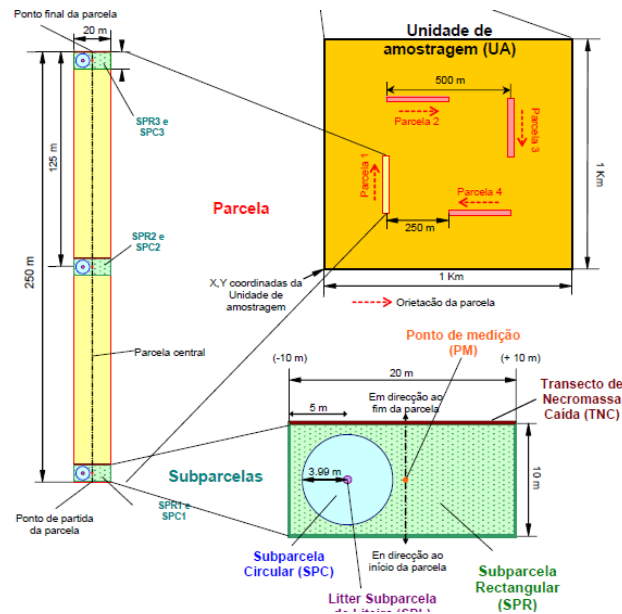


Fig. 23 Scheme of inventory plots

A GPS Garmin was used to recording UTM coordinates of each tract. In each tract, was recording UTM coordinates of each four inventory plots. Coordinates of tracts and inventory plots are show in the table below (Table 4).

Table 4 Coordinates of tracts and inventory plots

ÁREA	COORDINATES (UTM)				
Chiteta -Luvemba community (Bailundo-Huambo)	Central Coordinates	S 11°59.131' E 15°26.969'			
	PLOT	PLOT 1 (250mx20m)	PLOT 2 (250mx20m)	PLOT 3 (250mx20m)	PLOT 4 (250mx20m)
	Initial point	E 0585002	E 0584971	E 0585438	E 0585500
		N 8674644	N 8675191	N 8675162	N 8674564
	Middle point	E 0584977	E 0585096	E 058545	E 0585377
		N 8674760	N 8675178	N 8675040	N 8674562
	Final point	E 0584940	E 0585217	E 0585474	E 0585264
		N 8674882	N 8675180	N 8674916	N 8674543
Ngondo – Sambo community (Tchikala-Tcholo-hanga - Huambo)	Central Coordinates	S 1305.658 E 1618.850			
	PLOT	PLOT 1 (250mx20m)	PLOT 2 (250mx20m)	PLOT 3 (250mx20m)	PLOT 4 (250mx20m)
	Initial point	E 1616,713	E 1618,710	E 1618,854	E 1618,989

		N 1305,796	N 1305,524	N 1305,527	N 1305,794
	Middle point	E 1618,713	E 1618,779	E 1618,851	E 1618,920
		N 1305,729	N 1305,524	N 1305,854	N 1305,794
	Final point	E 1618,713	E 1618,848	E 1618,447	E 1618,850
		N 1305,662	N 1305,524	N 1305,241	N 1305,794

From inventory data (diameter and height) were calculated dasometric variables (basal area and volume) to each species. Also, density of each species and the potential productivity of charcoal were calculated with a general allometric equation for miombo species (Sanfillipo et al., 2013).

4. Deforestation study in miombo forest of Huambo

One of the bases of remote sensing is to measure at different wavelengths, electromagnetic energy that interacts with the material. According to the physical characteristics of the material, how reflection occurs change. This will ultimately depend on the refraction and absorption of each material (Fig, 24). These interactions can be measured through specific sections of the spectrum, as it is shown in the spectral signature. The spectral signature is unique and personal way to respond when the materials interact with light.

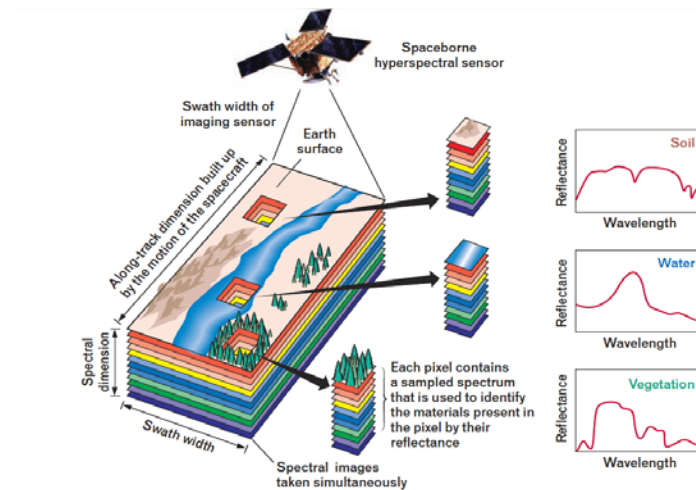


Fig. 24 Examples of reflectance of water, soil and vegetation in different wavelengths in different channels of Landsat ETM+.

The basis of the classification process will convert the reflectance of each pixel multispectral images from Landsat in a thematic map. Therefore, and taking advantage of the peculiarities of each spectral signature, each image will rank between 2002 and 2015 in forest and non-forest area. (Lillesand and Kiefer, 1979). Figure 25 shows the characteristics of the spectral signature of vegetation

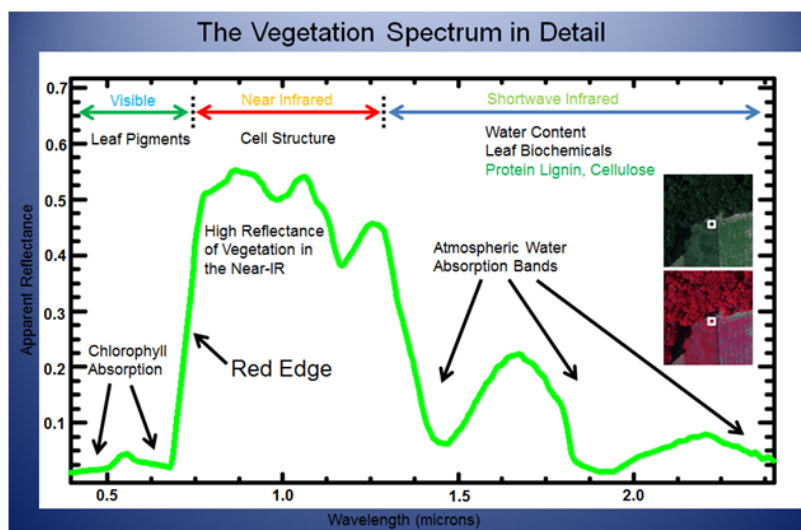


Fig. 25 Spectral signature of vegetation

4.1. Methodology

The classification processes to obtain the results of deforestation in miombo forest of Huambo follow the workflow in the figure 26

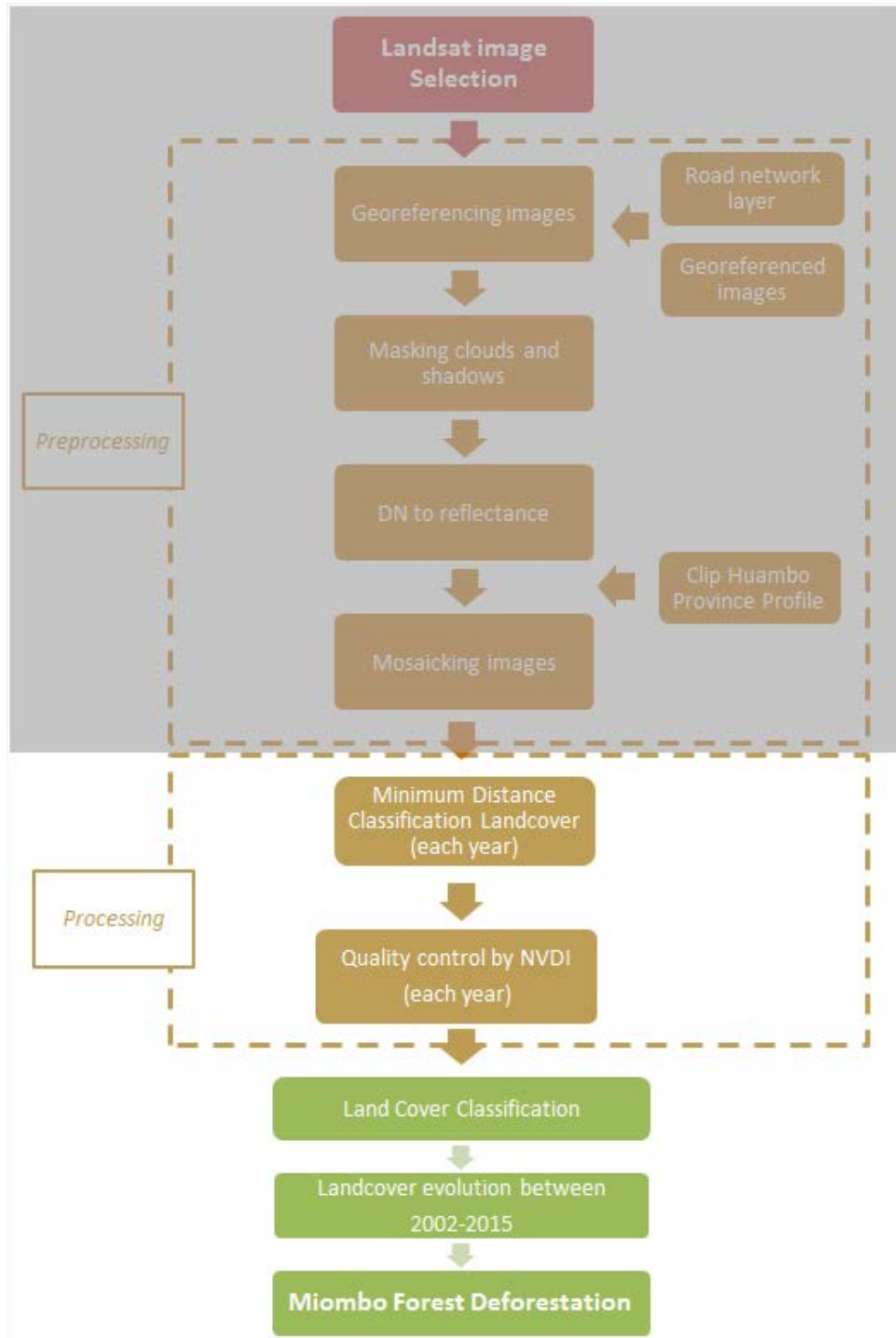


Fig. 26 Workflow of classification process

4.1.1. Classify the image mosaic with Minimum Distance algorithm

Supervised classification methods are used to generate a map with each pixel assigned to a class based on its multispectral composition. The classes are determined based on the spectral composition of training areas defined by the user. Figure 27 shows the basic workflow.

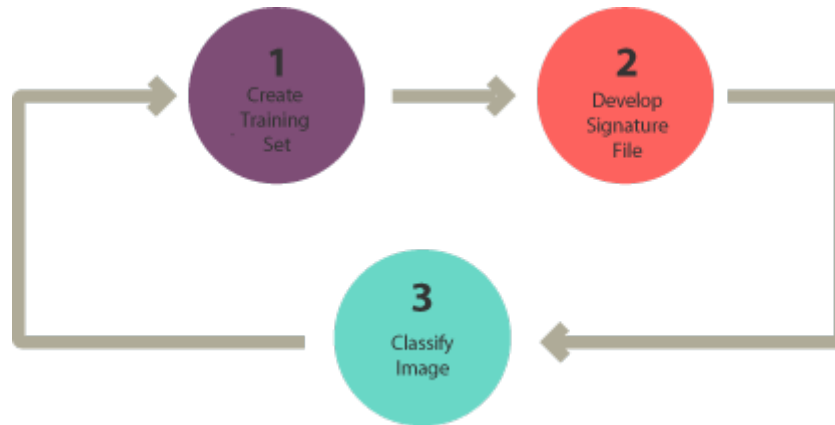


Fig. 27 Supervised Classification Diagram

The type of method implemented can profoundly affect the qualitative and quantitative estimates of the disturbance (Colwell and Weber, 1981). Even in the same environment, different approaches may yield different change maps. The selection of the appropriate method therefore takes on considerable significance.

The supervised classification (Fig. 28) it is very effective and accurate in classifying satellite images and can be applied at the individual pixel level or to image objects (groups of adjacent, similar pixels) (Al-Ahmadi and Hames, 2009). However, to make the process work more effectively, has been reinforced by previous knowledge of field (field data, aerial photographs...), climatic data, and biography about forest of Huambo and the classes of land cover types there are already located.

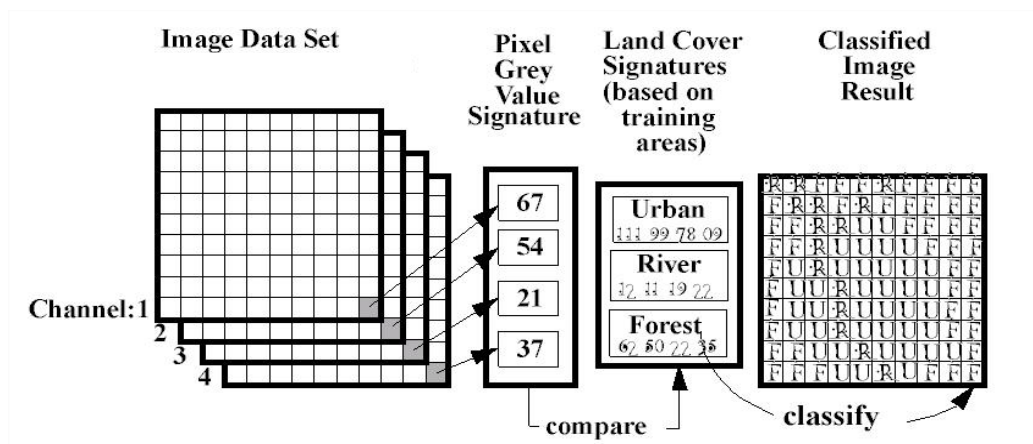


Fig. 28 Steps in Supervised classification

In supervised classification, the image processing software is guided by the user to specify the land cover classes of interest. The user defines “training regions” – areas in the map that are known to be representative of a particular land cover type – for each land cover type of interest.

The software determines the spectral signature of the pixels within each training area, and uses this information to define the mean and variance of the classes in relation to all of the input bands or layers. Each pixel in the image is then assigned, based on its spectral signature, to the class it most closely matches. In the classification stage, three supervised classification methods were selected to classify the images. Two methods, Maximum Likelihood and Minimum Distance-to-Mean had been performed to the images.

Maximum likelihood Classification is a statistical decision criterion to assist in the classification of overlapping signatures; pixels are assigned to the class of highest probability (Fig. 29). For mathematical reasons, a multivariate normal distribution is applied as the probability density function. In the case where the variance-covariance matrix is symmetric, the likelihood is the same as the Euclidian distance, while in case where the determinants are equal each other, the likelihood become the same as the Mahalanobis distances. (Ahmad and Quegan, 2012)

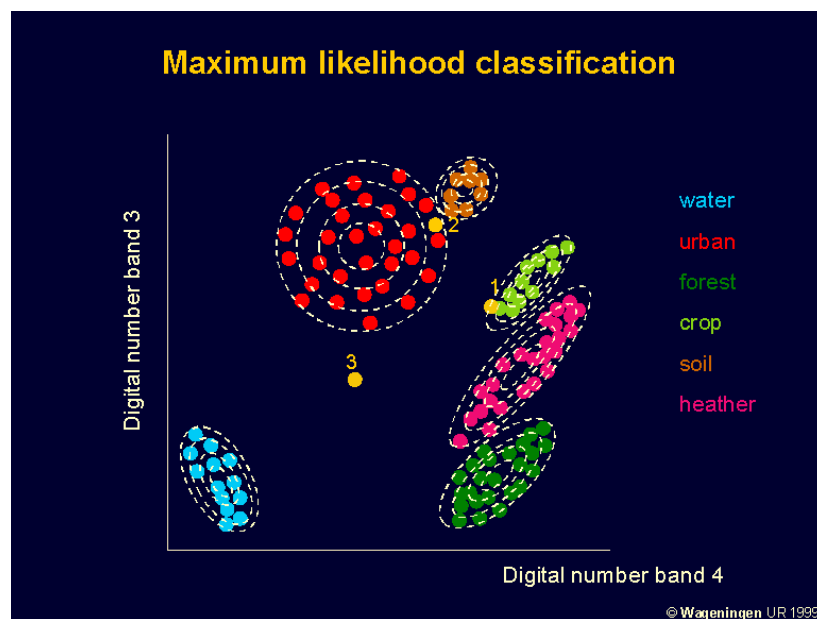


Fig. 29 Maximum likelihood classification. Source: Centre for Geo-information of Wageningen University and Research Centre, 1999

The maximum likelihood method has an advantage from the view point of probability theory, but care must be taken with respect to the following items. (Woodward et al., 1984)

1. Sufficient ground truth data should be sampled to allow estimation of the mean vector and the variance-covariance matrix of population.
2. The inverse matrix of the variance-covariance matrix becomes unstable in the case where there exists very high correlation between two bands or the ground truth data are very

homogeneous. In such cases, the number of bands should be reduced by a principal component analysis.

3. When the distribution of the population does not follow the normal distribution, the maximum likelihood method cannot be applied.

Otherwise, Minimum distance classifier image data on a database file using a set of 256 possible class signature segments as specified by signature parameter. Each segment specified in signature, for example, stores signature data pertaining to a particular class. Only the mean vector in each class signature segment is used. It means where the spectral distance between the target pixel and the average spectral value for each cover class are calculated. The class, to which the target pixel is closest, is assigned to that pixel in the output image (Fig, 30). A minimum distance classifier assumes that the image data follows a normal distribution and so it is a parametric classifier. (Wacker and Landgrebe, 1972)

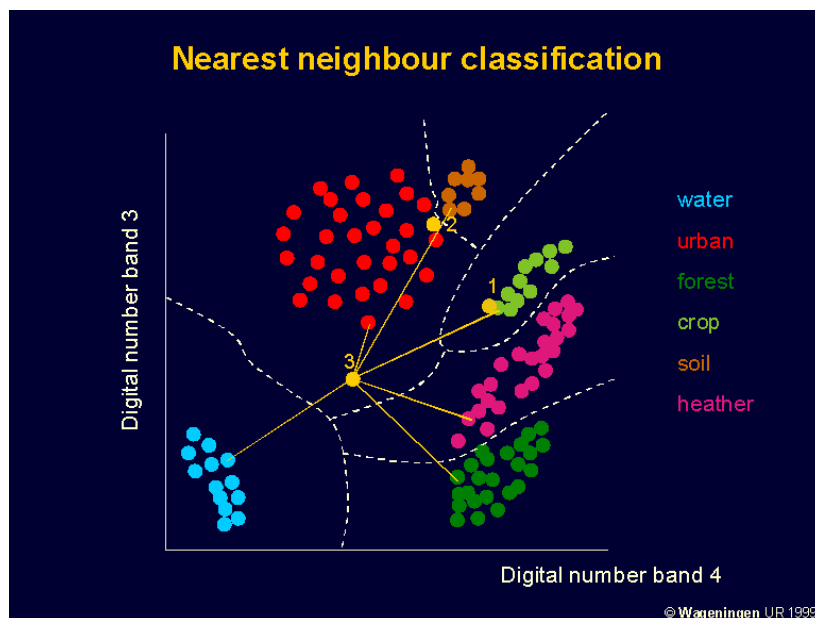


Fig. 30 Example of Minimum Distance Classifiers between spectral band 3 and 4. Source: Centre for Geo-information of Wageningen University and Research Centre, 1999

Minimum Distance algorithm calculates the Euclidean distance $d(x,y)$ between spectral signatures of image pixels and training spectral signatures, according to the following equation:

$$d(x, y) = \sqrt{\sum_{i=1}^n (x_i - y_i)^2}$$

where:

- x = spectral signature vector of an image pixel;
- y = spectral signature vector of a training area;

- n = number of image bands.

Therefore, the distance is calculated for every pixel in the image, assigning the class of the spectral signature that is closer, according to the following discriminant function (Richards and Jia, 2006):

$$x \in C_k \iff d(x, y_k) < d(x, y_j) \forall k \neq j$$

where:

- C_k = land cover class k ;
- y_k = spectral signature of class k ;
- y_j = spectral signature of class j .

It is possible to define a threshold T_i in order to exclude pixels below this value from the classification:

$$x \in C_k \iff d(x, y_k) < d(x, y_j) \forall k \neq j$$

and

$$d(x, y_k) < T_i$$

The result of the classification is a theme map directed to a specified database image channel. A theme map encodes each class with a unique level. The value used to encode a class is specified when the class signature is created.

In this project the two methods had been compared. It had been analysed the year 2002 and 2015 because are the furthest. It can see in the table 5, the algorithm of minimum distance had better results than Maximum Likelihood.

Table 5 The overall accuracy method and Kappa hat classification between two different algorithm of classification

Classification Method	Year	Overall Accuracy (%)	Kappa hat classification
Minimum Distance	2002	87.04	0.83
	2015	75.12	0.70
Maximum Likelihood	2002	83.27	0.78
	2015	73.95	0.67

4.1.2. Elaborating vegetation indices (NDVI)

The normalized difference vegetation index (NDVI) is an indicator of photosynthetic activity which measures the light reflected from vegetation; it was first used in 1974 by Rouse et al. from the Remote Sensing Centre of Texas A&M University (Rouse et al., 1974). In Fig. 31 it can observe the difference between NDVI in March and September in the same region. It uses the spectral bands of red and near-infrared, in the case of Landsat 7 corresponds to the bands 3

(R) and 4 (NIR) and Landsat 8 bands 4 (R) and 5 (NIR). NDVI served to ratify and improve the supervised classification of Minimum distance

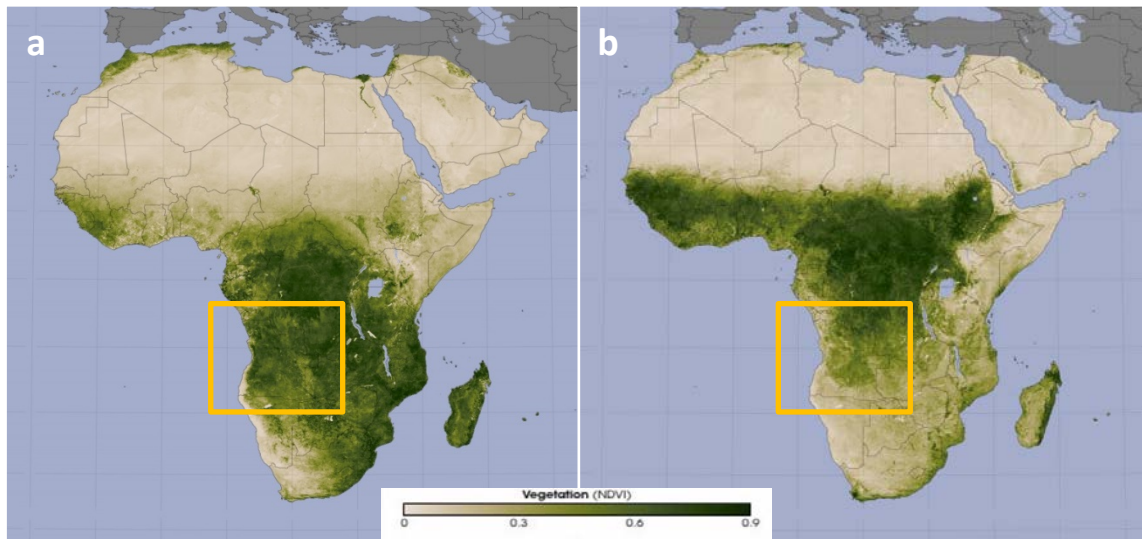


Fig. 31 Difference between NDVI index in March, 2004 (a) and September, 2004 (b) in Angola, Africa. (NASA, 2004)

NDVI is calculated on a per-pixel basis as the normalized difference between the red and near infrared bands from an image:

$$NDVI = \frac{NIR - RED}{NIR + RED}$$

Where NIR is the near infrared band value for a cell and RED is the red band value for the cell. NDVI can be calculated for any image that has a red and a near infrared band.

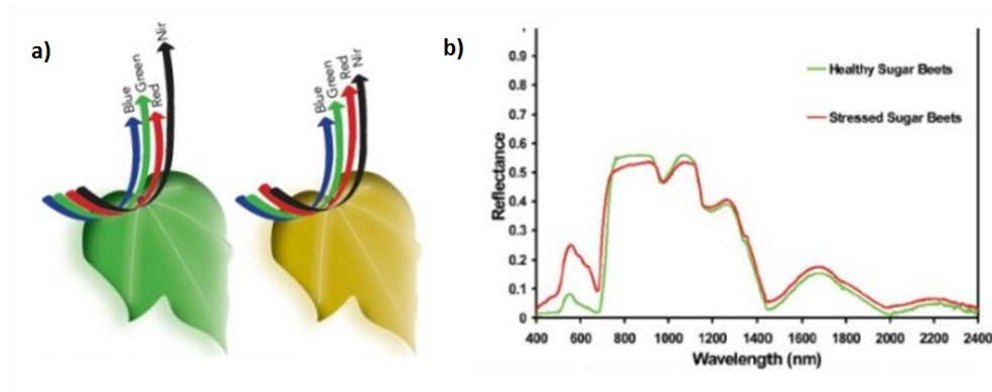


Fig. 32 a) Differences in reflected light between a healthy and unhealthy leaf and b) Change in spectral reflectance for a portion of the electromagnetic spectrum for healthy sugar beet plant and one under water stress

Vegetation with highest photosynthetic activity absorbs most of the visible light that hits it, and reflects a large portion of the near-infrared light. Unhealthy or sparse vegetation reflects more visible light and less near-infrared light. The spectral signatures on the Figure 32 are representative of vegetation values, but real vegetation is much more varied. (Jackson and Huete, 1991)

Finally, the data obtained by Minimum Distance algorithm was verified by comparing with the results obtained in the raster of NDVI. Figure 33 shows the differences of NDVI between the same area in forest or bare soil context. Thus, it checked that the results were very close to reality.

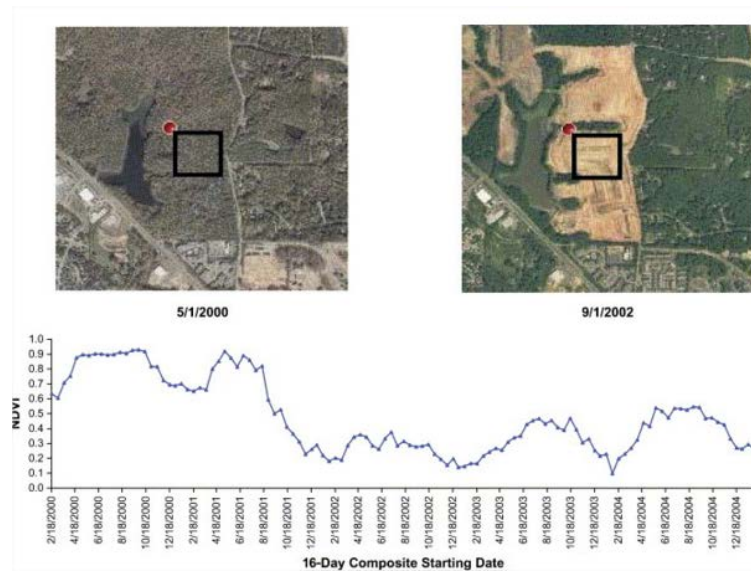


Fig. 33 Example about the difference between NDVI in forest and NDVI in bare soil in the same area

4.2. Results and discussion

4.2.1. Initial situation

The study begins checking the miombo situation in 2002 in the Huambo Province. In this year there were 2,596,536.09 ha of land covered by miombo woodland (a 78.41% of total Huambo surface). And for ending the study period has been checked the final situation in 2015. This year show 1,597,621.41 ha of land covered by miombo woodland. It means a 48.25% of the whole surface of Huambo Province in 2015 (Fig. 34). It can be observed a significant decrease in the surface covered by miombo woodlands. The results of the deforestation indicate that miombo forest in the Huambo Province (Angola) have been lost cover from 2002 to 2015. The main causes have been the primary necessities as heat, build houses or combustible as fuelwood, charcoal and agriculture. These will be described in detail later.

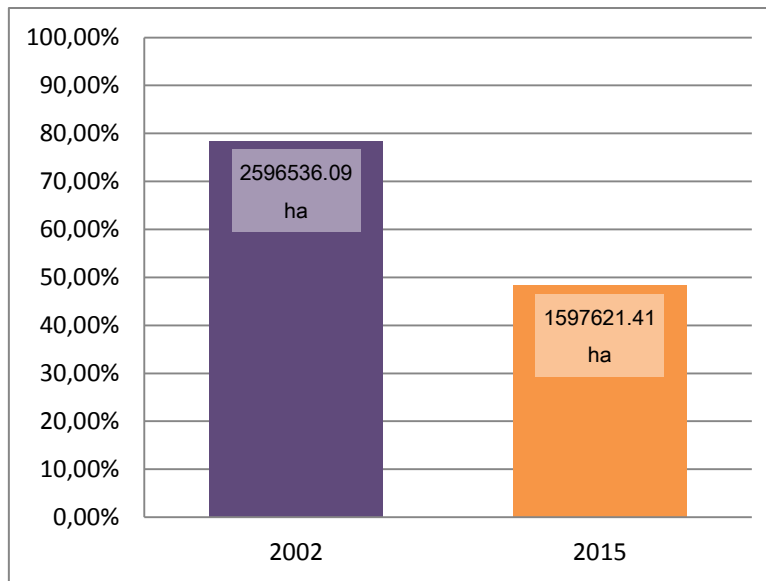


Fig. 34 Rate of miombo forest in Huambo province

4.2.2.Evaluation of cover change between 2002-2015

After checking the starting and ending situation (Annex VI. Land cover change (2002-2015)), is necessary to measure the deforestation process since 2002 to 2015 year by year. If evaluated the serial of year from 2002 to 2015 (Annex III. Evolution of cover of miombo between 2002-2015), these thirteen years shows that the current area of miombo forest has lost 48.74% of the initial surface; it is a 38.22% of the whole area of Huambo Province. Moreover, it gains 8.05% in the context of Huambo Province and the forest cover increases a 10.27%. In the other side, the miombo surface is unchanged in the 40.19% in the province of Huambo, means a 51.26% take into account the total miombo surface during the study years. (Table 6 and Figure 35)

Table 6 Percentage of gain, loss and no change of miombo forest in 2015

		Area (ha)	Area in Huambo province	Miombo cover changes between 2002-2015
Miombo forest 2015	Gain	266629.14	8.05%	10.27%
	Loss	1 265 543.82	38.22%	48.74%
	No change	1 330 992.27	40.19%	51.26%

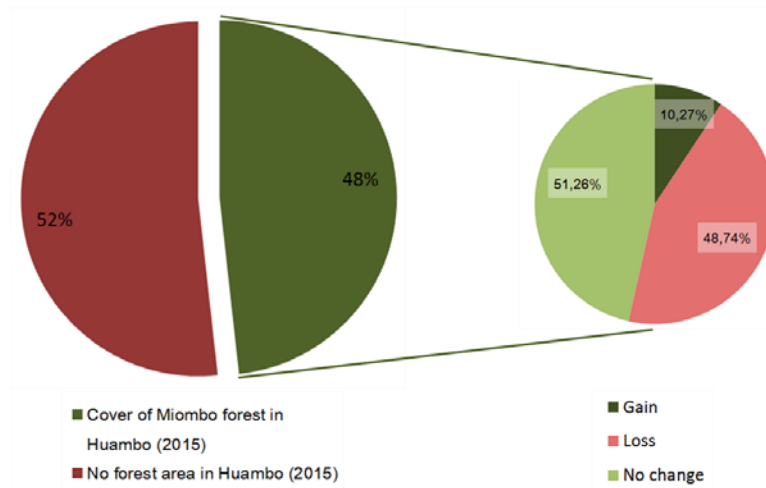


Fig. 35 Rate of Deforestation since 2002 on the context of Forest/No-forest land cover in the province of Huambo

The figure below (Fig 36) shows the distribution of deforestation since 2002 in the Huambo Province. The red colour area shows the largest loss of forest cover respect the other coloured areas in the Province. There are high concentration of deforestation in specific areas owing to the development of new sites and villages looking for forest areas to timber use and the increase of agriculture. Despite the high forest loss in some areas, the deforestation is homogeneous in whole province as it can see in the bottom part of the figure 36 (right map). The increase of forest cover is low and it is concentrated in the centre of the province.

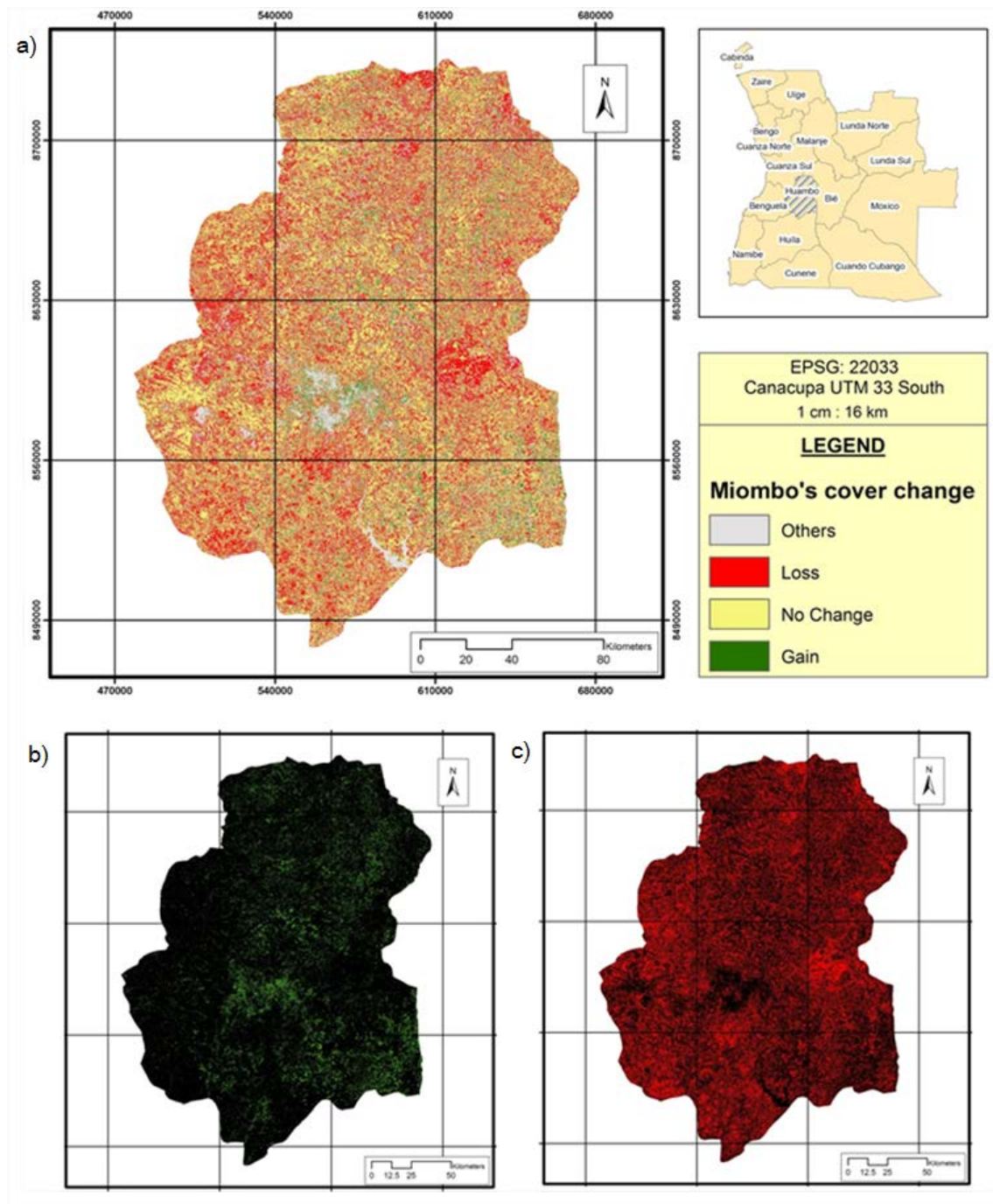


Fig. 36 a) Distribution of deforestation in Huambo (Angola), b) Detailed map of increased cover in miombo since 2002 c) Detailed map of miombo cover loss

Figures 37 and 38 show the evolution of deforestation through satellite images in the affected areas.

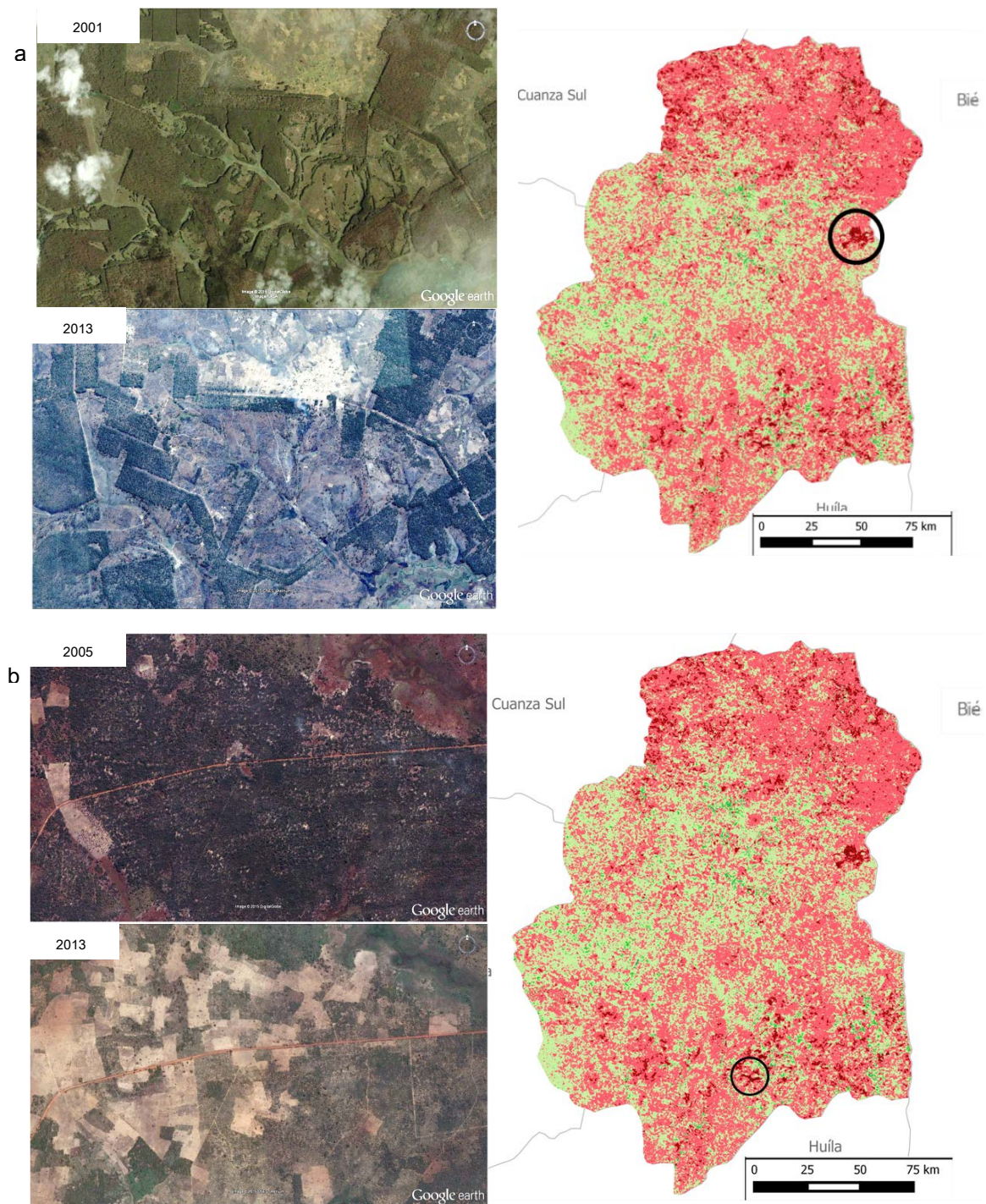


Fig. 37 Example of the most deforested area. a) Between 2001-2013, b) Between 2005-2013. Source: Google Earth

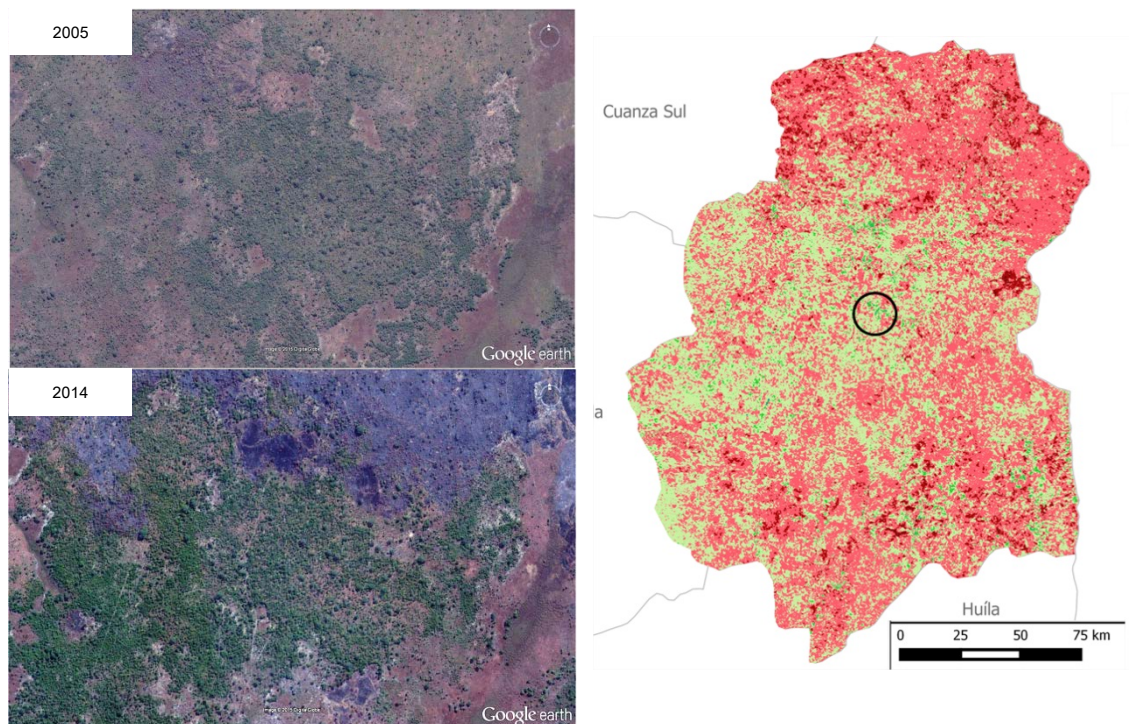


Fig. 38 Transformation from non-forest landcover to miombo cover, between 2005-2014. Source: Google Earth

4.2.3. Distribution of deforestation by type of landcover

A 1,532,172.96 ha of forest was altered, of which 266,629.14 ha have been changed from no-forest to miombo. Furthermore, 1,265,543.82 ha of miombo forest have been transformed to another land cover like agricultural or urban type through timber harvesting and/or the burning as explained above. The main transformation from miombo forest to another land cover is agricultural. It is equivalent to 63.24% from all of the deforestation types (Fig 39).

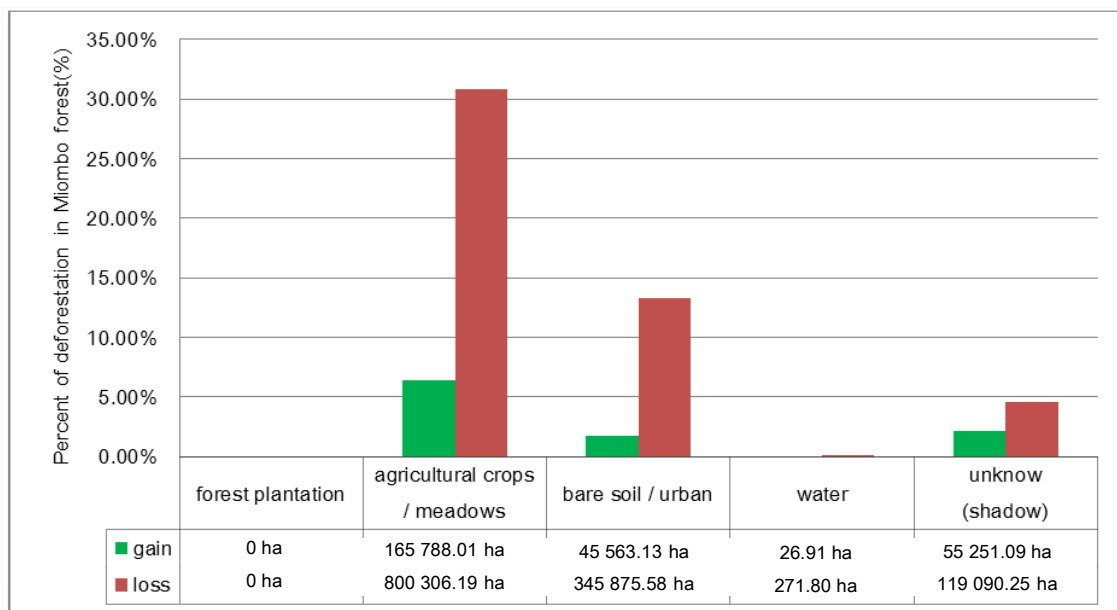


Fig. 39 Percentage of Gain/Loss miombo forest in Huambo Province from 2002

The second deforestation cause is the transformation to urban land because of new towns and the increase of some main cities. Also, some little village are abandoned because lack of timber resources, among others (categorized as bare soil).

In the table 8 it can see in detail how change the cover of miombo from 2002 to 2015.

Table 7 Detail of how it changed the landcover of miombo since 2002 to 2015

Land cover (2002)	Land cover (2015)	Area (ha)	Rate of gain/loss	Rate of Huambo province	Rate of miombo cover
Forest plantation	Miombo forest	0	0.00%	0.00%	0.00%
Agricultural crops / meadows		165,788.01	62.18%	5.01%	6.38%
Bare soil / urban		45,563.13	17.09%	1.38%	1.75%
Water		26.91	0.01%	0.00%	0.00%
Unknown (shadow)		55,251.09	20.72%	1.67%	2.13%
Total		266,629.14	100.00%	8.05%	10.27%
Miombo forest	Forest plantation	0	0.00%	0.00%	0.00%
	Agricultural crops / meadows	800,306.19	63.24%	24.17%	30.82%
	Bare soil / urban	345,875.58	27.33%	10.45%	13.32%
	Water	271.80	0.02%	0.01%	0.01%
	Unknown (shadow)	119,090.25	9.41%	3.60%	4.59%
Total		1,265,543.82	100.00%	38.22%	48.74%
Miombo forest	Miombo forest	1,330,992.27	100.00%	40.19%	51.26%

4.2.4. Distribution of deforestation by type of landcover and municipality

About the distribution by municipality, Figure 40 shows the percentage of miombo cover that has been gained and has been lost since 2002. The main affected zone is Bailundo, is the most deforested with 259,160.67 ha (10% loss in miombo cover since 2002) even if it is the most recovered with 64,988.73 ha (2.51% gain in miombo cover since 2002). Caala is a significant data because it is the only municipality that loss more miombo thought urban land cover than agricultural. Agriculture means the most change; a 792,204.3 ha have been lost in whole province since 2002 and only 165,455.82 ha have been recovered.

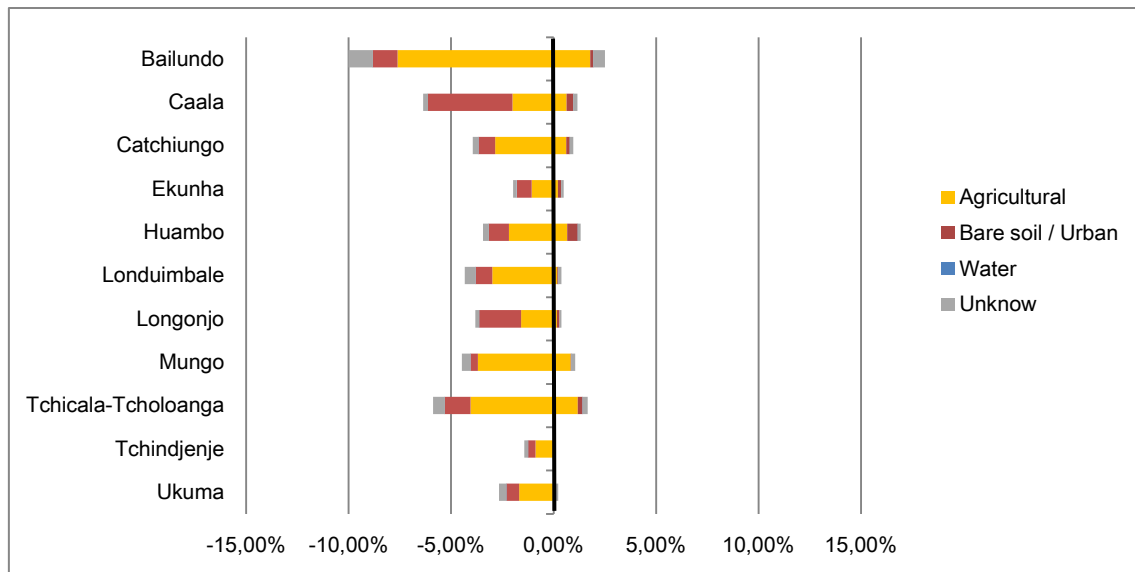


Fig. 40 Change of land cover from miombo to non-forest (percentage in negative) and change of land cover from non-forest to miombo (percentage in positive) since 2002

The background of the current cover miombo forest (Figure 41) is used to analyze the origin of the recovered miombo forest in each municipality.

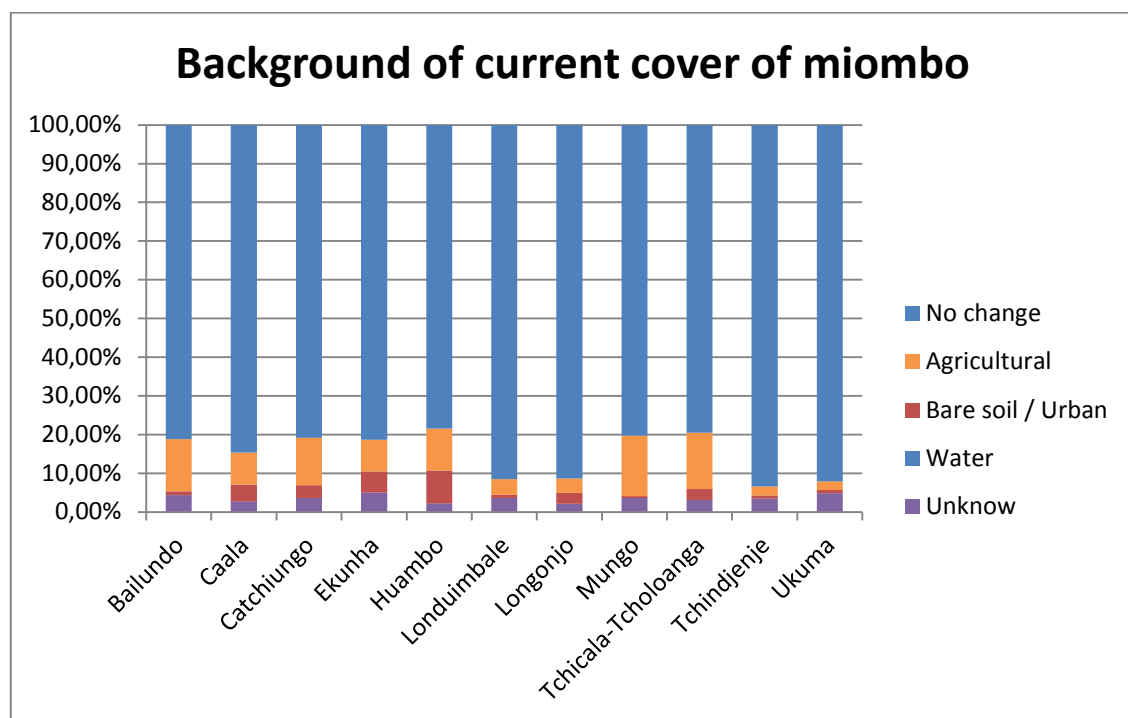


Fig. 41 Background of current cover of miombo by type of landcover and municipality

As shows Figure 41, in most cases, around of 80% of miombo cover by municipality in 2015 have not suffered changes. The main transformation from non-forest landcover to miombo is agriculture and the second is urban terrain. The municipalities that have had less change are Londuimbale and Longonjo. In the Figure 42 it can observe the real distribution in hectares.

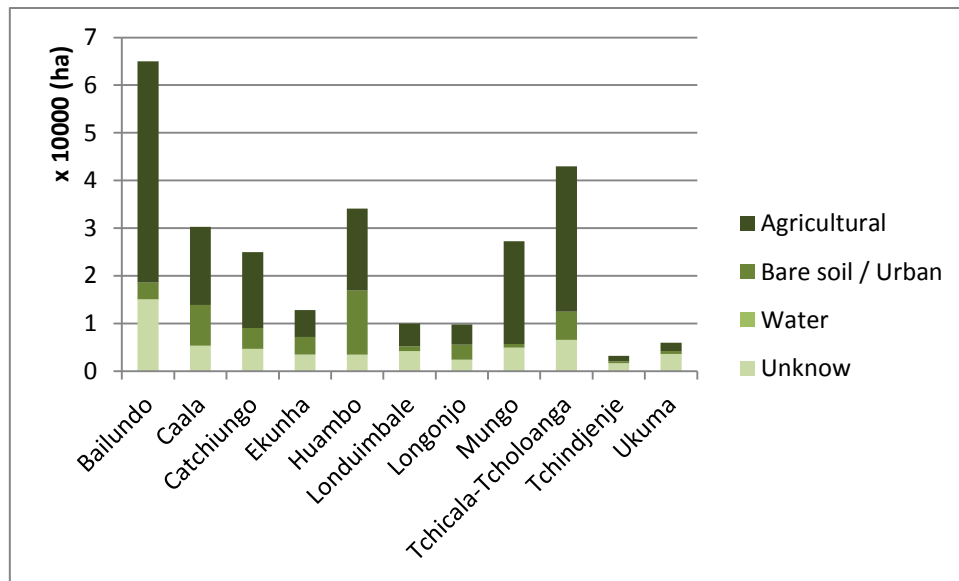


Fig. 42 Distribution of gain in miombo cover since 2002

In the deforestation context that Huambo Province are involve is necessary to highlight the miombo increment on the regional surface. As can see in Table 8, the high increment in miombo surface is Bailundo with a ratio of 24.41% respect the total miombo gain in Huambo Province and . The second municipality that increases the cover of miombo is Tchicala-Tcholoanga with 16.14%. The municipality with the lowest increase ratio is Tchindjenje.

It is necessary to stand out the date of the Transformation to agricultural to miombo in Bailundo. It is the most affected municipality by the deforestation, but has the highest rate of transformation from agricultural to miombo cover. It means that the fields in which have been an agricultural use, and was abandoned, are growing naturally miombo pioneer species. In the same way, in Huambo municipality are the highest transformation data from urban or bare soil to miombo forest. Tchindjenje, in general, it has the lowest transformation rates.

Table 8 a) Gain in cover of miombo between 2002 and 2015 in hectares, b) Rate of gain since 2002 c) Percentage of miombo cover in 2015

Municipality		Agricultural	Bare soil / Urban	Water	Unknown	Total
Bailundo	a	46441.53 ha	3433.14 ha	2.79 ha	15111.27 ha	64988.73 ha
	b	8.61%	0.64%	0.00%	2.80%	12.05%
	c	17.45%	1.29%	0.00%	5.68%	24.41%
Caala	a	16336.53 ha	8556.84 ha	6.12 ha	5343.3 ha	30242.79 ha
	b	4.92%	2.58%	0.00%	1.61%	9.10%
	c	6.14%	3.21%	0.00%	2.01%	11.36%
Catchiungo	a	15894.27 ha	4348.71 ha	2.25 ha	4683.69 ha	24928.92 ha
	b	7.65%	2.09%	0.00%	2.26%	12.00%

	c	5.97%	1.63%	0.00%	1.76%	9.36%
Ekunha	a	5643.9 ha	3755.52 ha	0 ha	3430.08 ha	12829.5 ha
	b	5.26%	3.50%	0.00%	3.20%	11.97%
	c	2.12%	1.41%	0.00%	1.29%	4.82%
Huambo	a	17171.19 ha	13442.49 ha	5.22 ha	3466.98 ha	34085.88 ha
	b	8.06%	6.31%	0.00%	1.63%	16.00%
	c	6.45%	5.05%	0.00%	1.30%	12.80%
Londumbale	a	4776.3 ha	996.39 ha	3.51 ha	4183.92 ha	9960.12 ha
	b	2.17%	0.45%	0.00%	1.90%	4.53%
	c	1.79%	0.37%	0.00%	1.57%	3.74%
Longonjo	a	4247.73 ha	3177 ha	0 ha	2381.76 ha	9806.49 ha
	b	2.10%	1.57%	0.00%	1.18%	4.84%
	c	1.60%	1.19%	0.00%	0.89%	3.68%
Mungo	a	21610.89 ha	728.91 ha	0.36 ha	4933.17 ha	27273.33 ha
	b	9.52%	0.32%	0.00%	2.17%	12.01%
	c	8.12%	0.27%	0.00%	1.85%	10.25%
Tchicala-Tcholoanga	a	30500.64 ha	5947.47 ha	4.77 ha	6517.62 ha	42970.5 ha
	b	9.55%	1.86%	0.00%	2.04%	13.46%
	c	11.46%	2.23%	0.00%	2.45%	16.14%
Tchindjenje	a	1126.35 ha	414.18 ha	0 ha	1648.08 ha	3188.61 ha
	b	1.37%	0.50%	0.00%	2.01%	3.88%
	c	0.42%	0.16%	0.00%	0.62%	1.20%
Ukuma	a	1706.49 ha	633.6 ha	0.09 ha	3591.18 ha	5931.36 ha
	b	1.24%	0.46%	0.00%	2.60%	4.30%
	c	0.64%	0.24%	0.00%	1.35%	2.23%
Province of Huambo	a	165455.82 ha	45434.25 ha	25.11 ha	55291.05 ha	266206.23 ha
	c	62.15%	17.07%	0.01%	20.77%	100%

Nevertheless in line with the study the next figure shows the distribution of loss in miombo cover by municipality and type of landcover (Fig. 41). Bailundo is the most affected municipality with 259,160.67 ha loss (20.70% of total loss as shows Table 9). The Second is Caala with 164,879.37 ha (13.17% of total loss) followed closely by Tchicala-Tcholoanga with 152,180.82 ha (12.15% of total loss).

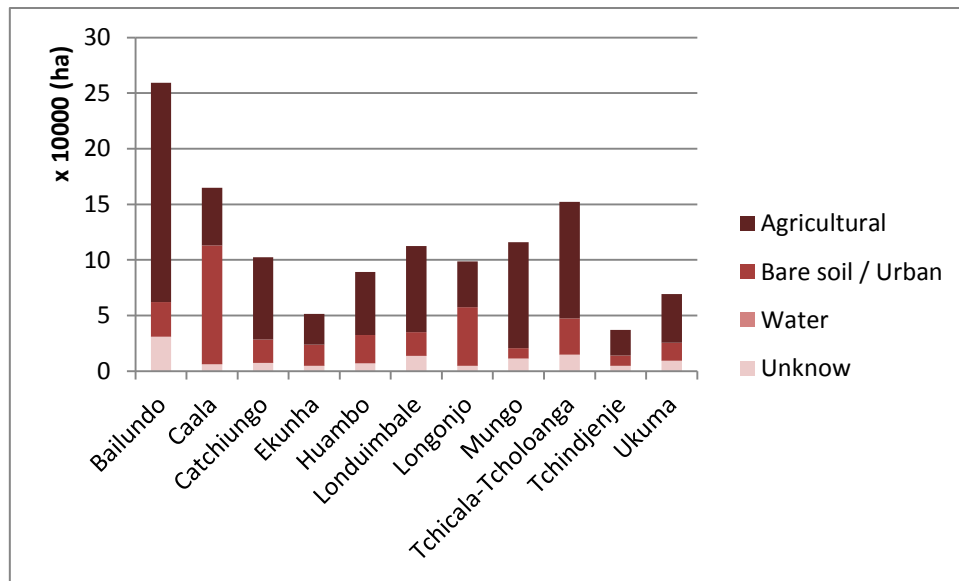


Fig. 43 Distribution in hectares the loss of miombo cover by municipality

The main change from miombo to non-forest landcover is agricultural terrain (792204.3 ha) for all municipalities except Caala. In Caala the main transformation is from miombo to urban terrain (106939.71 ha) with almost 70% of all loss in Caala as show figure 44. Longonjo proportions are similar as Caala.

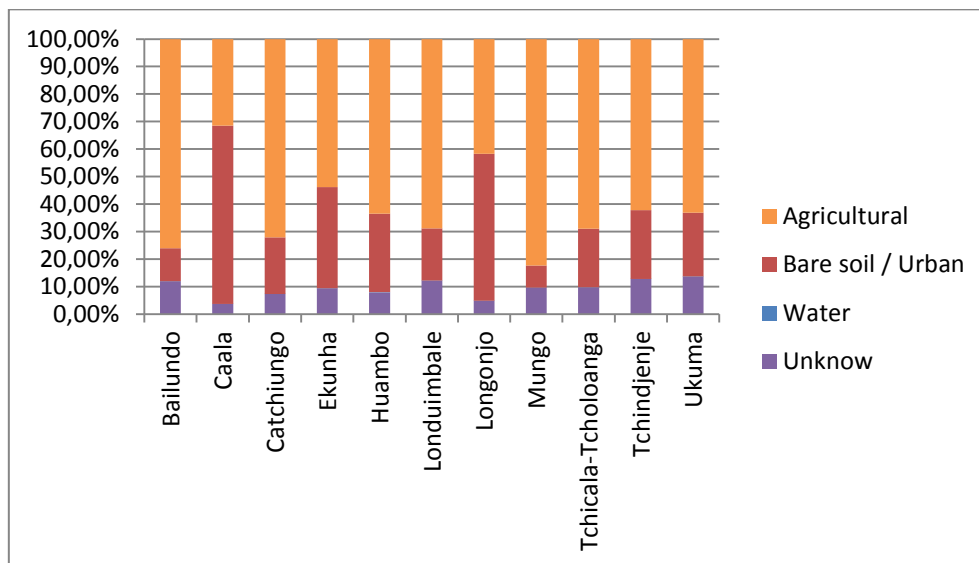


Fig. 44 Rate of loss in miombo cover by municipality

Table 9 shows the area of each type of landcover by municipality and the percentage of the miombo cover in 2002. The data present a high relation between the increments of the urban or bare soil areas, against the losses of miombo forest to agricultural. It can see in Caala municipality that have a high ratio in the bare soil/urban (32.19%) and a low ratio in agricultural (15.61%). This relationship maybe owing that the population in urban areas seeking other employment or supply sources. In Mungo municipality, have the opposite situation whit a high ratio in the agricultural causes (42.06%) and a low ratio in the bare soil/urban (4.08%). Rural

area and the dispersion of the population have been affecting more widely in the miombo woodland areas.

Table 9 a) Loss in cover of miombo between 2002 and 2015 in hectares, b) Rate of loss since 2002 c) Percentage of loss in miombo cover (2015)

Municipality		Agricultural	Bare soil / Urban	Water	Unknown	Total
Bailundo	a	197065.62 ha	31148.82 ha	35.1 ha	30911.13 ha	259160.67 ha
	b	36.55%	5.78%	0.01%	5.73%	48.07%
	c	15.74%	2.49%	0.00%	2.47%	20.70%
Caala	a	51841.17 ha	106939.71 ha	39.78 ha	6058.71 ha	164879.37 ha
	b	15.61%	32.19%	0.01%	1.82%	49.63%
	c	4.14%	8.54%	0.00%	0.48%	13.17%
Catchiungo	a	73770.84 ha	21028.05 ha	12.06 ha	7457.31 ha	102268.26 ha
	b	35.52%	10.12%	0.01%	3.59%	49.24%
	c	5.89%	1.68%	0.00%	0.60%	8.16%
Ekunha	a	27607.5 ha	18891.36 ha	3.6 ha	4814.73 ha	51317.19 ha
	b	25.75%	17.62%	0.00%	4.49%	47.87%
	c	2.21%	1.51%	0.00%	0.38%	4.10%
Huambo	a	56527.65 ha	25339.59 ha	108.72 ha	7015.05 ha	88991.01 ha
	b	26.53%	11.89%	0.05%	3.29%	41.77%
	c	4.52%	2.02%	0.01%	0.56%	7.11%
Londuibale	a	77239.44 ha	21391.38 ha	10.98 ha	13663.98 ha	112305.78 ha
	b	35.16%	9.74%	0.00%	6.22%	51.13%
	c	6.17%	1.71%	0.00%	1.09%	8.97%
Longonjo	a	41158.26 ha	52712.82 ha	0.9 ha	4784.58 ha	98656.56 ha
	b	20.32%	26.02%	0.00%	2.36%	48.70%
	c	3.29%	4.21%	0.00%	0.38%	7.88%
Mungo	a	95470.2 ha	9263.43 ha	9.54 ha	11233.44 ha	115976.61 ha
	b	42.06%	4.08%	0.00%	4.95%	51.09%
	c	7.63%	0.74%	0.00%	0.90%	9.26%
Tchicala-Tcholoanga	a	104916.24 ha	32435.55 ha	40.68 ha	14788.35 ha	152180.82 ha
	b	32.86%	10.16%	0.01%	4.63%	47.66%
	c	8.38%	2.59%	0.00%	1.18%	12.15%
Tchindjenje	a	23011.29 ha	9230.22 ha	3.69 ha	4745.79 ha	36990.99 ha
	b	28.03%	11.24%	0.00%	5.78%	45.06%
	c	1.84%	0.74%	0.00%	0.38%	2.95%

Ukuma	a	43596.09 ha	16033.95 ha	1.35 ha	9486.72 ha	69118.11 ha
	b	31.59%	11.62%	0.00%	6.88%	50.09%
	c	3.48%	1.28%	0.00%	0.76%	5.52%
Province of Huambo	a	792204.3 ha	344414.88 ha	266.4 ha	114959.79 ha	1251845.37 ha
	c	63.28%	27.51%	0.02%	9.18%	100%

5. Degradation study in Miombo forest of Huambo

The term degradation itself is ambiguous, not yet defined and far from being globally agreed. FAO (Hikojiro Katsuhisa and Peter Holmgren, 2005) define the forest degradation as “The reduction in the capacity of a forest to provide goods and services caused by human disturbances” (Fig. 45) or Article 3.4 of the Kyoto Protocol say that deforestation is “a direct human-induced long-term loss (persisting for X years or more) of at least Y % of forest carbon stocks (and forest values) since time T and not qualifying as deforestation or an elected activity under” (Grubb et al., 1999).

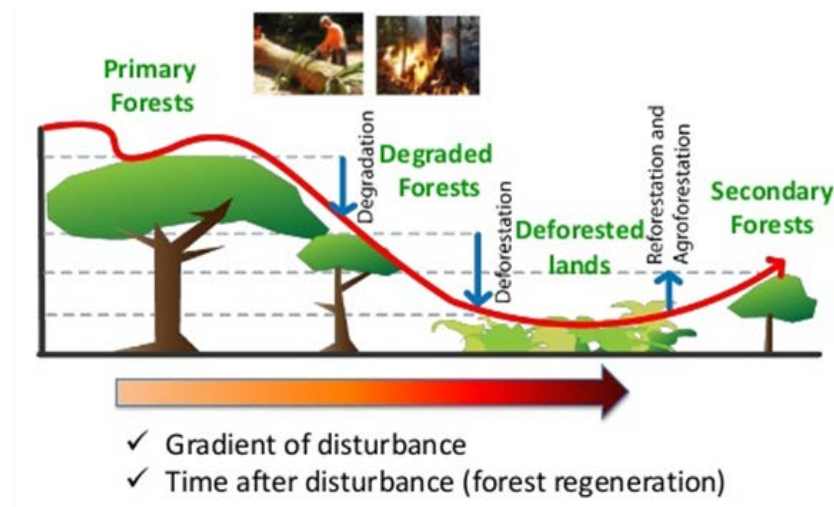


Fig. 45 Evolution of degraded forest. (P. Sist et al., 2015)

In strict degradation terms, it will only occur in a forest area if its rate of biomass loss is higher than the natural re-growth rate. As is well known, biomass assessment per se is an inaccurate and imprecise process unless very expensive, detailed inventory is conducted (Petrokofsky et al., 2012). Determining loss and re-growth rates is a complex task that requires long-term observations and intensive research which are not usually available in developing countries (Herold et al., 2011), or alternatively good statistical records (the “gain-loss” method).

Common degrading activities include it can show at figure 46 (GOFC-GOLD Project Office, Natural Resources Canada, 2009):



Fig. 46 Common degrading activities in forest

These activities vary greatly and render generalizations difficult (Murdiyarso et al., 2008). In percentage can observe in the figure 47

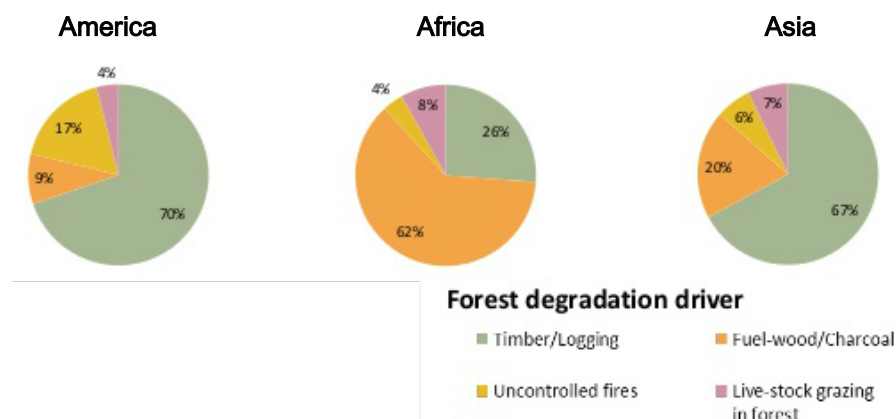


Fig. 47 Degradation drivers for each continent

Apart from selective logging, little analysis has been made of the impacts of these processes on the loss of forest biomass and the time needed for regrowth. Further, almost all studies have focused on tropical rainforest. However, degradation of dry forests by extraction of fuelwood for the extraction of basic survival (Fig. 48) is often more pronounced than by commercial timber harvesting (Skutsch and Trines 2008), and this is important since dry forests are generally more heavily populated than rainforest.



Fig. 48 Uses of miombo for the basic survival of the population

5.1. Methodology

The classification processes to obtain the results of deforestation in Miombo forest of Huambo follow the workflow (Fig 49):

1. Minimum Distance Classification
 - 1.1. Clip by mask of miombo cover
2. Quality control (some control points) and reclassification by NDVI
3. Obtain stages of degradation
 - 3.1. Generate cartography

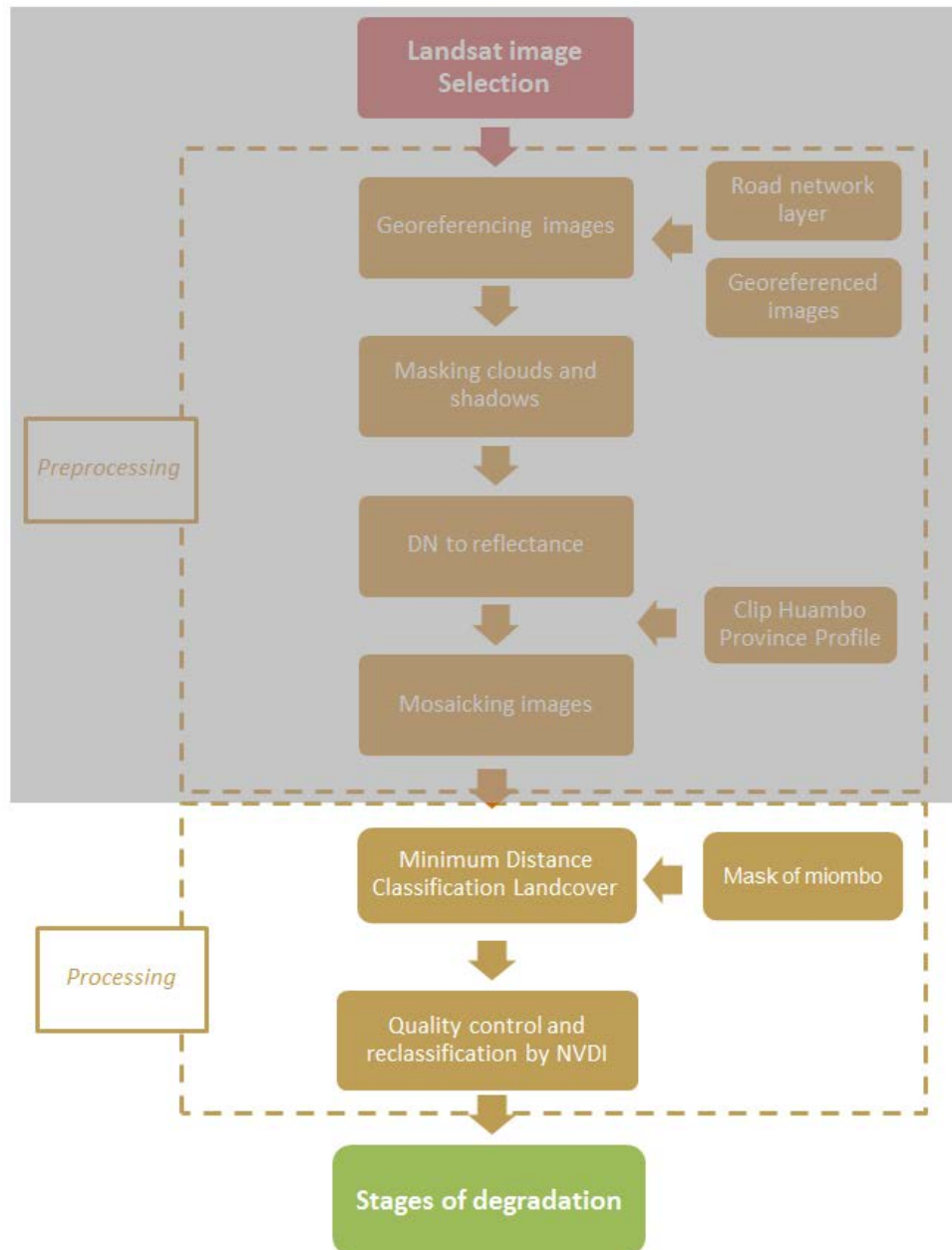


Fig. 49 Workflow of the degradation

5.1.1. Minimum Distance Classification Landcover

The first step to obtain the stages of degradation is to classify the landcover in 2015 in the province of Huambo. It keeping the previous procedure explained in 4.1.1. *Classifying the image mosaic with Minimum Distance algorithm*. It has been used the mask of Miombo forest to define the zone of interest in the Landcover of 2015.

5.1.2. Quality control and reclassification classification by NDVI

The second step was to classify the miombo according the stages of degradation. NDVI index have been used because localize the effects of degradation by passive remote sensing is quite difficult as show figure 50. Methods that detect and estimate the forest degradation usually are

uncertainty and prone to substantial confusion among classes due to differing classification thresholds. For example, severe forest degradation can be confused with intentional forest clearing in regional deforestation estimates [Cochrane, M.A., 1999] if forest damaging events are not accounted for in the classification process.

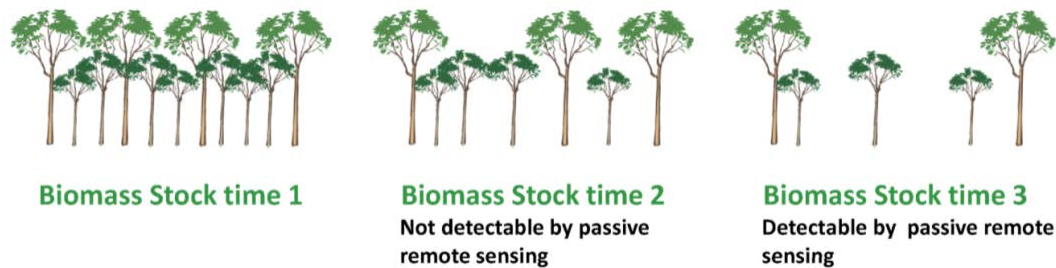


Fig. 50 Detect biomass by passive remote sensing

For this reason, it combines an index of vegetation (NDVI) with an analysis by observation and the results of landcover change that has been analysed in the chapter 4. *Deforestation study in Miombo forest of Huambo*. The process to calculate NDVI it has been explained thoroughly in 4.1.2. *Elaborating vegetation indices (NDVI)*.

Finally, different responses of miombo in NDVI had been studied. When the response was high, means that the forest of miombo was undegraded and when the response was low, there were a much degraded forest of miombo. It has been checked in some points in the area of study by satellite images.

5.2. Results and discussion

5.2.1. Initial situation

The cover of miombo in 2015 was 1,597,621.41 ha, a 48.25% in the province of Huambo (Fig. 51). This part of the study wants to analyse the situation of miombo forest currently and propose new ways to deal the degradation challenge.



Fig. 51 Miombo Woodlands. (A) Diversity of tree species; (B) Close up *Brachystegia bohemii*; (C) Regrowing area; (D) Recently burned area. Source: Tropical Research Institute, Portugal

5.2.2. Degradation in Huambo province

Degradation in Huambo's province had been analysed. Figure 52 shows the distribution of miombo NDVI. It would seem, at first sight, which the most part of the data are between 0.25 and 0.5 with the centre around 0.35. The NDVI range of miombo forest is between 0.2 and 1.

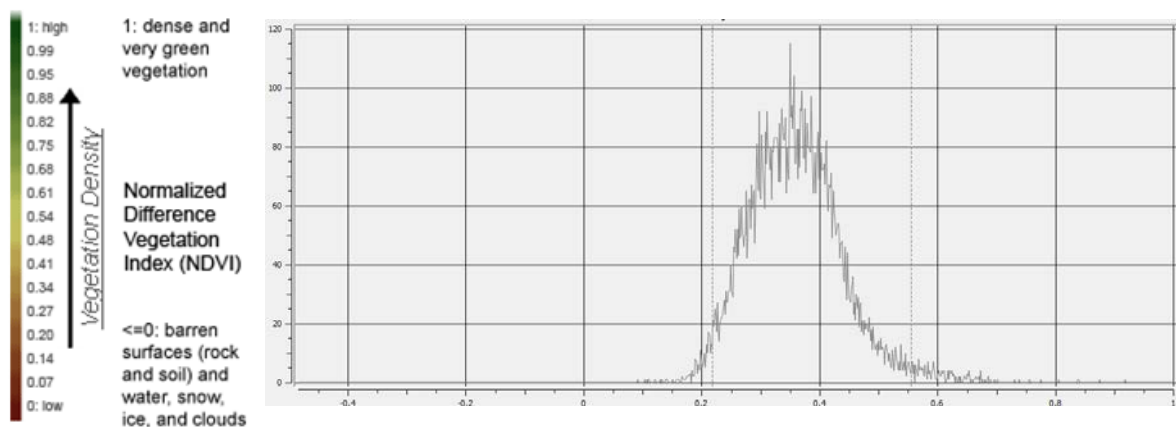


Fig. 52 Distribution of miombo NDVI

The results, as indicate in the figure 52, the major part of the forest of miombo is high degraded with 1,141,576.65 ha. This amounts to 72% of all miombo cover in 2015 as shows figure 53 (34.47% of whole Huambo's province area).

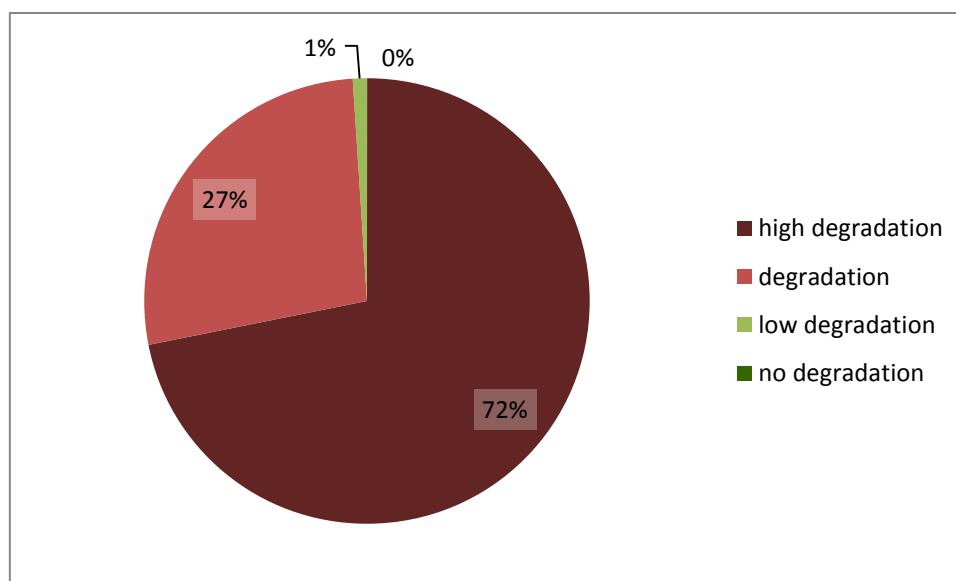


Fig. 53 Degradation's rate of miombo in 2015

Furthermore, only a 27% is degraded, 431,291.07 ha. One of the most important data is the little part of miombo that is classified as low degradation (15,978.06 ha).

It is highly remarkable; however, little of this data has undegraded forest (170.37 ha) in the whole miombo as shows table 10.

Table 10 Rate of miombo degradation

Type	Degradation	Rate of miombo cover	Rate of Huambo province
High Degradation	1141576.65 ha	71.84 %	34.47 %
Degradation	431291.07 ha	27.14 %	13.02 %
Low degradation	15978.06 ha	1.01 %	0.48 %
No degradation	170.37 ha	0.01 %	0.01 %

The map in the Figure 54 shows the distribution of degradation in the province of Huambo. High degradation and degradation are spread all over the province. There are small homogenous areas of low degradation located close to rivers or in the top of the hills.

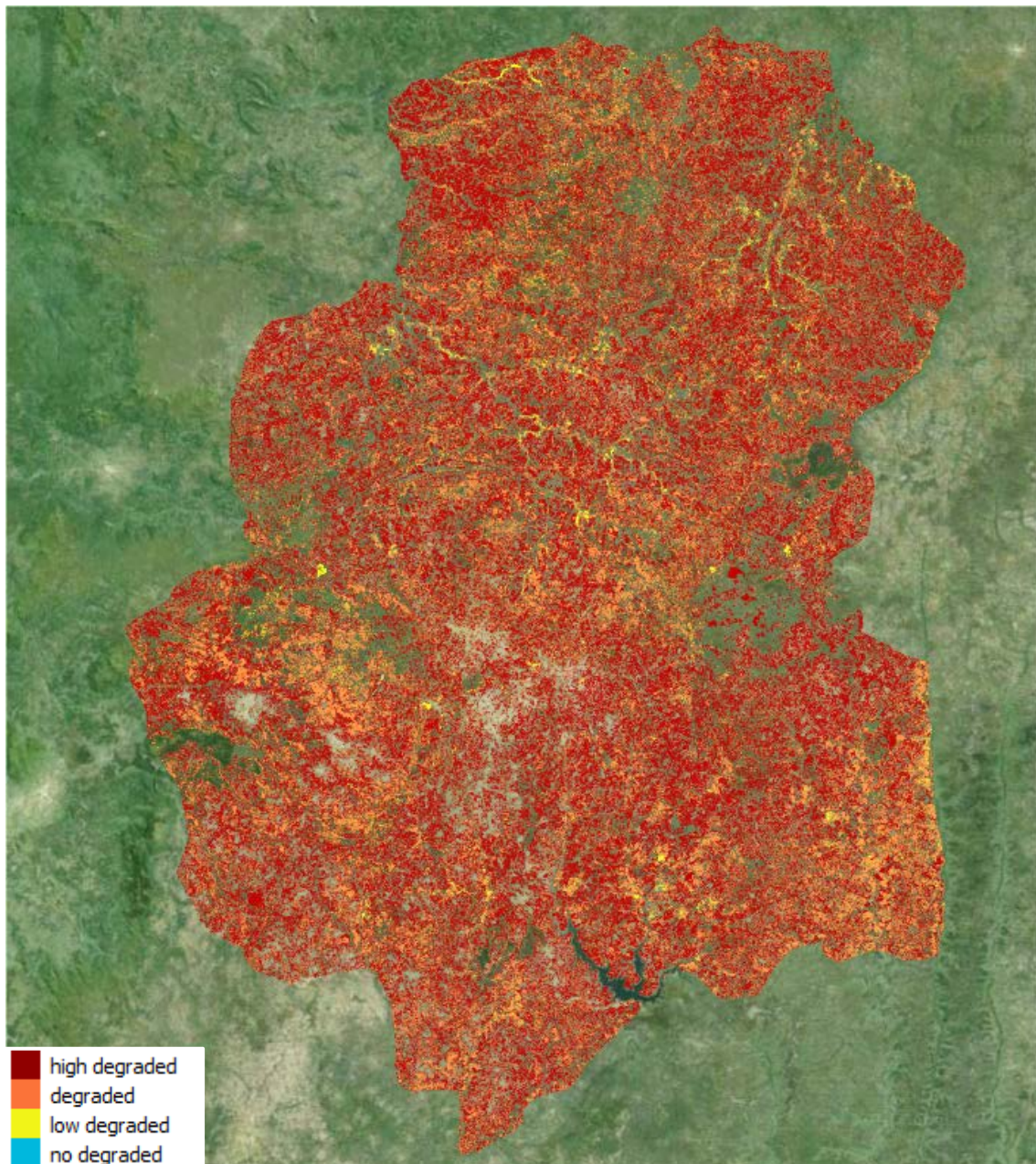


Fig. 54 Map of degradation in Huambo's Province

5.2.3. Degradation by municipality

If it analyses the degradation by municipality, the homogenous distribution of high degradation and degradation parameters are confirm as shows Figure 55.

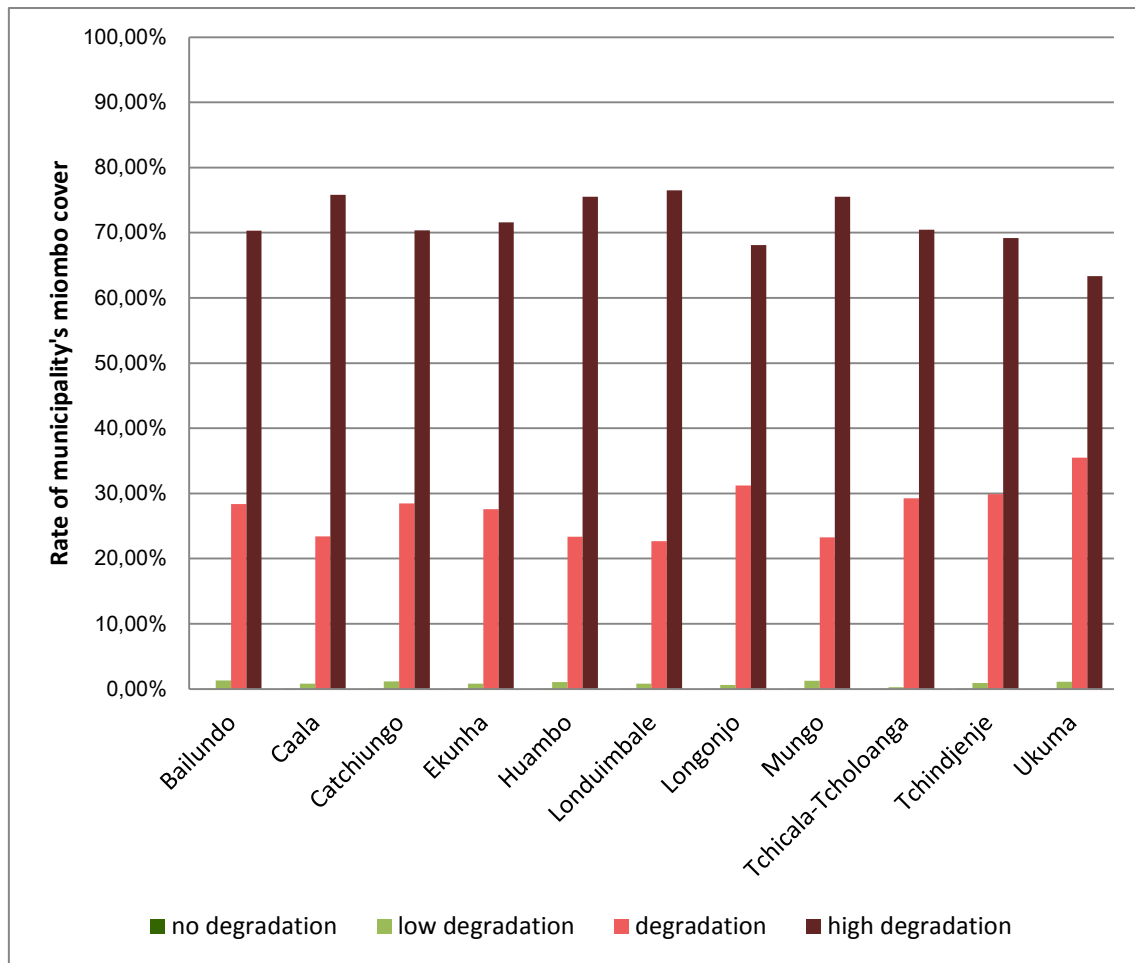


Fig. 55 Distribution of degradation by municipality.

All municipalities' cover of miombo are almost affected by the same percentage, around 70% is high degradation and between 20-30% is degradation. None of these achieves 1% of low and non-degradation. The Figure bellows (Fig. 56) shows the distribution of degradation in whole miombo cover by municipality. One of the most important data is the high degradation in Bailundo with 15.21% (241,672.77 ha) in opposition to no degradation data with only 30.33 ha.

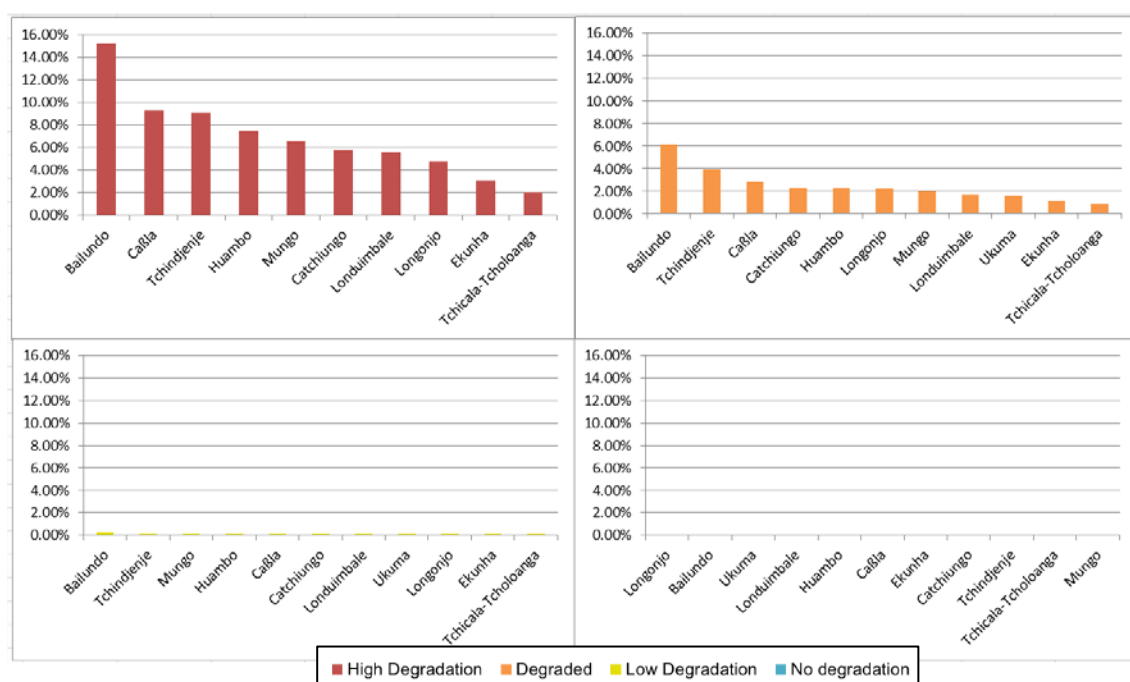


Fig. 56 Degradation by type and municipality in all miombo cover

Caála and Tchindjenje are the second most affected as it can see in table 11 with 147,716.19 ha and 144,519.03 ha, respectively. Less degraded municipality is Tchicala-Tcholoanga with 33,161.94 ha.

Table 11 Data of degradation by municipality and percentage in miombo cover and the province of Huambo

Category	Area	Municipality	Area (ha)	Rate of miombo cover	Rate of Huambo province
High Degradation	1141576.65 ha	Bailundo	241672.77	15.21%	7.30%
		<i>Caála</i>	<i>147716.19</i>	<i>9.30%</i>	<i>4.46%</i>
		Tchindjenje	144519.03	9.09%	4.36%
		Huambo	118155.96	7.44%	3.57%
		Mungo	104164.02	6.56%	3.15%
		Catchiungo	91231.38	5.74%	2.76%
		Londuimbale	88788.6	5.59%	2.68%
		Longonjo	76637.97	4.82%	2.31%
		Ekunha	48749.31	3.07%	1.47%
		Tchicala-Tcholoanga	33161.94	2.09%	1.00%
Degraded	431291.07 ha	Bailundo	97459.74	6.13%	2.94%
		<i>Tchindjenje</i>	<i>62495.19</i>	<i>3.93%</i>	<i>1.89%</i>
		Caála	45595.71	2.87%	1.38%
		Catchiungo	36914.49	2.32%	1.11%
		Huambo	36555.84	2.30%	1.10%
		Longonjo	35133.3	2.21%	1.06%
		Mungo	32048.19	2.02%	0.97%
		Londuimbale	26309.79	1.66%	0.79%

		Ukuma	26207.37	1.65%	0.79%
		Ekunha	18793.35	1.18%	0.57%
		Tchicala-Tcholoanga	13778.1	0.87%	0.42%
Low Degradation	15978.06 ha	Bailundo	4487.94	0.28%	0.14%
		<i>Tchindjenje</i>	<i>1935.63</i>	<i>0.12%</i>	<i>0.06%</i>
		Mungo	1707.75	0.11%	0.05%
		Huambo	1679.58	0.11%	0.05%
		Caala	1550.79	0.10%	0.05%
		Catchiungo	1490.4	0.09%	0.05%
		Londuibale	953.28	0.06%	0.03%
		Ukuma	835.92	0.05%	0.03%
		Longonjo	672.3	0.04%	0.02%
		Ekunha	543.6	0.03%	0.02%
		Tchicala-Tcholoanga	120.87	0.01%	0.00%
		Longonjo	56.52	0.00%	0.00%
		<i>Bailundo</i>	<i>30.33</i>	<i>0.00%</i>	<i>0.00%</i>
		Ukuma	16.2	0.00%	0.00%
No degradation	170.37 ha	Londuibale	15.93	0.00%	0.00%
		Huambo	12.96	0.00%	0.00%
		Caala	11.79	0.00%	0.00%
		Ekunha	9.63	0.00%	0.00%
		Catchiungo	8.73	0.00%	0.00%
		Tchindjenje	6.57	0.00%	0.00%
		Tchicala-Tcholoanga	0.99	0.00%	0.00%
		Mungo	0.72	0.00%	0.00%

6. Conclusion

Based on the results, the main conclusions of the study are presented below:

Results of the deforestation study indicate that the miombo forest in Huambo Province have been the loss of coverage of 48.74% between 2002 and 2015. From 2,596,536.09 ha in 2002 to 1,597,621.41 ha, a percentage of 78.41% of whole surface of Huambo fall down to 48.25%. Basic needs, fuelwood and charcoal transformation and agricultural border progress can be mentioned as causes.

With a deep analysis, we can observed that in the thirteen last years, 40.19% the miombo surface is unchanged, while 38.22% surface was lost and only 8.05% of surface is changed from another vegetation formations to miombo forest.

The distribution of deforestation in the province of Huambo is homogeneous. The most of the concentration of deforestation is localized in specific areas with high development of urban centres, or timber and agricultural areas, while the little increase of forest cover areas is concentrated in the centre of the province.

Studying the distribution of deforestation by type of land cover, 1,265,543.82 ha of miombo forest have been transformed to another land cover, principally to agricultural use (63.24% from deforestation area). Only 266,629.14 ha have been changed to miombo forest surface.

Bailundo is the municipality with most change rate. From 2002 to 2015, 259,160.67 ha were lost for deforestation. However 64,988.73 ha were transformed from another landcover to miombo forest, caused by colonisation of miombo pioneer species.

In relation to the gain of miombo surface, Bailundo has the highest rate of transformation from agricultural to miombo cover while Huambo has the highest transformation rate from urban or bare soil to miombo forest. Tchindjenje is the municipality with the lowest transformation rates.

The transformation of miombo is, first of all from forest surface to agricultural areas and then to urban surfaces. In most of municipalities, miombo has become to cover agricultural land except in Caala and Longonjo, where the transformation has been to bare or urban soil.

In general, exist a high relation between the increments of the urban or bare soil areas, against the losses of miombo forest to agricultural. Caala is the best example of this situation with a high ratio of bare soil/urban (32.19%) and a low ratio in agricultural (15.61%). In the opposite side, Mungo has a high ratio in the agricultural gain (42.06%) and a low ratio in the bare soil/urban (4.08%).

From study of NDVI index of miombo, can be observed that, from 1,597,621.41 ha of miombo forest present in 2015, 1,141,576.65 ha (72%) are highly degraded (about 34.47% of whole Huambo's province area). Only a 1% of the surface is low degraded followed by 27%

considered degraded. The surface non-degraded is practically non-existent (170.37 ha of whole surface).

The distribution of degradation is homogenous throughout the province: the miombo surface of all municipalities is similarly affected, with rates around 70% of high degradation and between 20-30% of degradation.

Bailundo is the province with the most rate of his surface highly degraded (15.21%) and Tchicala-Tcholoanga have got “the best rates” (2.09%).

7. Bibliography

- Ahmad, A., Quegan, S., 2012. Analysis of Maximum Likelihood classification technique on Landsat 5 TM satellite data of tropical land covers, in: 2012 IEEE International Conference on Control System, Computing and Engineering (ICCSCE). Presented at the 2012 IEEE International Conference on Control System, Computing and Engineering (ICCSCE), pp. 280–285. doi:10.1109/ICCSCE.2012.6487156
- Akinnifesi F.K., Kwesiga F., Mhango J., Chilanga T., Mkonda A., Kadu C.A.C., Kadzere I., Mithofer D., Saka J.D.K., Sileshi G., Ramadhani T., Dhliwayo P. 2006. Towards the development of miombo fruit trees as commercial tree crops in southern Africa. *Forests, Trees and Livelihoods* 16: 103–121.
- Al-Ahmadi, F., Hames, A., 2009. Comparison of Four Classification Methods to Extract Land Use and Land Cover from Raw Satellite Images for Some Remote Arid Areas, Kingdom of Saudi Arabia. *J. King Abdulaziz Univ.-Earth Sci.* 20, 167–191. doi:10.4197/Ear.20-1.9
- Aldrich, R.C., 1975. Detecting disturbances in a forest environment. [ERTS land use surveys. Photogramm. Eng. Remote Sens.
- Arnold, J.E.M. & Dewees, P.A. (eds). 1995. *Tree management in farmers strategies*. Oxford University press, Oxford. 287 pp.
- Backéus, I.; Petterson, B.; Stromquist, L. & Ruffo, C. 2006. Tree Communities And Structural Dynamics In Miombo (*Brachystegia-Julbernardia*) Woodland, Tanzania. In: *Forest Ecology Management*. N° 230. pp 171–178.
- Banda, T.; Schwartz, M. W. & Caro, T. 2006. Woody Vegetation Structure And Composition Along a Protection Gradient In a Miombo Ecosystem Of Western Tanzania. In: *Forest Ecology and Management*. N° 230. pp 179–185.
- Cabral A. I. R., Vasconcelos M. J., Oom D., & Sardinha R. 2009. Deforestation or regrowth? A quantification of forest extension in the Miombo of Angola for the period 1990–2000.
- Cabral A.I.R., Vasconcelos M.J., Oom D., Sardinha R.. 2010. Spatial dynamics and quantification of deforestation in the central-plateau woodlands of Angola (1990-2009). *Applied Geography* 31 (2010) 1185-1193.
- Campbell B. 1996. *The Miombo in Transition: Woodlands and Welfare in Africa*. Center for International Forestry Research (CIFOR)
- Campbell B. M., Angelsen A., Cunningham A., Katerere Y., Siteo A., & Wunder S. 2007. *Miombo woodlands—opportunities and barriers to sustainable forest management*. CIFOR.

- Campbell B.M., Jeffrey S., Luckert M., Mutamba M., and Zindi C. 2002. "Household Livelihoods in Semi-Arid Regions: Options and Constraints." Bogor, Indonesia: CIFOR.
- Chidumayo E. N. 2002 Changes in miombo woodland structure under different land tenure and use systems in central Zambia. *Journal of Biogeography*. 29, Issue 12 Pages 1619–1626.
- Chidumayo, E. N. 1987a. A Shifting Cultivation Land Use System Under Population Pressure In Zambia. In: AGROFOR. Syst. Nº 5, pp 15–25.
- Chidumayo, E.N. 1987b. Woodland structure, destruction and conservation in the copperbelt area of Zambia. *Biological Conservation* 40, 89-100.
- Climate Change Knowledge Portal. http://sdwebx.worldbank.org/climateportal/index.cfm?page=country_historical_climate&ThisRegion=Africa&ThisCCode=AGO. Review in November of 2015.
- Cochrane, M.A.; Alencar, A.; Schulze, M.D.; Souza, C.M.; Nepstad, D.C.; Lefebvre, P.; Davidson, E.A. Positive feedbacks in the fire dynamic of closed canopy tropical forests. *Science* 1999, 284, 1832–1835.
- COLWELL, J. E., and WEBER, F. P., 1981, Forest change detection. *Proceedings of the 15th International Symposium on Remote Sensing of Environment held in Ann Arbor in 1981* (Ann Arbor, Michigan: Environmental Research Institute of Michigan), pp. 839-852.
- Davies, G.M., Pollard, L., Mwenda M. D. 2010. Perceptions of land-degradation, forest restoration and fire management: a case study from Malawi. *Land Degrad. Develop.* 21: 546–556.
- Dean, W.R.J. 2000. *The Birds of Angola: An annotated checklist*. BOU Checklist No. 18. British Ornithologists' Union, Herts, U.K.
- Delgado-Matas, C., Pukkala T. 2011. Growth and yield of nine pine species in Angola. *Journal of Forestry Research*, 23(2): 197–204.
- Desanker, P. V., Prentice, I. C. 1994. Miombo - A vegetation dynamics model for the Miombo woodlands of Zambezi Africa. *Forest Ecology and Management* 69: 87–95.
- Deweese, P., B. Campbell, Y. Katerere, A. Siteo, A.B. Cunningham, A. Angelsen and S. Wunder. 2011. *Managing the Miombo Woodlands of Southern Africa: Policies, incentives, and options for the rural poor*. Washington DC: Program on Forests (PROFOR).
- Dovala Luísa F. L. 2015. Estrutura e resposta da regeneração e sua resposta à humidade e densidade da copa de uma população de Miombo, na reserva Brito Teixeira, Chianga, Huambo, Angola. Tesis de Licenciatura en Ingeniería Forestal. 91 pp.

- Frost, P. 1996. The Ecology Of Miombo Woodlands. in: Campbell, B.(ED.), The Miombo In Transition: Woodlands And Welfare In Africa. CIFOR. Bogor. pp. 11–55.
- GOFC-GOLD Project Office, Natural Resources Canada, 2009. Reducing Greenhouse Gas Emissions from Deforestation and Degradation in Developing Countries: a Sourcebook of Methods and Procedures for Monitoring, Measuring and Reporting. GOFC-GOLD Project Office, Natural Resources Canada.
- Grubb, M., Vrolijk, C., Brack, D., 1999. The Kyoto Protocol. A guide and assessment.
- Herold, M., Román-Cuesta, R., Mollicone, D., Hirata, Y., Van Laake, P., Asner, G.P., Souza, C., Skutsch, M., Avitabile, V., MacDicken, K., 2011. Options for monitoring and estimating historical carbon emissions from forest degradation in the context of REDD+. Carbon Balance Manag. 6, 13. doi:10.1186/1750-0680-6-13
- Hikojiro Katsuhisa, Peter Holmgren, 2005. Third Expert Meeting on Harmonizing Forest-related Definitions for Use by Various Stakeholders.
- Hyde WF, Köhlin G. 2000. Social forestry reconsidered. Silva Fennica 34: 285–314.
- Stocker, T.F., D. Qin, G.-K. Plattner, M. Tignor, S.K. Allen, J. Boschung, A. Nauels, Y. Xia, V. Bex y P.M. Midgley (eds.). Resumen para responsables de políticas. En: Cambio Climático 2013: Bases físicas. Contribución del Grupo de trabajo I al Quinto Informe de Evaluación del Grupo Intergubernamental de Expertos sobre el Cambio Climático” . Cambridge University Press, Cambridge, Reino Unido y Nueva York, NY, Estados Unidos de América. IPCC, 2013.
- Jackson, R.D., Huete, A.R., 1991. Interpreting vegetation indices. Prev. Vet. Med. 11, 185–200. doi:10.1016/S0167-5877(05)80004-2
- Lillesand, T.M., Kiefer, R.W., 1979. Remote Sensing and Image Interpretation. Wiley.
- Lowore J. 2006. Miombo woodlands and rural livelihoods in Malawi. Center for International Forestry Research: Bogor, Indonesia.
- Lund, G., 1983. Lund, H. Gyde. 1983. In: Bell, John F.; Atterbury, Toby, eds. Renewable resource inventories for monitoring changes and trends. Proceedings; 15-19 August 1983; Corvallis, OR. SAF 83-14. Corvallis, OR: Oregon State University; 211-213. <http://home.comcast.net/~gyde/1983change.doc> .
- Luoga E. J. 2002. Harvested and standing wood stocks in protected and communal miombo woodlands of eastern Tanzania Volume 164, Issues 1–3, Pages 15–30.

- Malimbwi, R. E.; Solberg, B. & Luoga, E. 1994. Estimation Of Biomass And Volume In Miombo Woodland At Kitulungalo Forest Reserve, Tanzania. In: Journal of Tropical Forest Science. Nº 7. Vol. 2.
- Ministério de Agricultura e do Desenvolvimento Rural. 2009. Estrategia Nacional de Segurança Alimentar.
- Ministério de Agricultura e do Desenvolvimento Rural. 2009. Política Nacional de Florestas, Fauna Selvagem e Áreas de Conservação.
- Moges, A., Holden NM. 2007. Farmers' perceptions of soil erosion and soil fertility loss in southern Ethiopia. *Land Degradation & Development* 18: 543–554.
- Murdiyarso, D., Skutsch, M.M., Guariguata, M., Kanninen, M., Luttrell, C., Verweij, P.A., Stella, O., 2008. Measuring and monitoring forest degradation for REDD : implications of country circumstances. *Tijdschr. Tijdel. Onbekend* 16.
- Ngangula Cassiva Augusto. 2015. Caracterização morfológica de algumas espécies nativas do Miombo angolano presentes nos municípios de Wako-Kungo, província de Kwanza Sul e Huambo, província do Huambo e elaboração de uma ferramenta digital de apoio para a identificação destas espécies. Tesis de Licenciatura em Ingeniería Forestal. 58 pp.
- P. Sist, J. Chave, E. Rutishauser, 2015. Tropical Forest Degradation in the context of climate change: increas.... Cirad, CNRS, CarboFor-Expert, Montpellier.
- Pérez, F. C. y Sicard, T. E. L. 2003. Modelo conceptual del papel ecológico de la hormiga arriera (*atta laevigata*) en los ecosistemas de sabana estacional (vichada, colombia). *Caldasia* 25: 403-417.
- Ribeiro, N.; Siteo, A. A. ; Guedes, B. S. & Staiss, C. 2002. Manual de Silvicultura Tropical. Publicado com apoio da FAO, Projecto GCP/Moz/056/Net. 123 pp.
- Richards, J. A. & Jia, X., 2006. Remote Sensing Digital Image Analysis: An Introduction. Berlin, Germany: Springer
- Rouse, J.W., Jr., Haas, R.H., Schell, J.A., Deering, D.W., 1974. Monitoring Vegetation Systems in the Great Plains with Ert. *NASA Spec. Publ.* 351, 309.
- Sanfilippo, M. 2013. Trinta Árvores E Arbustos Do Miombo Angolano. Guia de campo para a identificação. 76 pp.
- Sayer, J. & Campbell, B.M. 2004. The science of sustainable development: local livelihoods and the global environment. Cambridge University Press, Cambridge. 268 pp.

- Shackleton C.M., Clarke J.M. 2007. Research and Management of Miombo Woodlands for Products in Support of Local Livelihoods. Genesis Analytcs.
- Skutsch, M. and Trines, E. 2008 Operationalising reduced degradation within REDD.
[http://www. communitycarbonforestry.org](http://www.communitycarbonforestry.org)
- The Worldwide Reference System « Landsat Science, n.d.
- Wacker, A., Landgrebe, D., 1972. Minimum Distance Classification in Remote Sensing. LARS Tech. Rep.
- Walker SM, Desanker PV. 2004. The impact of land use on soil carbon in Miombo woodlands of Malawi. *Forest Ecology and Management* 203: 345–360.
- WFP/VAM. (2005). Food security and livelihoods survey in the central highland of rural Angola. World Food Programme report.
- White, F. 1983. The vegetation of Africa, a descriptive memoir to accompany the UNESCO/AETFAT/UNSO Vegetation Map of Africa (3 Plates, Northwestern Africa, Northeastern Africa, and Southern Africa). 1:5,000,000. UNESCO. Paris.
- Woodward, W.A., Parr, W.C., Schucany, W.R., Lindsey, H., 1984. A Comparison of Minimum Distance and Maximum Likelihood Estimation of a Mixture Proportion. *J. Am. Stat. Assoc.* 79, 590–598. doi:10.2307/2288405

Annexes

Table of contents

Annex I.....	73
Annex II. Remote Sensing.....	74
MODIS 74	
LANDSAT 7 ETM +	79
LANDSAT 8 OLI	81
Annex III. Evolution of miombo cover between 2002-2015.....	85
Annex IV. Land cover change 2002 and 2015.....	169
Annex V. Deforestation between 2002-2015	170
Annex VI. Degradation of miombo in 2015.....	177

Index of Figures

Fig A. 1 MODIS (Moderate Resolution Imaging Spectroradiometer)	74
Fig A. 2 Nasa's MODIS satellites take images of the entire planet every two days	75
Fig A. 3 Components of MODIS.....	76
Fig A. 4 Images of MOD13Q1.....	78
Fig A. 5 Landsat 7 satellite in the cleanroom prior to launch.....	79
Fig A. 6 A schematic of the Landsat 7 satellite	80
Fig A. 7 Landsat 8 OLI	81


Index of Tables

Table A 1 Coordinates of tracts and inventory plots.....	73
Table A 2 Coordinates of tracts and inventory plots Study area/scope.....	73
Table A 3 Spectral bands of MODIS.....	76
Table A 4 ETM+ Bands.....	81
Table A 5 OLI Bands.....	83
Table A 6 TIRS bands.....	84

Annex I

Table A 1 Coordinates of tracts and inventory plots

Table A 2 Coordinates of tracts and inventory plots Study area/scope	Residues type	Biomass quantities [t/year]	Energy potential [GJ/year]	Biomass access restrictions	GIS based method	Sources
Portugal/Country	Forestry	1,097,000	-	No	Yes	[11]
Portugal/Local	Forestry and agricultural	10,600	106,000	No	Yes	[12]
Portugal/Local	Forestry, agricultural and timber industry	135,000	-	No	Yes	[13]
Portugal/Local	Forestry and agricultural	-	4,500,000	Yes	Yes	[14]
Mozambique/Local	Forestry	1,200,000	17,300,000	No	Yes	[15]
Spain/Local	Forestry	463,000	5,800,000	Yes	Yes	[16]
Spain/Country	Forestry and agricultural	-	118,000,000	Yes	Yes	[17]

Table A 2 (i) Crop areas and (ii) amount of usable energy in Andalusia¹ ²

¹ Sebastián Nogués F, García-Galindo D, Rezeau A. 2010. Energías Renovables. Energía de la biomasa, vol. I. Prensas Universitarias de Zaragoza;

² Ministerio de Medio Ambiente y Medio Rural y Marino. Informes de mapas de cultivos. Sistema de Información Geográfica de datos Agrarios (SIGA). Available at <<http://sig.marm.es/siga/>> [August 2010].

Annex II. Remote Sensing

MODIS

MODIS (or Moderate Resolution Imaging Spectroradiometer) is a key instrument aboard the Terra (originally known as EOS AM-1) and Aqua (originally known as EOS PM-1) satellites. Terra's orbit around the Earth is timed so that it passes from north to south across the equator in the morning, while Aqua passes south to north over the equator in the afternoon. Terra MODIS and Aqua MODIS are viewing the entire Earth's surface every 1 to 2 days, acquiring data in 36 spectral bands, or groups of wavelengths (see MODIS Technical Specifications). These data will improve our understanding of global dynamics and processes occurring on the land, in the oceans, and in the lower atmosphere. MODIS is playing a vital role in the development of validated, global, interactive Earth system models able to predict global change accurately enough to assist policy makers in making sound decisions concerning the protection of our environment.

MODIS Design

The MODIS instrument provides high radiometric sensitivity (12 bit) in 36 spectral bands ranging in wavelength from 0.4 μm to 14.4 μm . The responses are custom tailored to the individual needs of the user community and provide exceptionally low out-of-band response. Two bands are imaged at a nominal resolution of 250 m at nadir, with five bands at 500 m, and the remaining 29 bands at 1 km. A ± 55 -degree scanning pattern at the EOS orbit of 705 km achieves a 2,330-km swath and provides global coverage every one to two days.

The Scan Mirror Assembly uses a continuously rotating double-sided scan mirror to scan ± 55 -degrees and is driven by a motor encoder built to operate at 100 percent duty cycle throughout the 6-year instrument design life. The optical system consists of a two-mirror off-axis afocal telescope, which directs energy to four refractive objective assemblies; one for each of the VIS, NIR, SWIR/MWIR and LWIR spectral regions to cover a total spectral range of 0.4 to 14.4 μm .

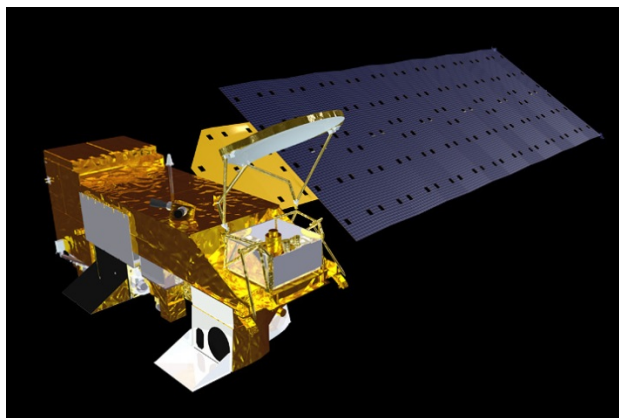


Fig A. 1 MODIS (Moderate Resolution Imaging Spectroradiometer)

A high-performance passive radiative cooler provides cooling to 83K for the 20 infrared spectral bands on two HgCdTe Focal Plane Assemblies (FPAs). Novel photodiode-silicon readout technology for the visible and near infrared provides unsurpassed quantum efficiency and low-noise readout with exceptional dynamic range. Analog programmable gain and offset and FPA clock and bias electronics are located near the FPAs in two dedicated electronics modules, the Space-viewing Analog Module (SAM) and the Forward-viewing Analog Module (FAM). A third module, the Main Electronics Module (MEM) provides power, control systems, command and telemetry, and calibration electronics.

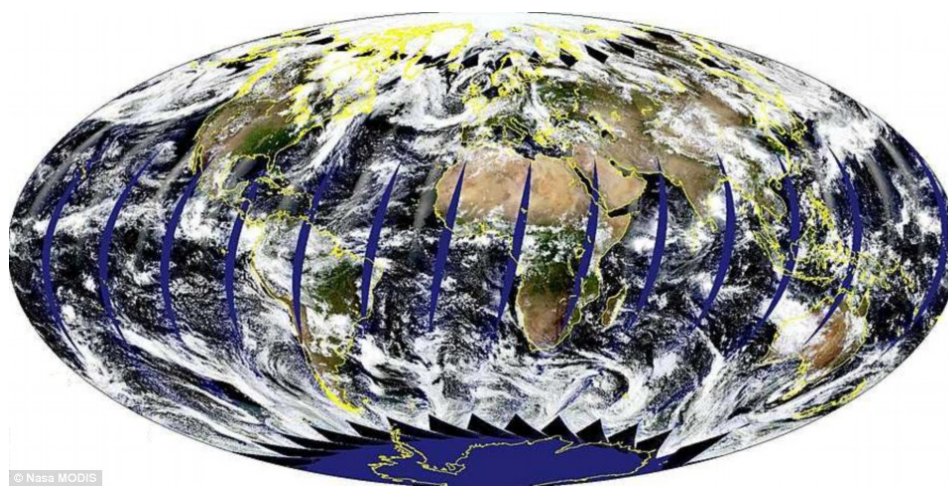


Fig A. 2 Nasa's MODIS satellites take images of the entire planet every two days

The system also includes four on-board calibrators as well as a view to space: A Solar Diffuser (SD), a v-groove Blackbody (BB), a Spectroradiometric calibration assembly (SRCA), and a Solar Diffuser Stability Monitor (SDSM).

The first MODIS Flight Instrument, ProtoFlight Model or PFM, is integrated on the Terra (EOS AM-1) spacecraft. Terra successfully launched on December 18, 1999. The second MODIS flight instrument, Flight Model 1 or FM1, is integrated on the Aqua (EOS PM-1) spacecraft; it was successfully launched on May 4, 2002. These MODIS instruments offer an unprecedented look at terrestrial, atmospheric, and ocean phenomenology for a wide and diverse community of users throughout the world.

Components

The MODIS instrument has been designed and developed since the Engineering Model (EM) was completed in mid-1995. Since then, two spaceflight units, the Protoflight Model (PFM) (aboard the Terra Satellite), and the Flight Model 1 (FM1) (aboard the Aqua Satellite) have been completed and launched. Terra was launched on December 18, 1999, and Aqua was launched on May 4, 2002. The MODIS instruments — built to NASA specifications by Santa Barbara

Remote Sensing — represent the finest in engineering of spaceflight hardware for remote sensing.

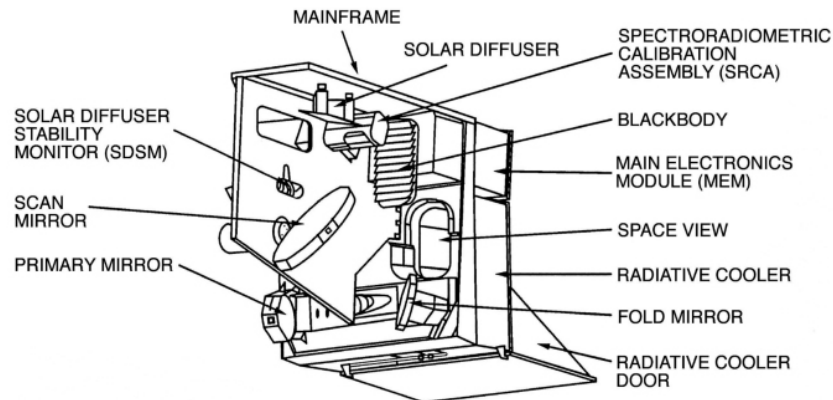


Fig A. 3 Components of MODIS

Specifications

Orbit: 705 km, 10:30 a.m. descending node (Terra) or 1:30 p.m. ascending node (Aqua), sun-synchronous, near-polar, circular

Scan Rate: 20.3 rpm, cross track

Swath Dimensions: 2330 km (cross track) by 10 km (along track at nadir)

Telescope: 17.78 cm diam. off-axis, afocal (collimated), with intermediate field stop

Size: 1.0 x 1.6 x 1.0 m

Weight: 228.7 kg

Power: 162.5 W (single orbit average)

Data Rate: 10.6 Mbps (peak daytime); 6.1 Mbps (orbital average)

Quantization: 12 bits

Spatial Resolution: 250 m (bands 1-2), 500 m (bands 3-7), 1000 m (bands 8-36) Design Life: 6 years

Table A 3 Spectral bands of MODIS

Primary Use	Band	Bandwidth ¹	Spectral Radiance ²	Required SNR ³
Land/Cloud/Aerosols Boundaries	1	620 - 670	21.8	128
	2	841 - 876	24.7	201
Land/Cloud/Aerosols Properties	3	459 - 479	35.3	243
	4	545 - 565	29.0	228
	5	1230 - 1250	5.4	74
	6	1628 - 1652	7.3	275

	7	2105 - 2155	1.0	110
Ocean Colour/ Phytoplankton/ Biogeochemistry	8	405 - 420	44.9	880
	9	438 - 448	41.9	838
	10	483 - 493	32.1	802
	11	526 - 536	27.9	754
	12	546 - 556	21.0	750
	13	662 - 672	9.5	910
	14	673 - 683	8.7	1087
	15	743 - 753	10.2	586
	16	862 - 877	6.2	516
Atmospheric Water Vapour	17	890 - 920	10.0	167
	18	931 - 941	3.6	57
	19	915 - 965	15.0	250
Primary Use	Band	Bandwidth ¹	Spectral Radiance ²	Required NE[Δ]T(K) ⁴
Surface/Cloud Temperature	20	3.660 - 3.840	0.45(300K)	0.05
	21	3.929 - 3.989	2.38(335K)	2.00
	22	3.929 - 3.989	0.67(300K)	0.07
	23	4.020 - 4.080	0.79(300K)	0.07
Atmospheric Temperature	24	4.433 - 4.498	0.17(250K)	0.25
	25	4.482 - 4.549	0.59(275K)	0.25
Cirrus Clouds Water Vapour	26	1.360 - 1.390	6.00	150(SNR)
	27	6.535 - 6.895	1.16(240K)	0.25
	28	7.175 - 7.475	2.18(250K)	0.25
Cloud Properties	29	8.400 - 8.700	9.58(300K)	0.05
Ozone	30	9.580 - 9.880	3.69(250K)	0.25
Surface/Cloud Temperature	31	10.780 - 11.280	9.55(300K)	0.05
	32	11.770 - 12.270	8.94(300K)	0.05
Cloud Top Altitude	33	13.185 - 13.485	4.52(260K)	0.25
	34	13.485 - 13.785	3.76(250K)	0.25
	35	13.785 - 14.085	3.11(240K)	0.25
	36	14.085 - 14.385	2.08(220K)	0.35
¹ Bands 1 to 19 are in nm; Bands 20 to 36 are in μm ² Spectral Radiance values are (W/m ² -μm-sr) ³ SNR = Signal-to-noise ratio ⁴ NE(Δ)T = Noise-equivalent temperature difference Note: Performance goal is 30-40% better than required				

Vegetation Indices 16-Day L3 Global 250m

MOD13Q1

Short Name: MOD13Q1

The MOD13Q1 images shown are samples of the MODIS/Terra Vegetation Indices 16-Day L3 Global 250m SIN Grid. The NDVI and EVI have been pseudo-coloured to represent the biomass health of the western United States using tile h08v05 from June 25 July 10, 2000.

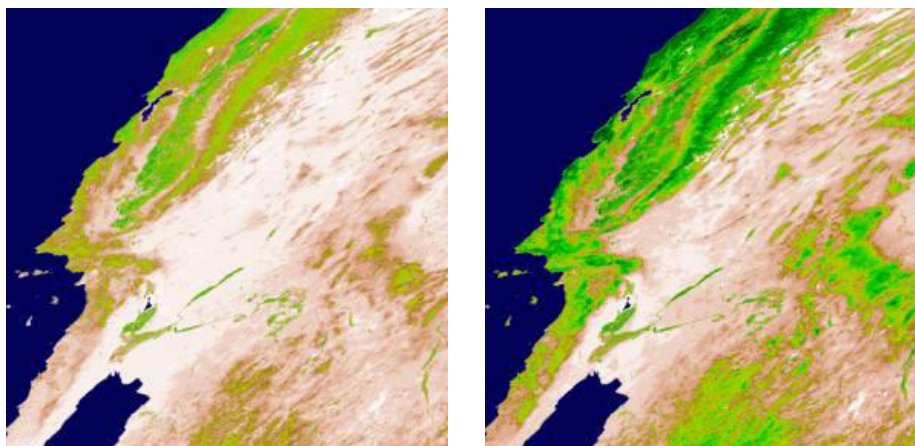


Fig A. 4 Images of MOD13Q1

Due to their simplicity, ease of application, and widespread familiarity, vegetation indices have a wide range of usage within the user community. Some of the more common applications may include global biogeochemical and hydrologic modelling, agricultural monitoring and forecasting, land-use planning, land cover characterization, and land cover change detection.

Global MODIS vegetation indices are designed to provide consistent spatial and temporal comparisons of vegetation conditions. Blue, red, and near-infrared reflectance, centred at 469-nanometers, 645-nanometers, and 858-nanometers, respectively, are used to determine the MODIS daily vegetation indices.

The MODIS Normalized Difference Vegetation Index (NDVI) complements NOAA's Advanced Very High Resolution Radiometer (AVHRR) NDVI products and provides continuity for time series historical applications. MODIS also includes a new Enhanced Vegetation Index (EVI) that minimizes canopy background variations and maintains sensitivity over dense vegetation conditions. The EVI also uses the blue band to remove residual atmosphere contamination caused by smoke and sub-pixel thin cloud clouds. The MODIS NDVI and EVI products are computed from atmospherically corrected bi-directional surface reflectance that have been masked for water, clouds, heavy aerosols, and cloud shadows.

Global MOD13Q1 data are provided every 16 days at 250-meter spatial resolution as a gridded level-3 product in the Sinusoidal projection. Lacking a 250m blue band, the EVI algorithm uses the 500m blue band to correct for residual atmospheric effects, with negligible spatial artefacts.

Vegetation indices are used for global monitoring of vegetation conditions and are used in products displaying land cover and land cover changes. These data may be used as input for modelling global biogeochemical and hydrologic processes and global and regional climate.

These data also may be used for characterizing land surface biophysical properties and processes, including primary production and land cover conversion.

Version-5 MODIS Vegetation Indices products have attained Validation Stage 3.

- Change Points of Interest
 - Phased production between Terra and Aqua products for improved temporal frequency (Terra 16-day period starting Day 001, Aqua 16-day period starting Day 009)
 - Replaced NDVI_QA and EVI_QA with one VI_QA Science Data Set
 - Reduced file volume by using internal compression
 - More: MODIS Vegetation Index Product Series Collection 5 Change Summary

LANDSAT 7 ETM +

The government-owned Landsat 7 was successfully launched on April 15, 1999, from the Western Test Range of Vandenberg Air Force Base, California, on a Delta-II expendable launch vehicle. The Earth observing instrument on Landsat 7, the Enhanced Thematic Mapper Plus (ETM+), replicates the capabilities of the highly successful Thematic Mapper instruments on Landsat 4 and 5.



Fig A. 5 Landsat 7 satellite in the cleanroom prior to launch

The ETM+ also includes additional features that make it a more versatile and efficient instrument for global change studies, land cover monitoring and assessment, and large area mapping than its design forebears.

These features are:

- a panchromatic band with 15m spatial resolution
- on-board, full aperture, 5% absolute radiometric calibration
- a thermal IR channel with 60m spatial resolution
- an on-board data recorder

Landsat 7 is the most accurately calibrated Earth-observing satellite, i.e., its measurements are extremely accurate when compared to the same measurements made on the ground. Landsat 7's sensor has been called "the most stable, best characterized Earth observation instrument ever placed in orbit." Landsat 7's rigorous calibration standards have made it the validation choice for many coarse-resolution sensors.

The excellent data quality, consistent global archiving scheme, and reduced pricing (\$600) of Landsat 7 led to a large increase of Landsat data users. In October 2008, USGS made all Landsat 7 data free to the public (all Landsat data were made free in January 2009 leading to a 60-fold increase of data downloads).

Considered a calibration-triumph, the Landsat 7 mission went flawlessly until May 2003 when a hardware component failure left wedge-shaped spaces of missing data on either side of Landsat 7's images.

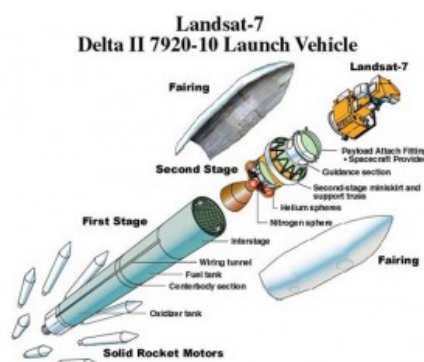


Fig A. 6 A schematic of the Landsat 7 satellite

Sensor ETM+

The Enhanced Thematic Mapper Plus (ETM+) instrument is a fixed "whisk-broom", eight-band, multispectral scanning radiometer capable of providing high-resolution imaging information of the Earth's surface. It detects spectrally-filtered radiation in VNIR, SWIR, LWIR and panchromatic bands from the sun-lit Earth in a 183 km wide swath when orbiting at an altitude of 705 km.

The primary new features on Landsat 7 are a panchromatic band with 15 m spatial resolution, an on-board full aperture solar calibrator, 5% absolute radiometric calibration and a thermal IR channel with a four-fold improvement in spatial resolution over TM.

Landsat 7 collects data in accordance with the World Wide Reference System 2, which has catalogued the world's land mass into 57,784 scenes, each 183 km wide by 170 km long. The ETM+ produces approximately 3.8 gigabits of data for each scene. An ETM+ scene has an Instantaneous Field Of View (IFOV) of 30 meters x 30 meters in bands 1-5 and 7 while band 6 has an IFOV of 60 meters x 60 meters on the ground and the band 8 an IFOV of 15 meters.

Please visit the L7 Science Data Users Handbook for a detailed description of ETM+ spatial characteristics.

Table A 4 ETM+ Bands

Band Number	μm	Resolution
1	0.45-0.515	30 m
2	0.525-0.605	30 m
3	0.63-0.69	30 m
4	0.775-0.90	30 m
5	1.55-1.75	30 m
6	10.4-12.5	60 m
7	2.08-2.35	30 m
8	0.52-0.9	15 m

ETM+ Technical Specifications

- Sensor type: opto-mechanical
- Spatial Resolution: 30 m (60 m – thermal, 15-m pan)
- Spectral Range: 0.45 – 12.5 μm
- Number of Bands: 8
- Temporal Resolution: 16 days
- Image Size: 183 km X 170 km
- Swath: 183 km
- Programmable: yes

LANDSAT 8 OLI



Fig A. 7 Landsat 8 OLI

Landsat 8 launched on February 11, 2013, from Vandenberg Air Force Base, California, on an Atlas-V 401 rocket, with the extended payload fairing (EPF) from United Launch Alliance, LLC. The Landsat 8 satellite payload consists of two science instruments—the Operational Land Imager (OLI) and the Thermal Infrared Sensor (TIRS). These two sensors provide seasonal coverage of the global landmass at a spatial resolution of 30 meters (visible, NIR, SWIR); 100 meters (thermal); and 15 meters (panchromatic).

Landsat 8 was developed as a collaboration between NASA and the U.S. Geological Survey (USGS). NASA led the design, construction, launch, and on-orbit calibration phases, during which time the satellite was called the Landsat Data Continuity Mission (LDCM). On May 30, 2013, USGS took over routine operations and the satellite became Landsat 8. USGS leads post-launch calibration activities, satellite operations, data product generation, and data archiving at the Earth Resources Observation and Science (EROS) center.

Evolutionary Advances

Landsat 8 instruments represent an evolutionary advance in technology. OLI improves on past Landsat sensors using a technical approach demonstrated by a sensor flown on NASA's experimental EO-1 satellite. OLI is a push-broom sensor with a four-mirror telescope and 12-bit quantization. OLI collects data for visible, near infrared, and short wave infrared spectral bands as well as a panchromatic band. It has a five-year design life. The graphic below compares the OLI spectral bands to Landsat 7's ETM+ bands. OLI provides two new spectral bands, one tailored especially for detecting cirrus clouds and the other for coastal zone observations

TIRS collects data for two more narrow spectral bands in the thermal region formerly covered by one wide spectral band on Landsats 4–7. The 100 m TIRS data will be registered to the OLI data to create radiometrically, geometrically, and terrain-corrected 12-bit data products.

Landsat 8 is required to return 400 scenes per day to the USGS data archive (150 more than Landsat 7 is required to capture). Landsat 8 has been regularly acquiring 550 scenes per day (and Landsat 7 is acquiring 438 scenes per day). This increases the probability of capturing cloud-free scenes for the global landmass. The Landsat 8 scene size is 185-km-cross-track-by-180-km-along-track. The nominal spacecraft altitude is 705 km. Cartographic accuracy of 12 m or better (including compensation for terrain effects) is required of Landsat 8 data products.

Sensor OLI

The Operational Land Imager (OLI), built by the Ball Aerospace & Technologies Corporation, measures in the visible, near infrared, and short wave infrared portions of the spectrum. Its images have 15-meter (49 ft.) panchromatic and 30-meter multi-spectral spatial resolutions along a 185 km (115 miles) wide swath, covering wide areas of the Earth's landscape while providing sufficient resolution to distinguish features like urban centers, farms, forests and other land uses. The entire Earth will fall within view once every 16 days due to Landsat 8's near-polar orbit.

OLI's design is an advancement in Landsat sensor technology and uses an approach demonstrated by the Advanced Land Imager sensor flown on NASA's experimental EO-1 satellite. Instruments on earlier Landsat satellites employed scan mirrors to sweep the instrument fields of view across the surface swath width and transmit light to a few detectors. The OLI instead uses long detector arrays, with over 7,000 detectors per spectral band, aligned

across its focal plane to view across the swath. This “push-broom” design results in a more sensitive instrument providing improved land surface information with fewer moving parts. With an improved signal-to-noise ratio compared to past Landsat instruments, engineers expect this new OLI design to be more reliable and to provide improved performance.

Table A 5 OLI Bands

Band Number	μm	Resolution
1	0.433–0.453	30 m
2	0.450–0.515	30 m
3	0.525–0.600	30 m
4	0.630–0.680	30 m
5	0.845–0.885	30 m
6	1.560–1.660	60 m
7	2.100–2.300	30 m
8	0.500–0.680	15 m
9	1.360–1.390	30 m

OLI Technical Specifications

- Sensor type: push broom
- Spatial Resolution: 30 m (15-m pan)
- Spectral Range: 0.43 – 1.39 μm
- Number of Bands: 9
- Temporal Resolution: 16 days
- Image Size: 185 km X 180 km
- Swath: 185 km
- Programmable: yes

SENSOR TIRS

The Thermal Infrared Sensor (TIRS) measures land surface temperature in two thermal bands with a new technology that applies quantum physics to detect heat.

TIRS was added to Landsat 8 when it became clear that state water resource managers rely on the highly accurate measurements of Earth’s thermal energy obtained by Landsat 5 and Landsat 7 to track how land and water are being used. With nearly 80 percent of the fresh water

in the Western U.S. being used to irrigate crops, TIRS is an invaluable tool for managing water consumption.

TIRS uses Quantum Well Infrared Photodetectors (QWIPs) to detect long wavelengths of light emitted by the Earth whose intensity depends on surface temperature. These wavelengths, called thermal infrared, are well beyond the range of human vision. QWIPs are a new, lower-cost alternative to conventional infrared technology and were developed at NASA's Goddard Space Flight Center in Greenbelt, Md.

The QWIPs TIRS uses are sensitive to two thermal infrared wavelength bands, helping it separate the temperature of the Earth's surface from that of the atmosphere. Their design operates on the complex principles of quantum mechanics. Gallium arsenide semiconductor chips trap electrons in an energy state 'well' until the electrons are elevated to a higher state by thermal infrared light of a certain wavelength. The elevated electrons create an electrical signal that can be read out and recorded to create a digital image.

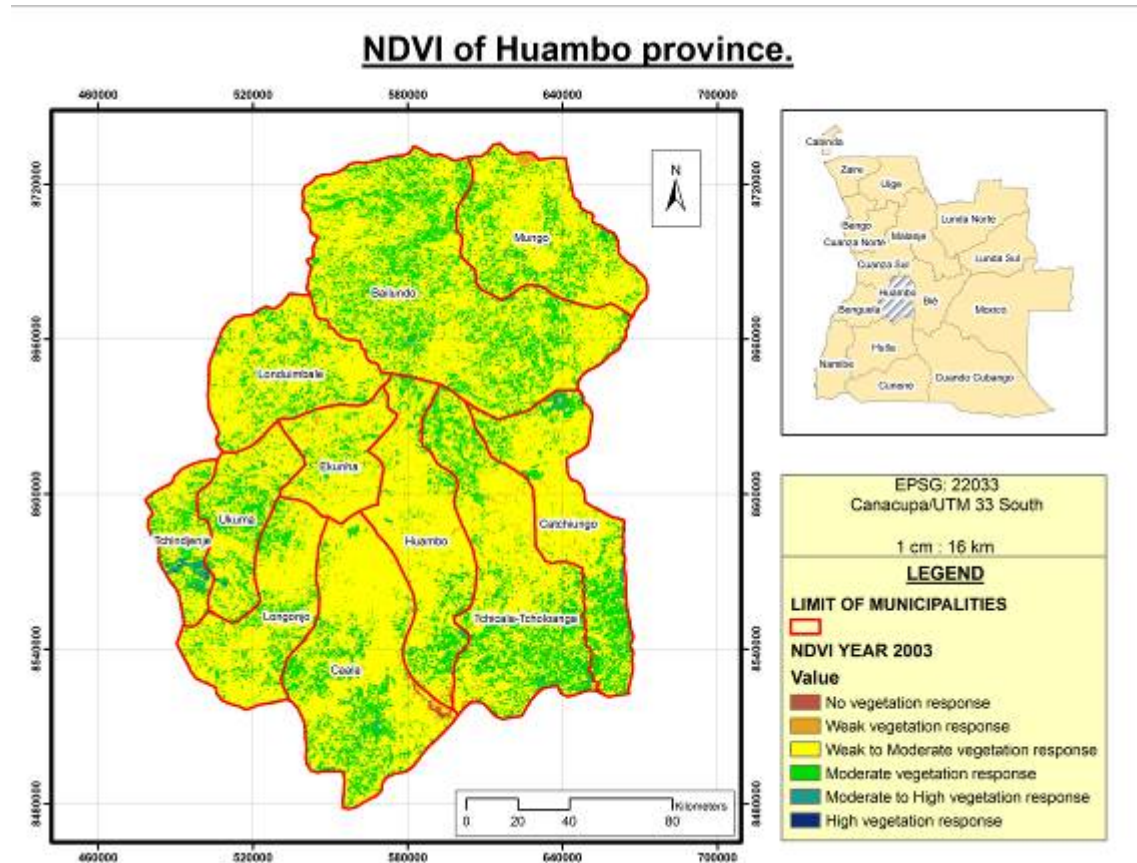
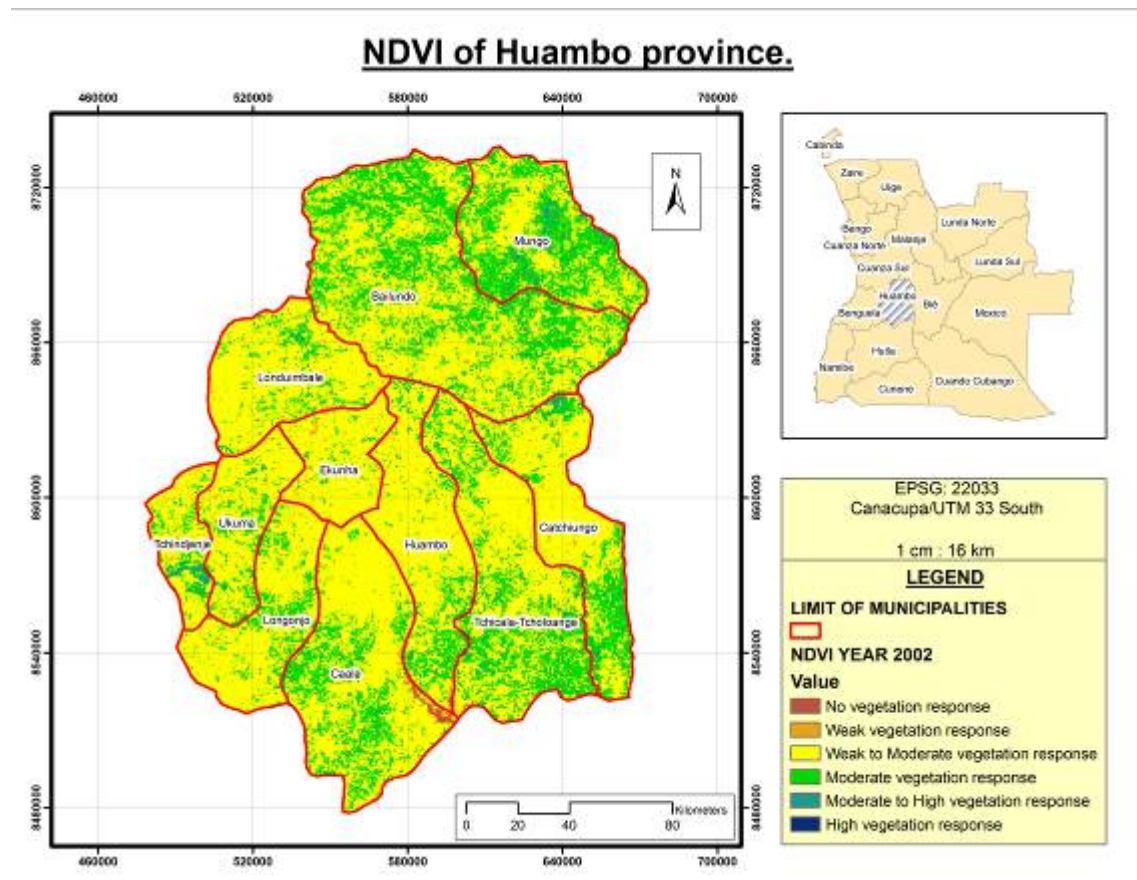
Table A 6 TIRS bands

Band Number	μm	Resolution
10	10.6-11.2	100 m
11	11.5-12.5	100 m

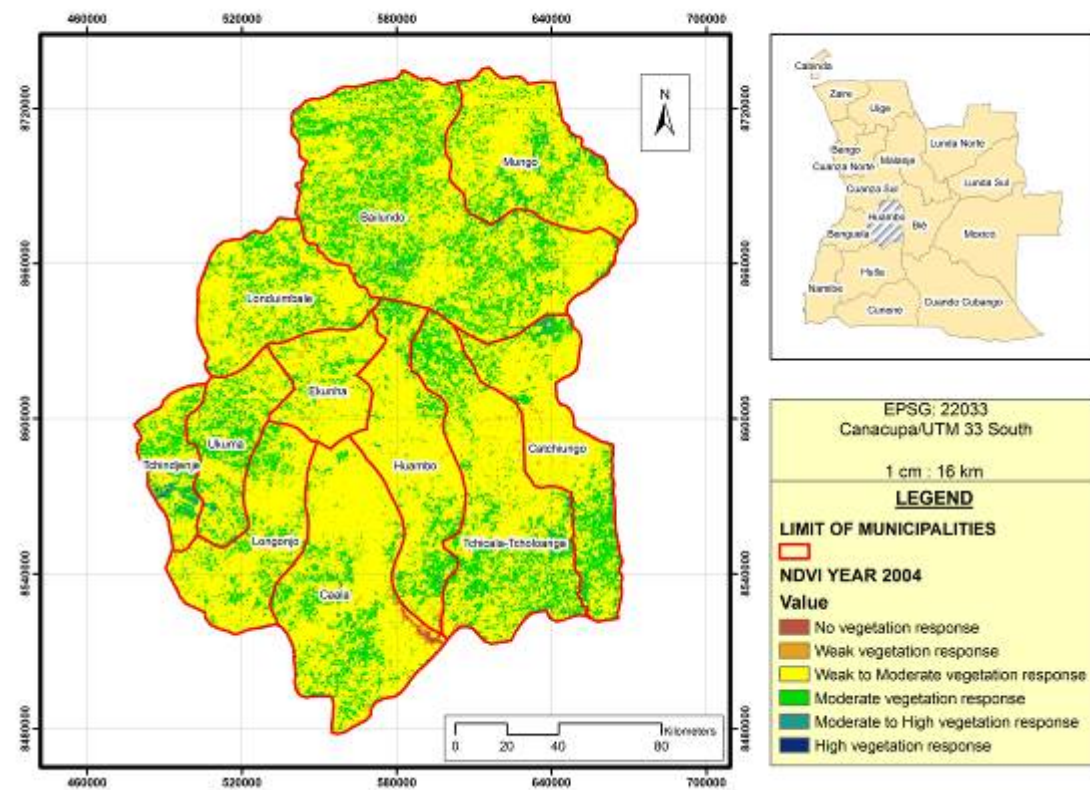
TIRS Technical Specifications

- Sensor type: push broom
- Spatial Resolution: 100 m
- Spectral Range: 10.6 – 12.5 μm
- Number of Bands: 2
- Temporal Resolution: 16 days
- Image Size: 185 km X 180 km
- Swath: 185 km
- Programmable: yes

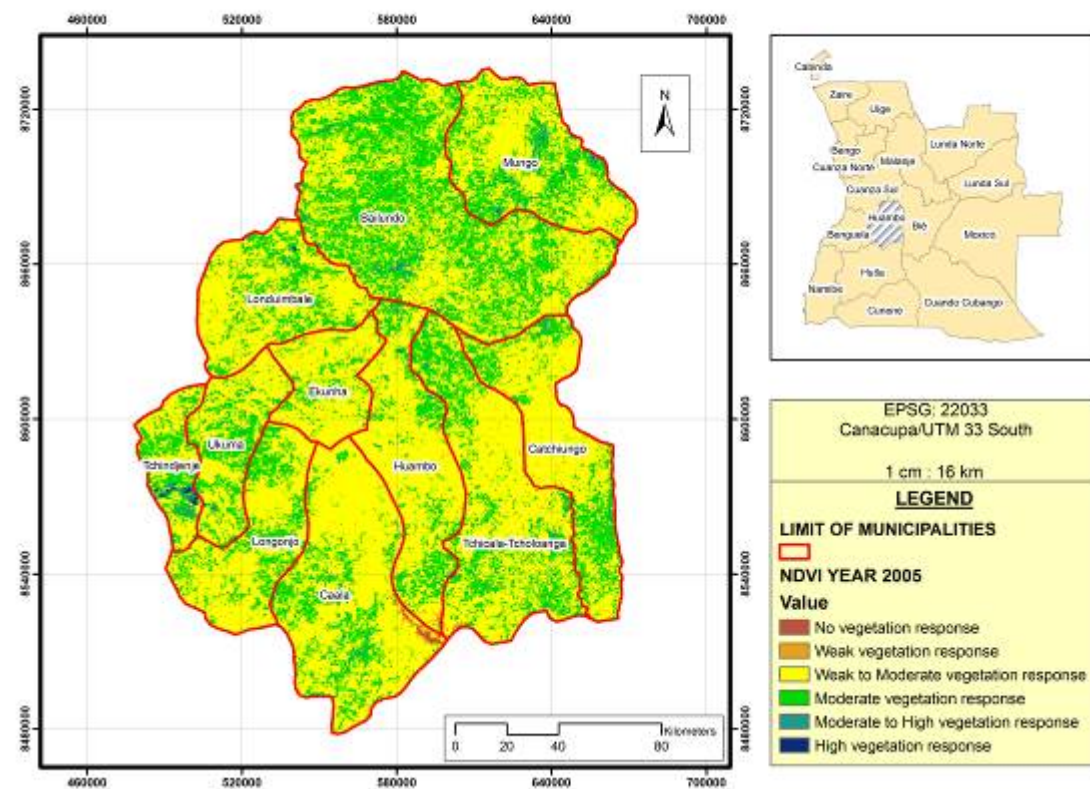
Annex III. Evolution of miombo cover between 2002-2015



NDVI of Huambo province.

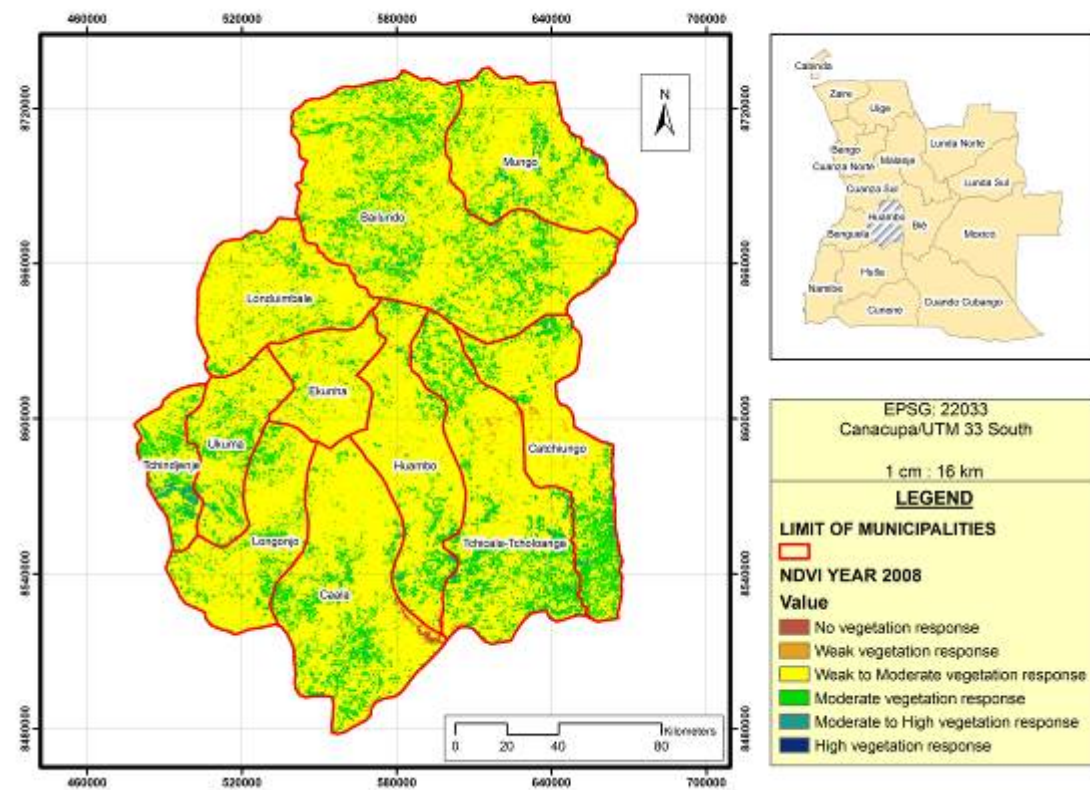


NDVI of Huambo province.

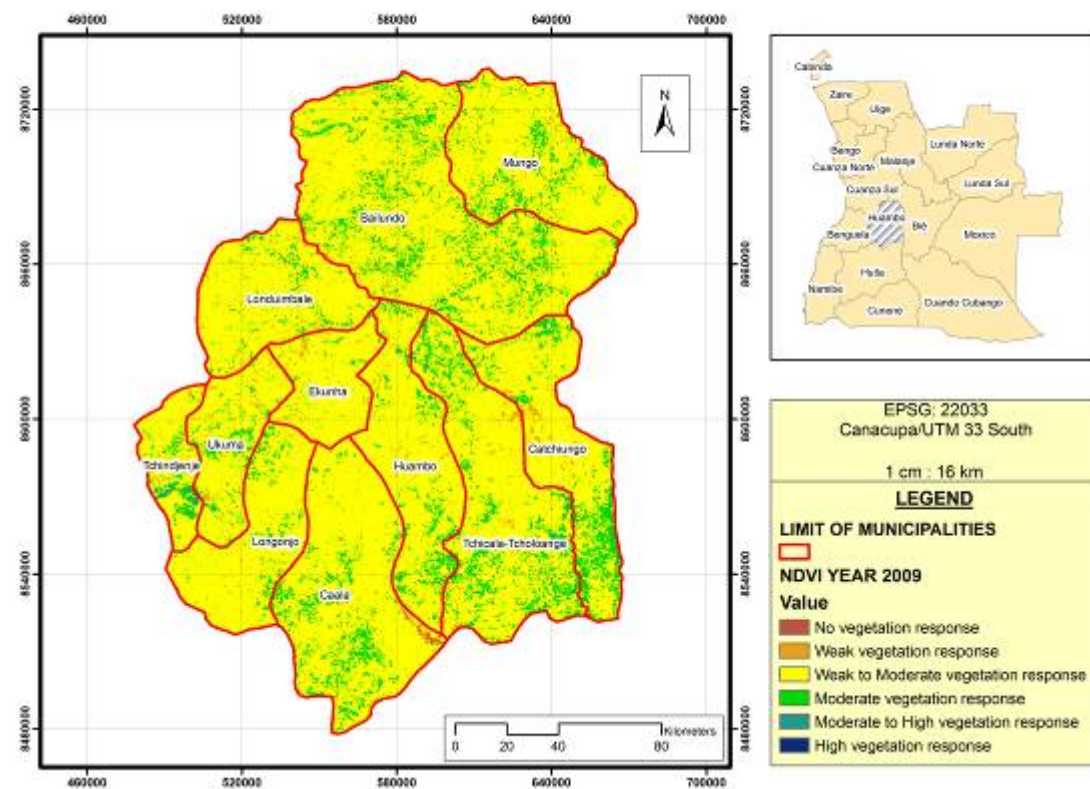




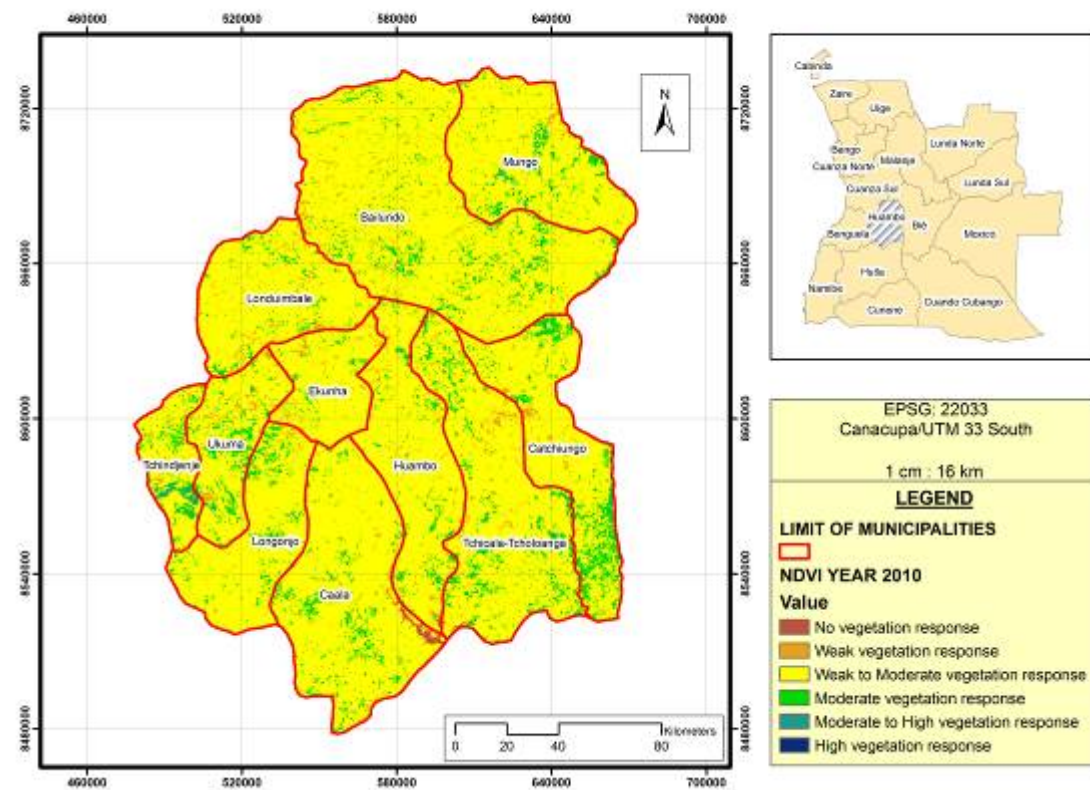
NDVI of Huambo province.



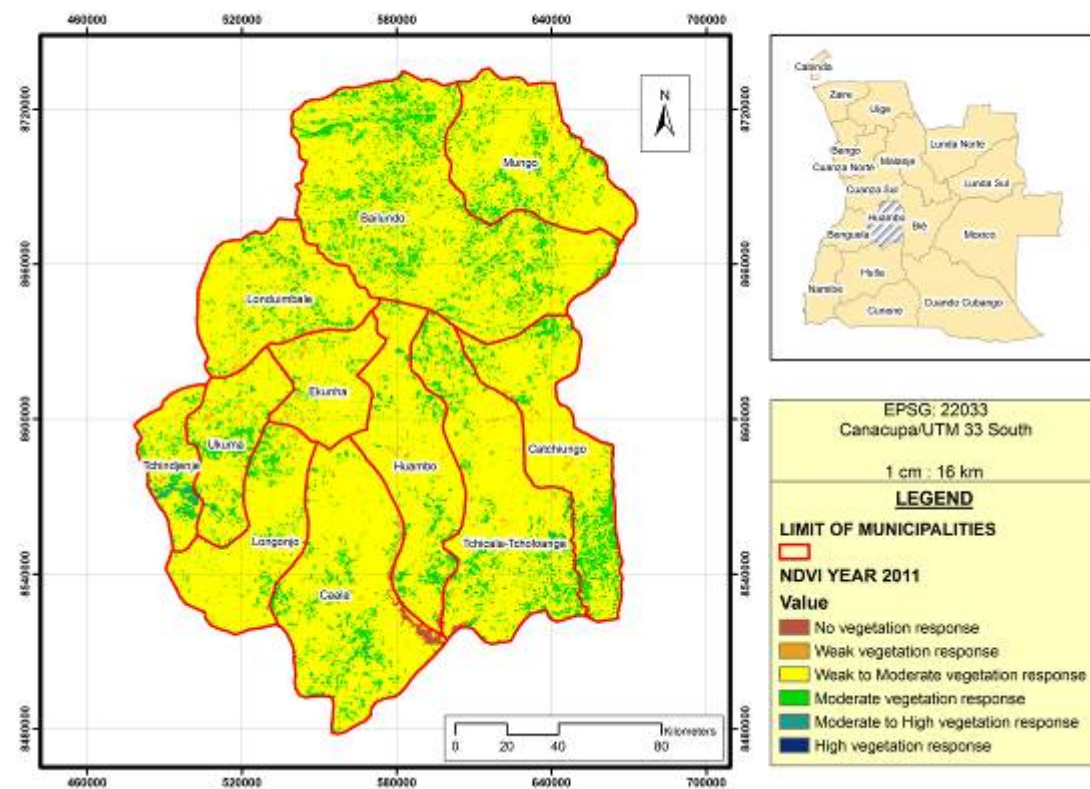
NDVI of Huambo province.



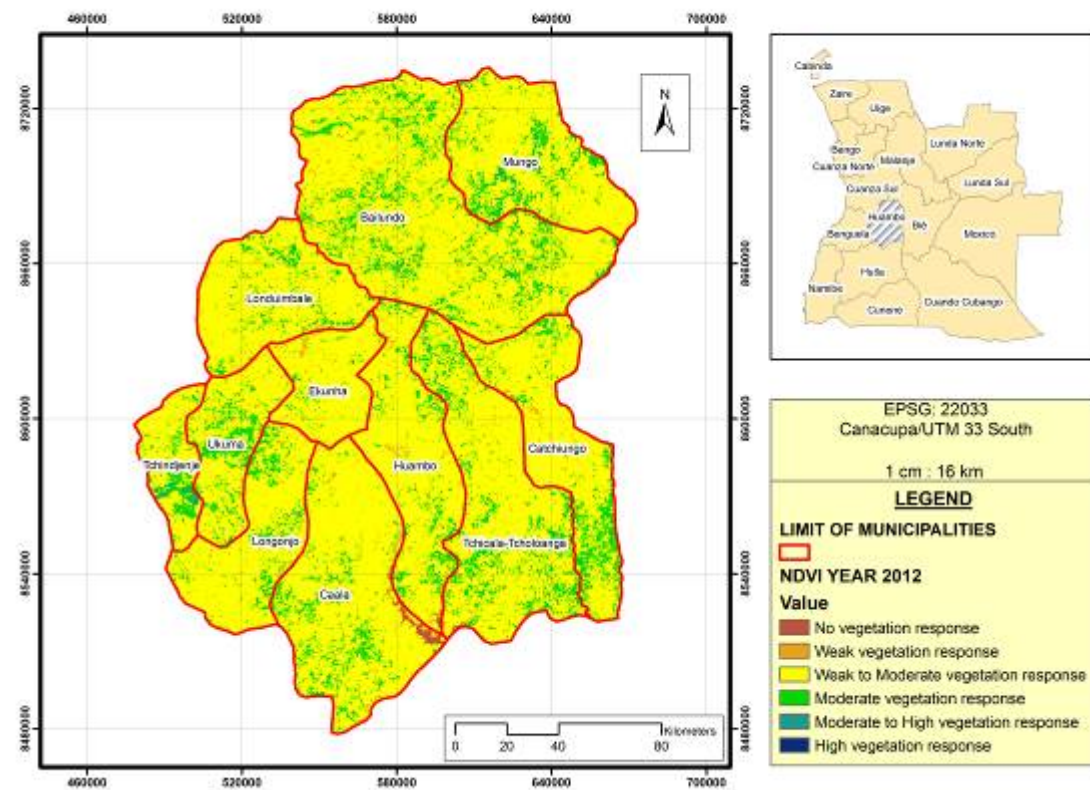
NDVI of Huambo province.



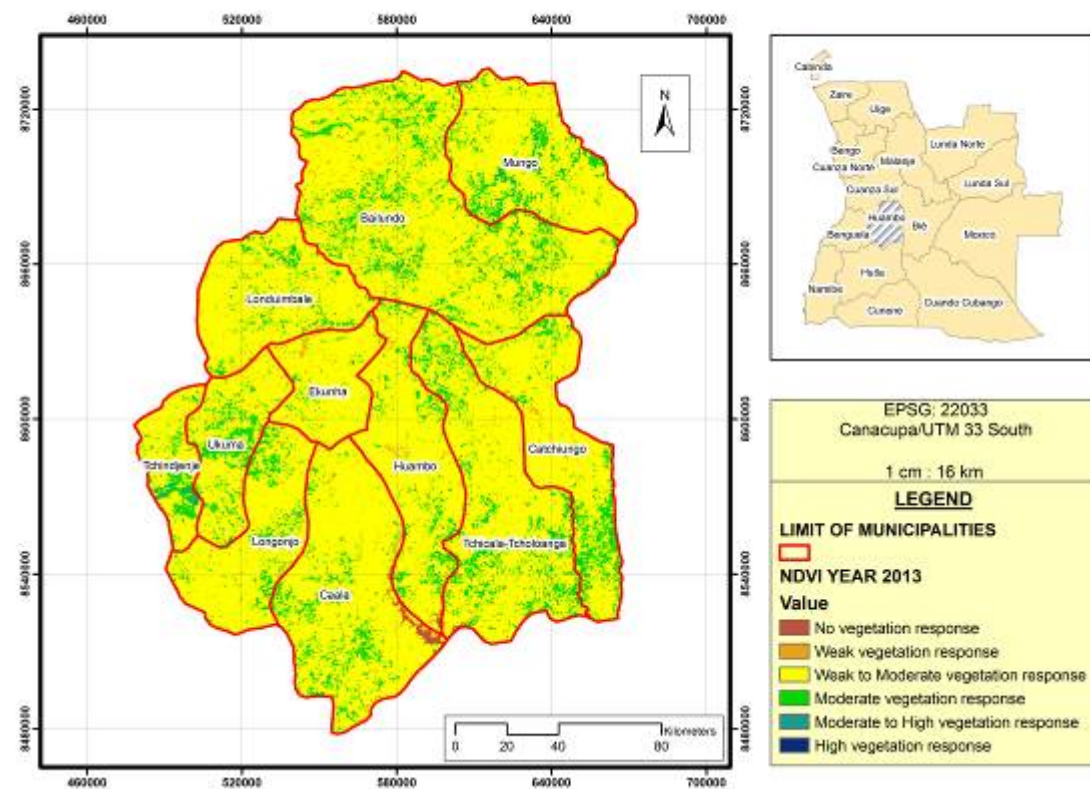
NDVI of Huambo province.



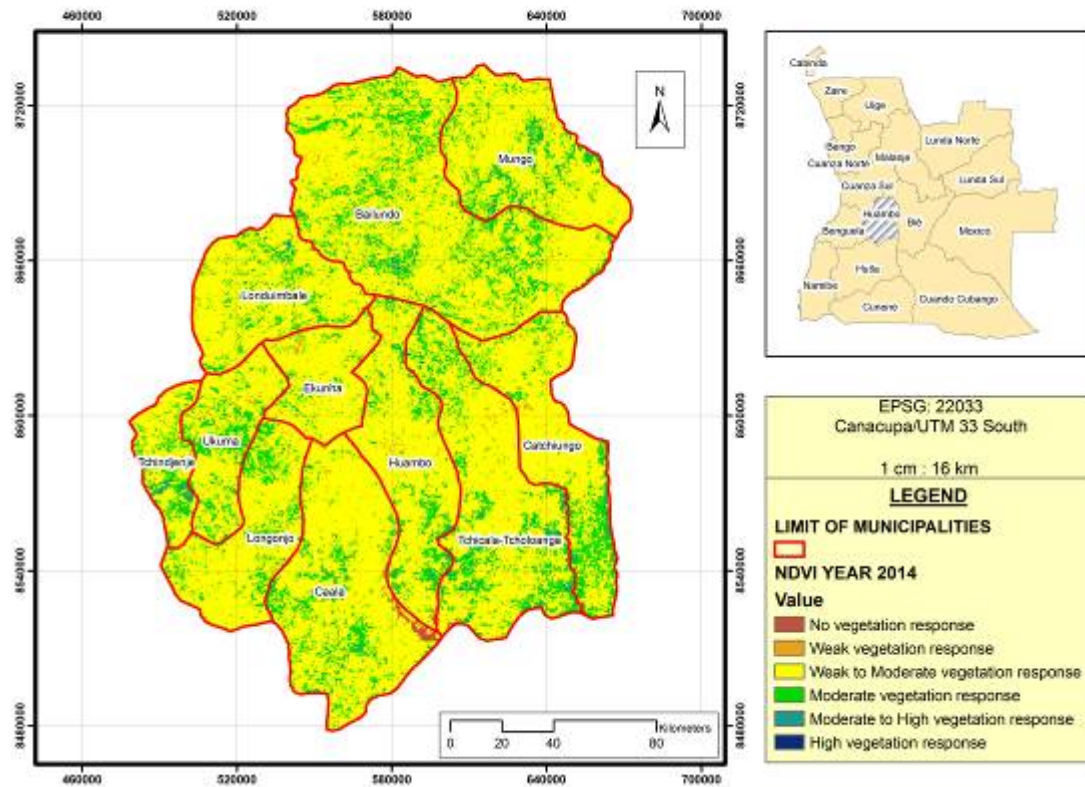
NDVI of Huambo province.



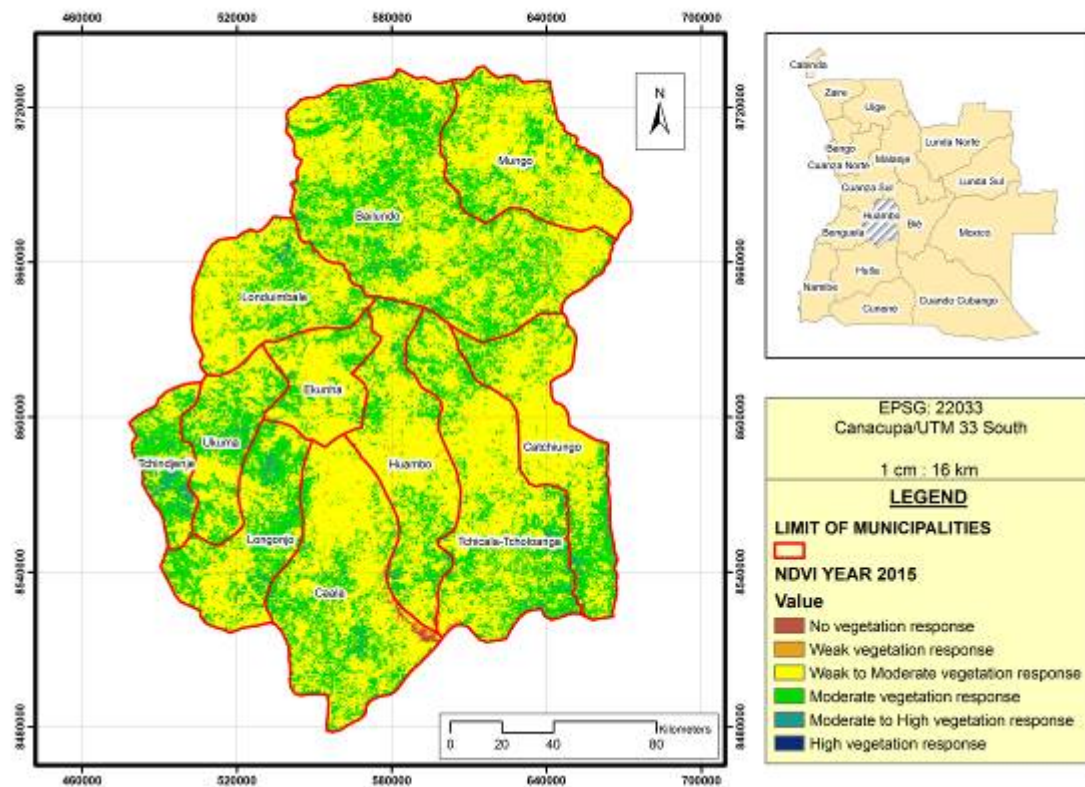
NDVI of Huambo province.



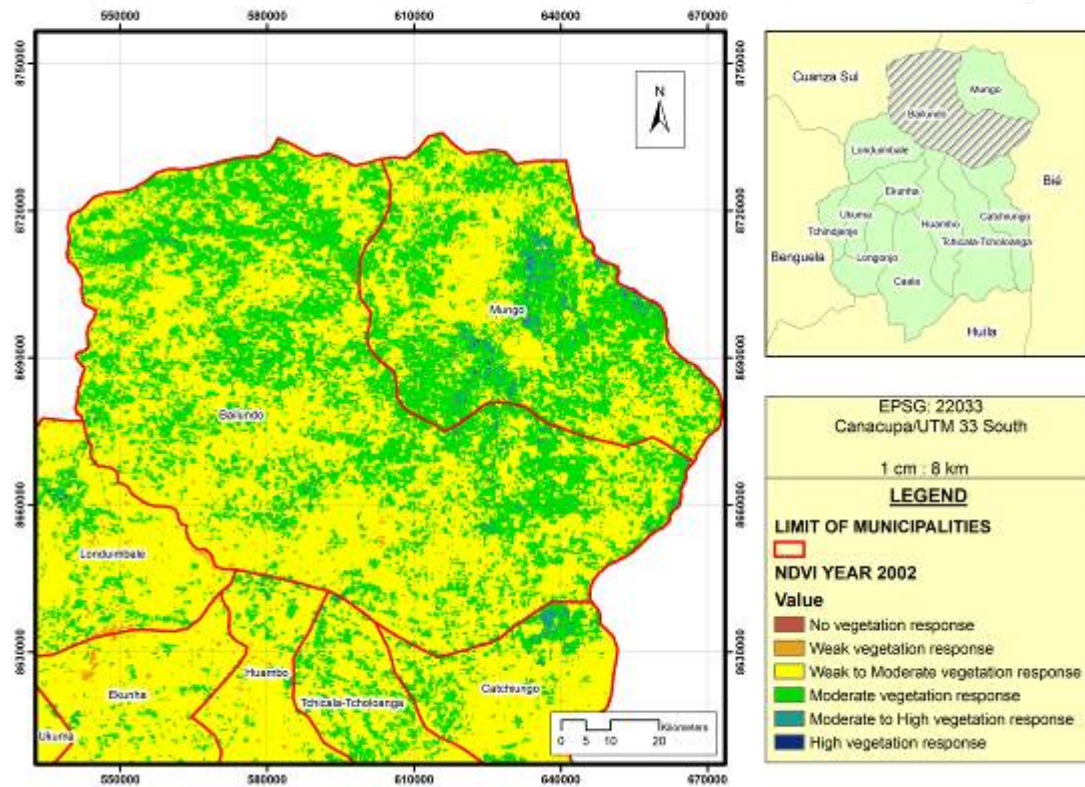
NDVI of Huambo province.



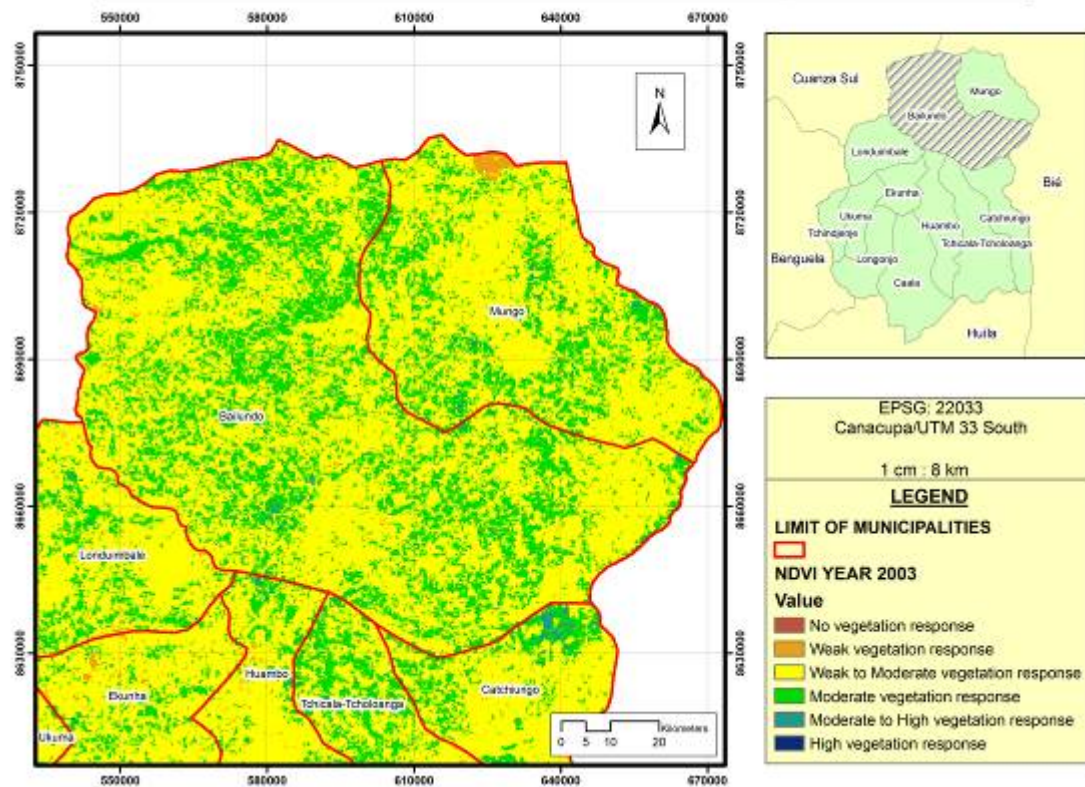
NDVI of Huambo province.



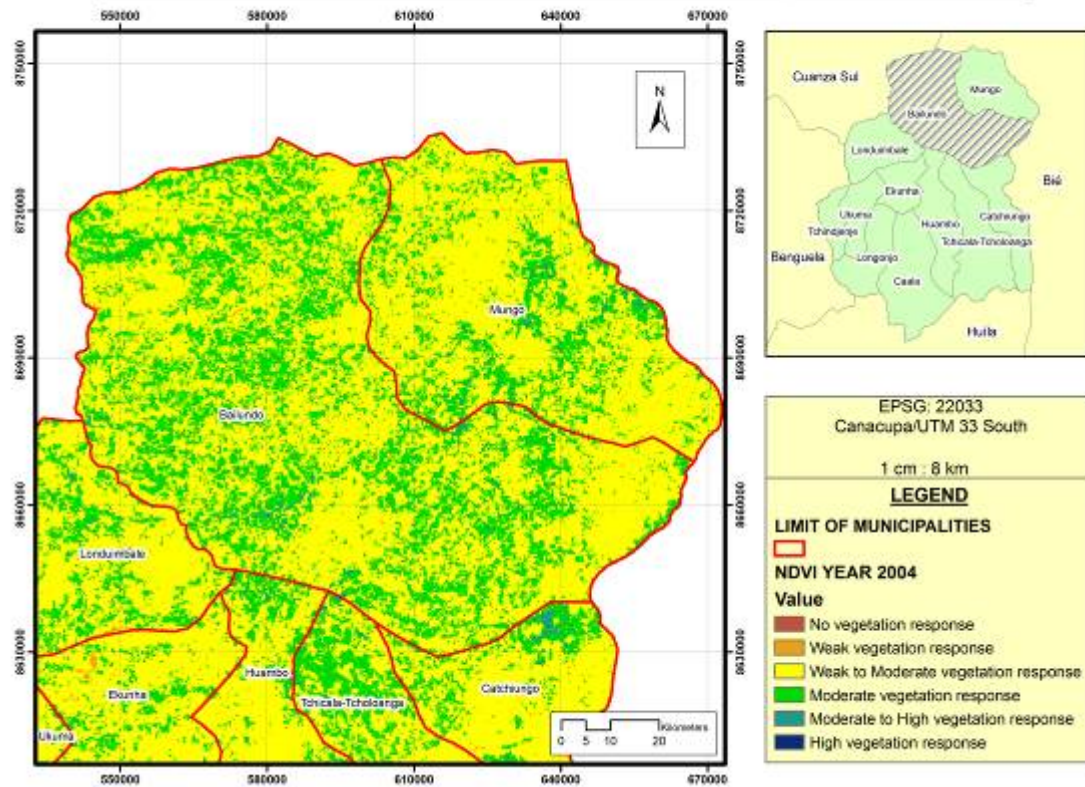
NDVI of Huambo province, municipality of Bailundo.



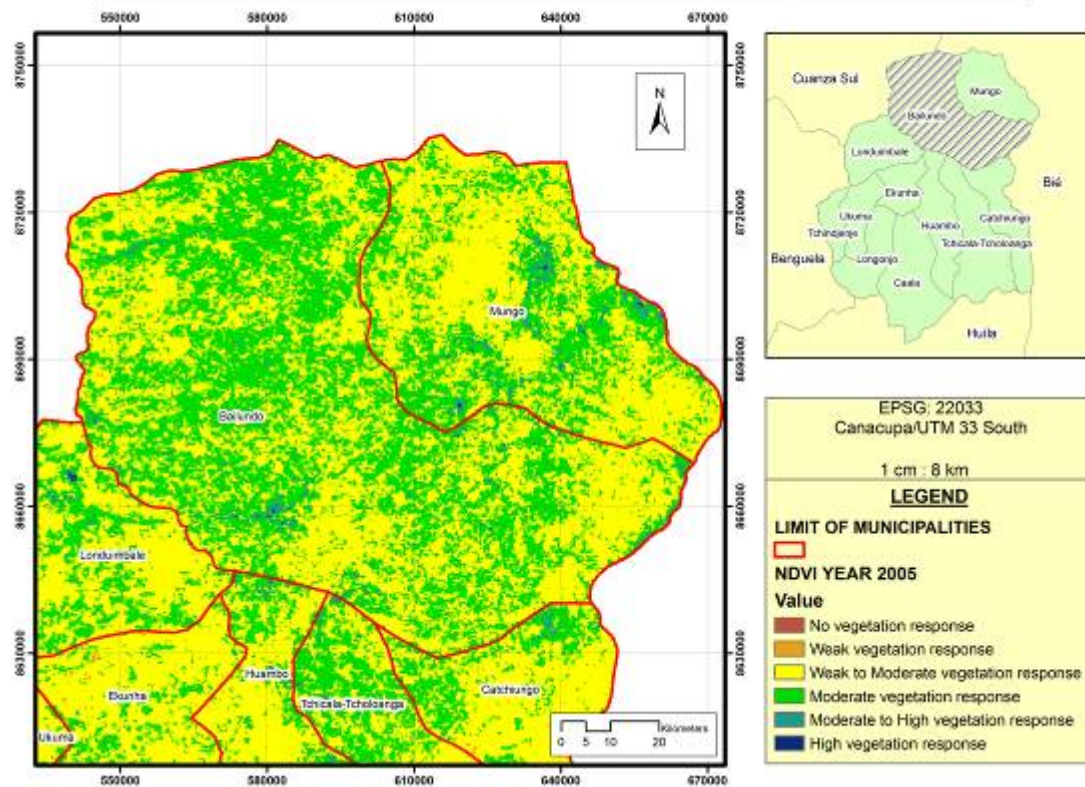
NDVI of Huambo province, municipality of Bailundo.



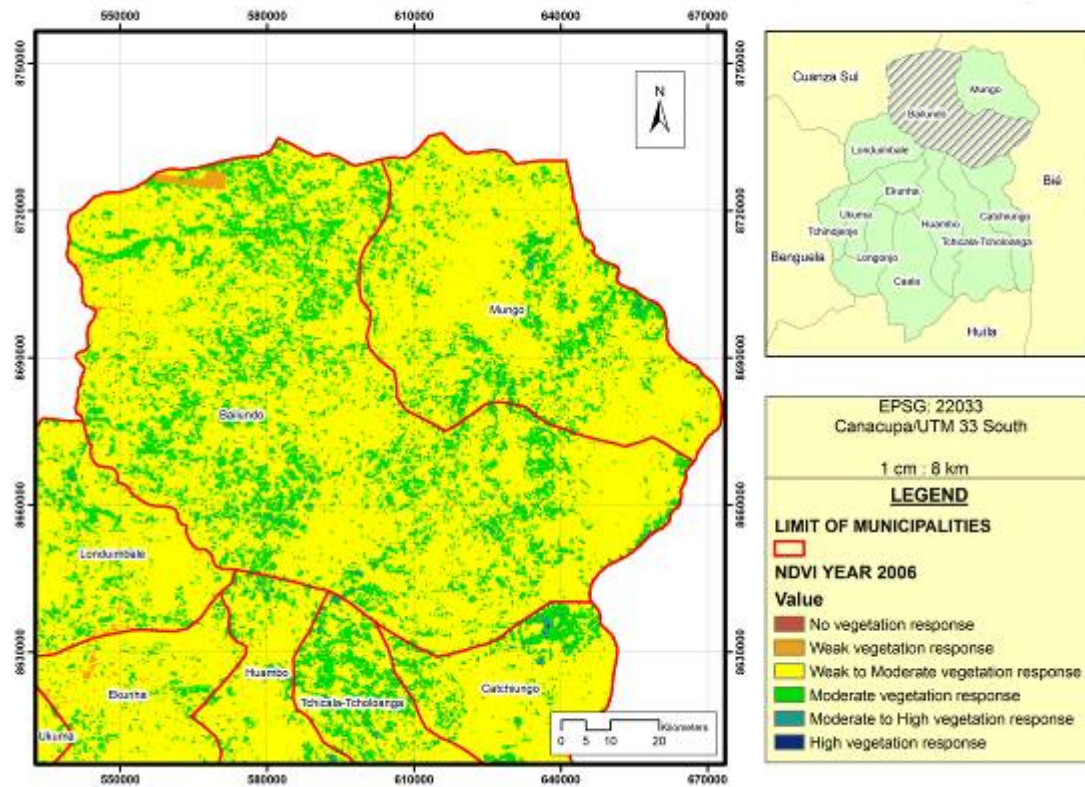
NDVI of Huambo province, municipality of Bailundo.



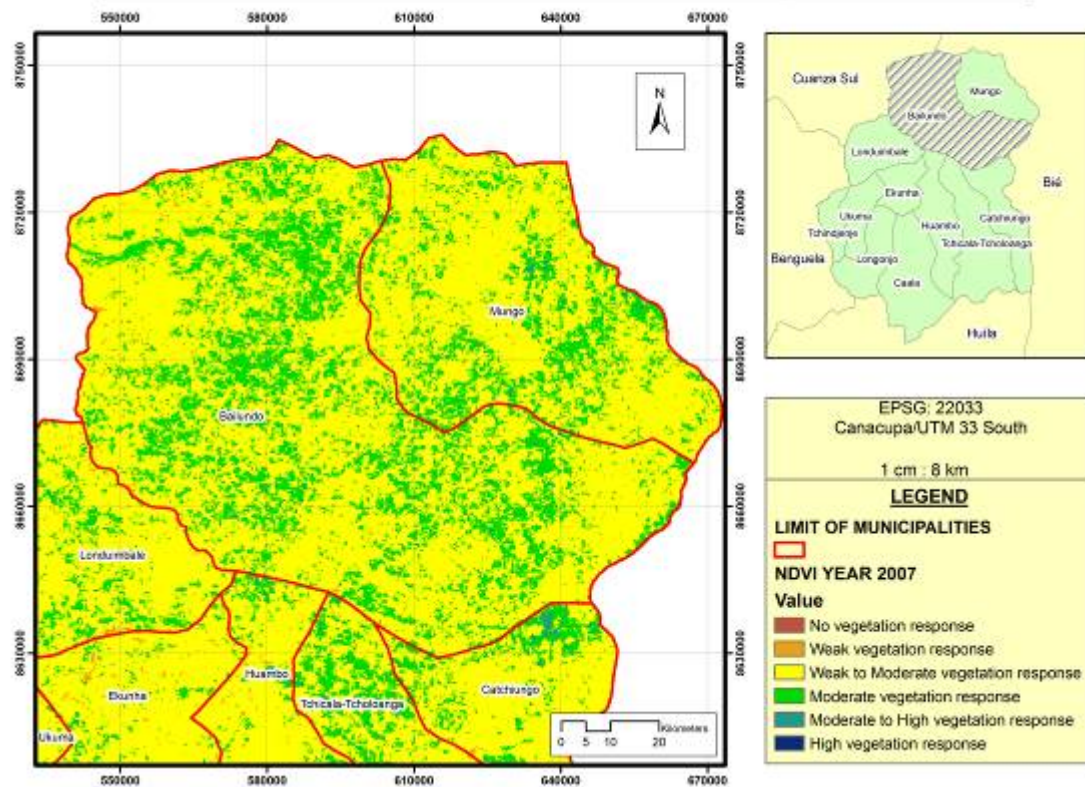
NDVI of Huambo province, municipality of Bailundo.



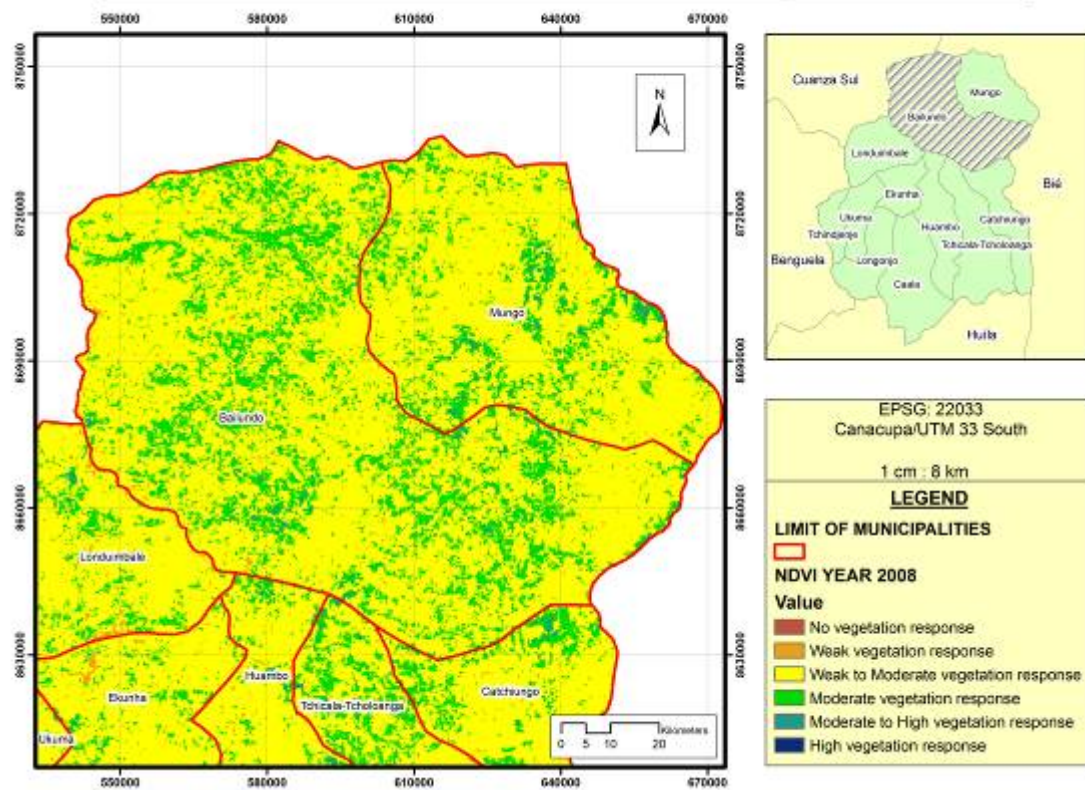
NDVI of Huambo province, municipality of Bailundo.



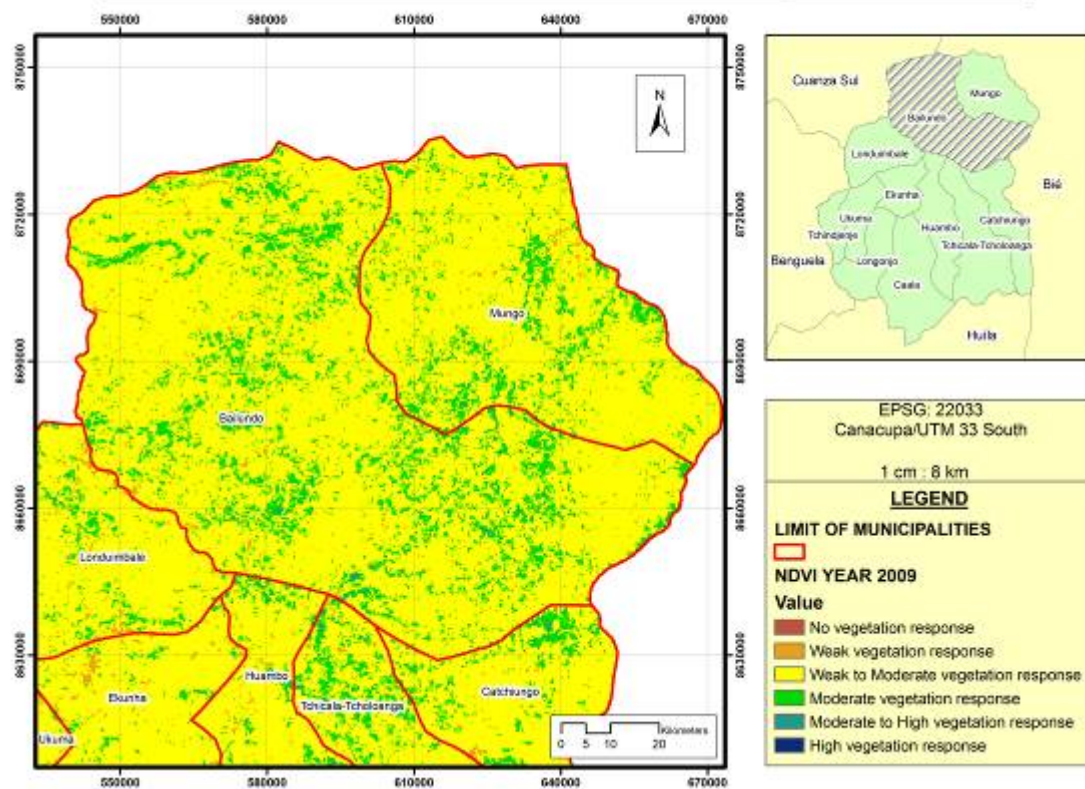
NDVI of Huambo province, municipality of Bailundo.



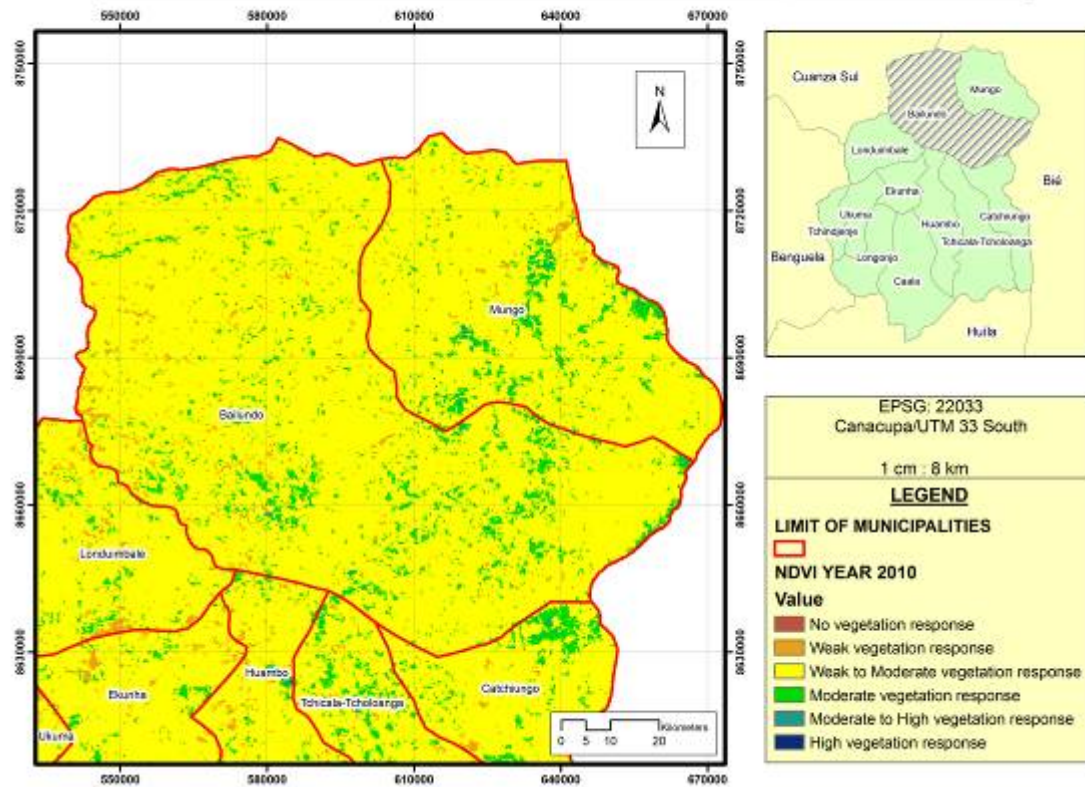
NDVI of Huambo province, municipality of Bailundo.



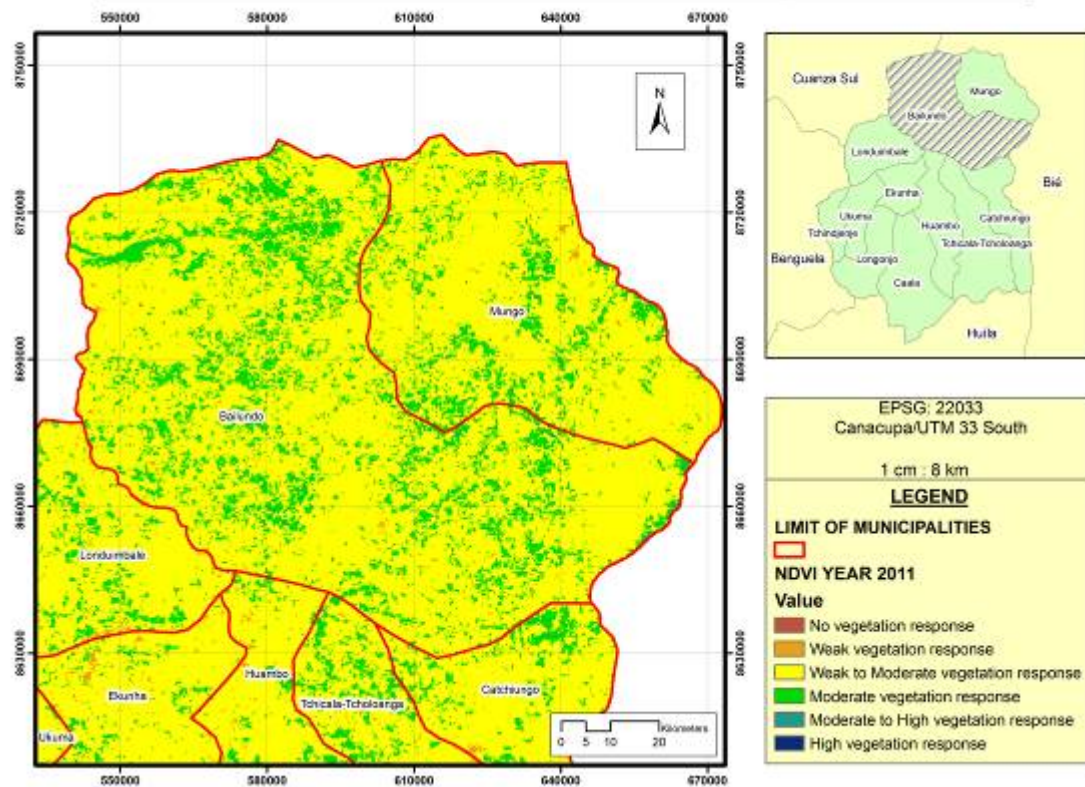
NDVI of Huambo province, municipality of Bailundo.



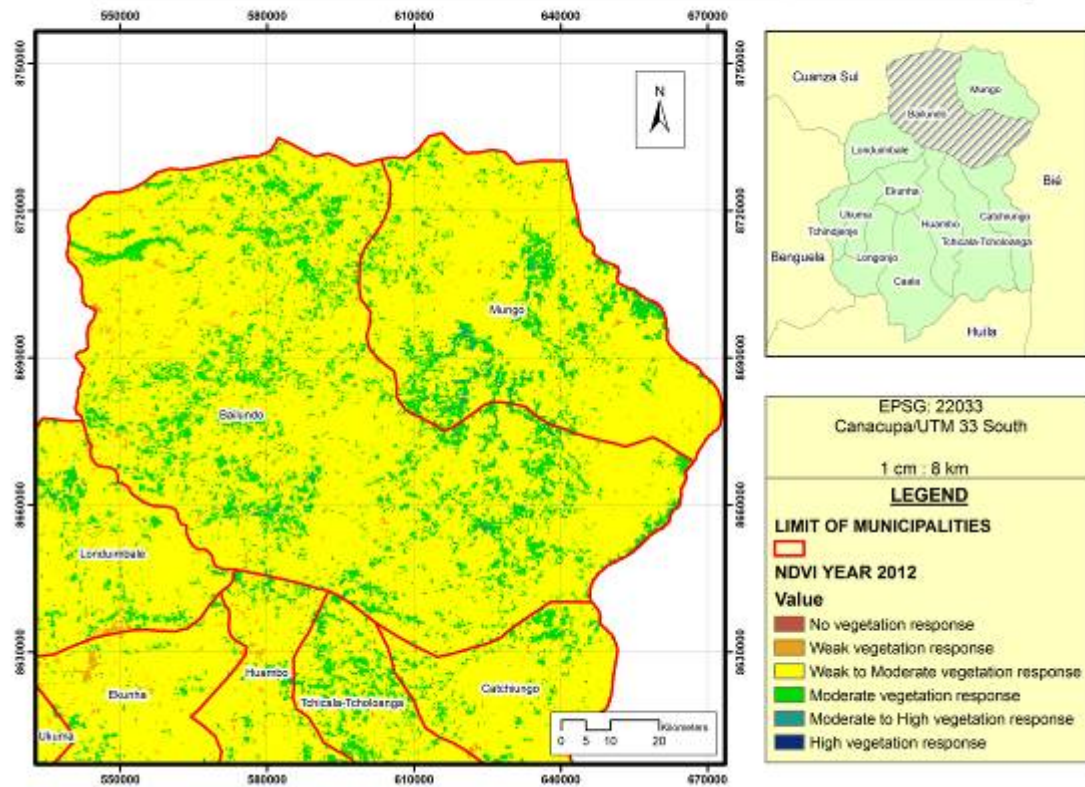
NDVI of Huambo province, municipality of Bailundo.



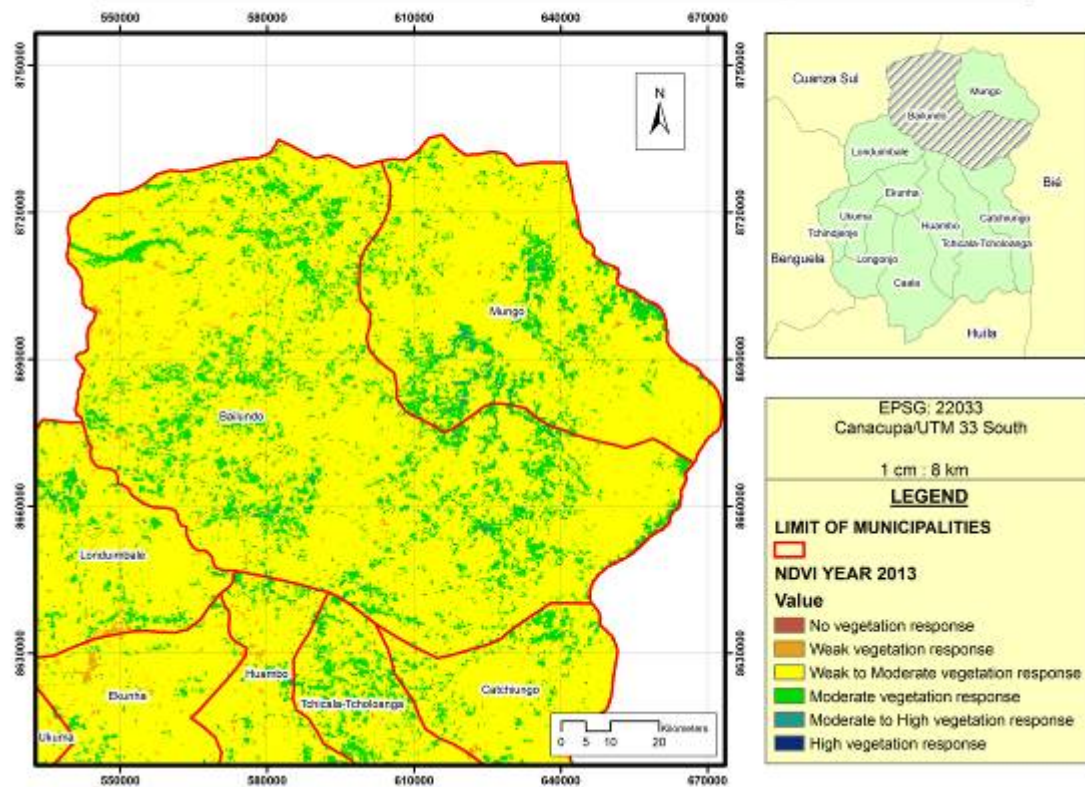
NDVI of Huambo province, municipality of Bailundo.



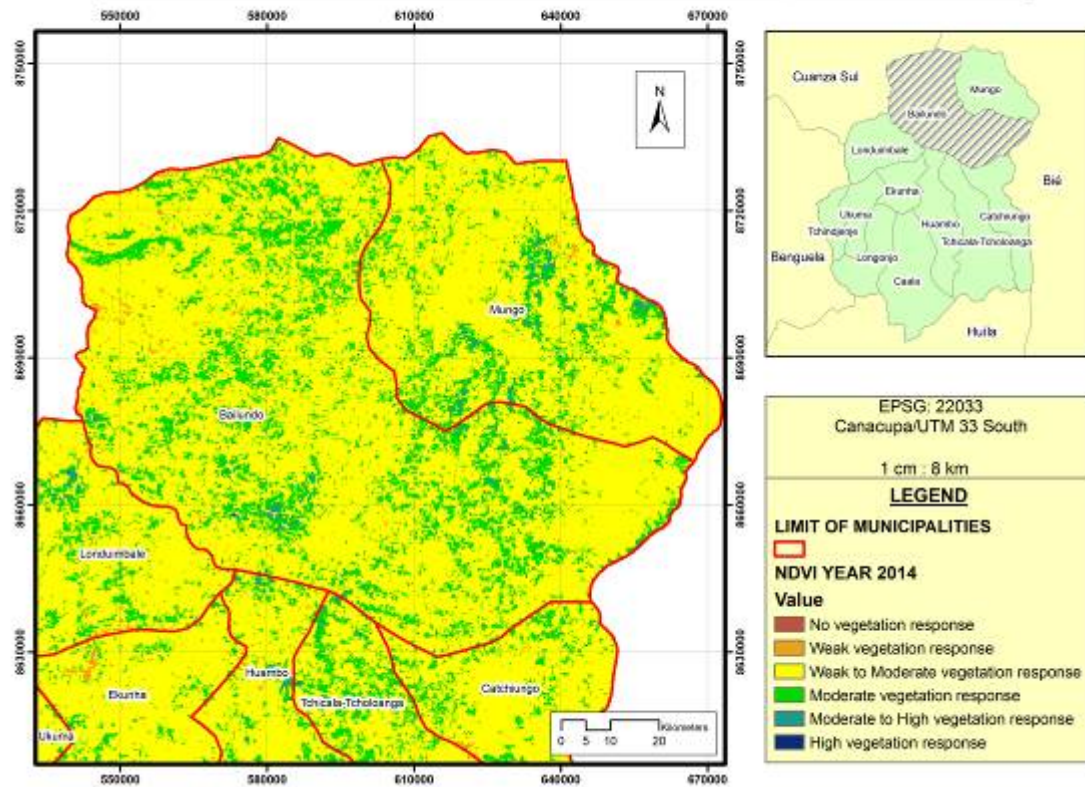
NDVI of Huambo province, municipality of Bailundo.



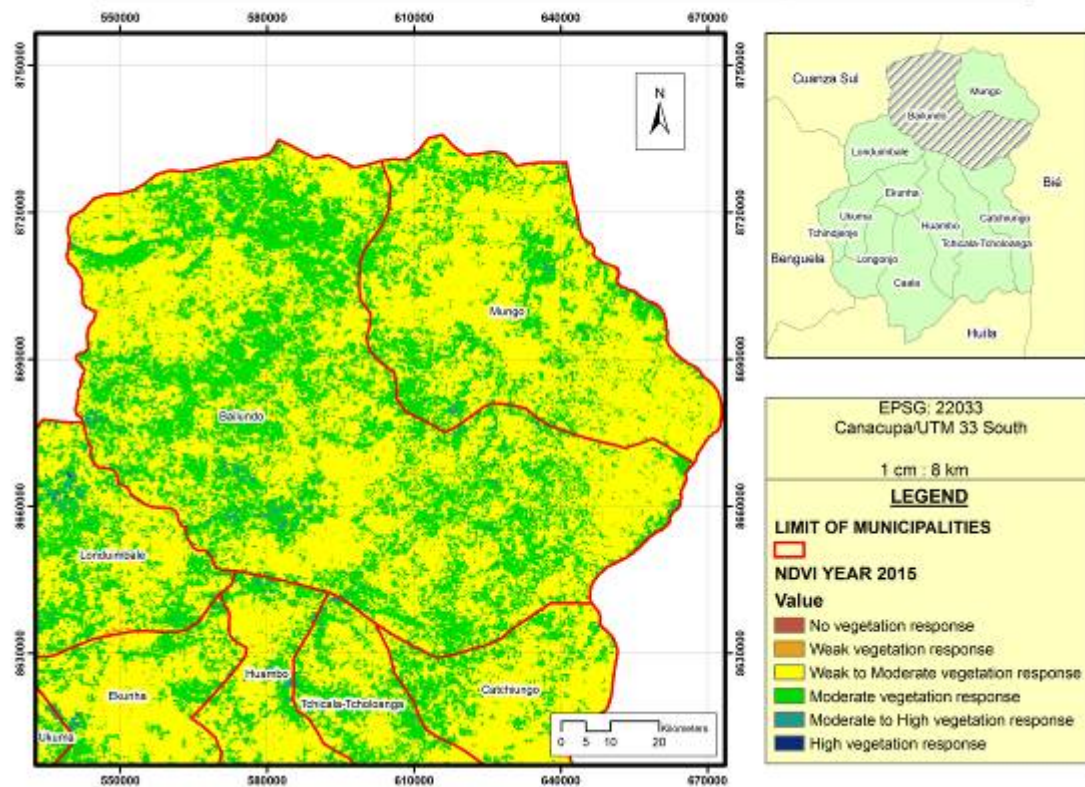
NDVI of Huambo province, municipality of Bailundo.



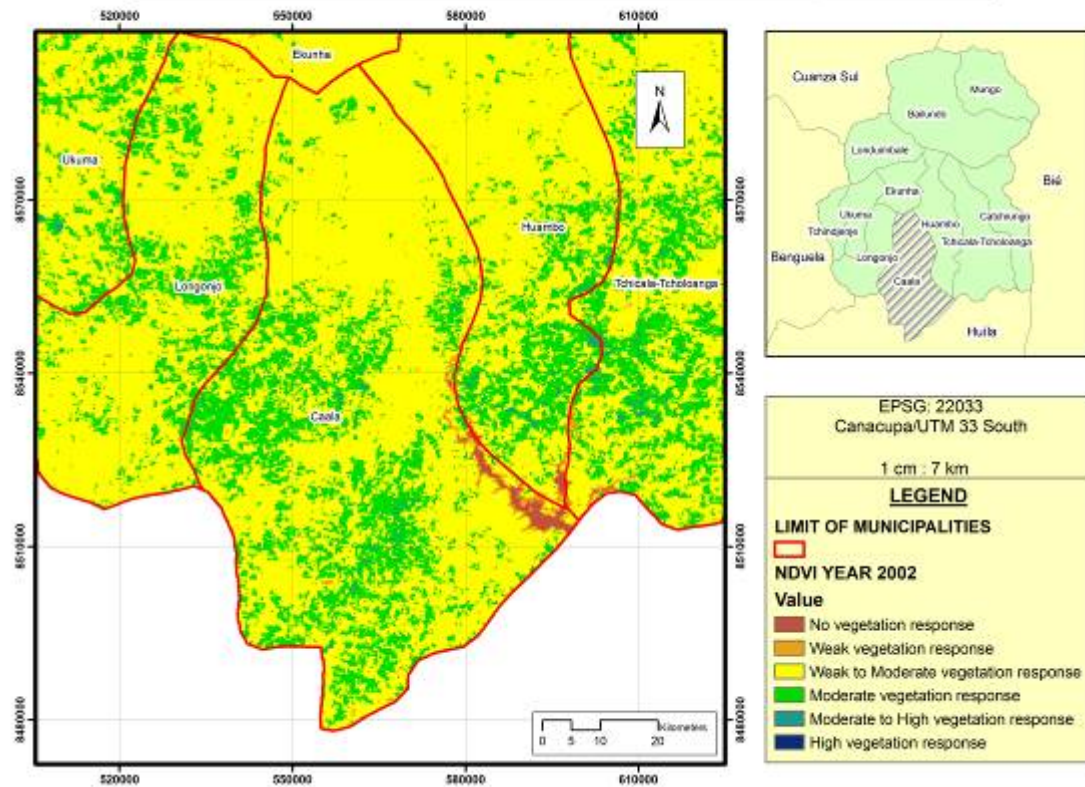
NDVI of Huambo province, municipality of Bailundo.



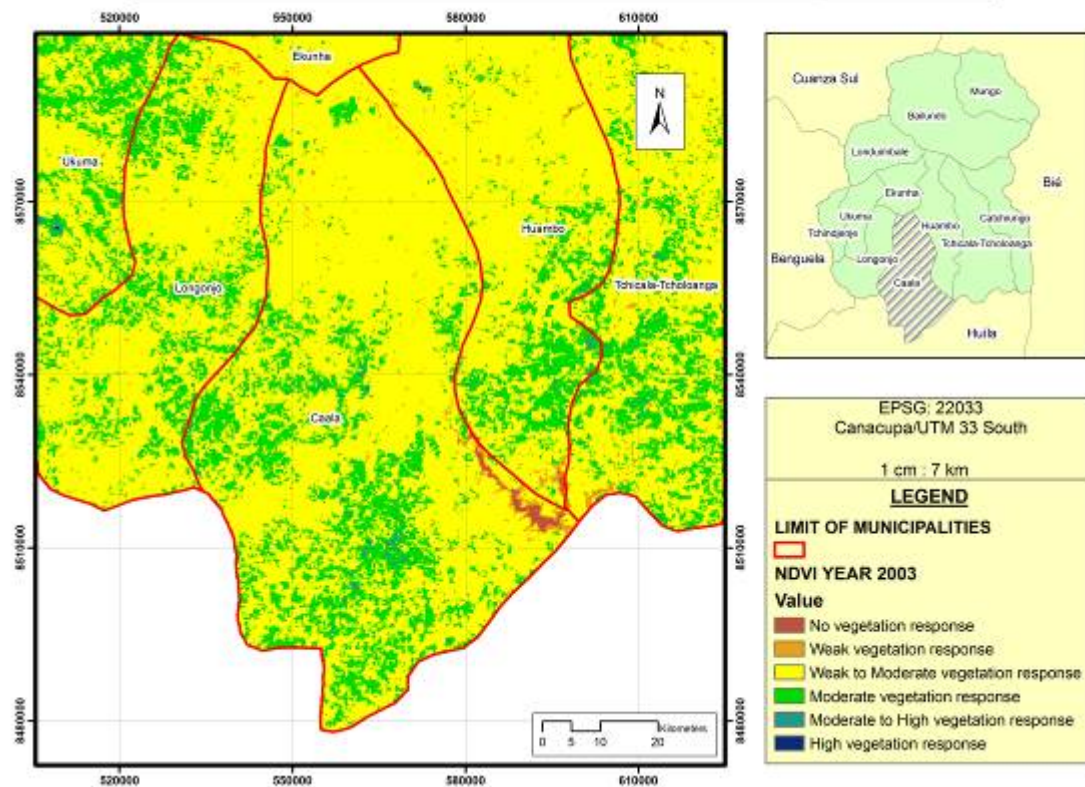
NDVI of Huambo province, municipality of Bailundo.



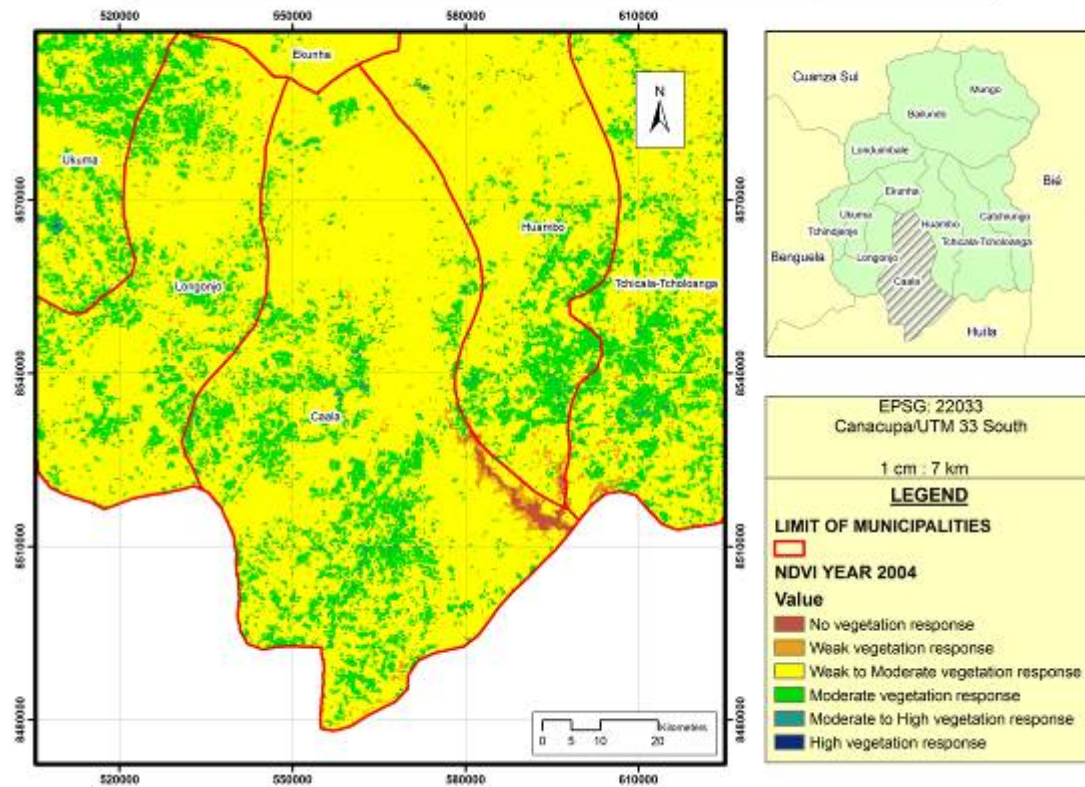
NDVI of Huambo province, municipality of Caala.



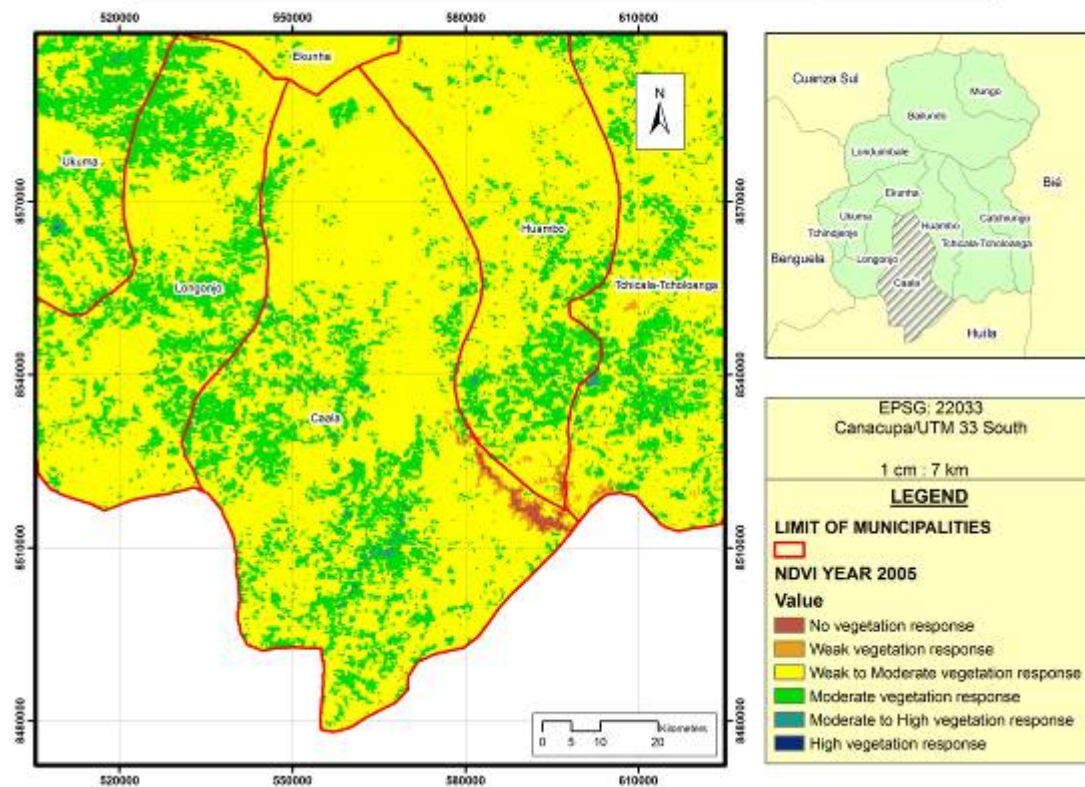
NDVI of Huambo province, municipality of Caala.



NDVI of Huambo province, municipality of Caala.

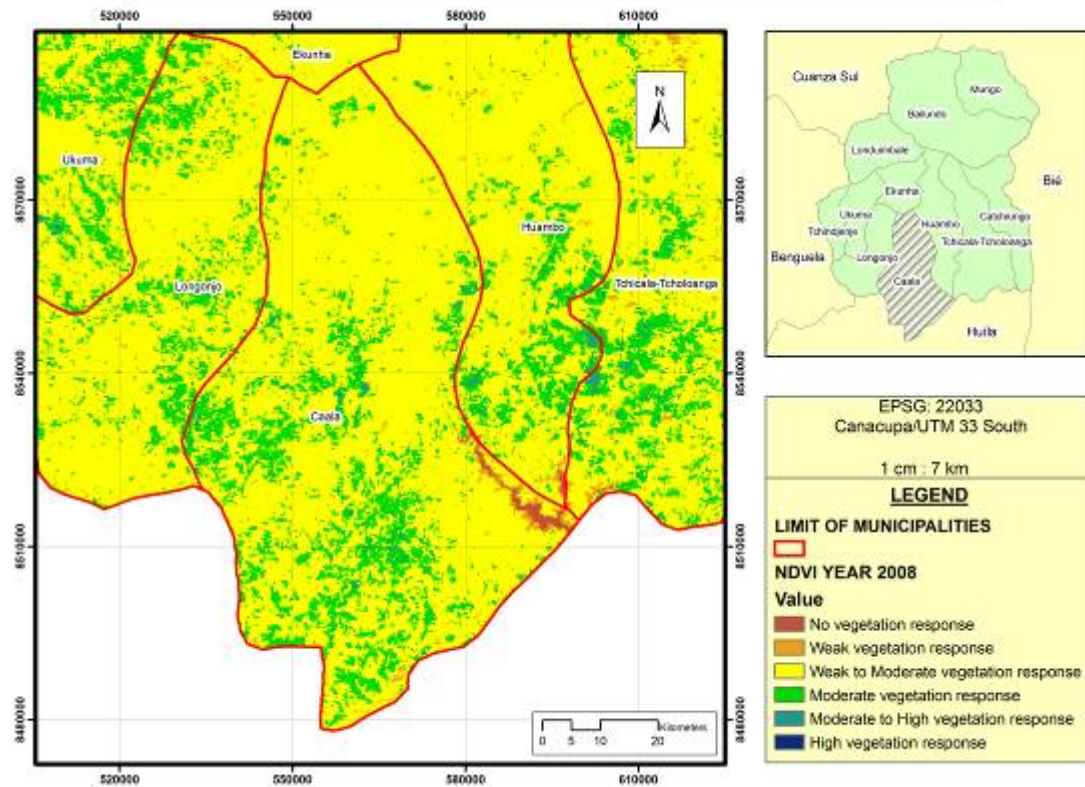


NDVI of Huambo province, municipality of Caala.

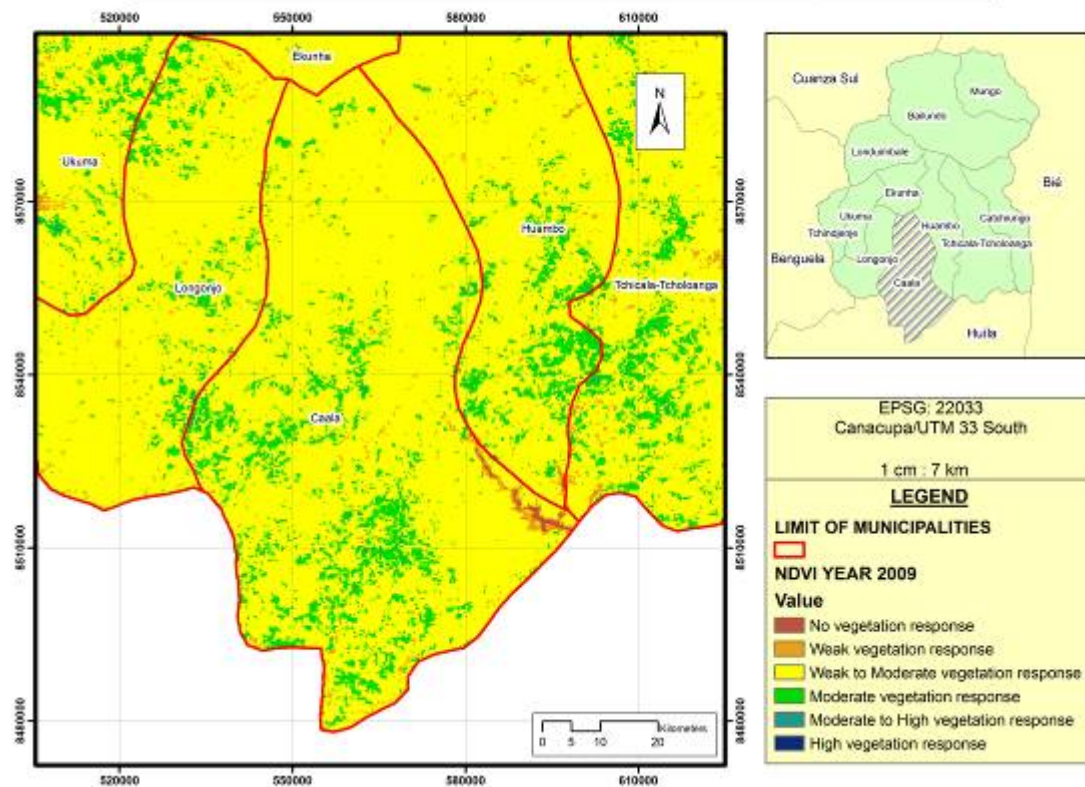




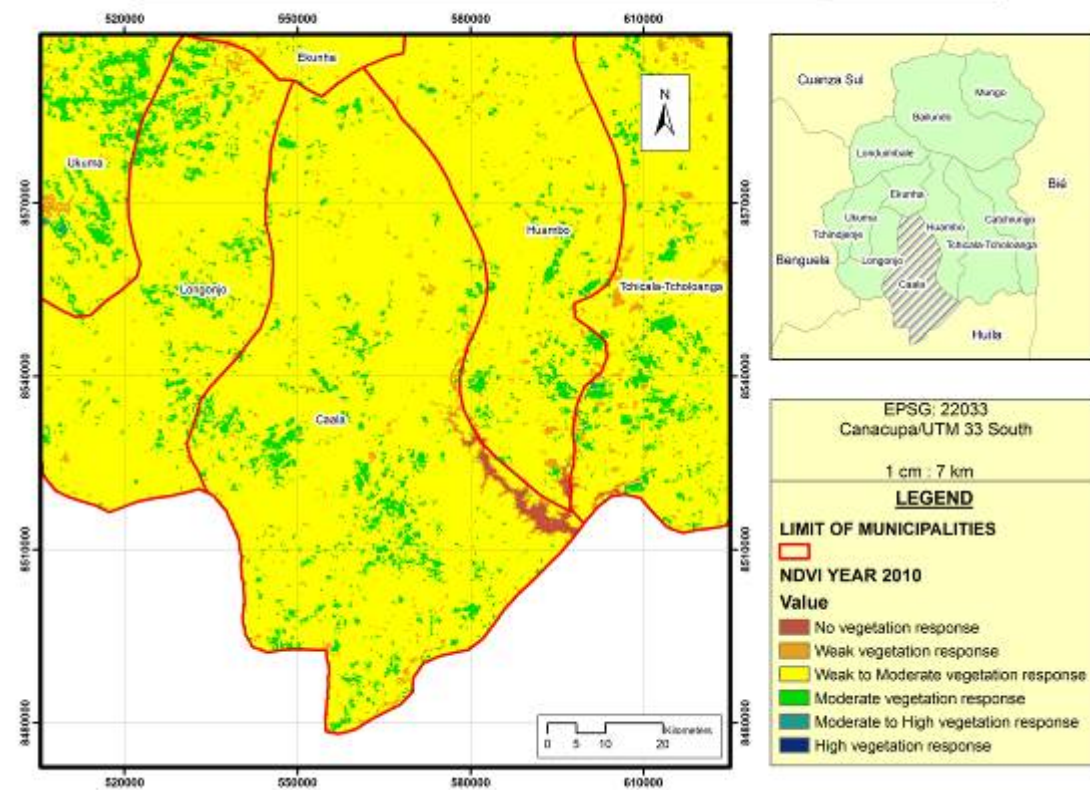
NDVI of Huambo province, municipality of Caala.



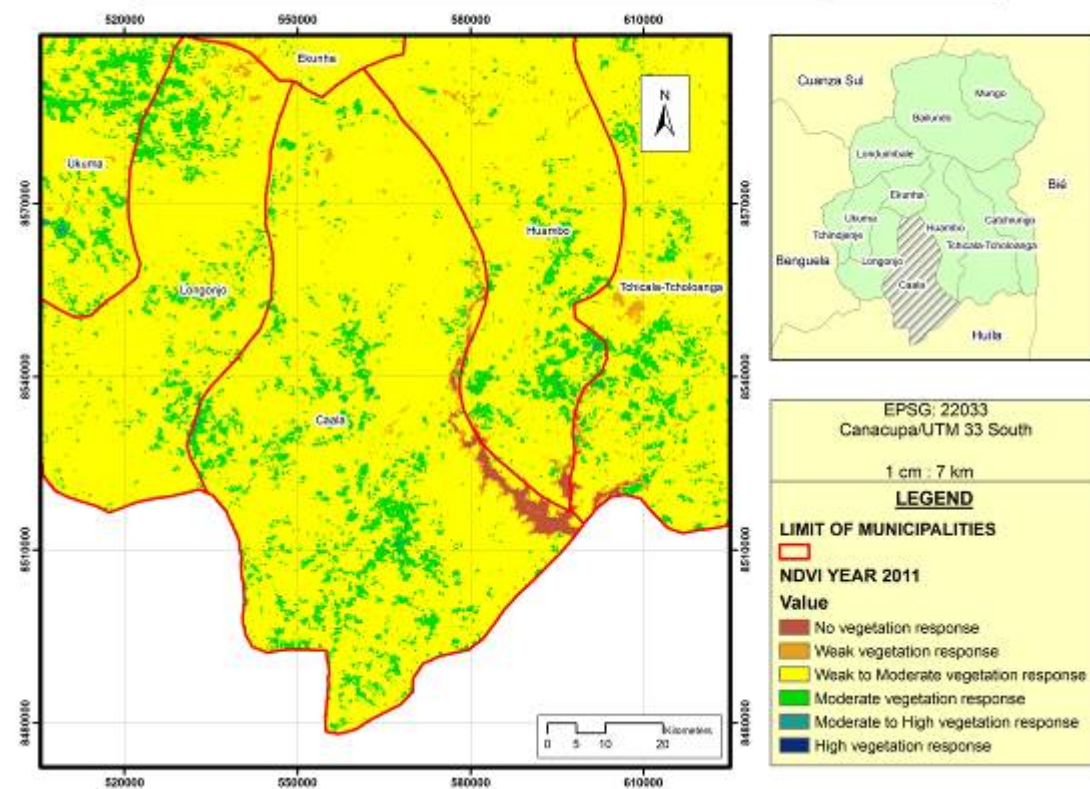
NDVI of Huambo province, municipality of Caala.



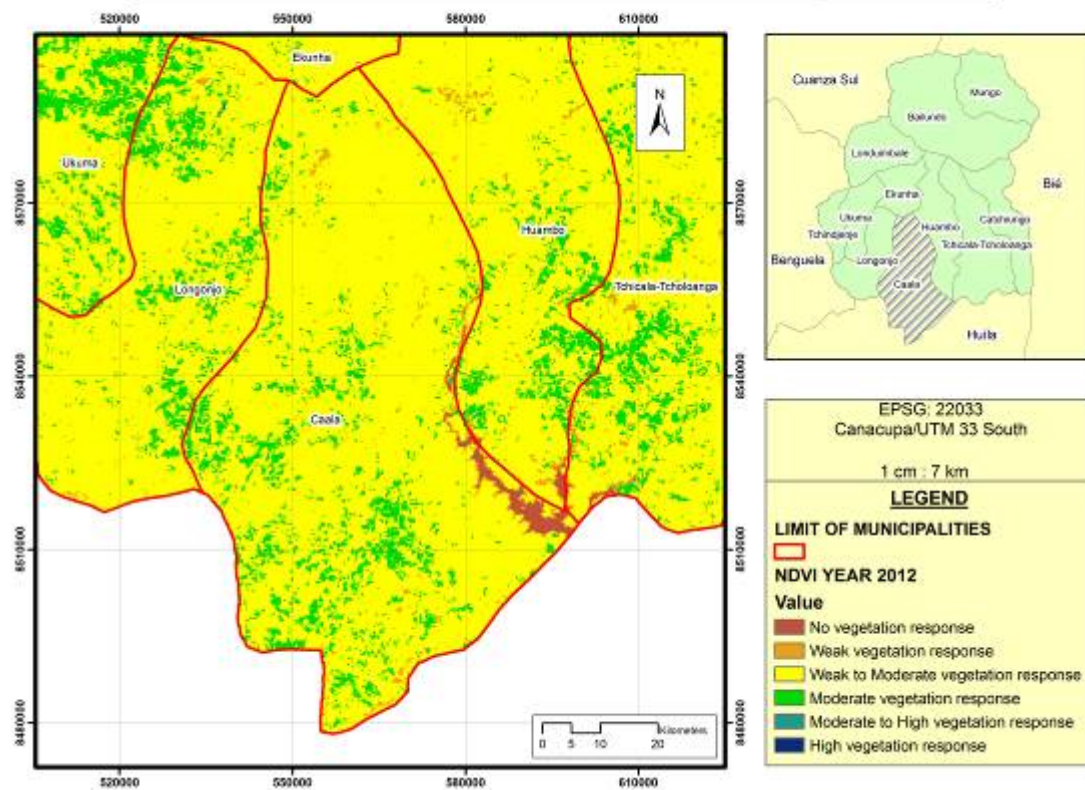
NDVI of Huambo province, municipality of Caala.



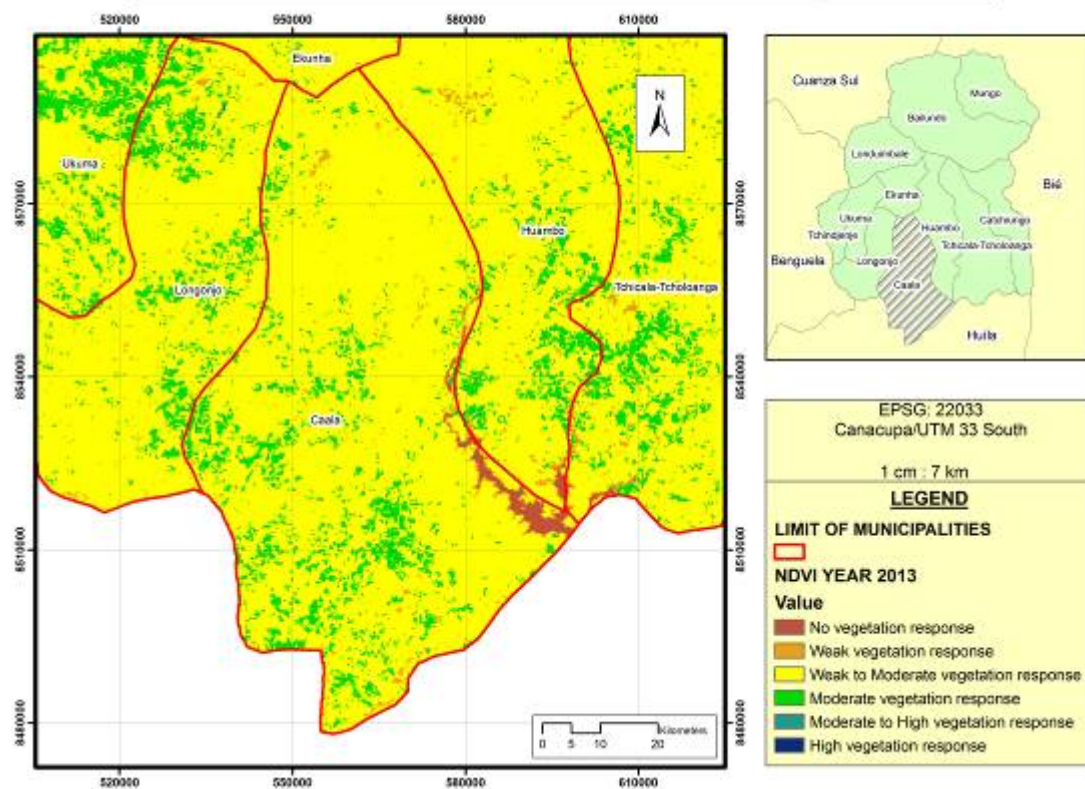
NDVI of Huambo province, municipality of Caala.



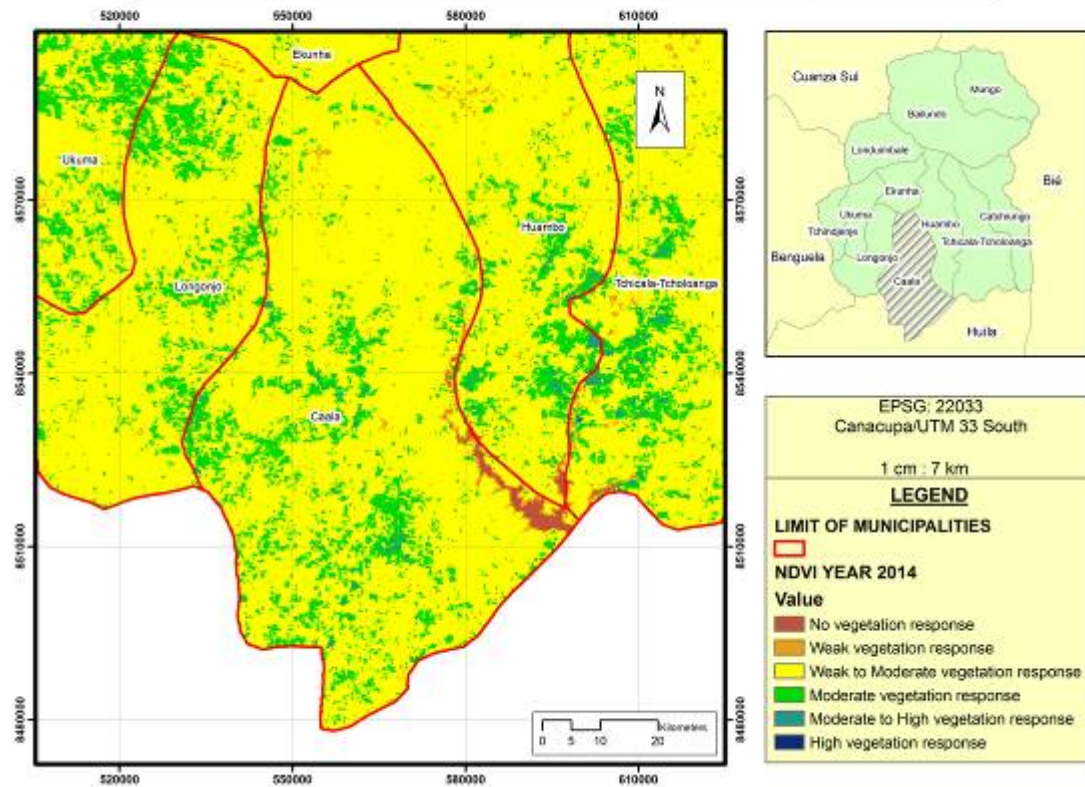
NDVI of Huambo province, municipality of Caala.



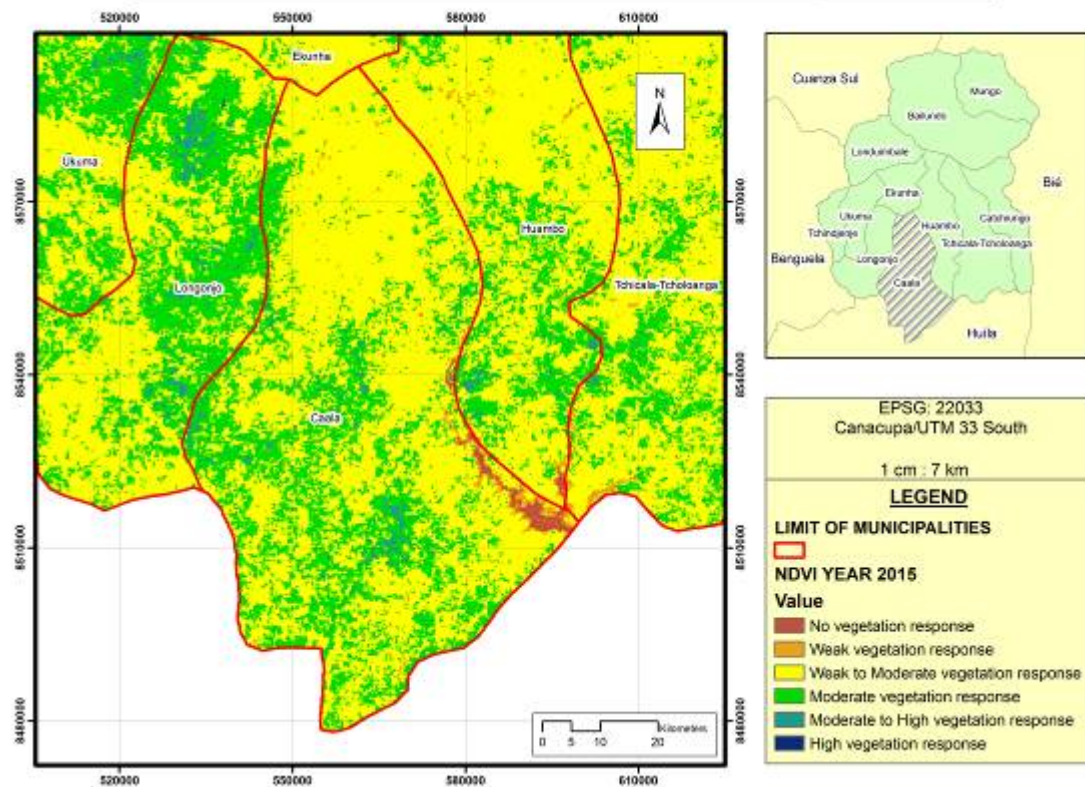
NDVI of Huambo province, municipality of Caala.



NDVI of Huambo province, municipality of Caala.

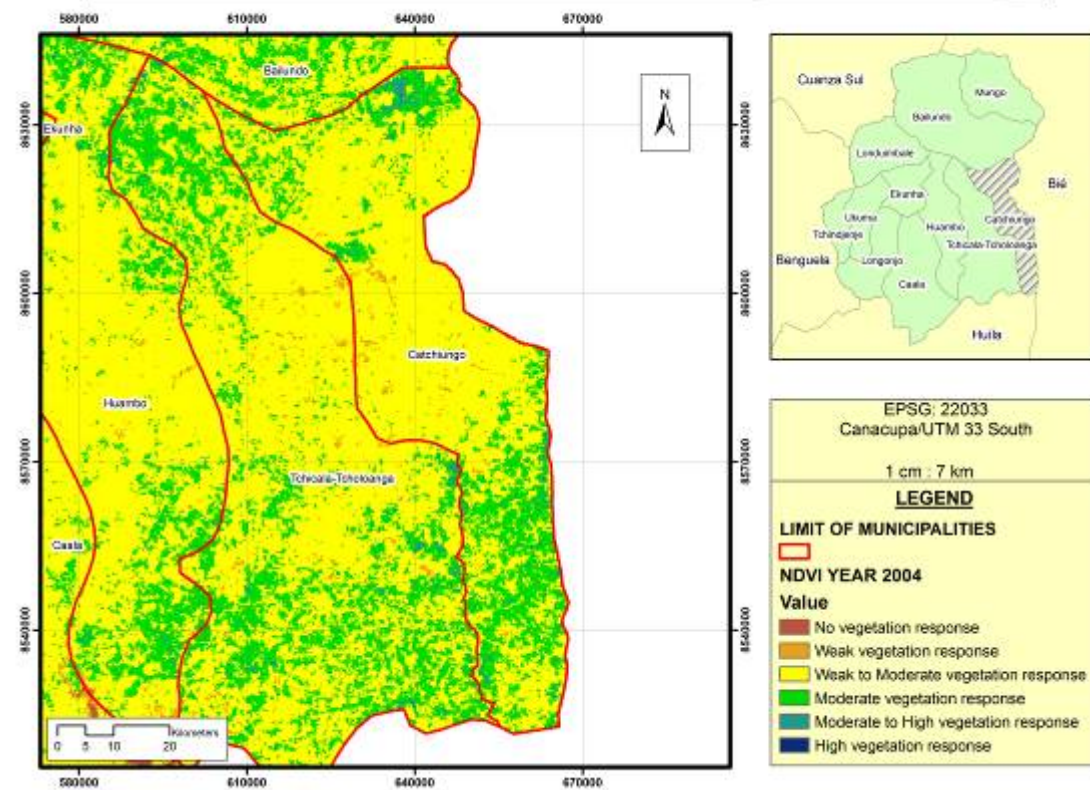


NDVI of Huambo province, municipality of Caala.

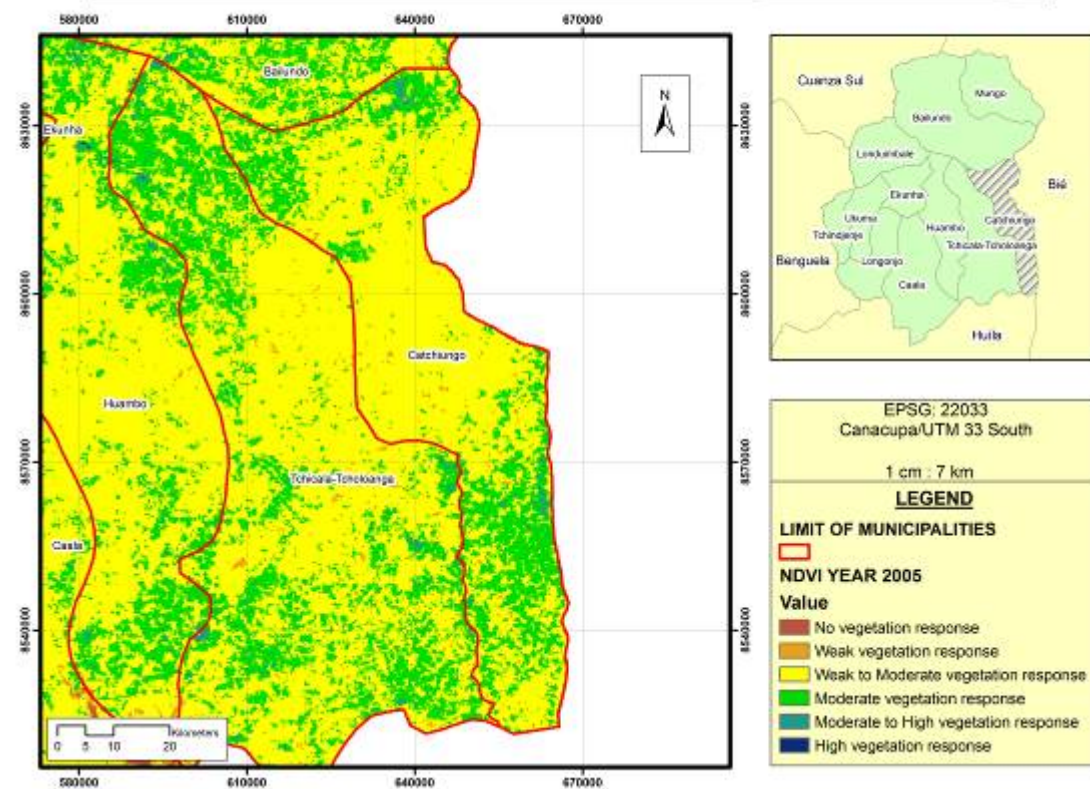




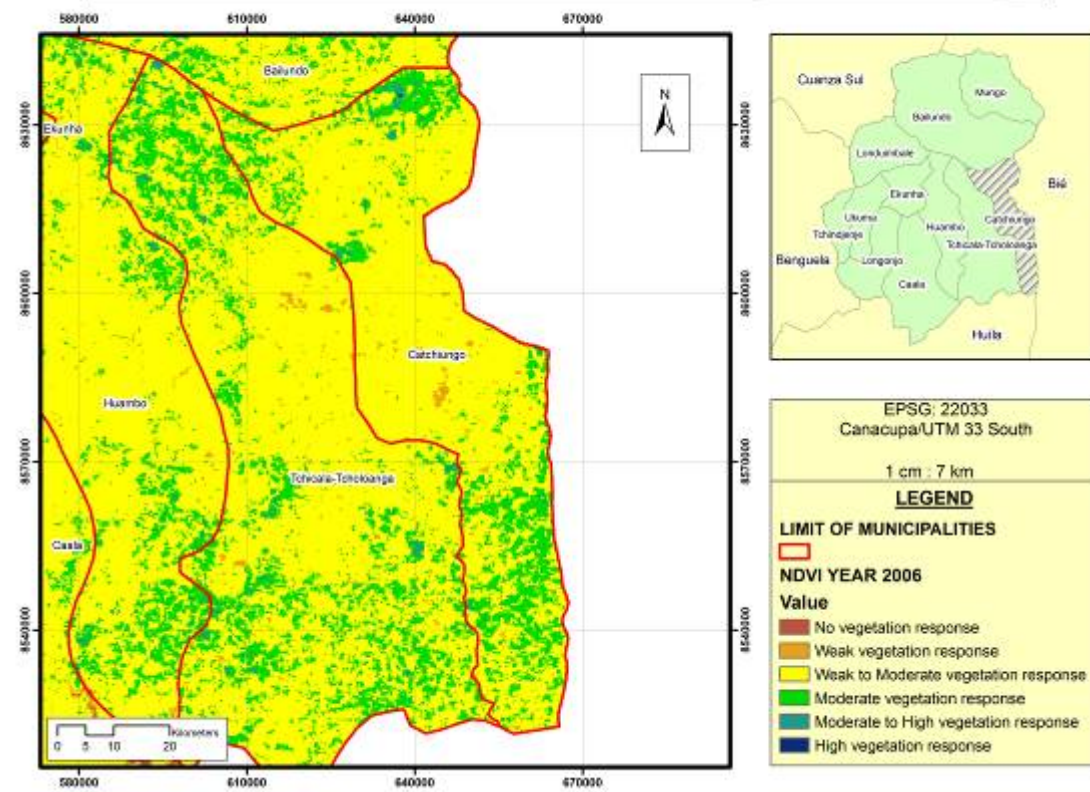
NDVI of Huambo province, municipality of Catchiungo.



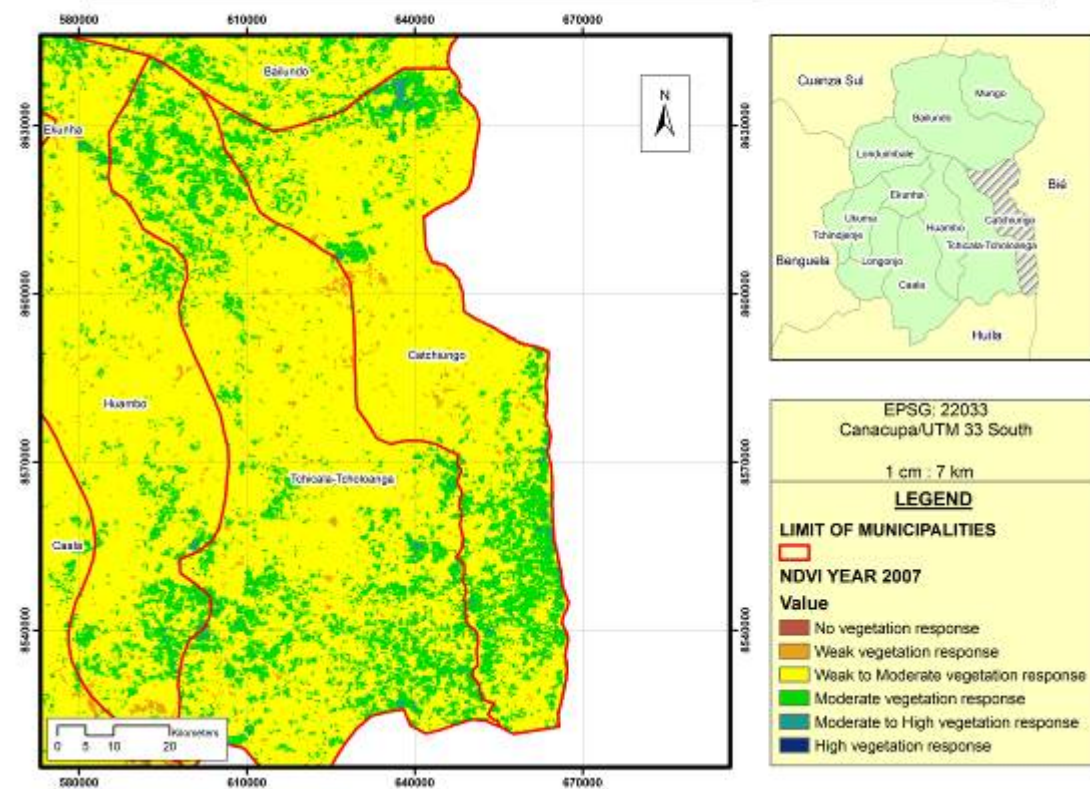
NDVI of Huambo province, municipality of Catchiungo.



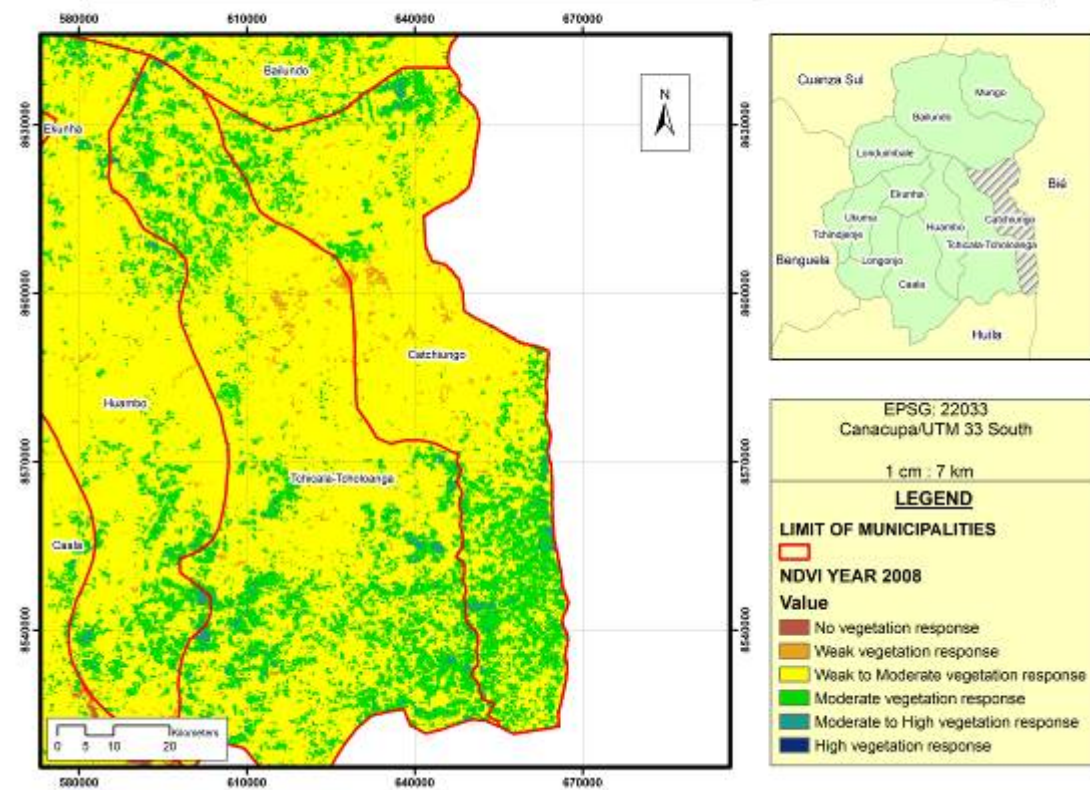
NDVI of Huambo province, municipality of Catchiungo.



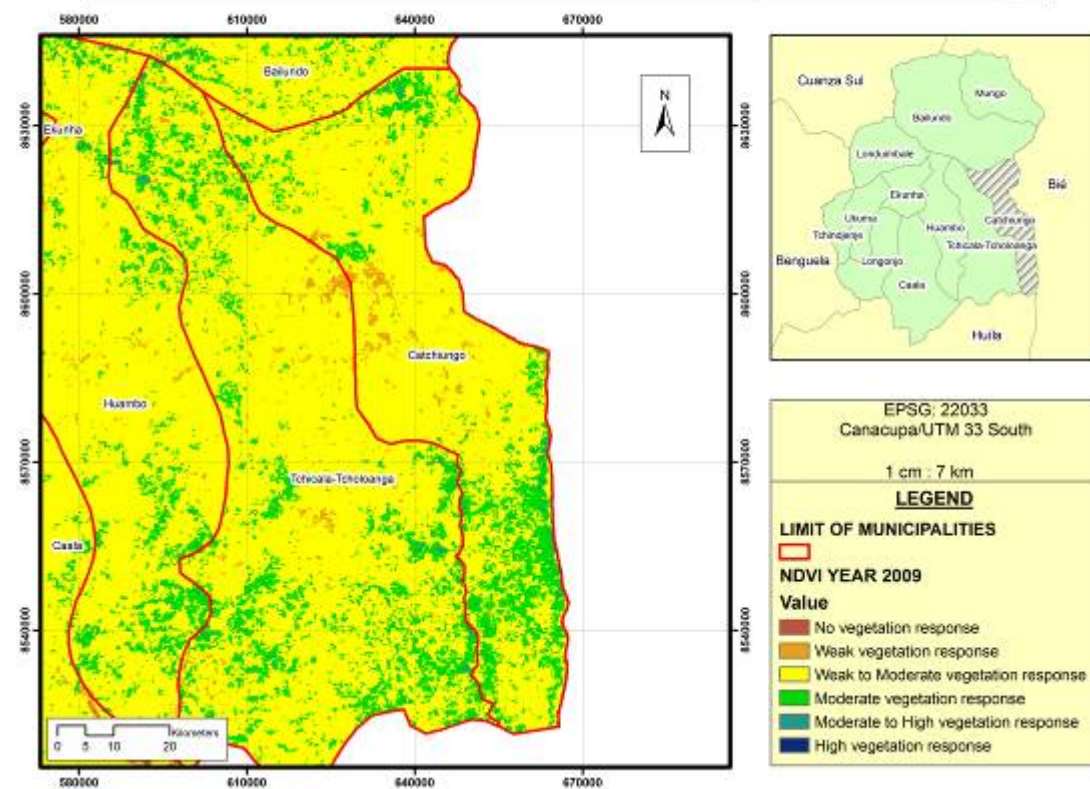
NDVI of Huambo province, municipality of Catchiungo.



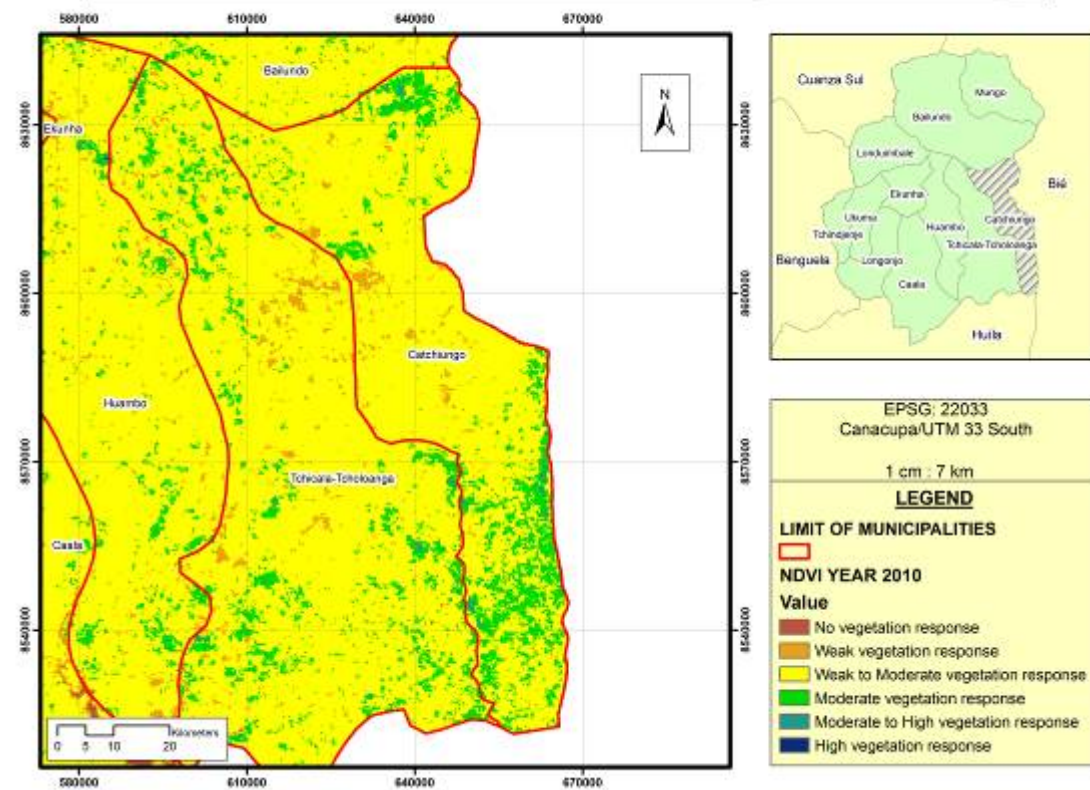
NDVI of Huambo province, municipality of Catchiungo.



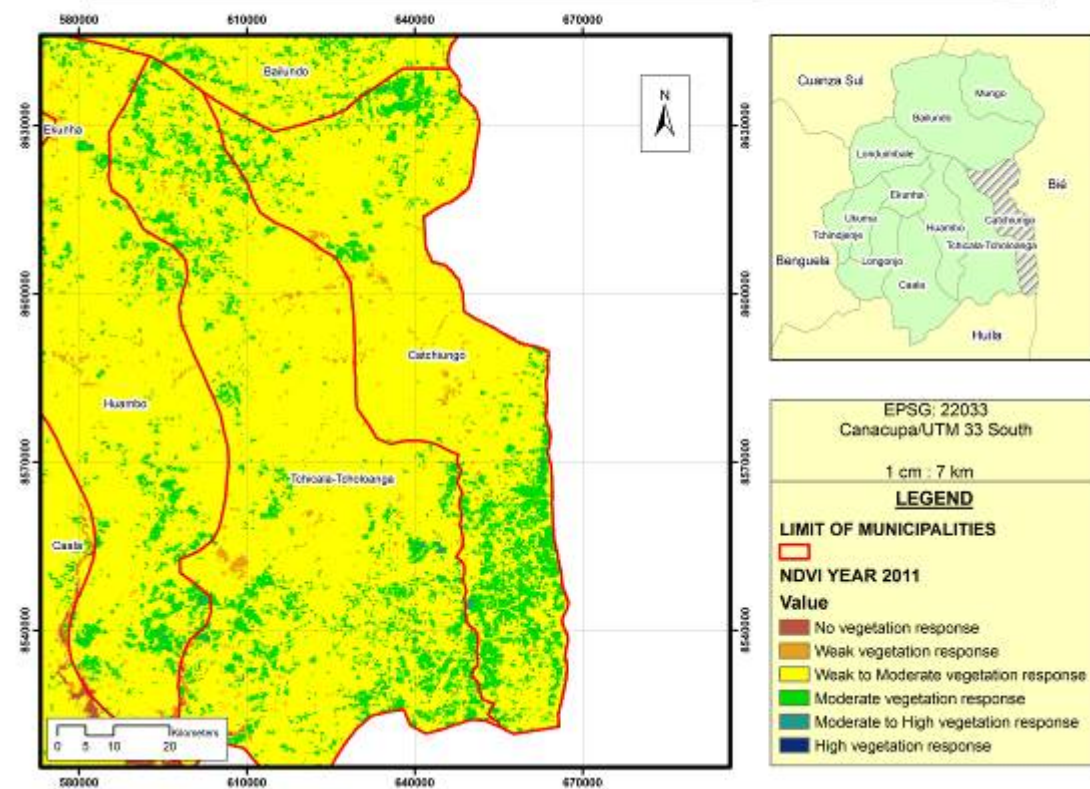
NDVI of Huambo province, municipality of Catchiungo.



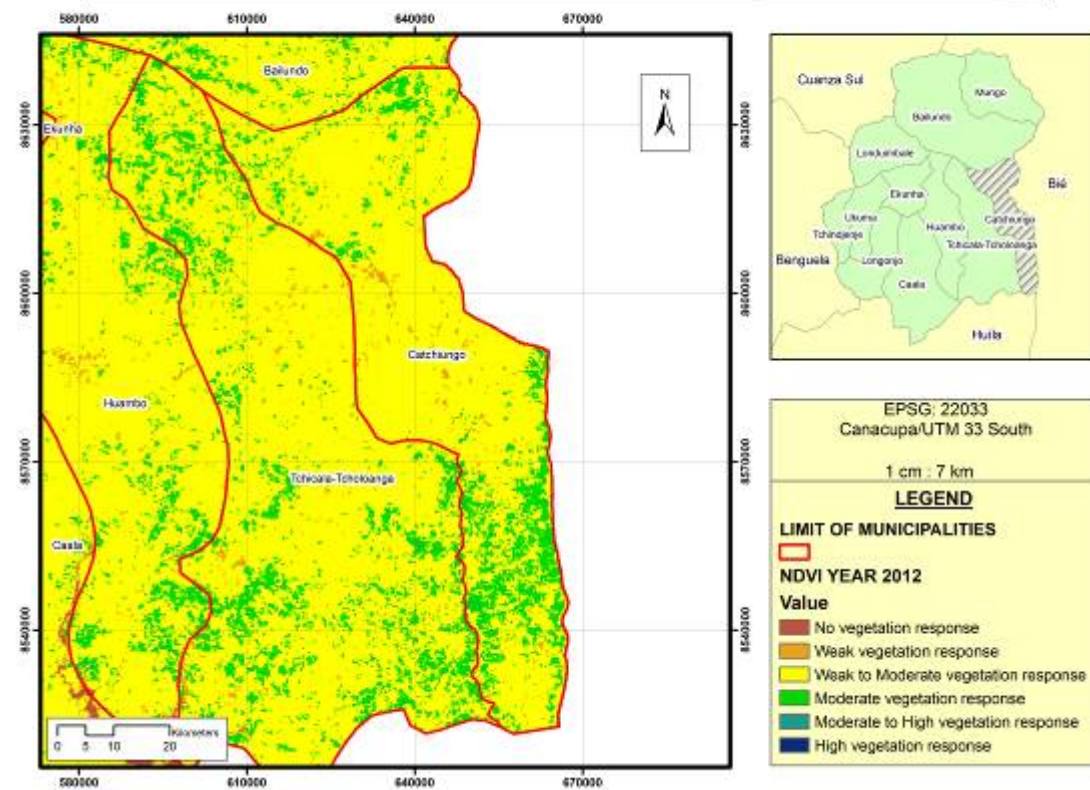
NDVI of Huambo province, municipality of Catchiungo.



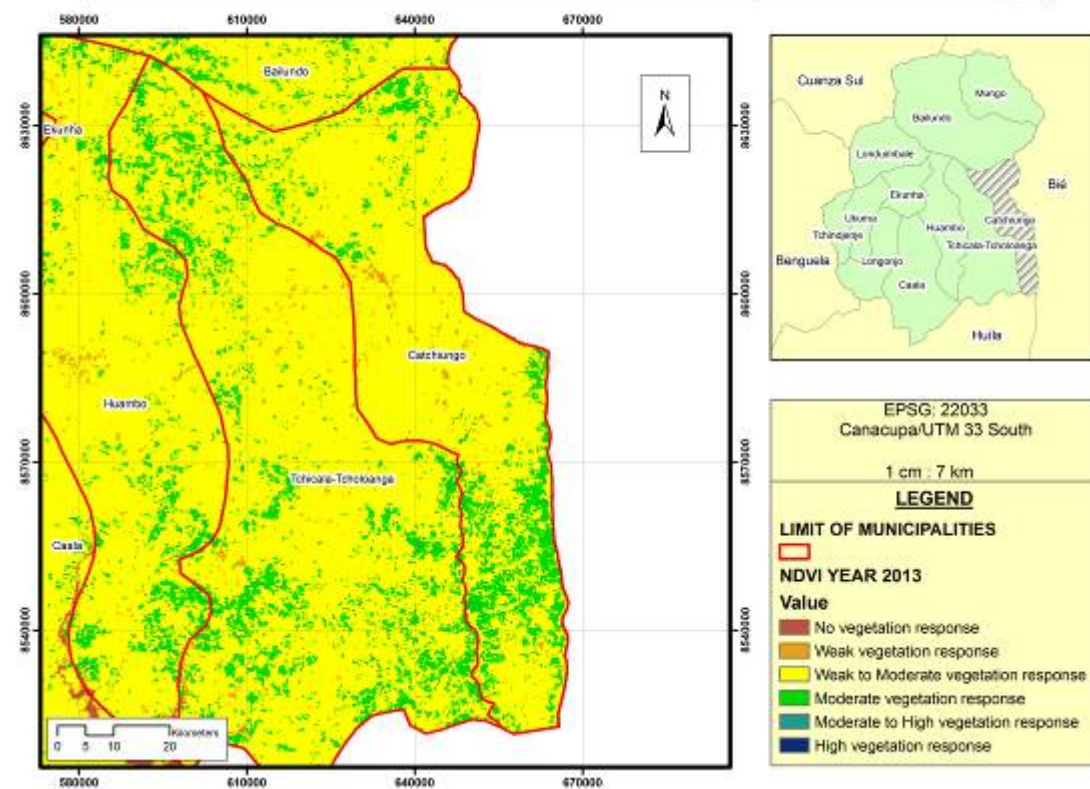
NDVI of Huambo province, municipality of Catchiungo.



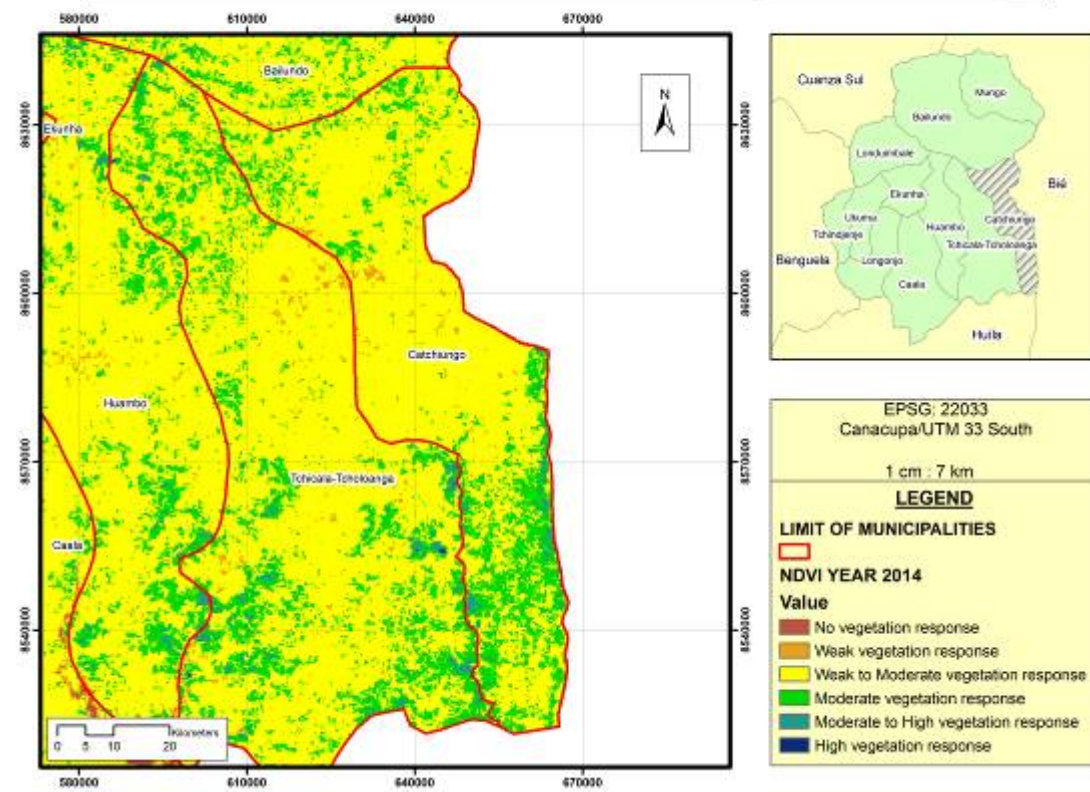
NDVI of Huambo province, municipality of Catchiungo.



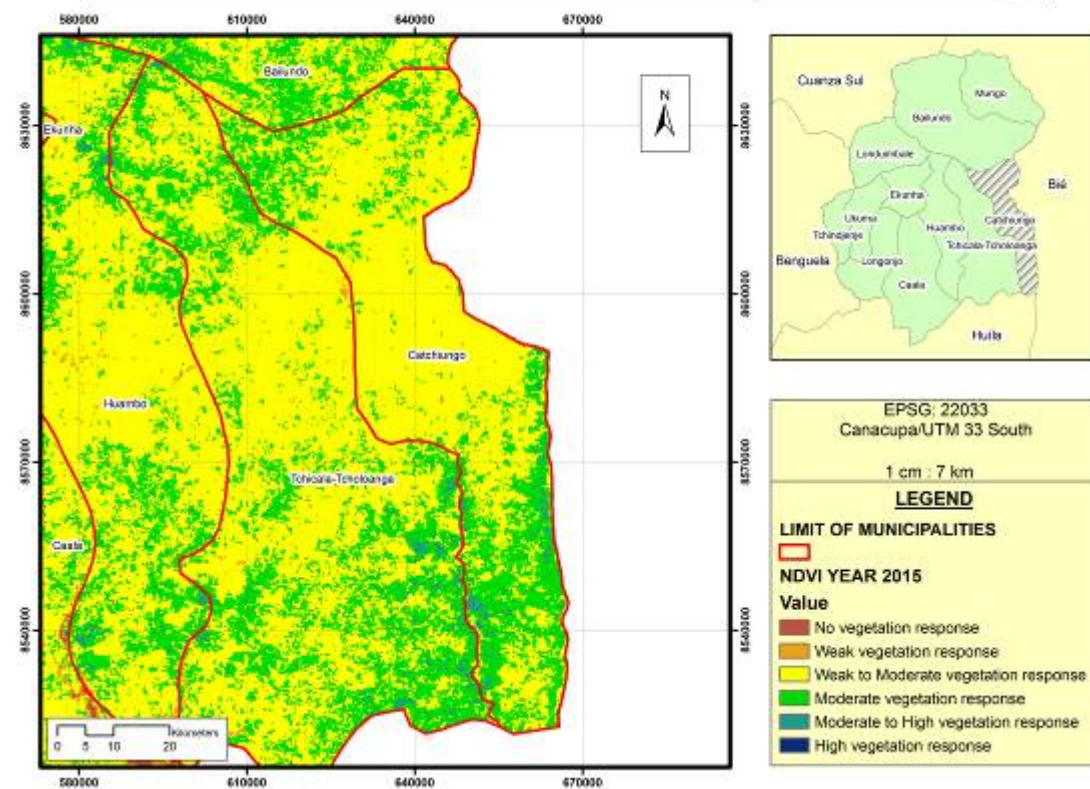
NDVI of Huambo province, municipality of Catchiungo.



NDVI of Huambo province, municipality of Catchiungo.

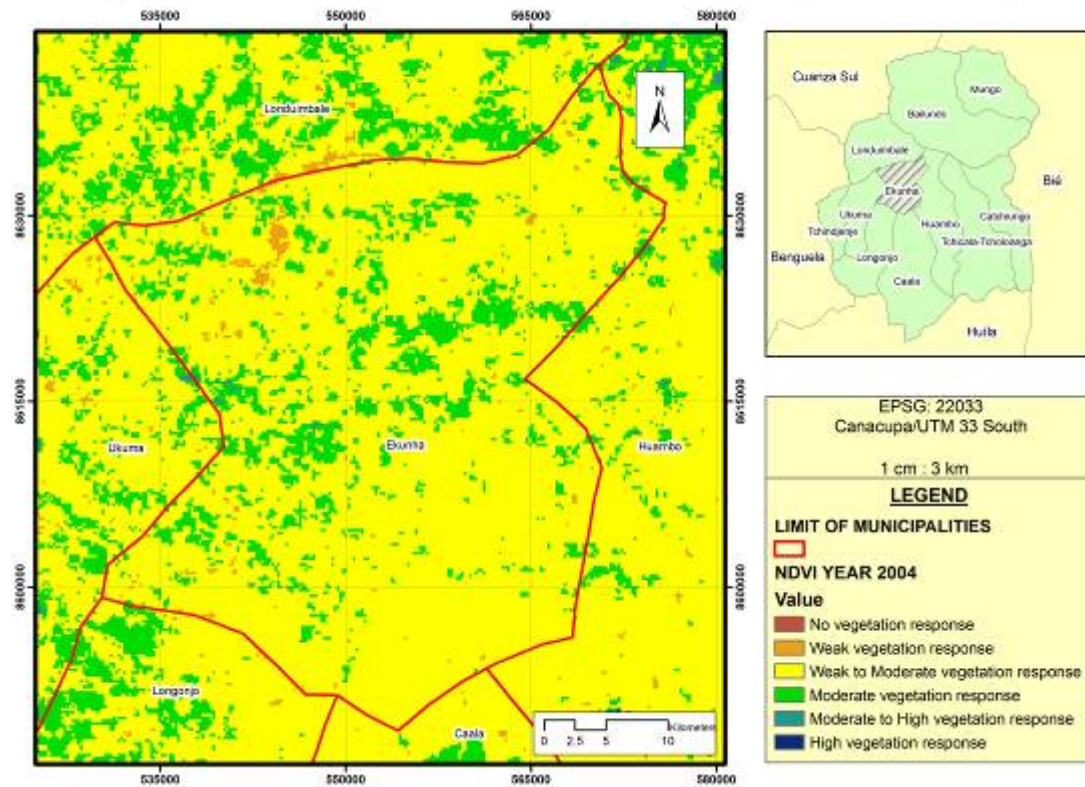


NDVI of Huambo province, municipality of Catchiungo.

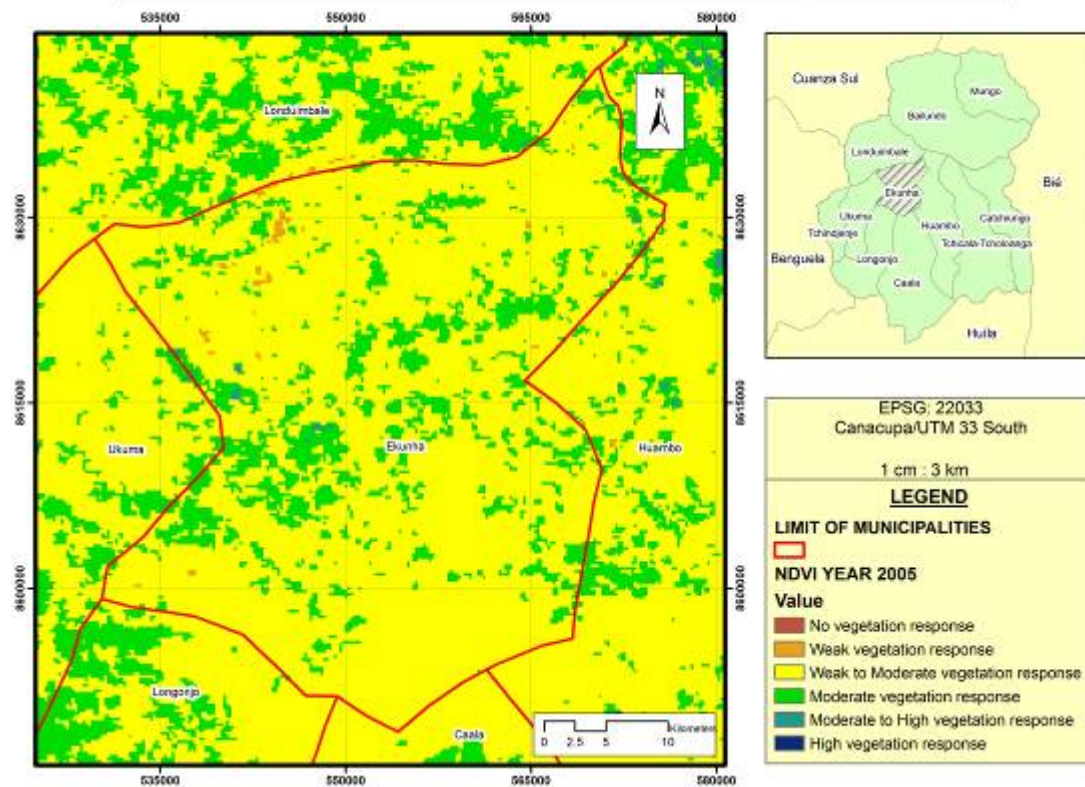




NDVI of Huambo province, municipality of Ekunha.

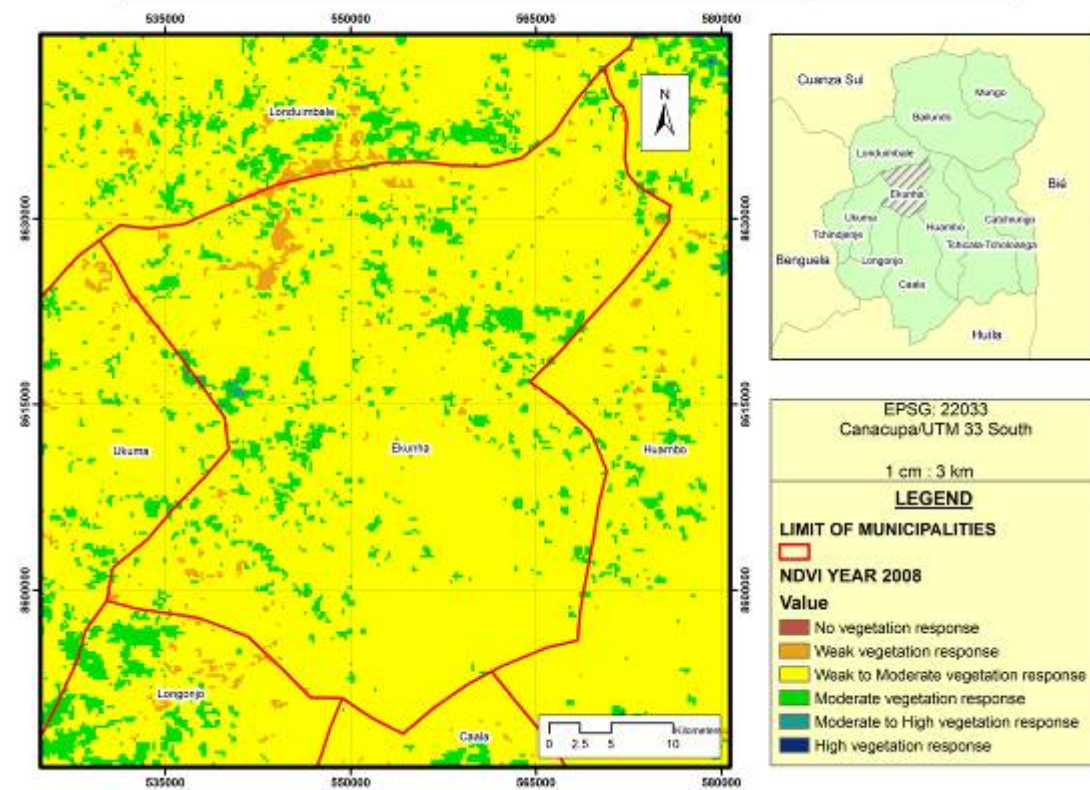


NDVI of Huambo province, municipality of Ekunha.

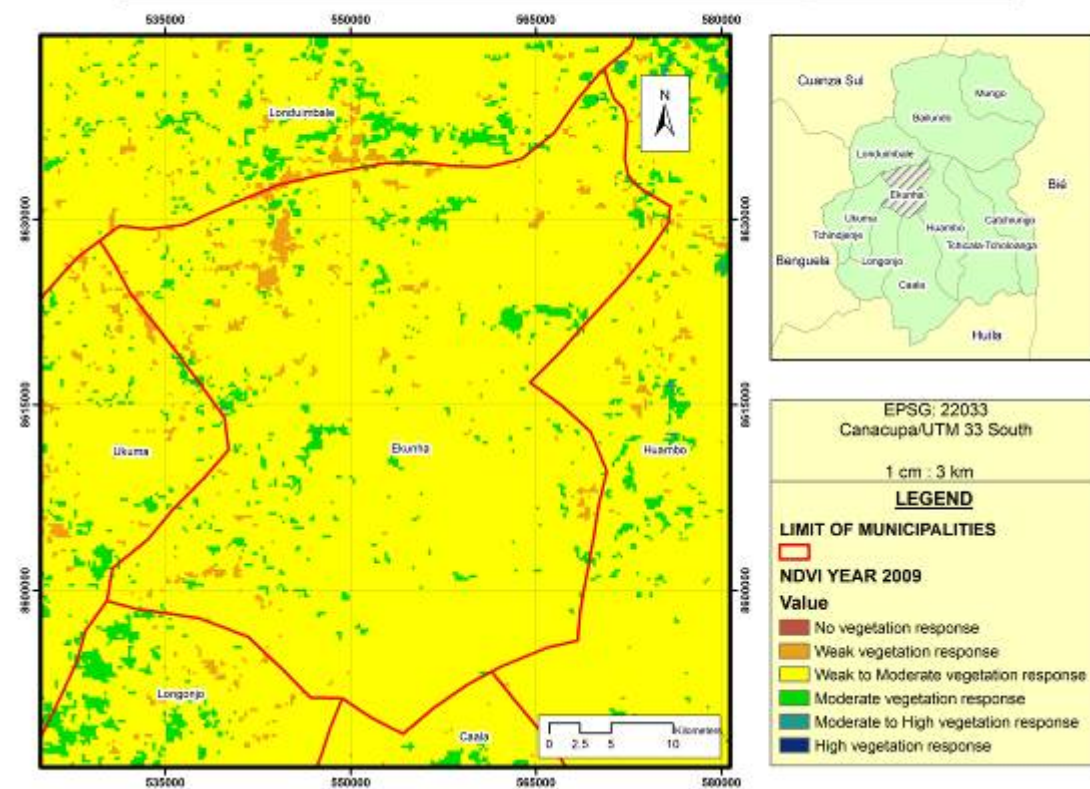




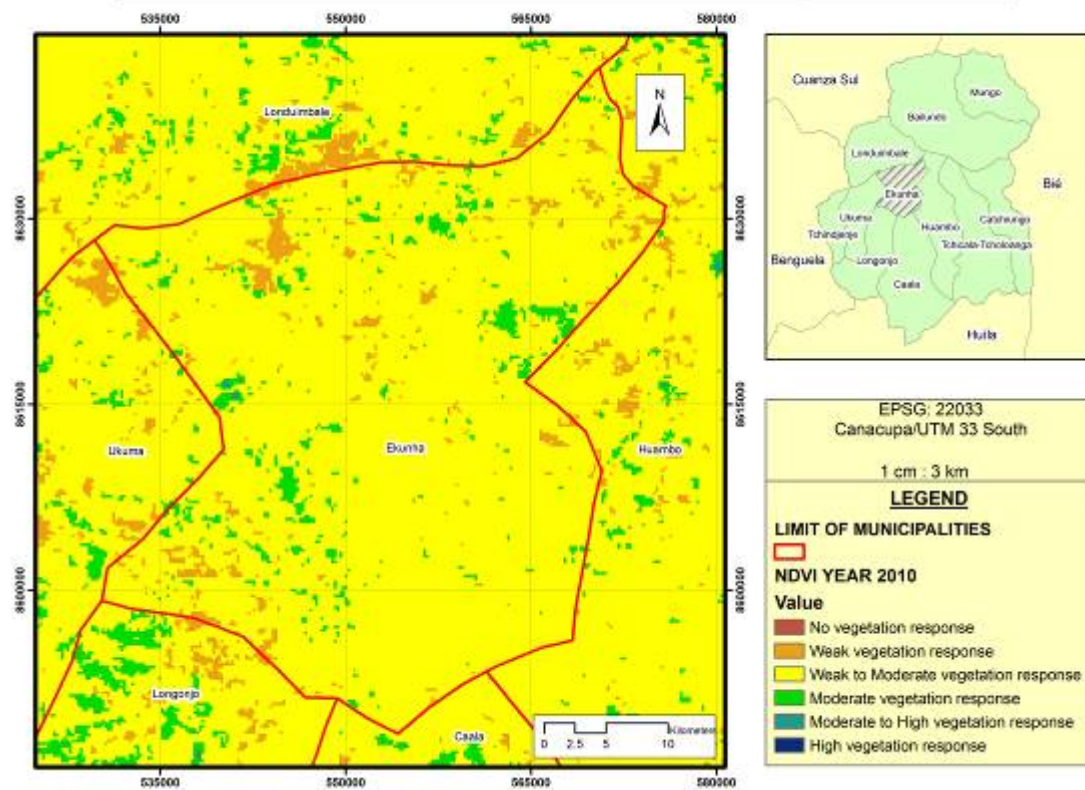
NDVI of Huambo province, municipality of Ekunha.



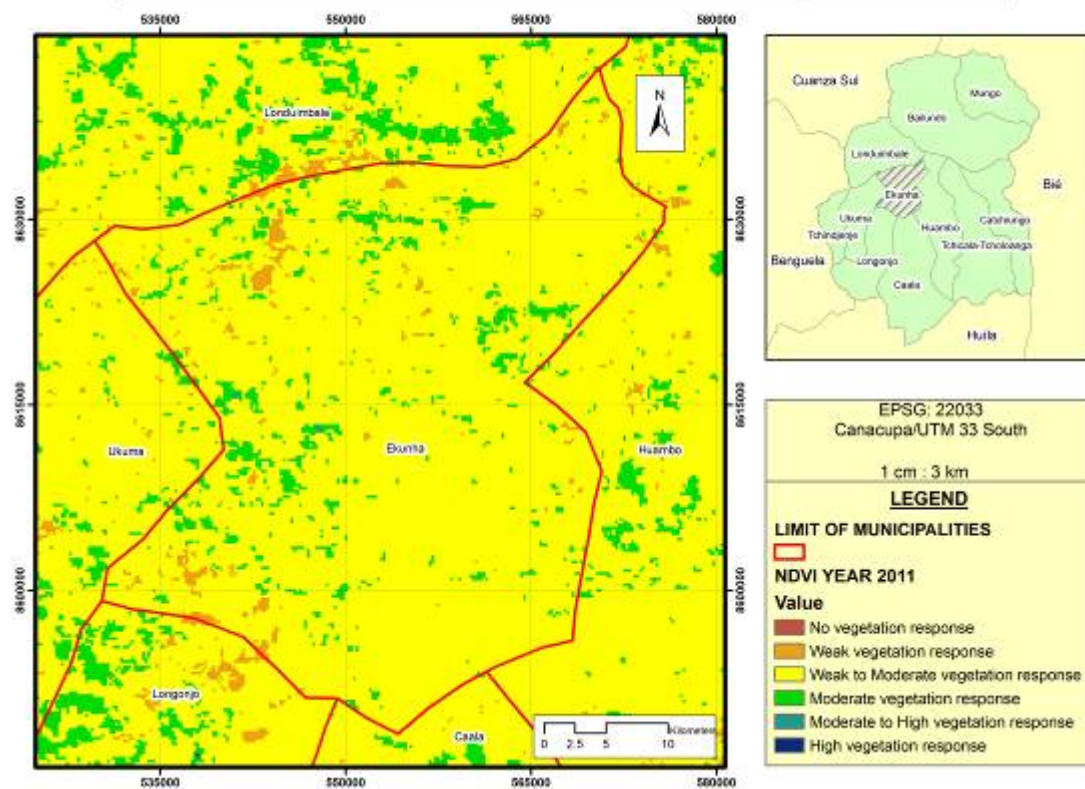
NDVI of Huambo province, municipality of Ekunha.



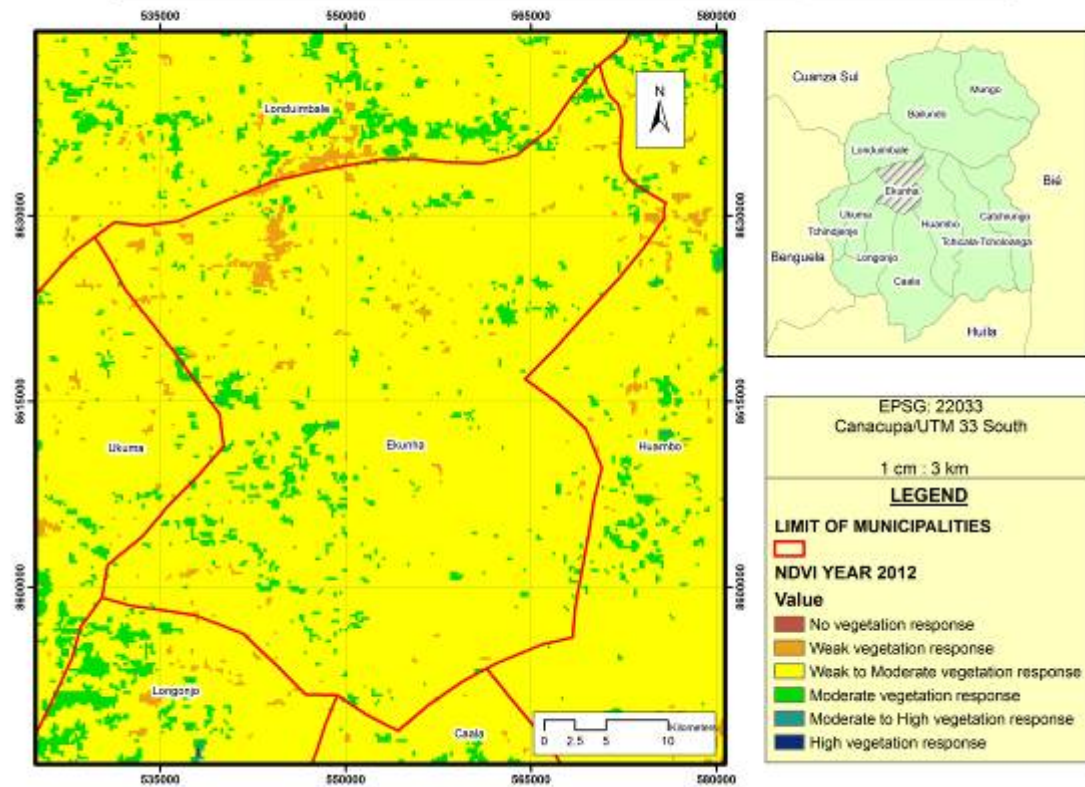
NDVI of Huambo province, municipality of Ekunha.



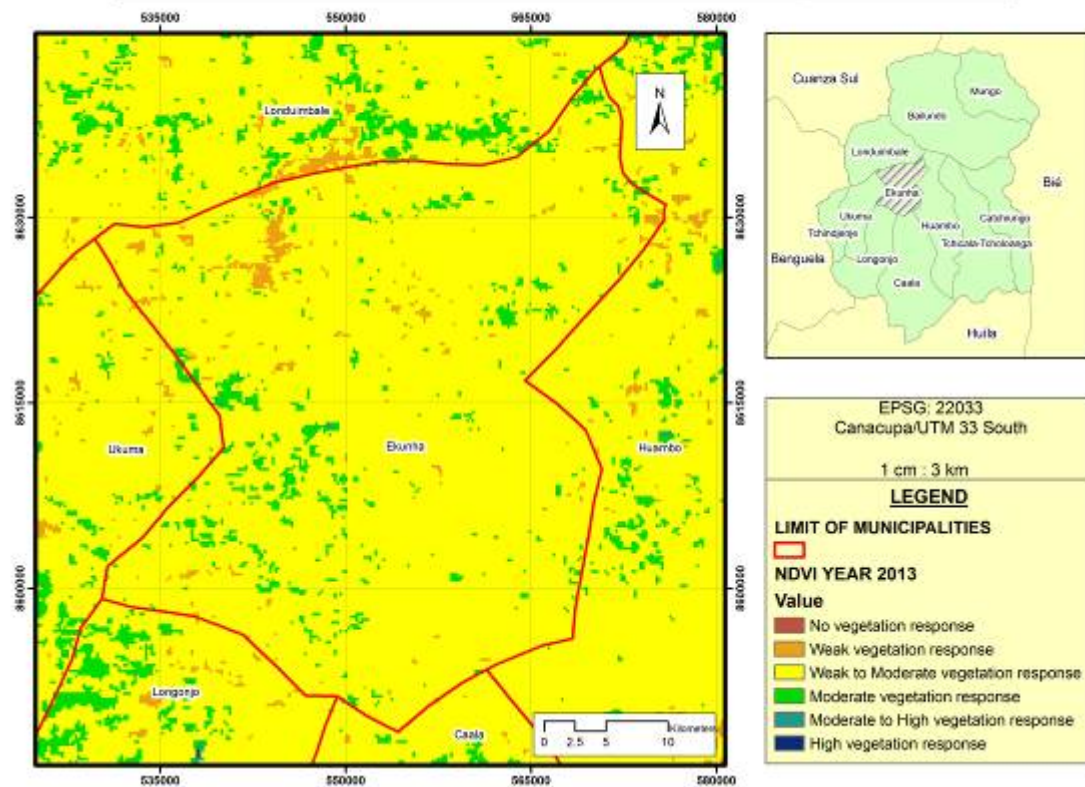
NDVI of Huambo province, municipality of Ekunha.

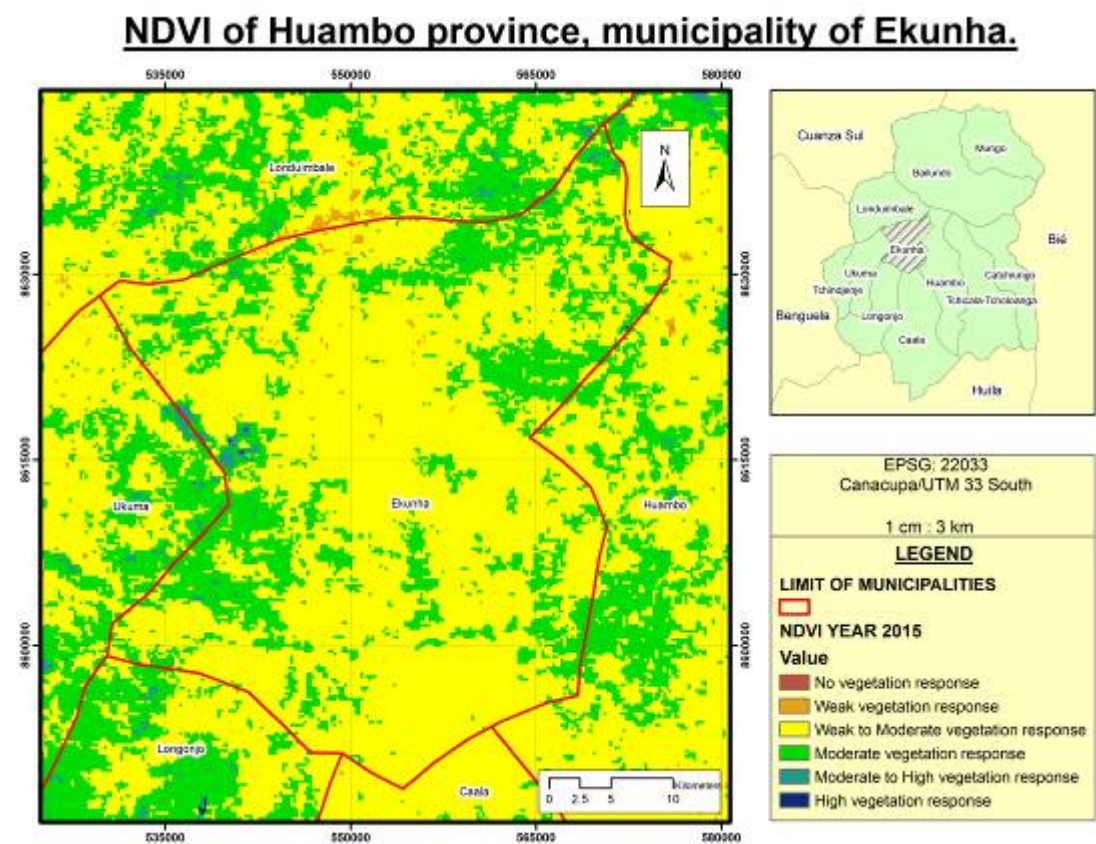
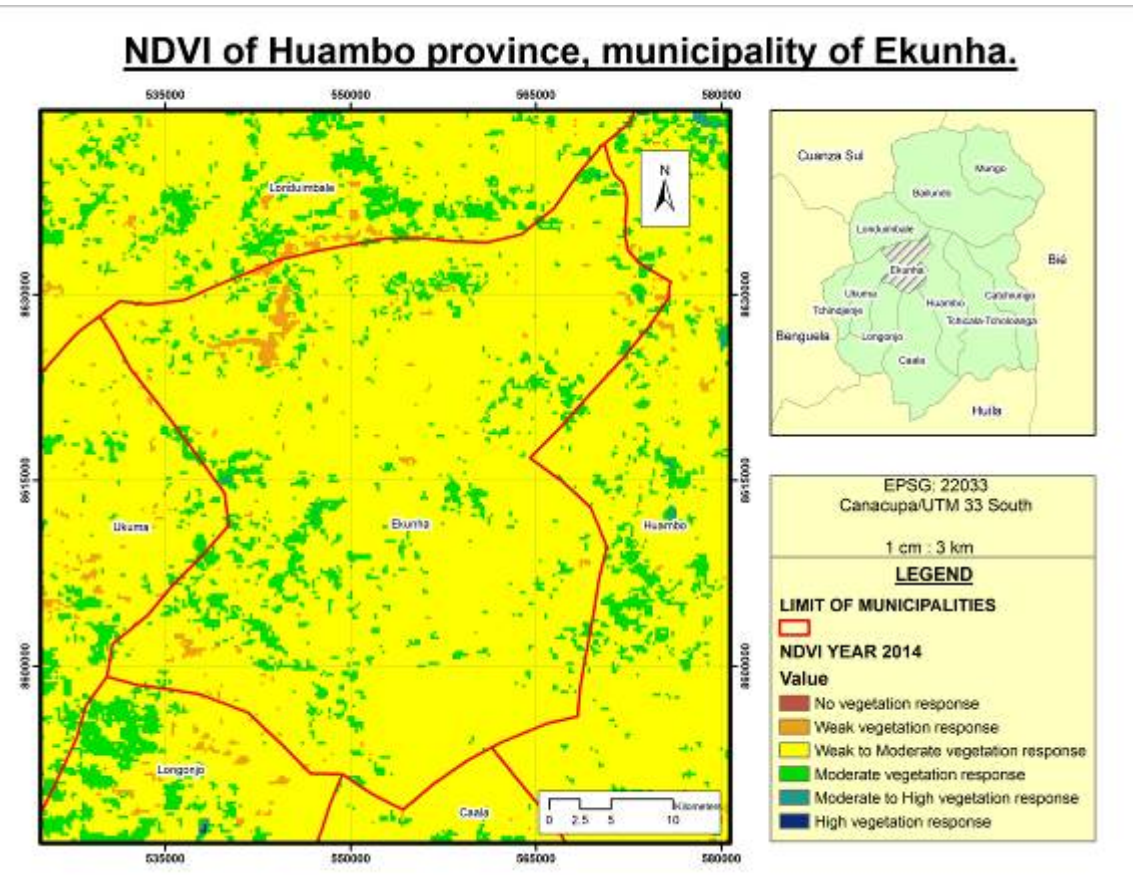


NDVI of Huambo province, municipality of Ekunha.

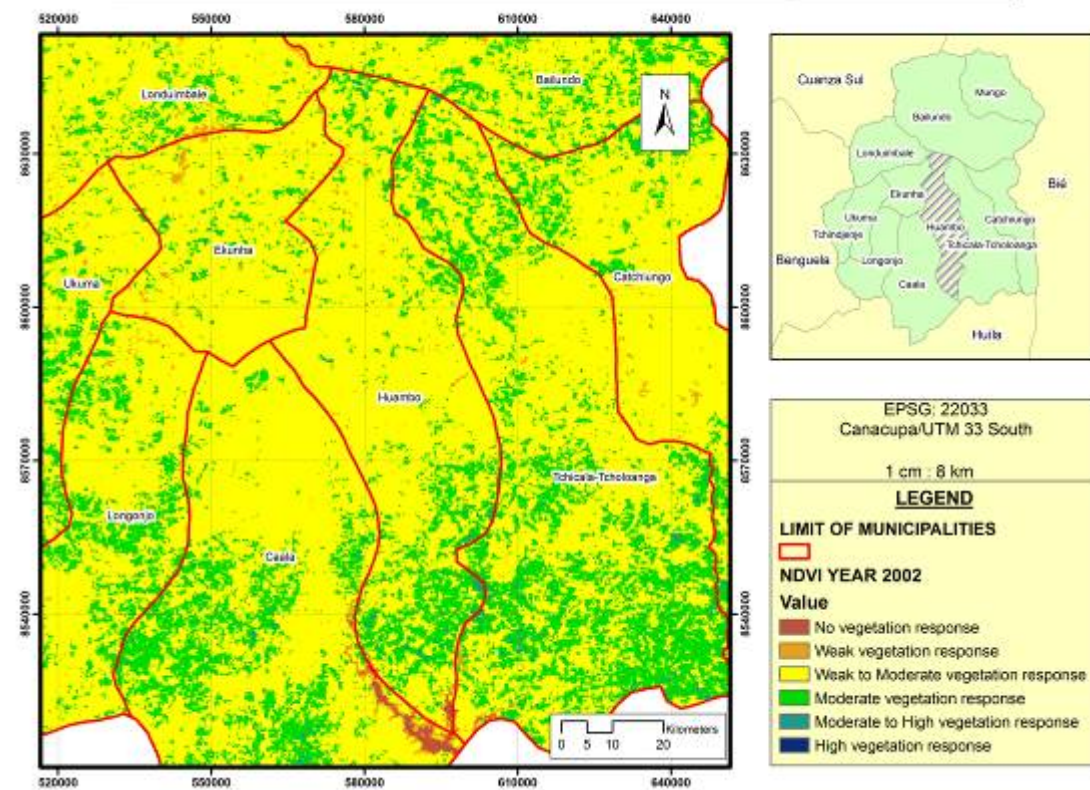


NDVI of Huambo province, municipality of Ekunha.

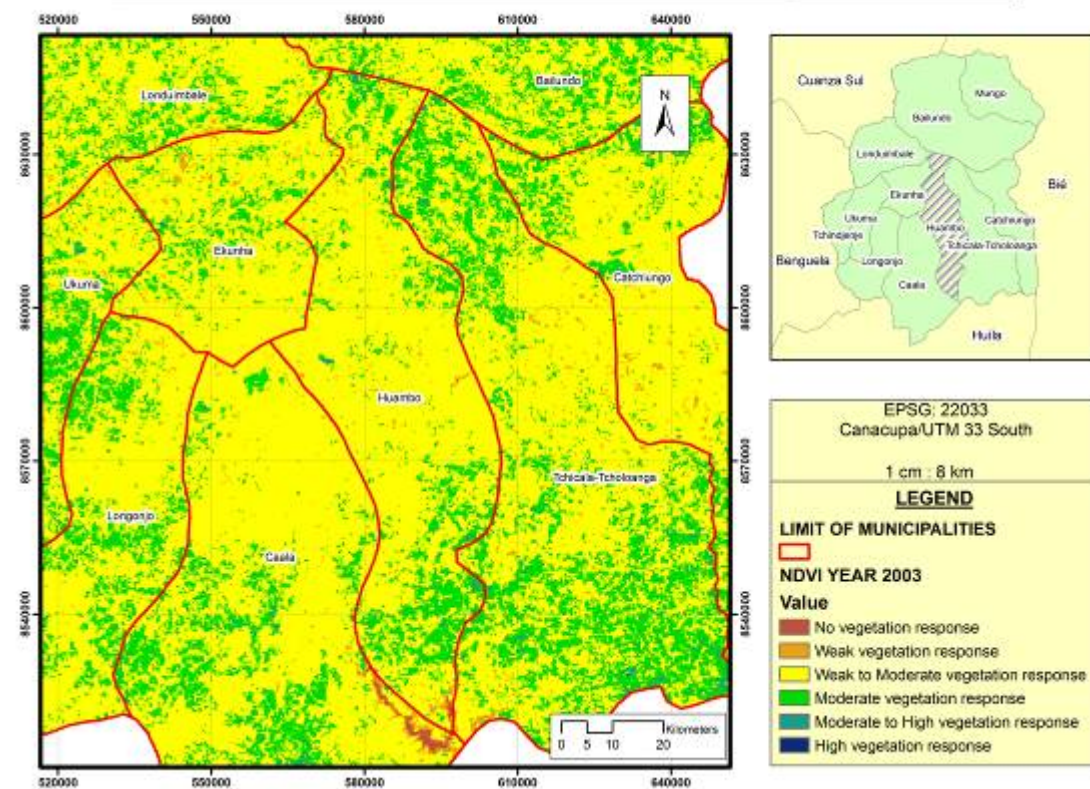




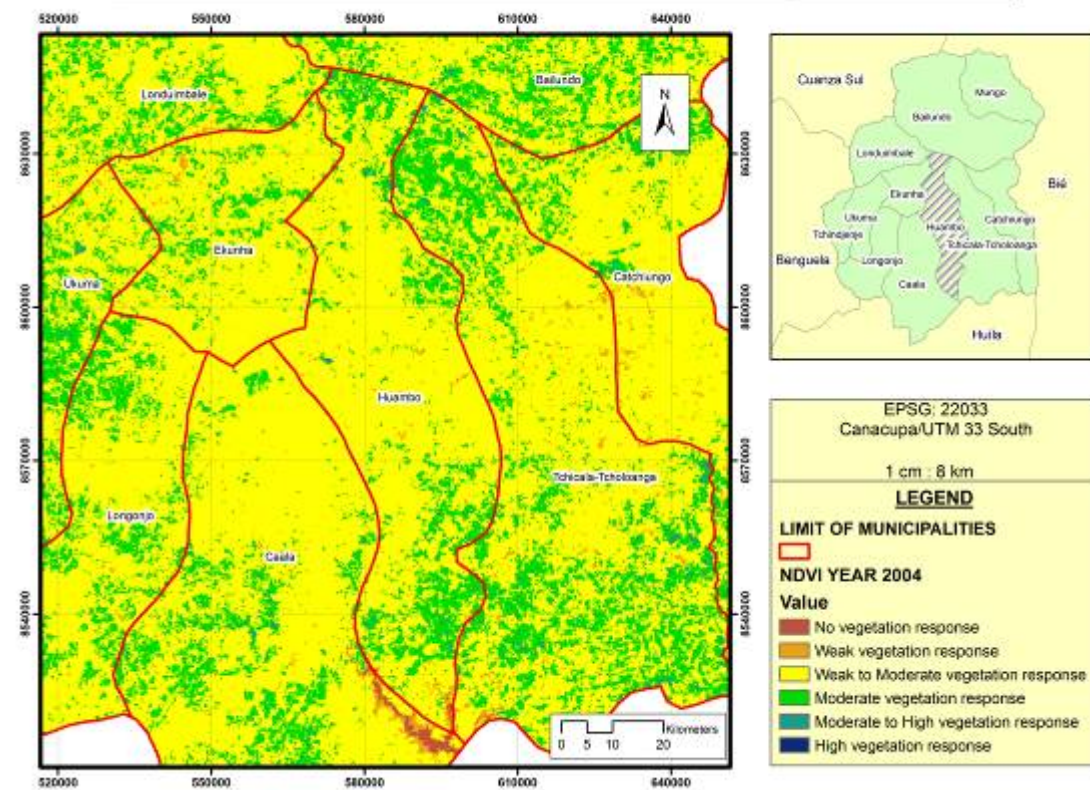
NDVI of Huambo province, municipality of Huambo.



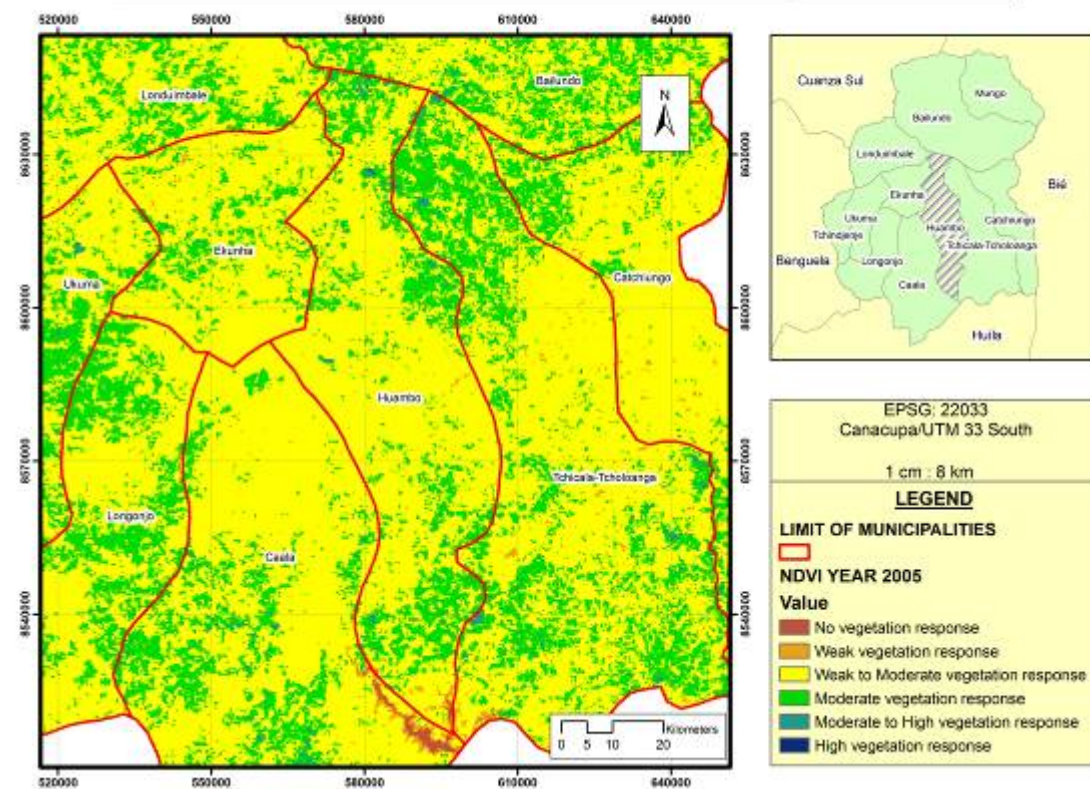
NDVI of Huambo province, municipality of Huambo.



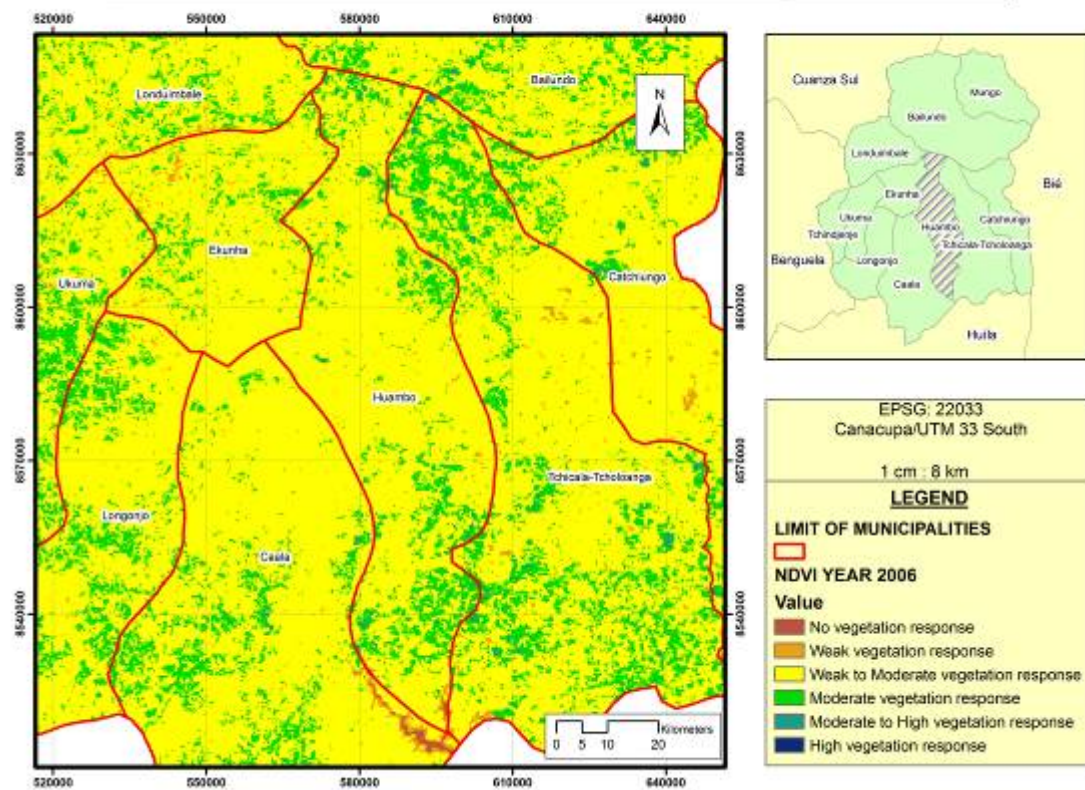
NDVI of Huambo province, municipality of Huambo.



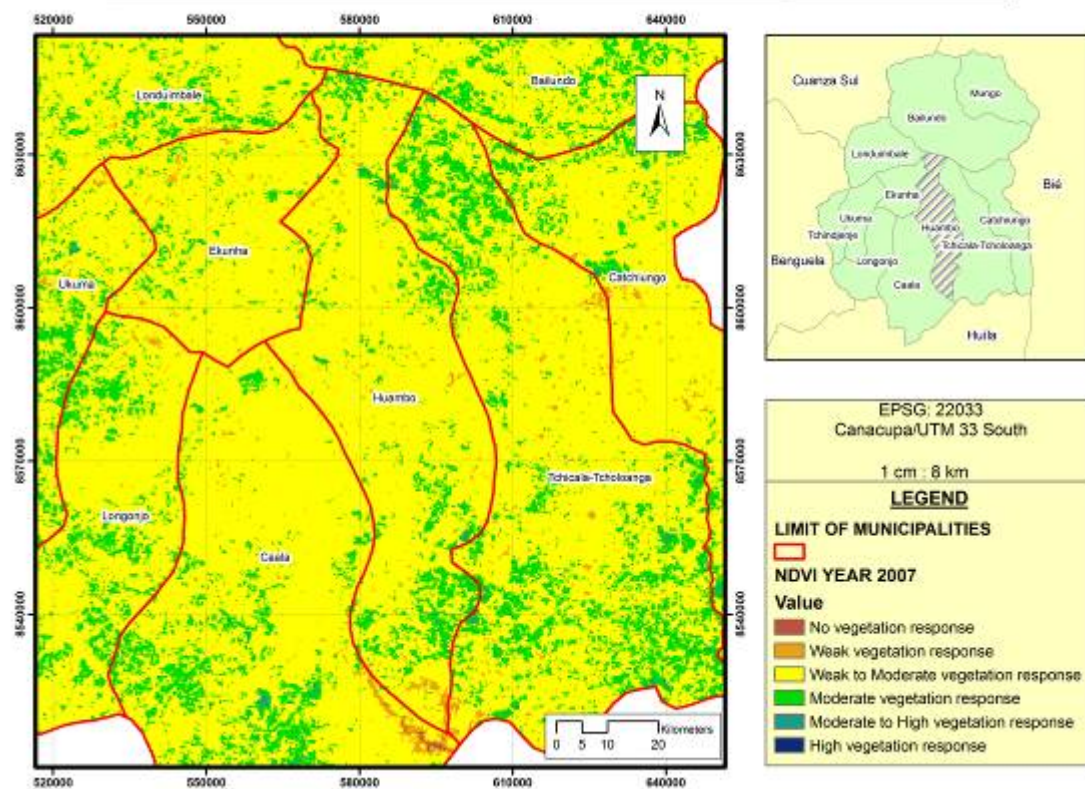
NDVI of Huambo province, municipality of Huambo.



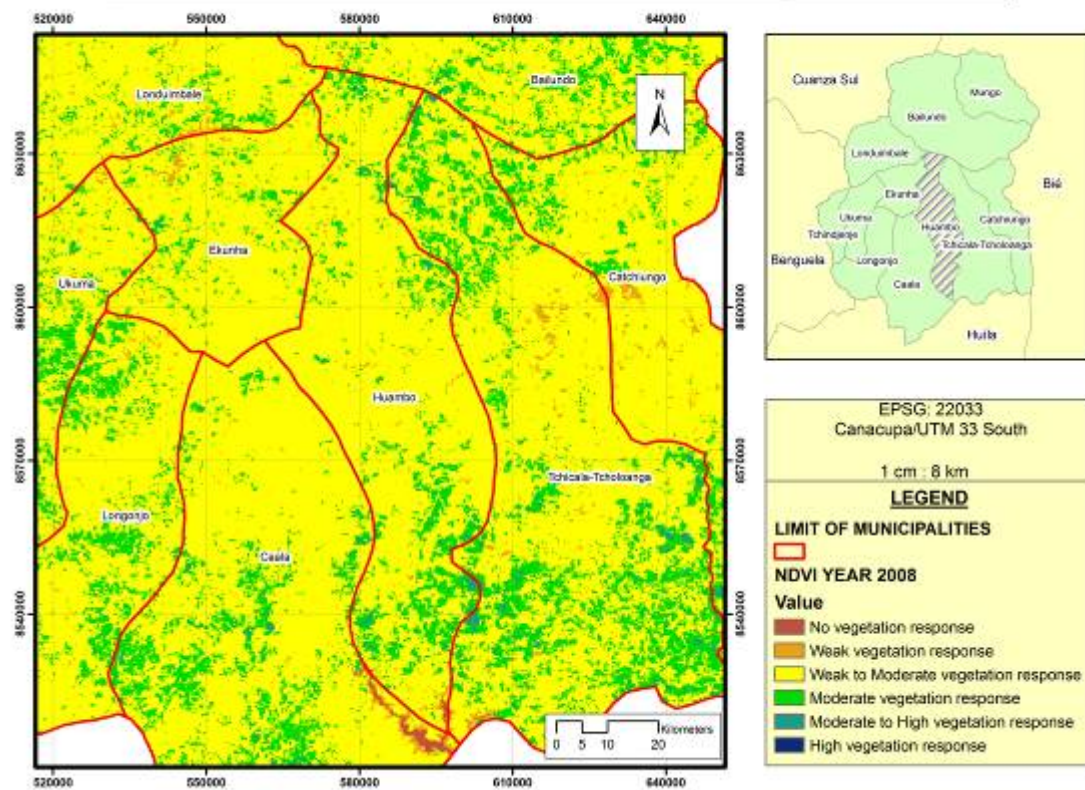
NDVI of Huambo province, municipality of Huambo.



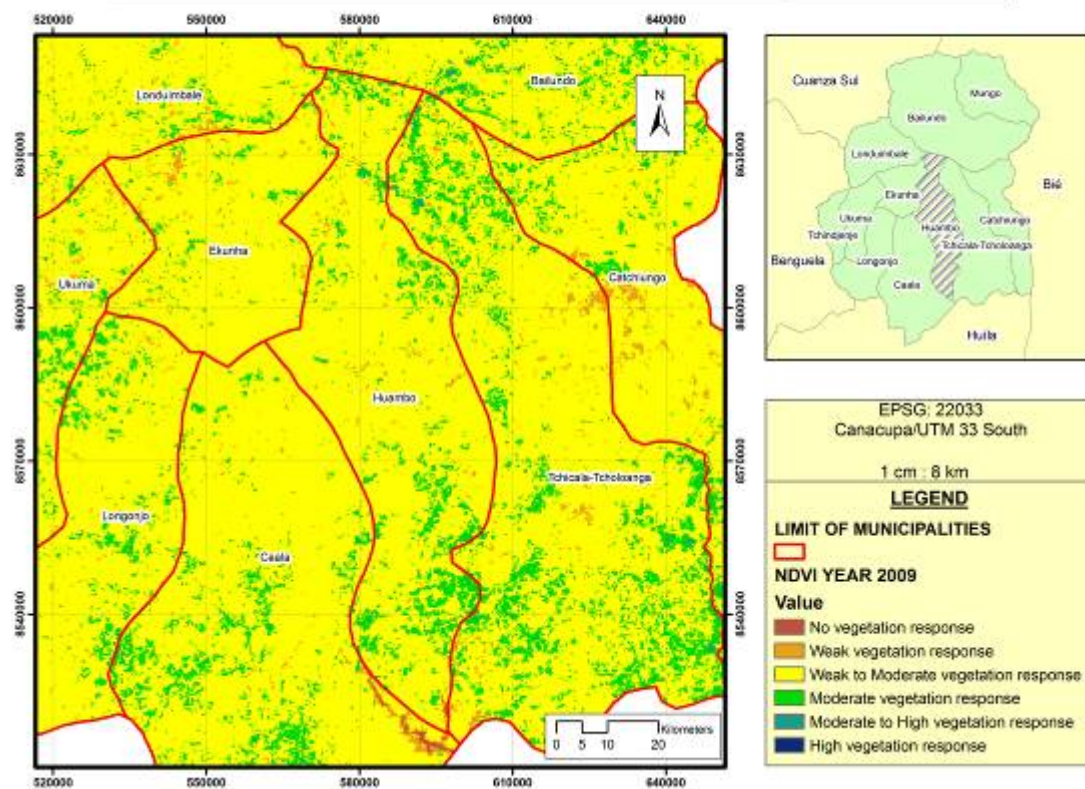
NDVI of Huambo province, municipality of Huambo.



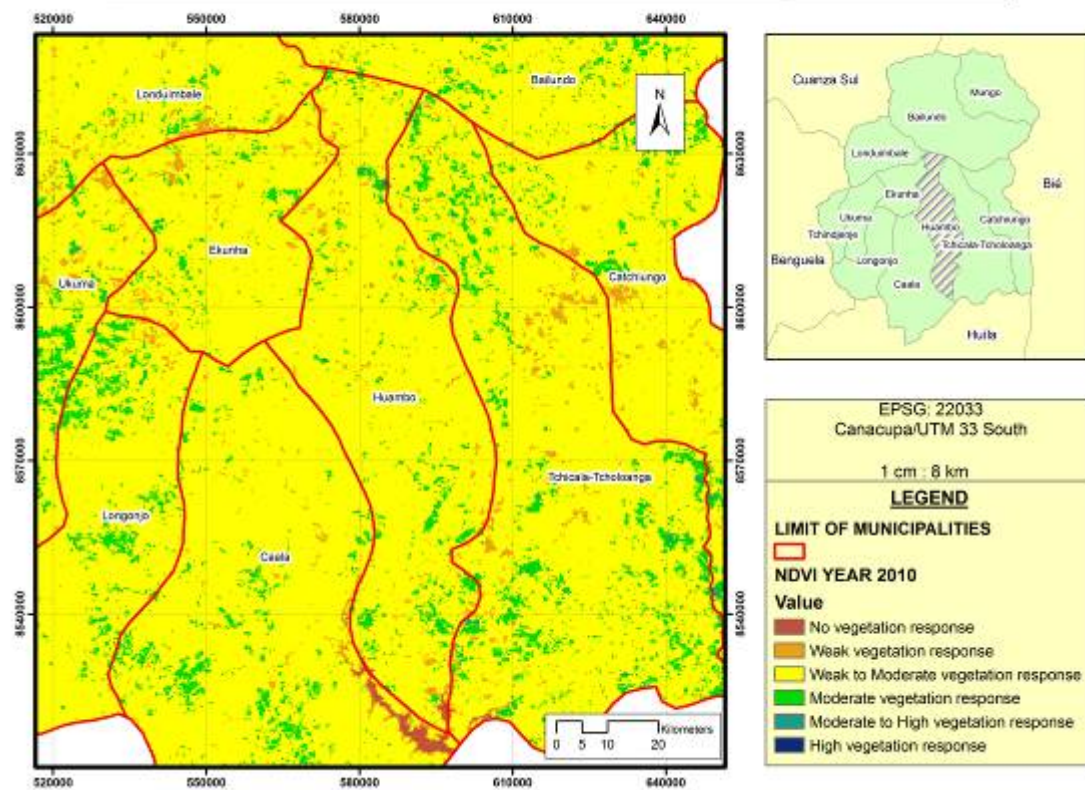
NDVI of Huambo province, municipality of Huambo.



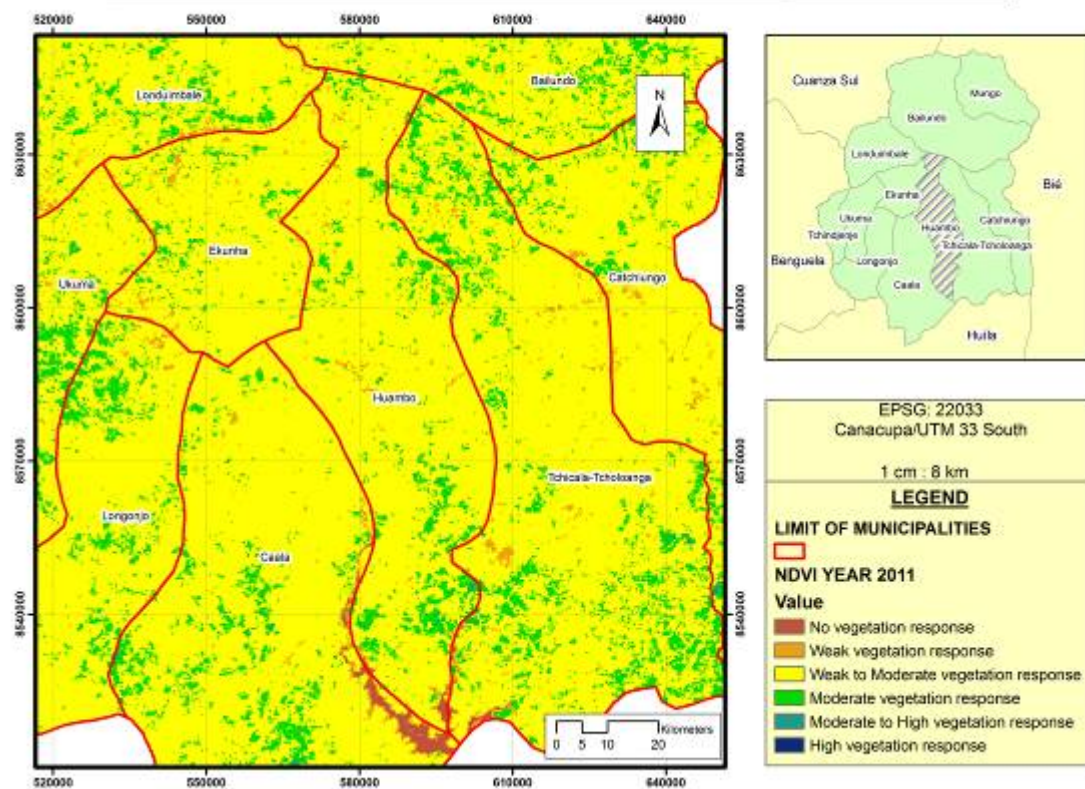
NDVI of Huambo province, municipality of Huambo.



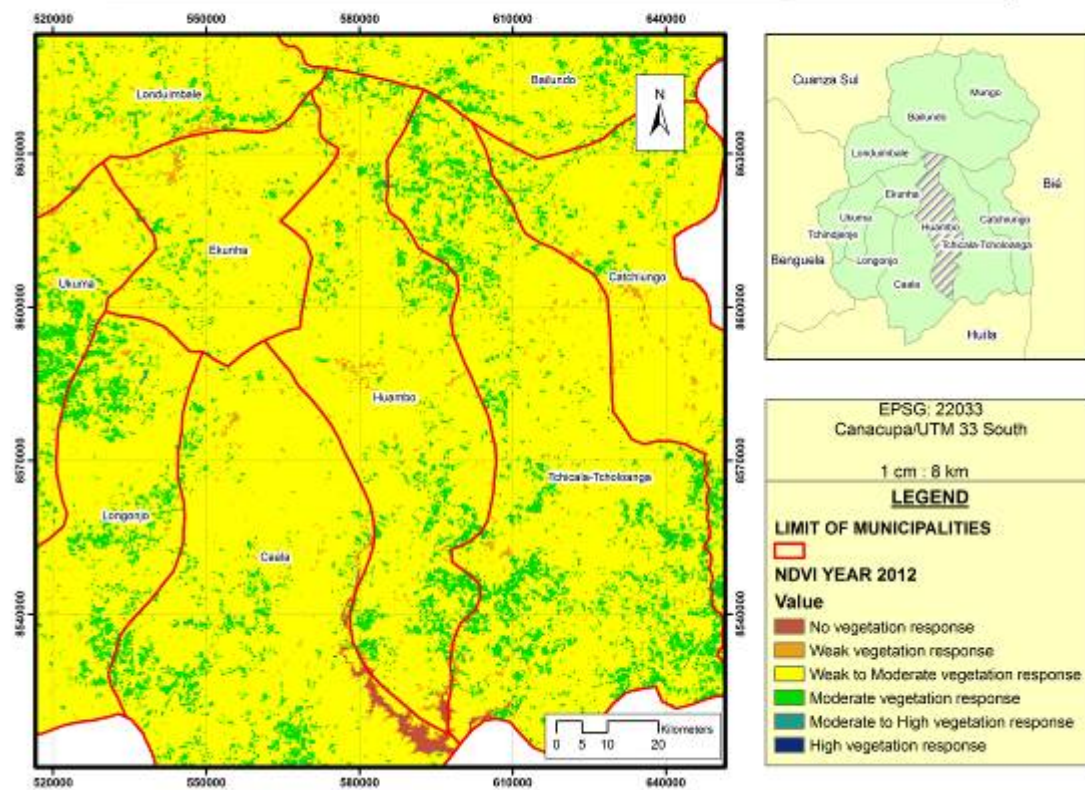
NDVI of Huambo province, municipality of Huambo.



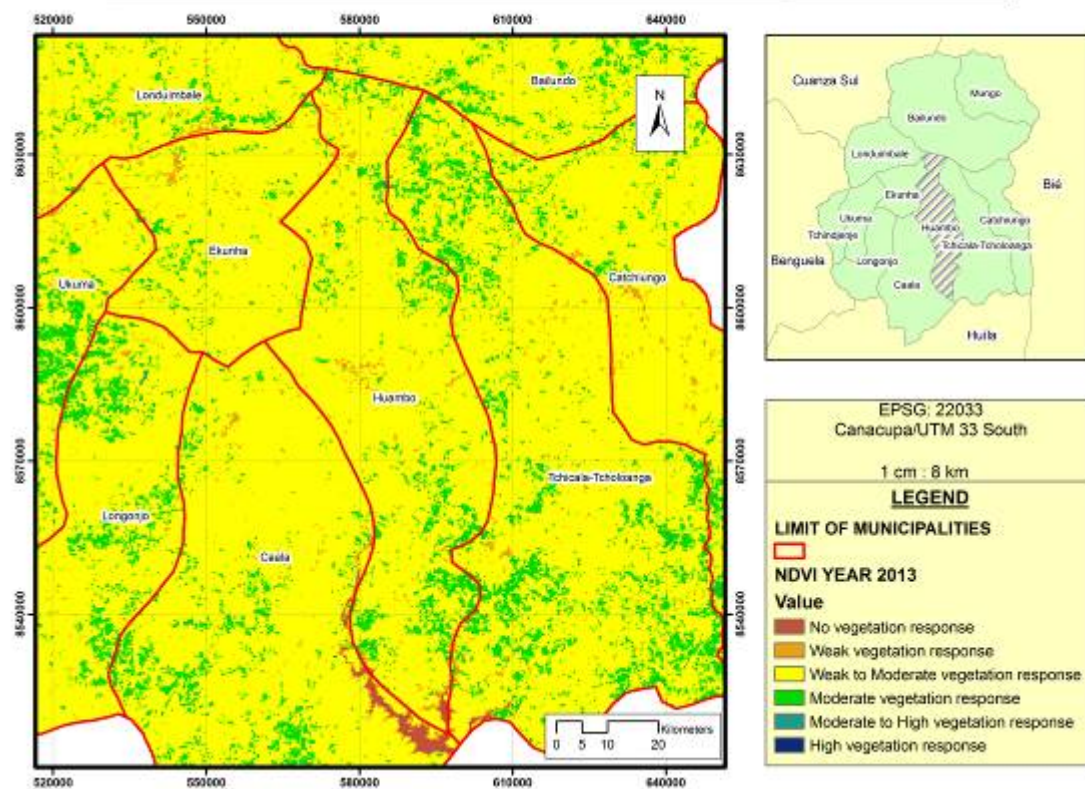
NDVI of Huambo province, municipality of Huambo.



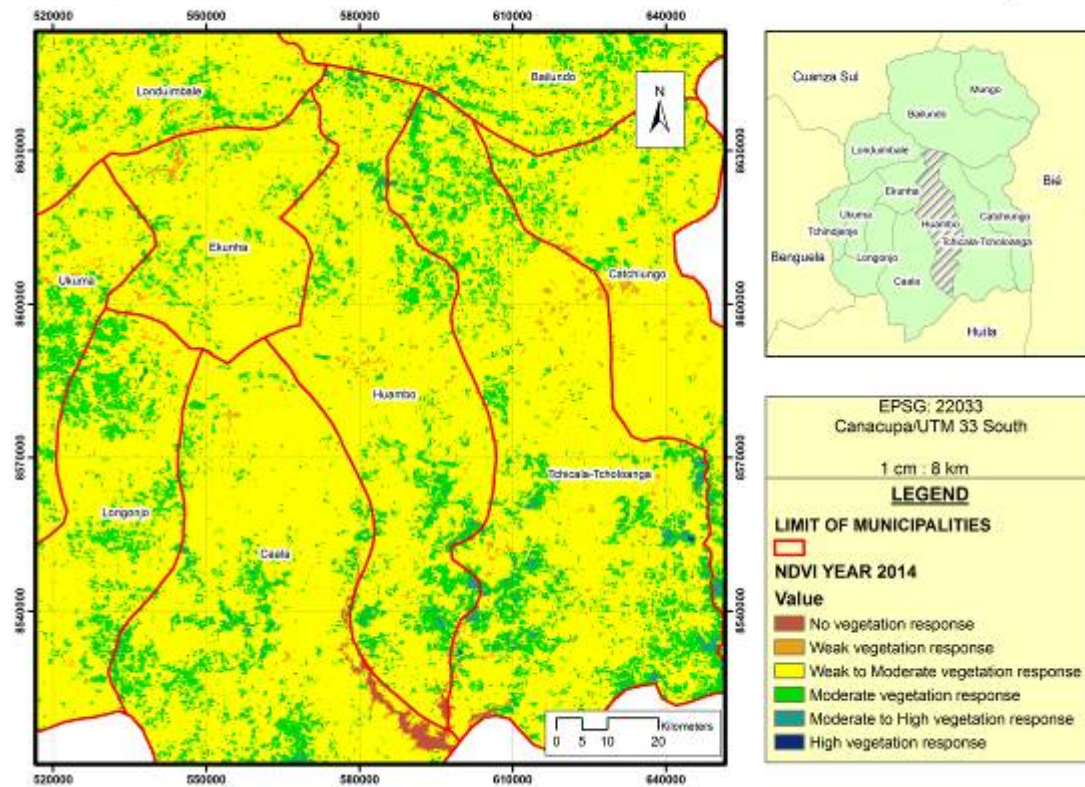
NDVI of Huambo province, municipality of Huambo.



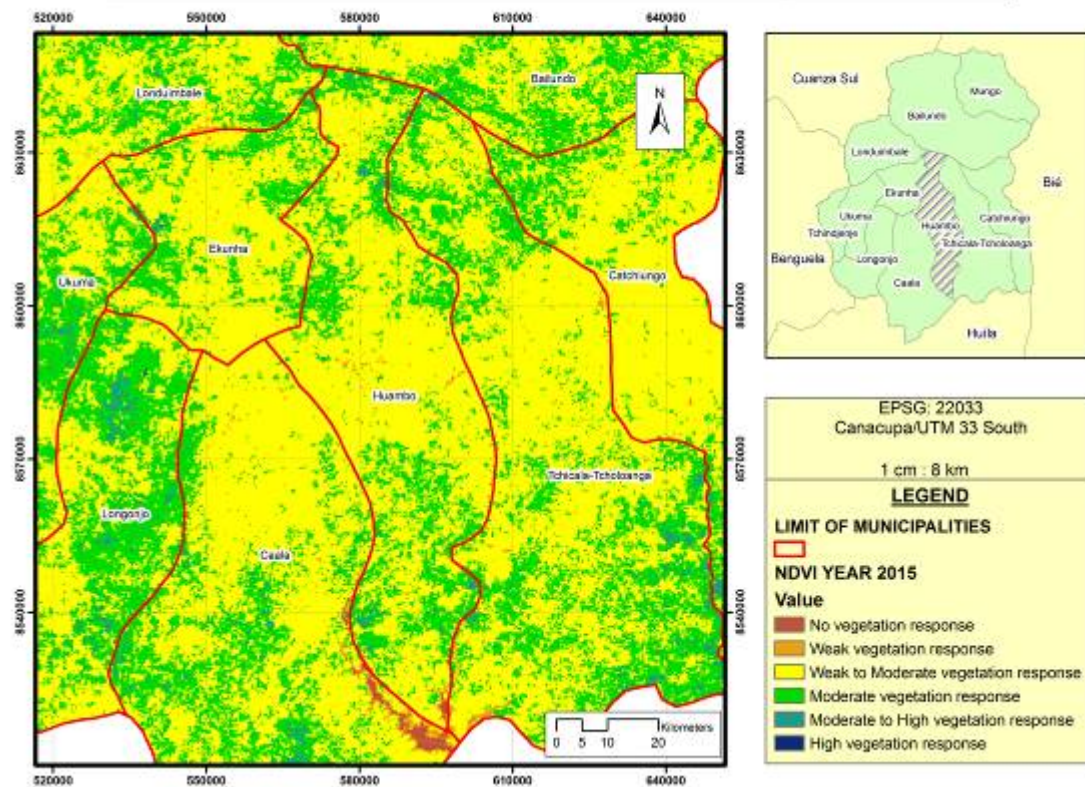
NDVI of Huambo province, municipality of Huambo.



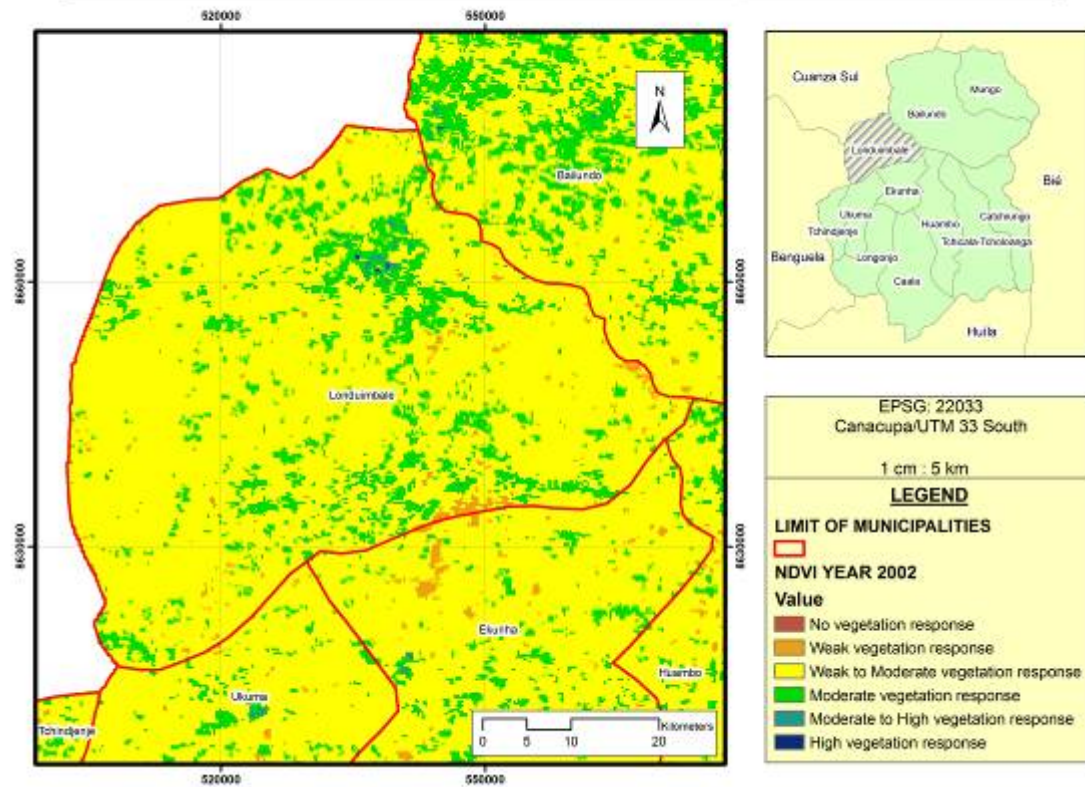
NDVI of Huambo province, municipality of Huambo.



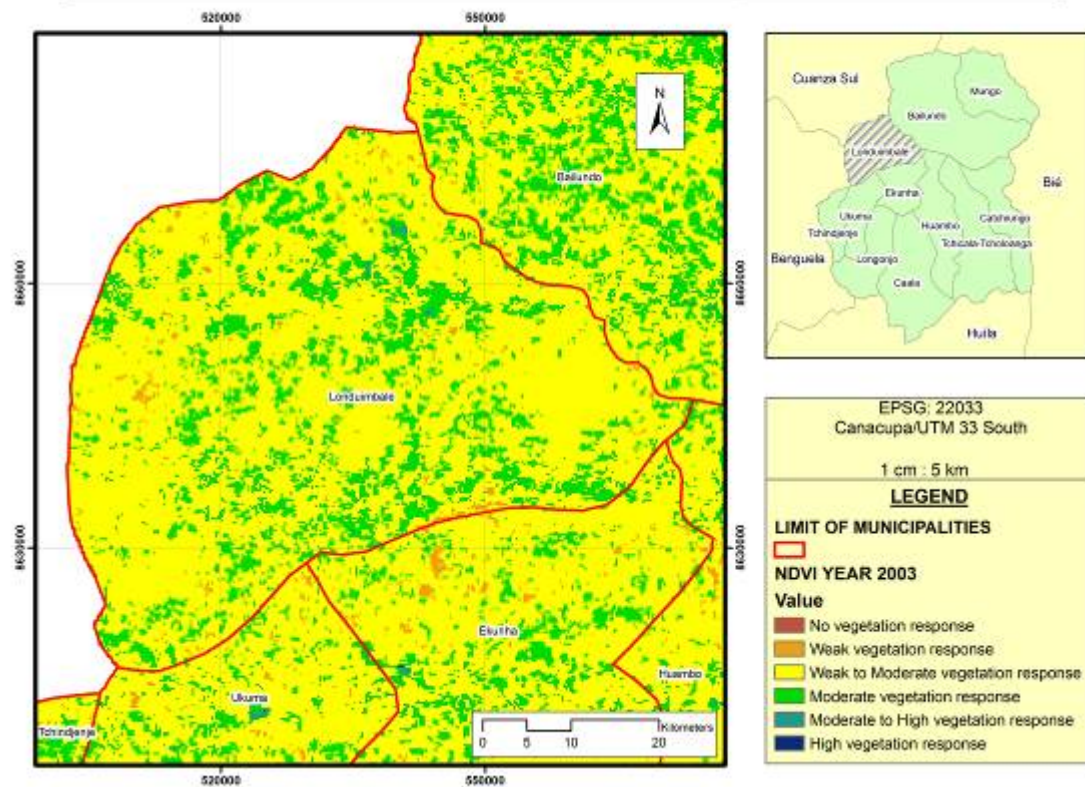
NDVI of Huambo province, municipality of Huambo.



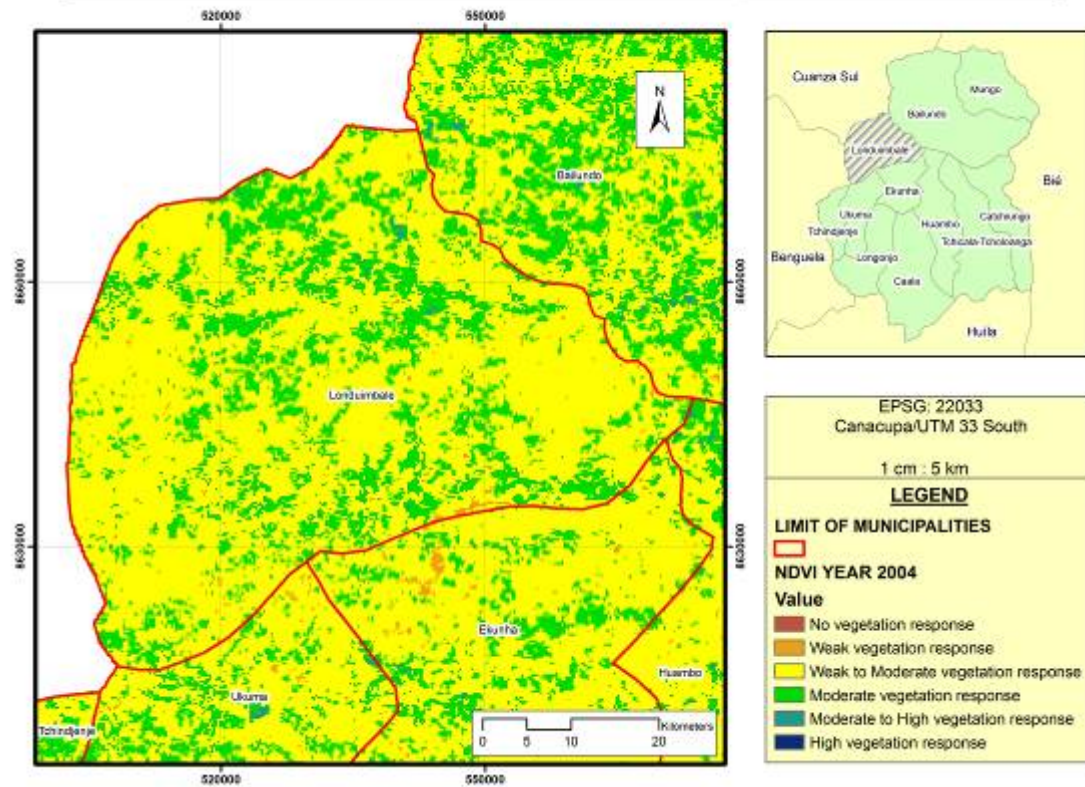
NDVI of Huambo province, municipality of Londuimbale.



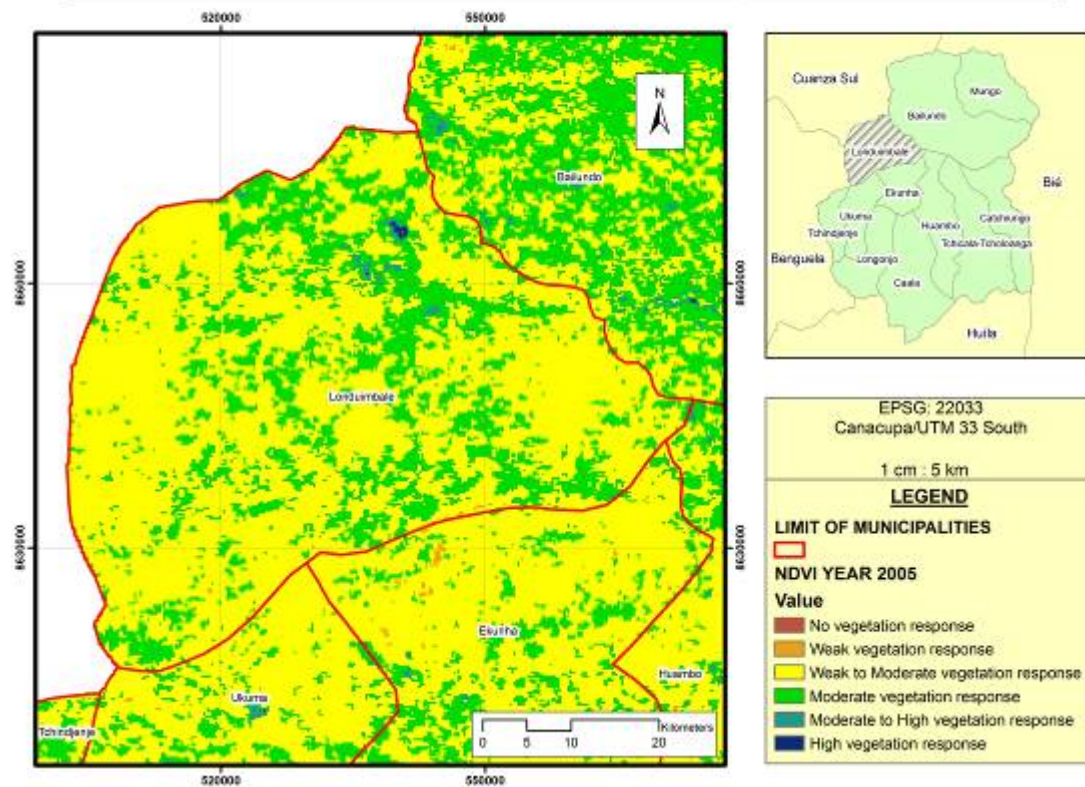
NDVI of Huambo province, municipality of Londuimbale.



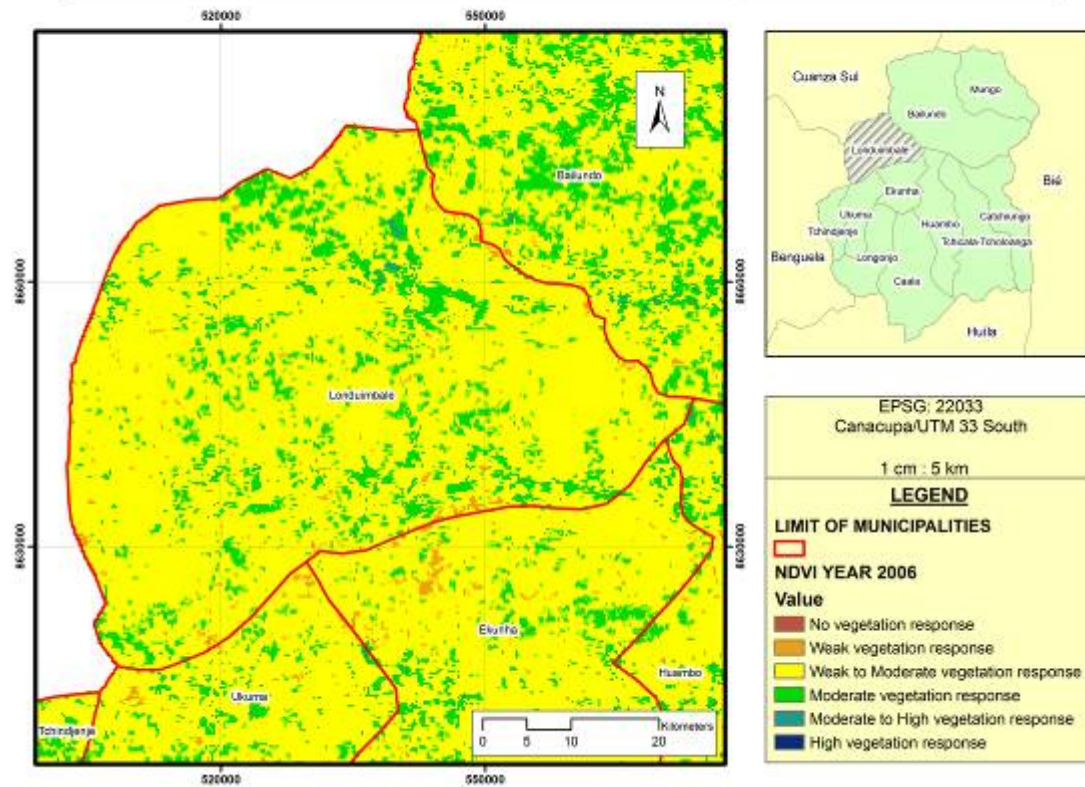
NDVI of Huambo province, municipality of Londuimbale.



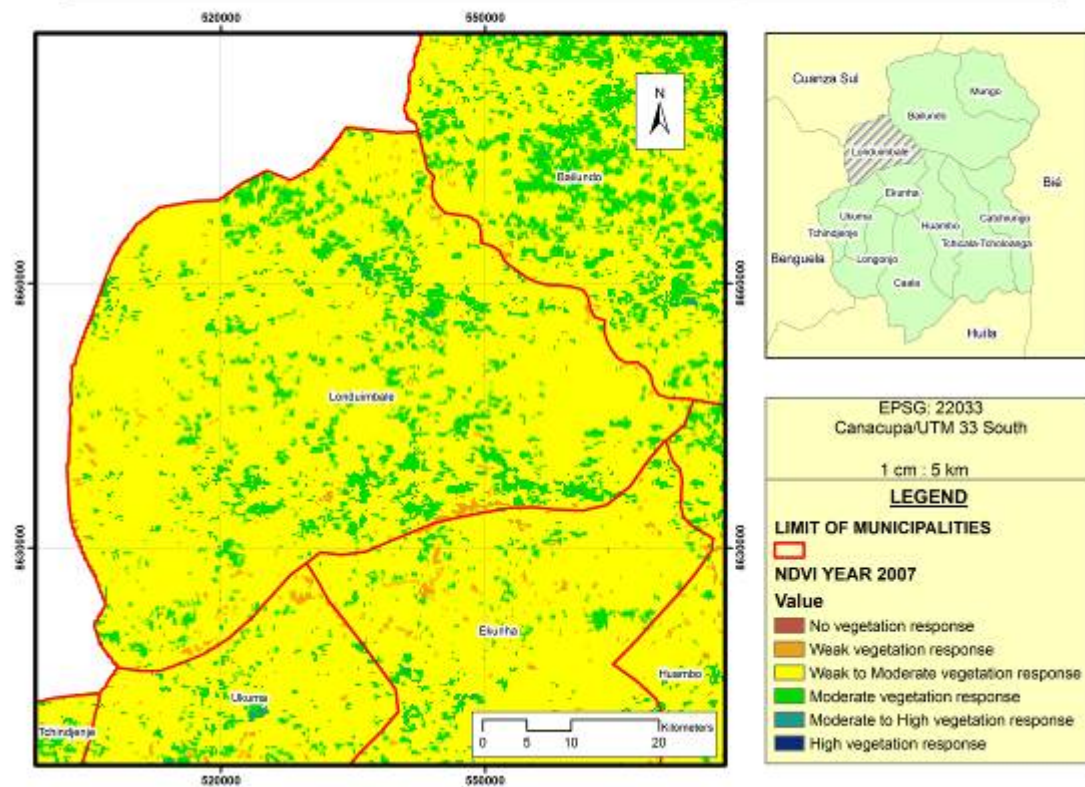
NDVI of Huambo province, municipality of Londuimbale.



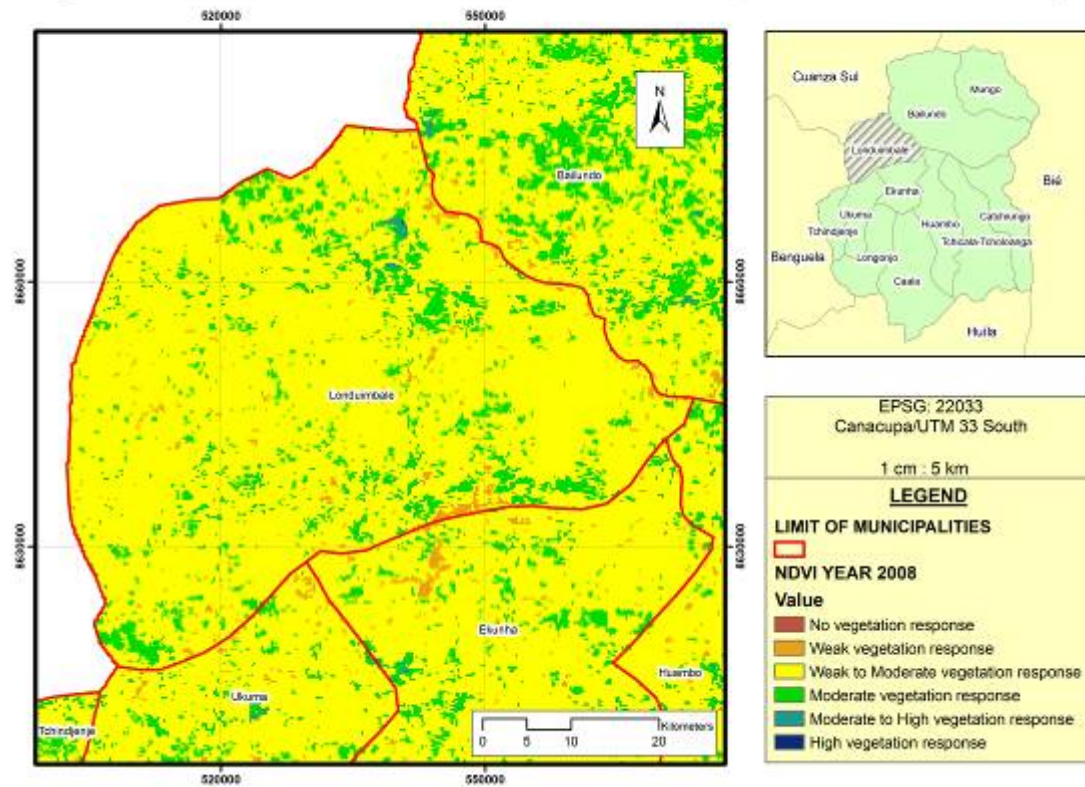
NDVI of Huambo province, municipality of Londuimbale.



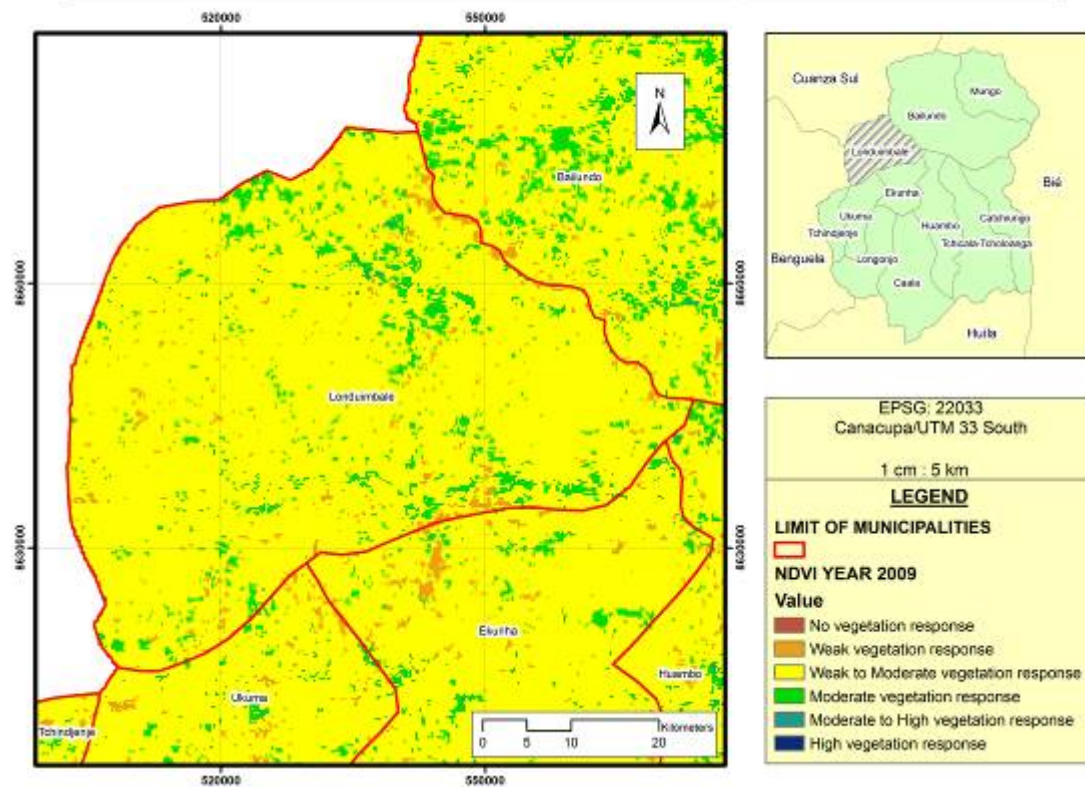
NDVI of Huambo province, municipality of Londuimbale.



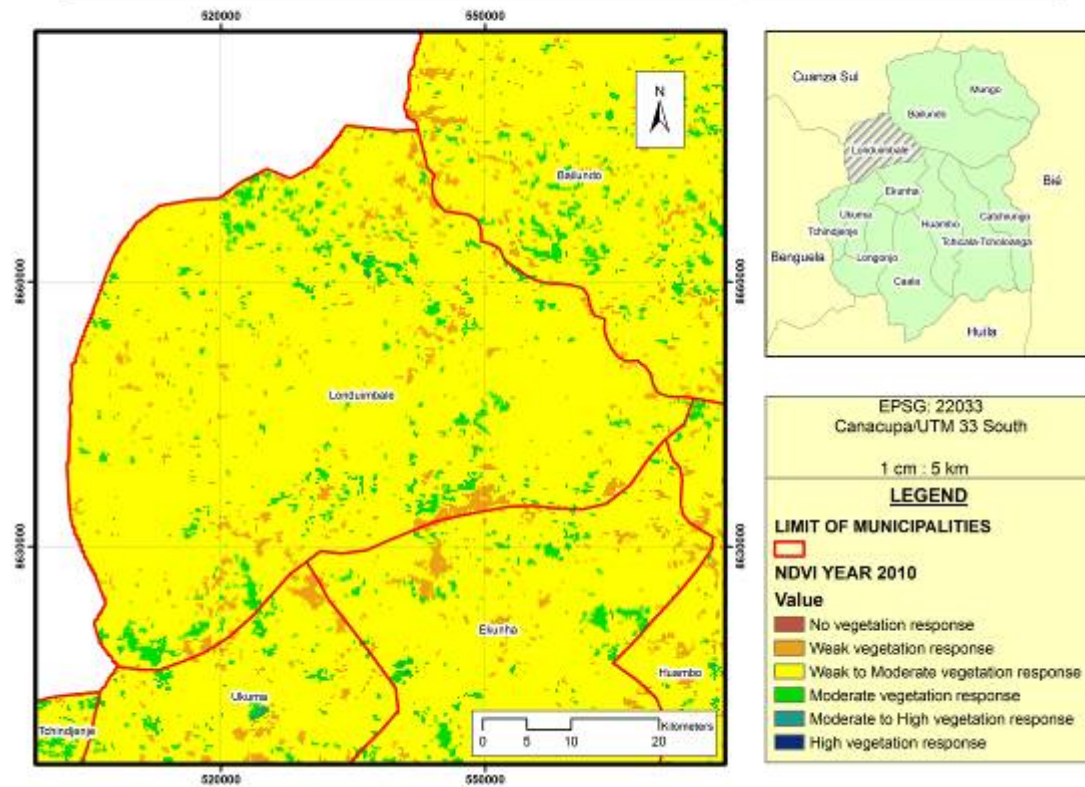
NDVI of Huambo province, municipality of Londuimbale.



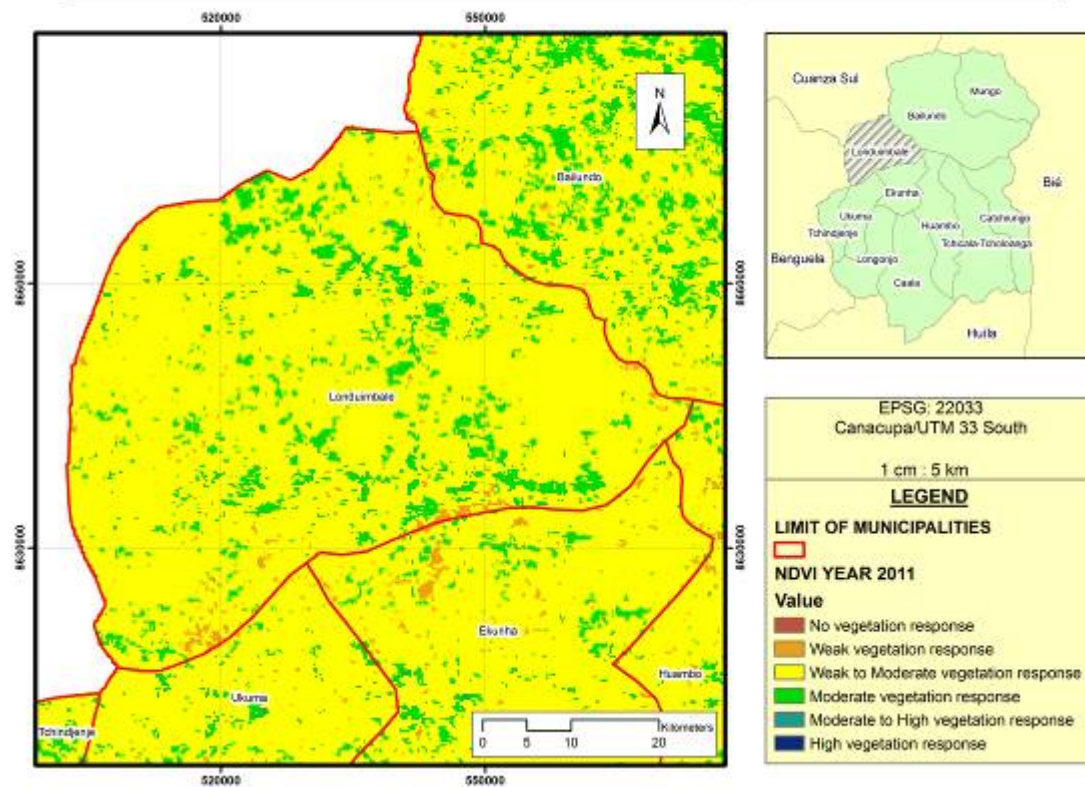
NDVI of Huambo province, municipality of Londuimbale.



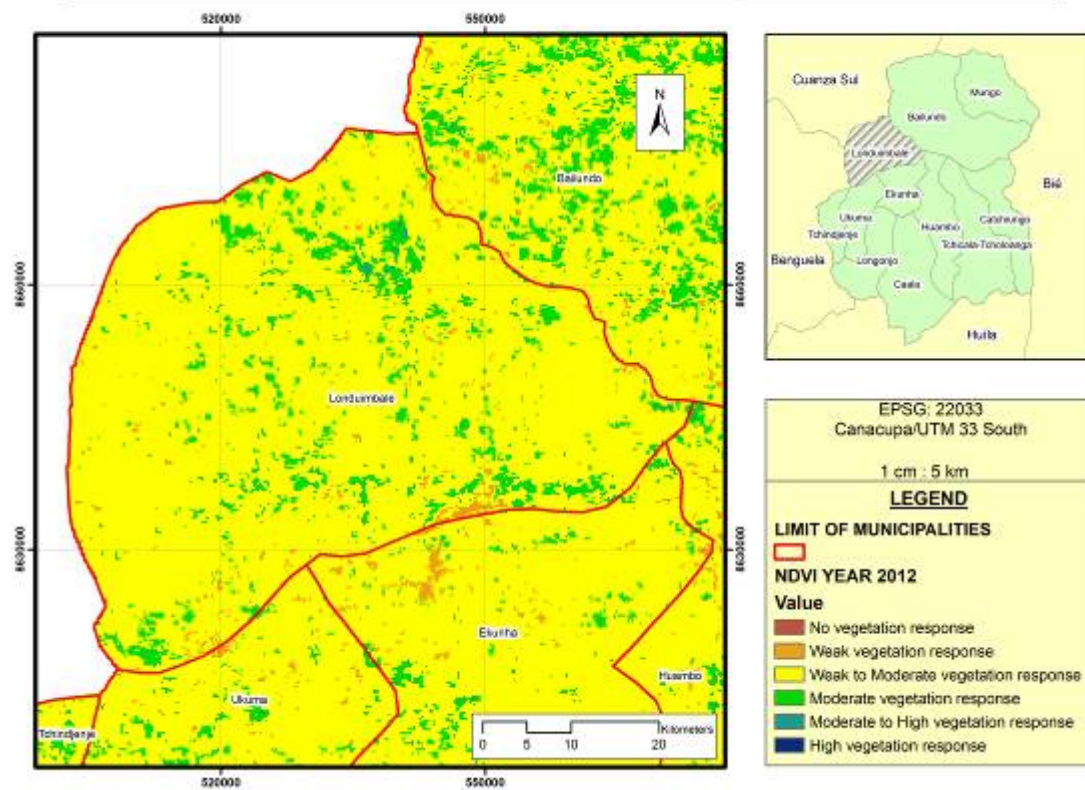
NDVI of Huambo province, municipality of Londuimbale.



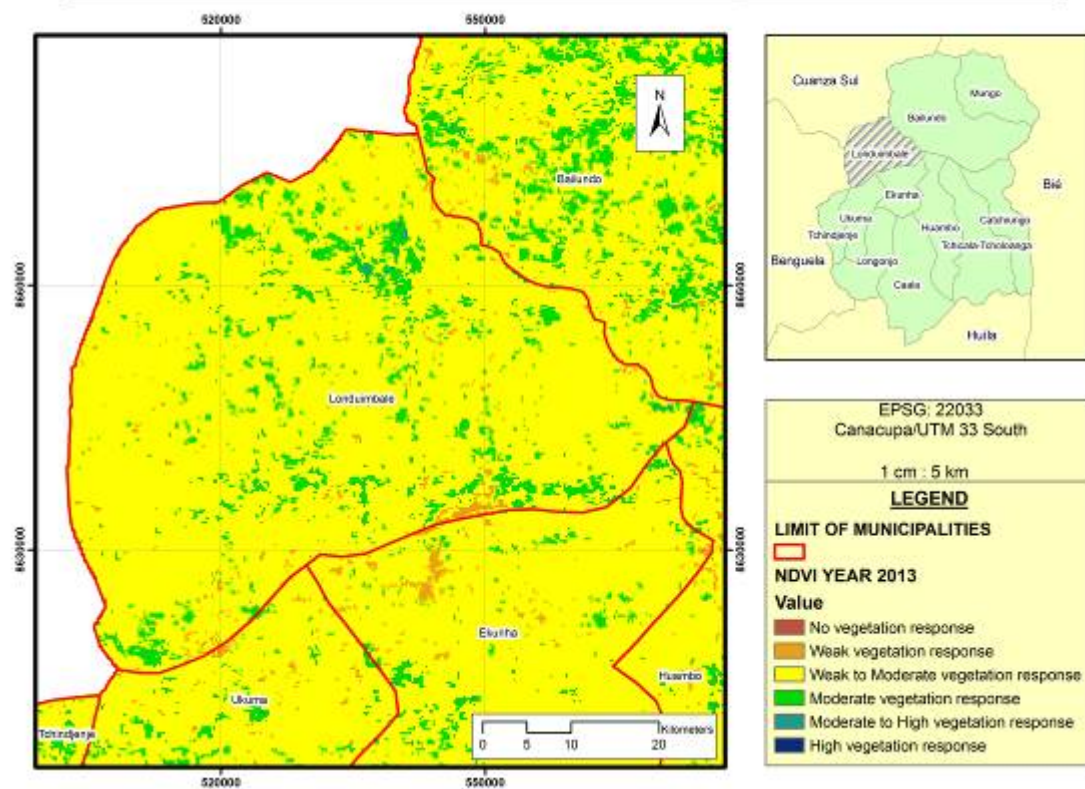
NDVI of Huambo province, municipality of Londuimbale.



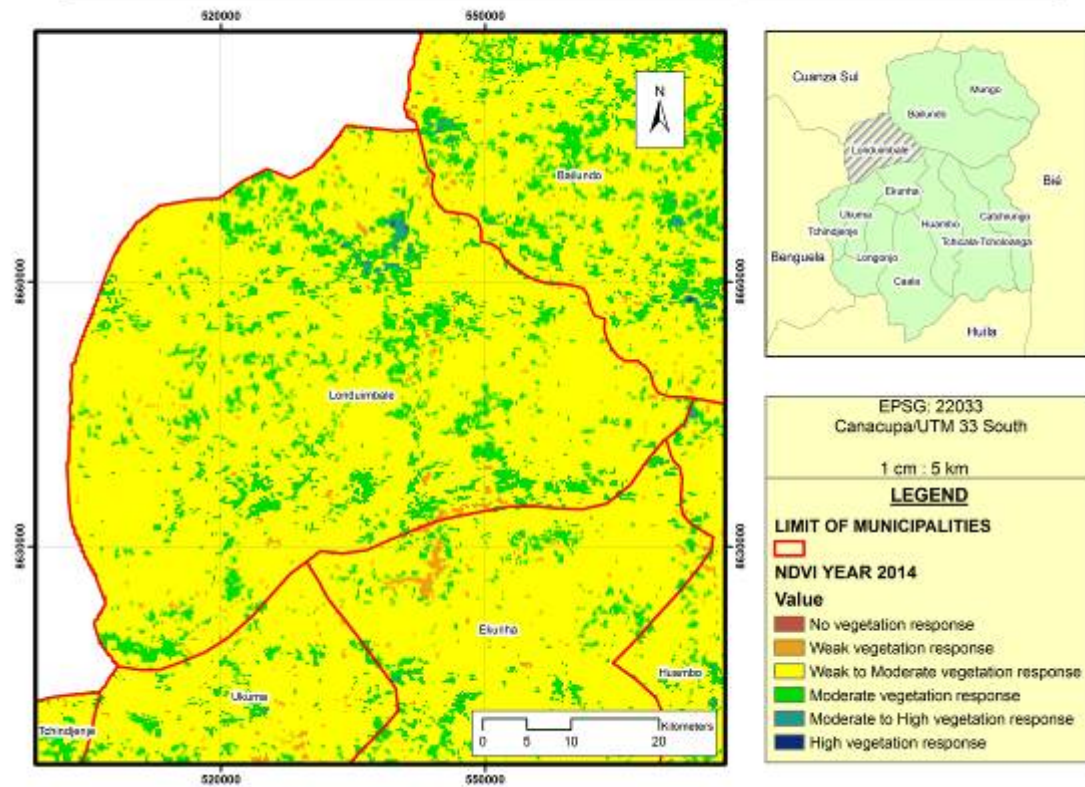
NDVI of Huambo province, municipality of Londuimbale.



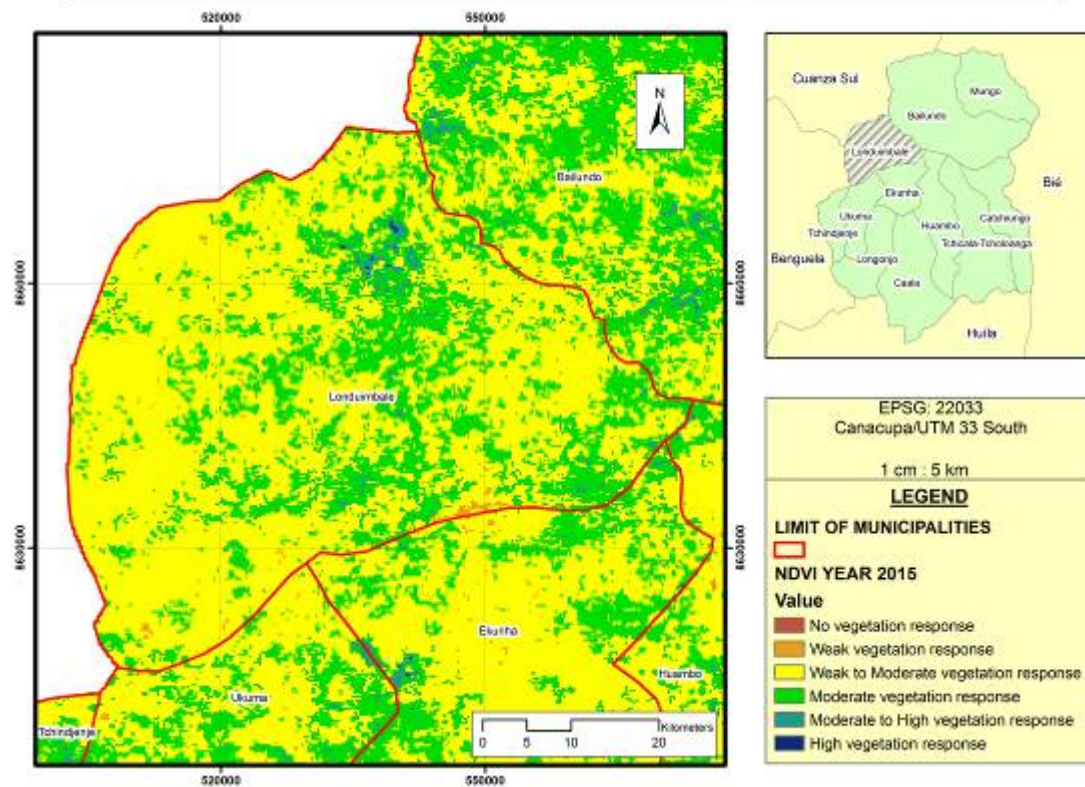
NDVI of Huambo province, municipality of Londuimbale.



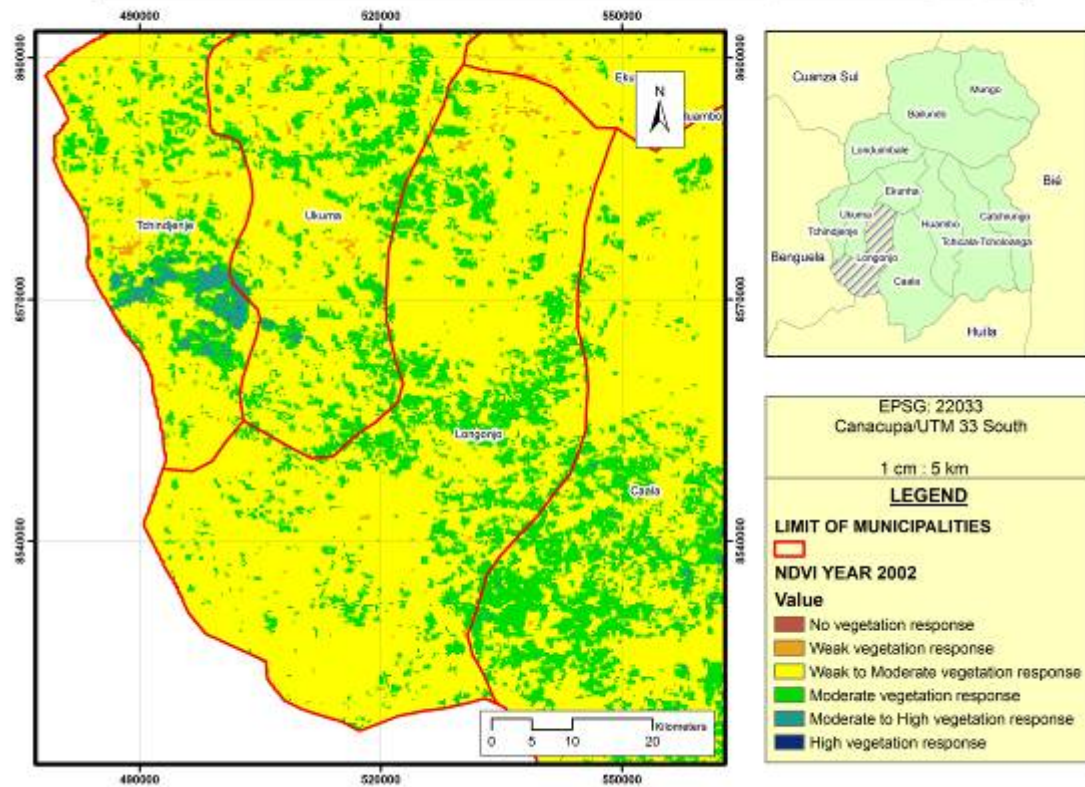
NDVI of Huambo province, municipality of Londuimbale.



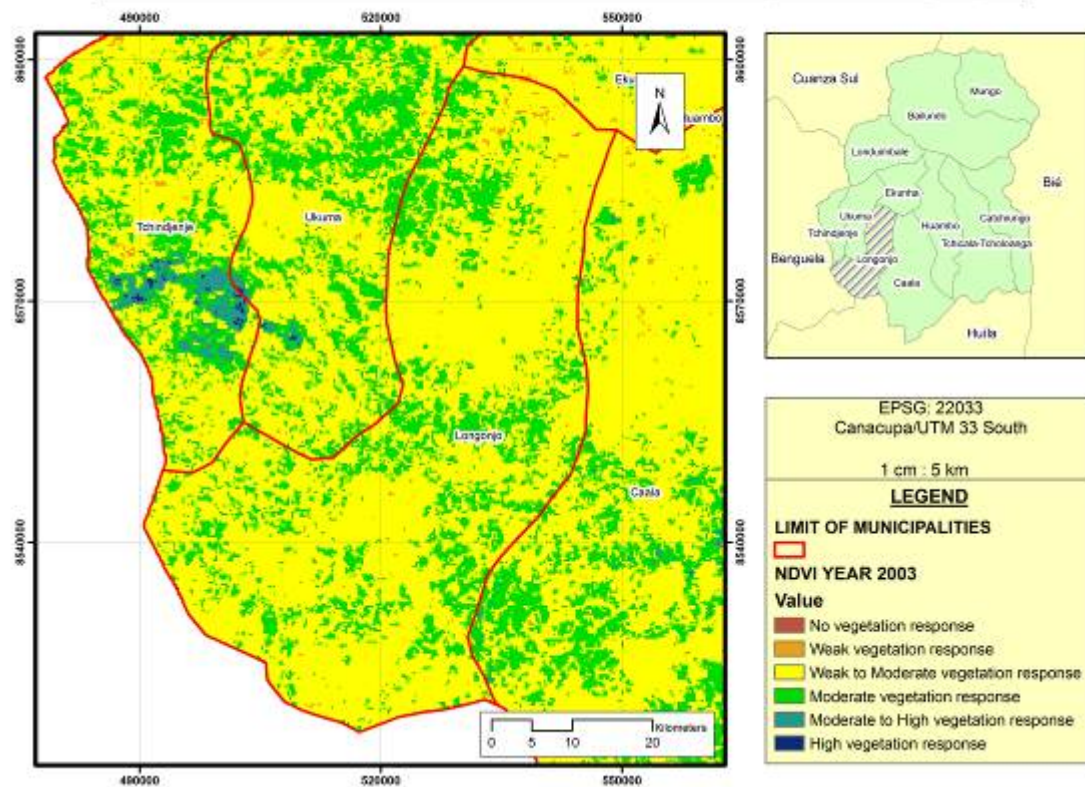
NDVI of Huambo province, municipality of Londuimbale.



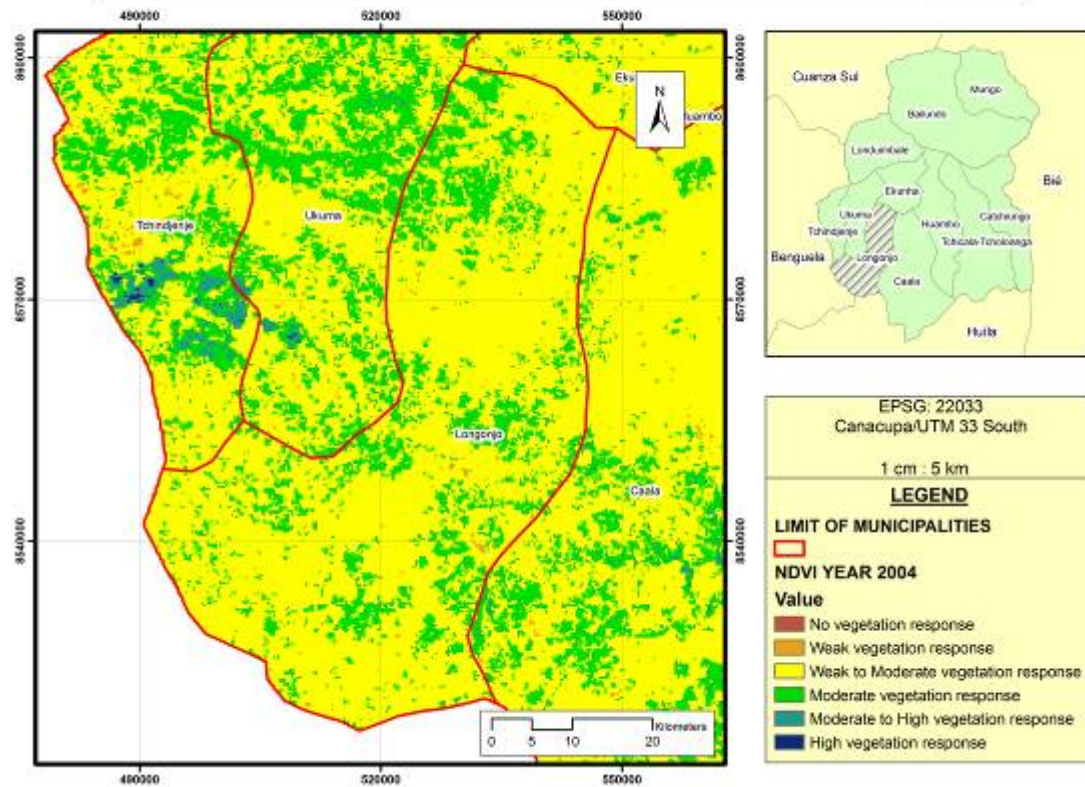
NDVI of Huambo province, municipality of Longonjo.



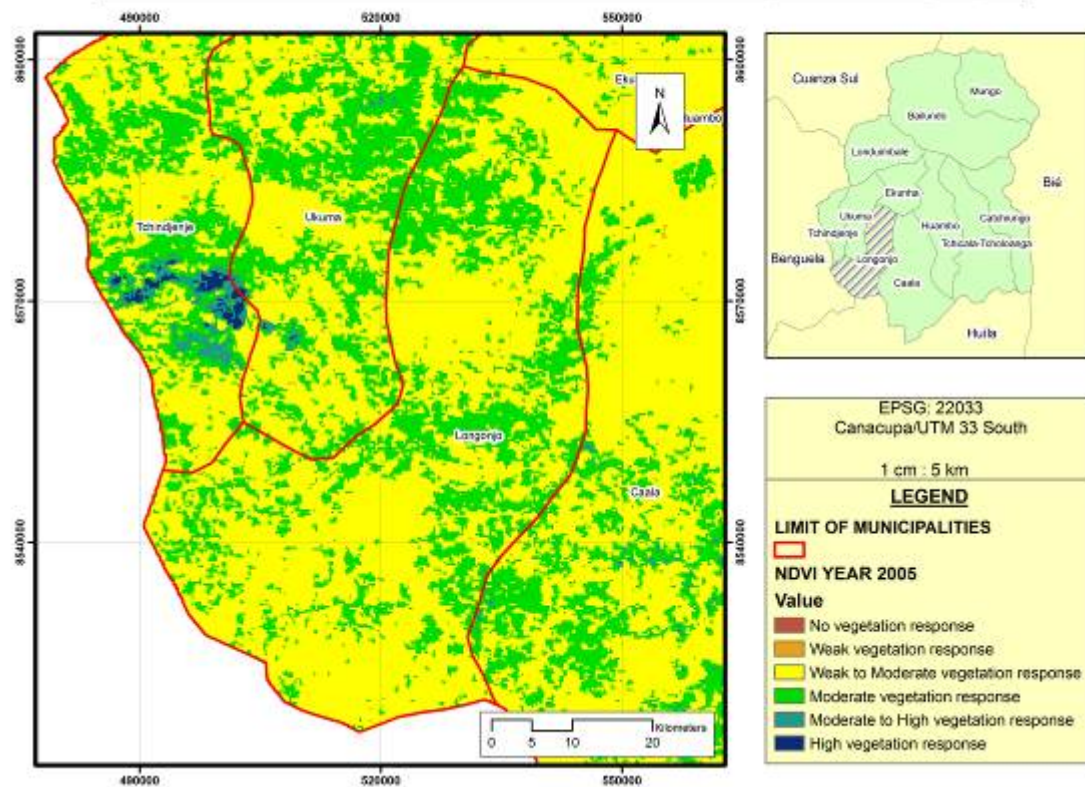
NDVI of Huambo province, municipality of Longonjo.



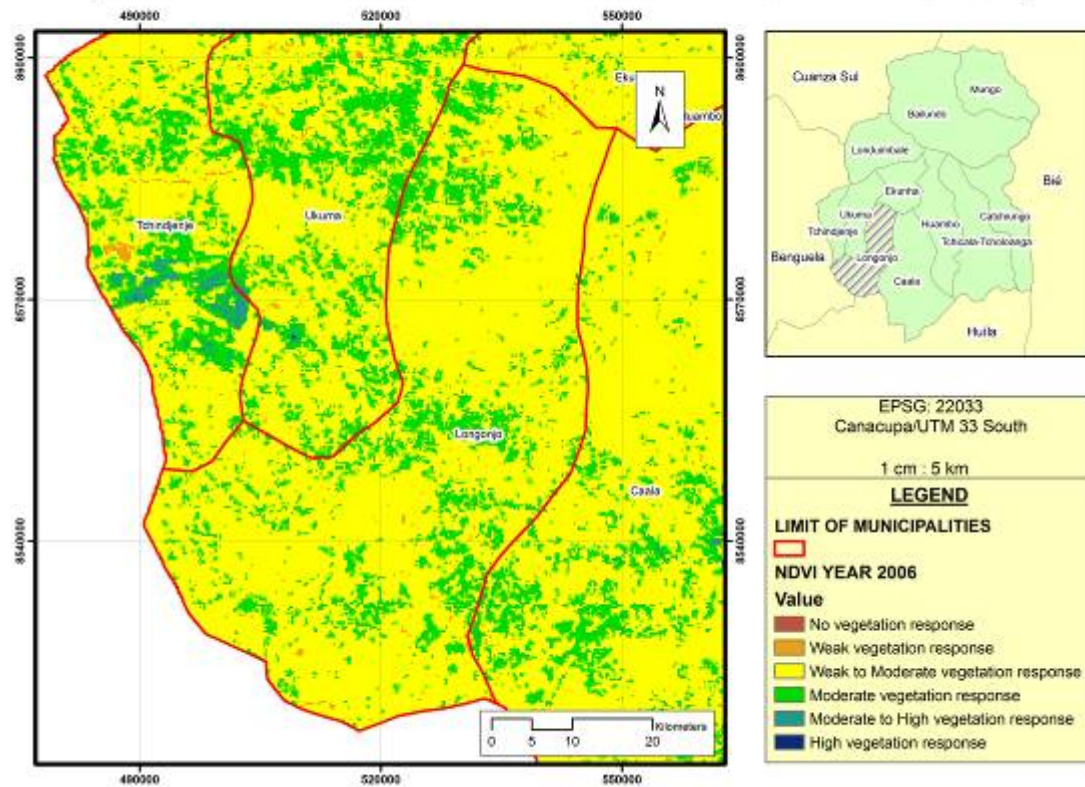
NDVI of Huambo province, municipality of Longonjo.



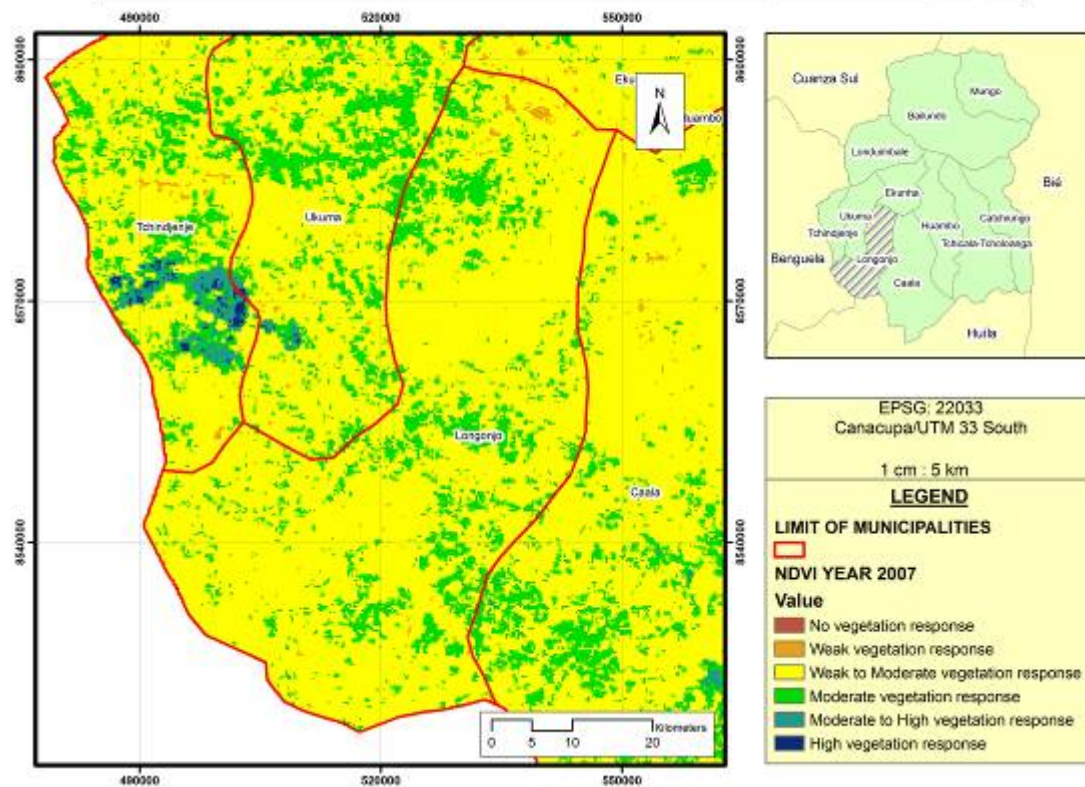
NDVI of Huambo province, municipality of Longonjo.



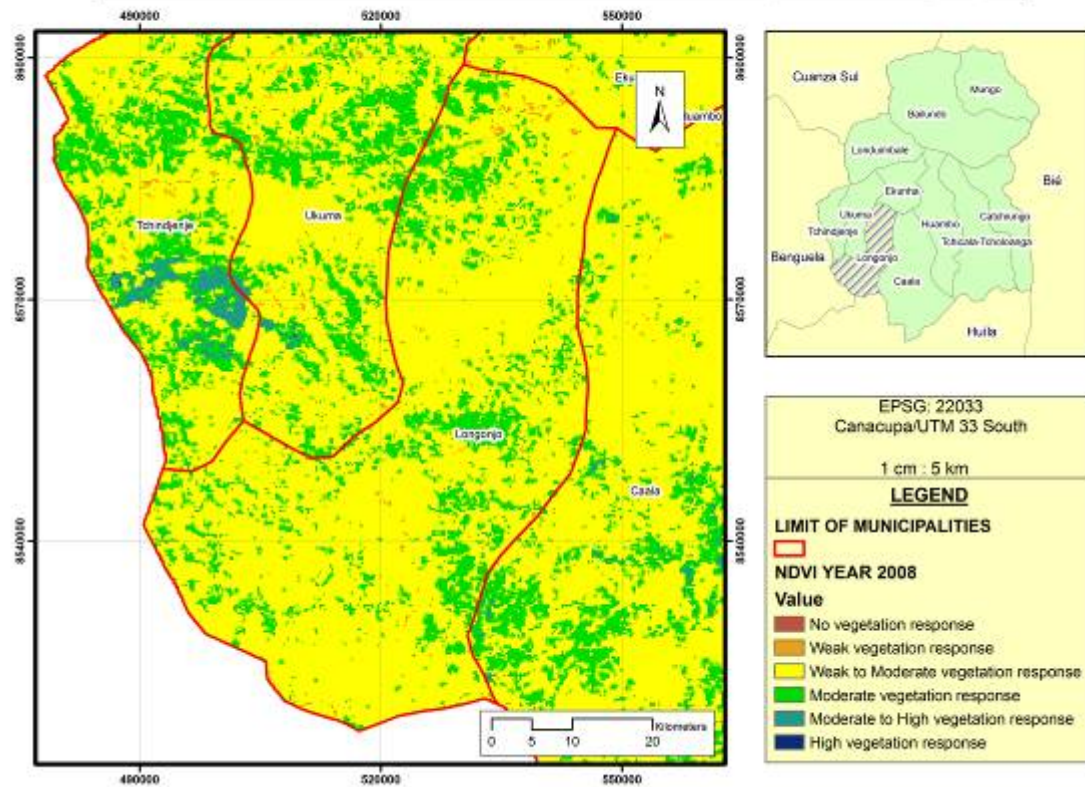
NDVI of Huambo province, municipality of Longonjo.



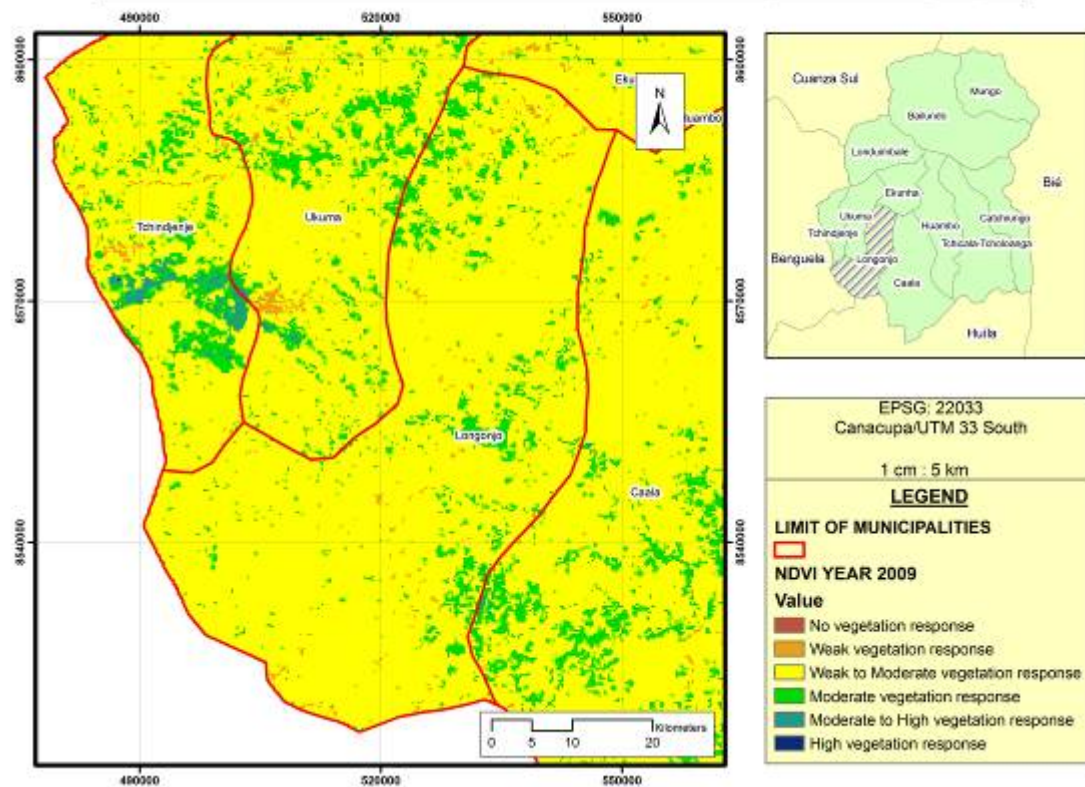
NDVI of Huambo province, municipality of Longonjo.



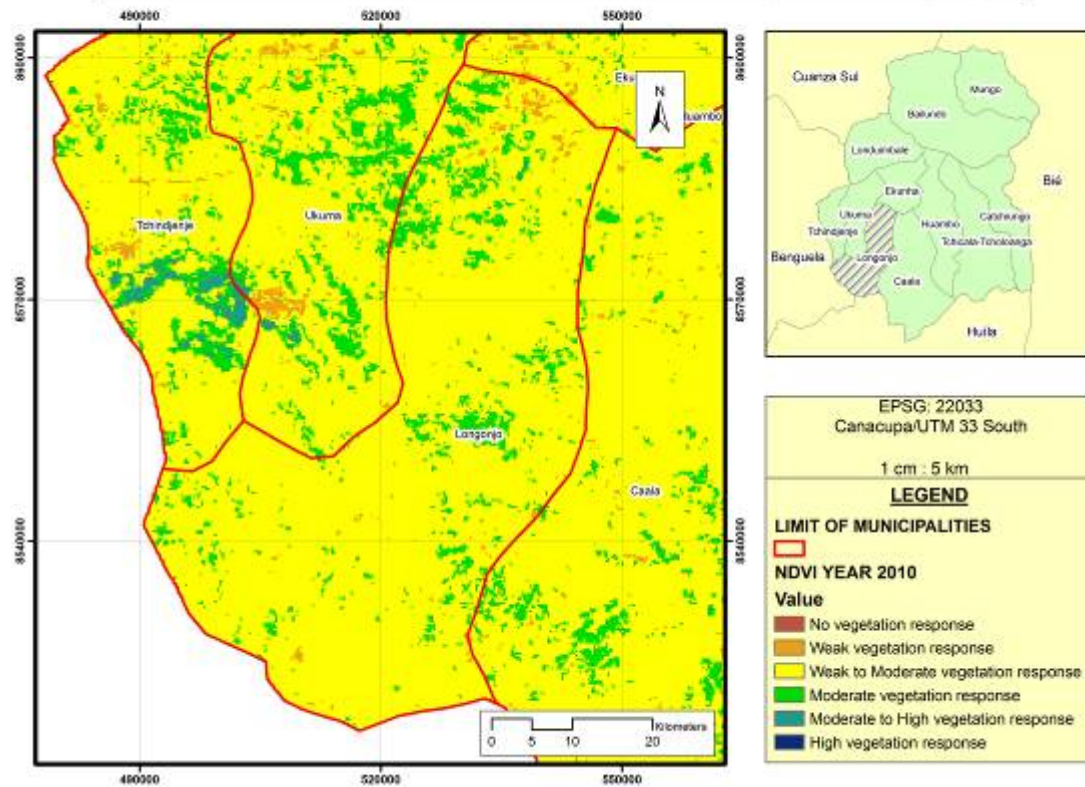
NDVI of Huambo province, municipality of Longonjo.



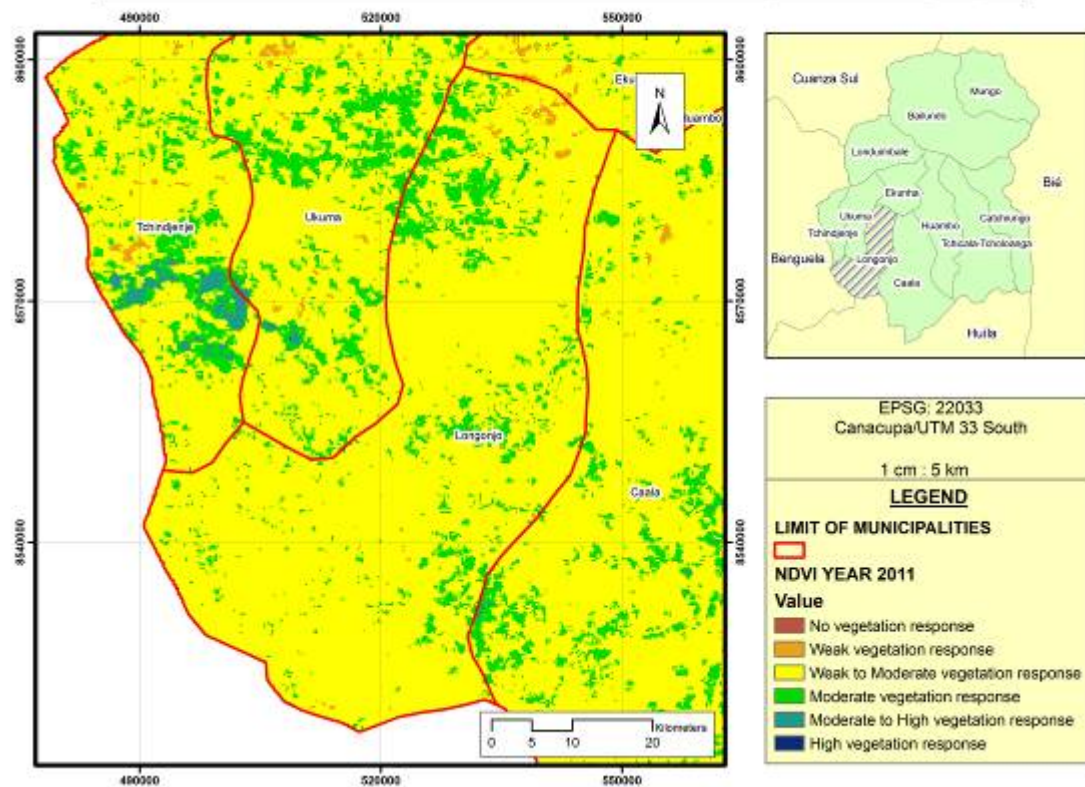
NDVI of Huambo province, municipality of Longonjo.



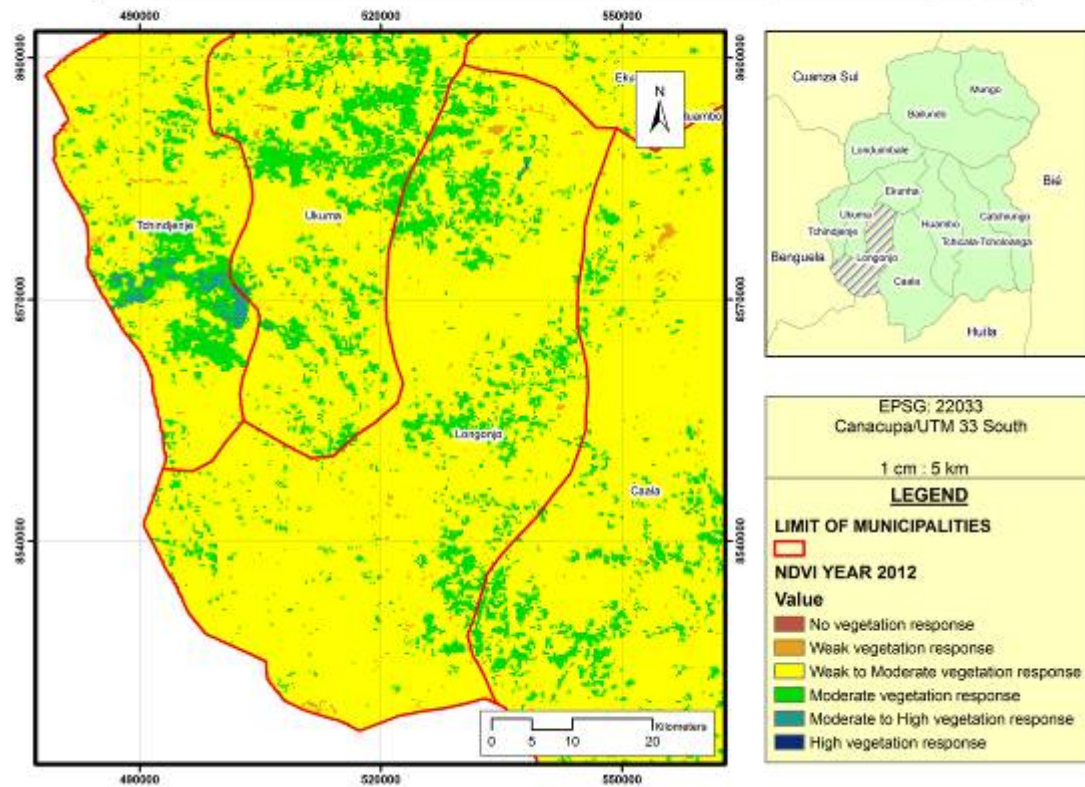
NDVI of Huambo province, municipality of Longonjo.



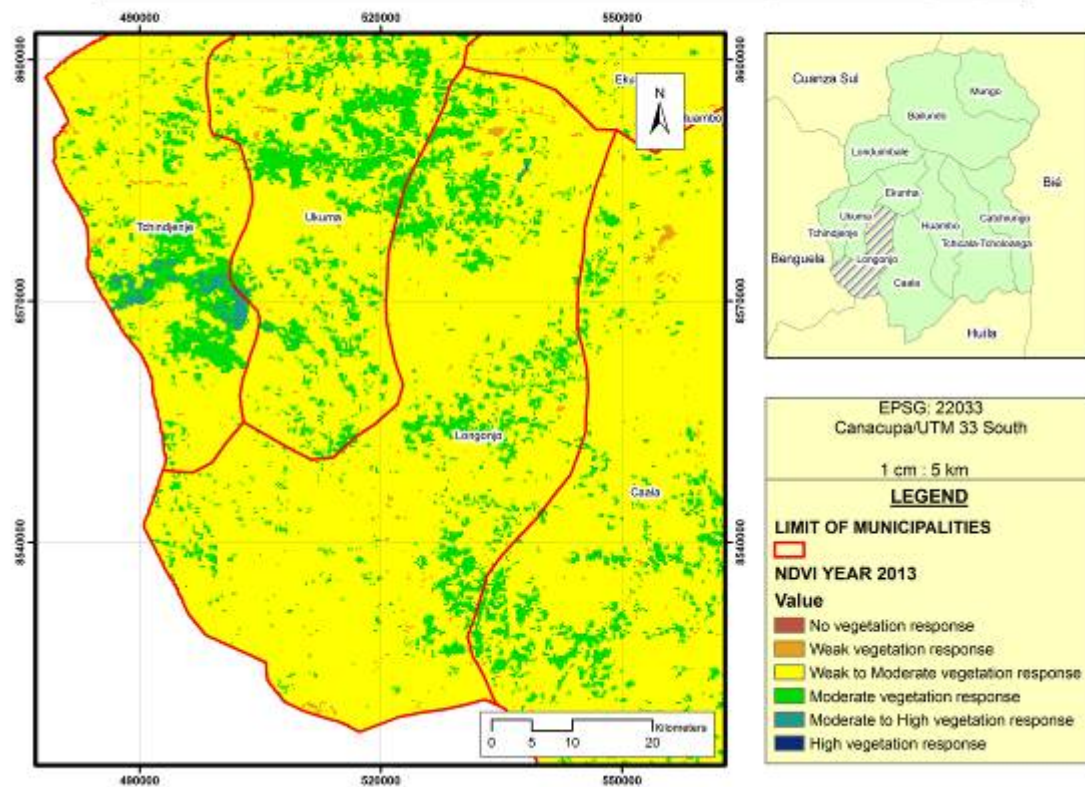
NDVI of Huambo province, municipality of Longonjo.



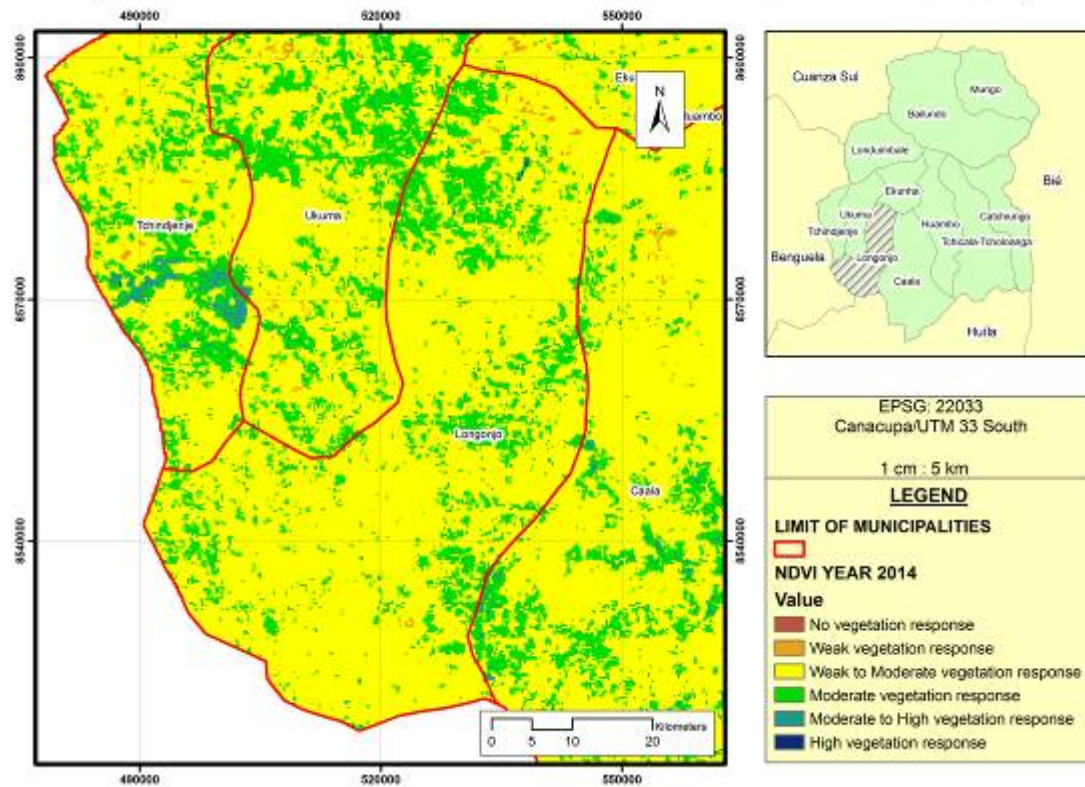
NDVI of Huambo province, municipality of Longonjo.



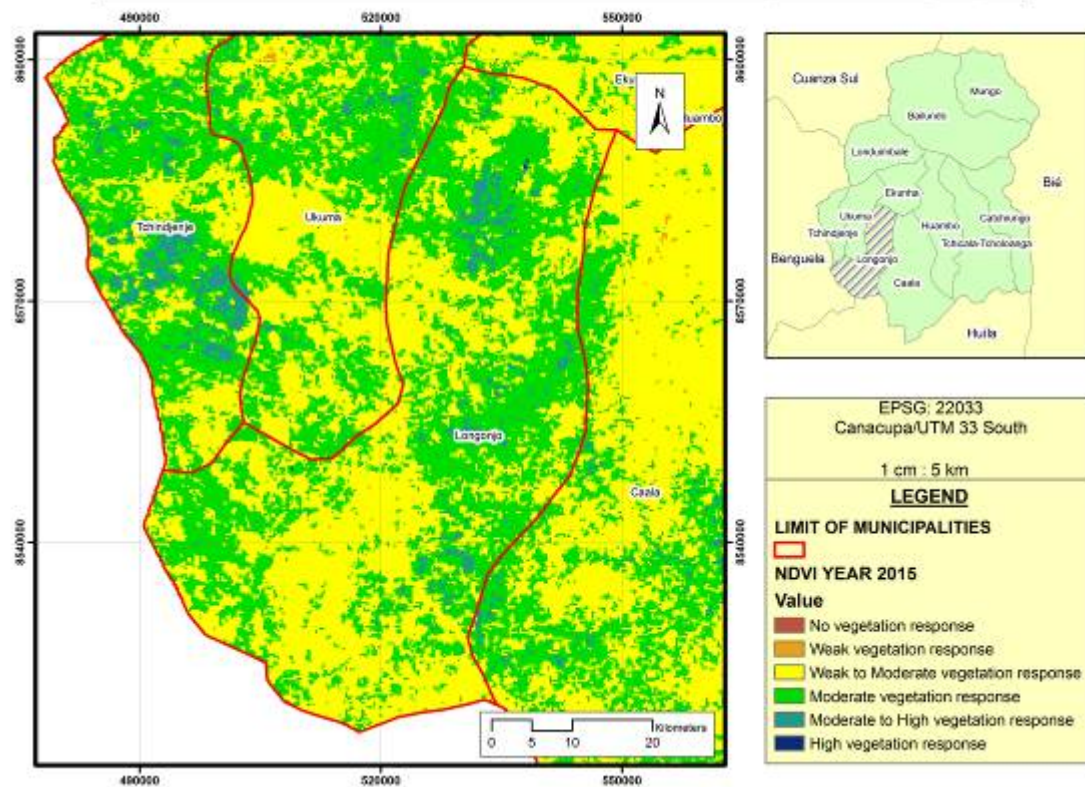
NDVI of Huambo province, municipality of Longonjo.



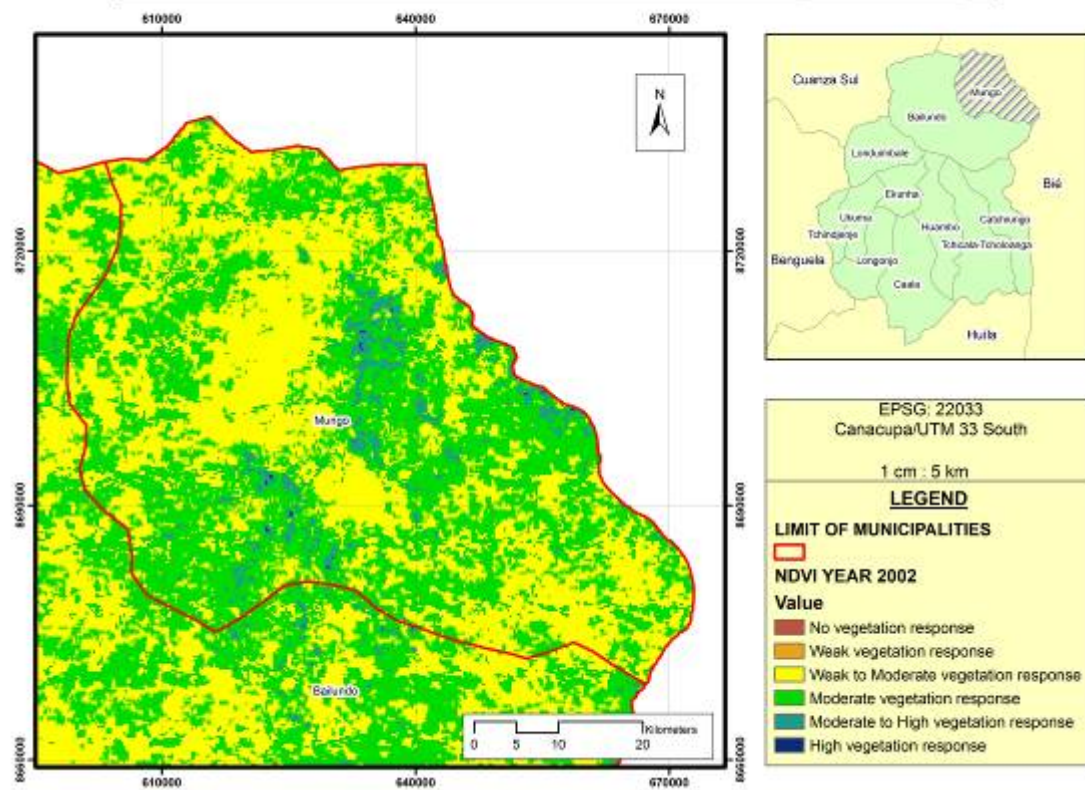
NDVI of Huambo province, municipality of Longonjo.



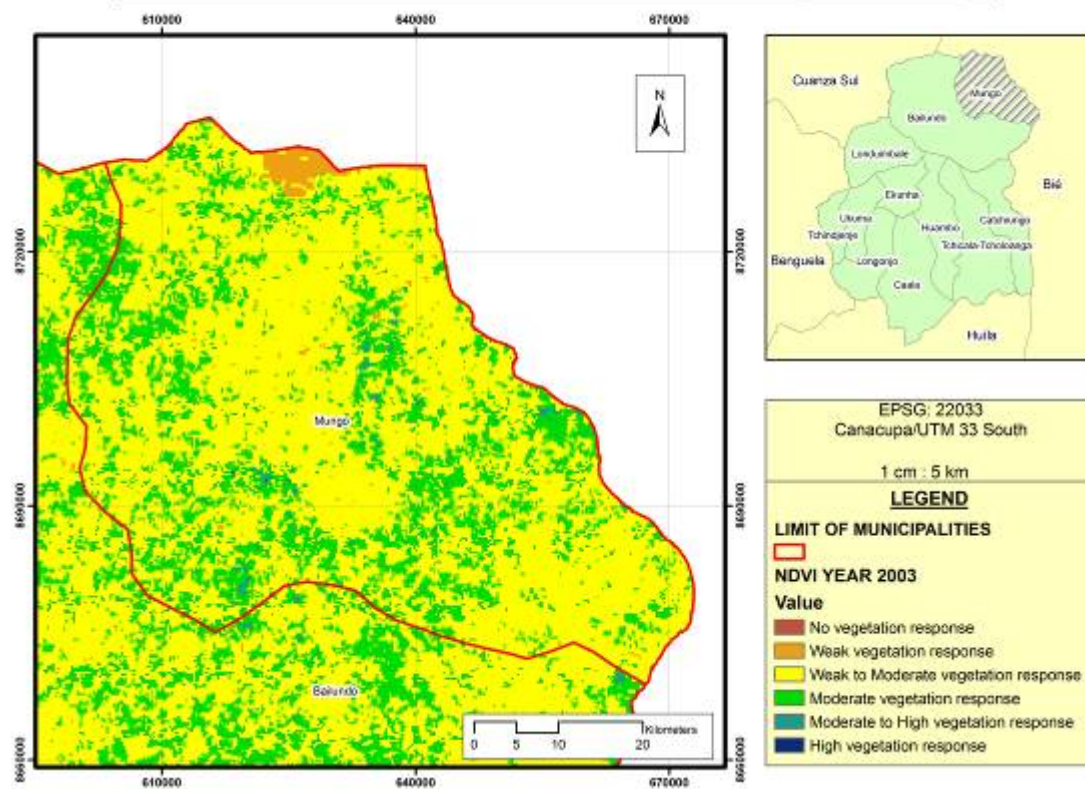
NDVI of Huambo province, municipality of Longonjo.



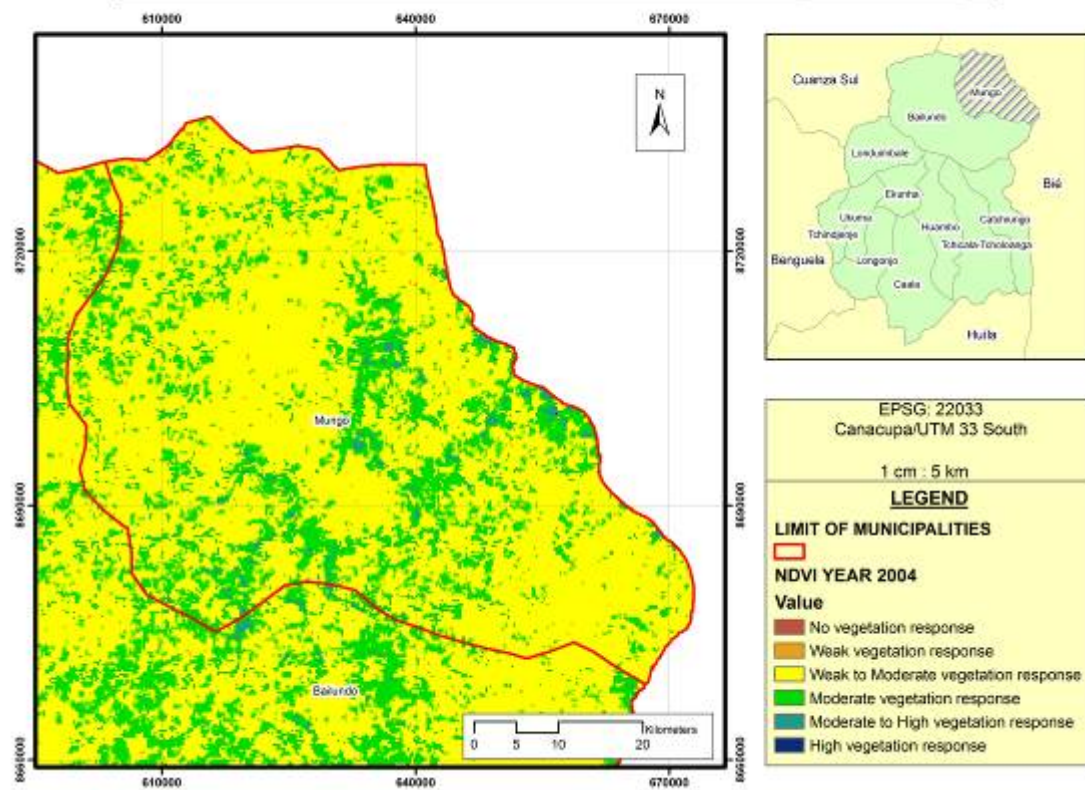
NDVI of Huambo province, municipality of Mungo.



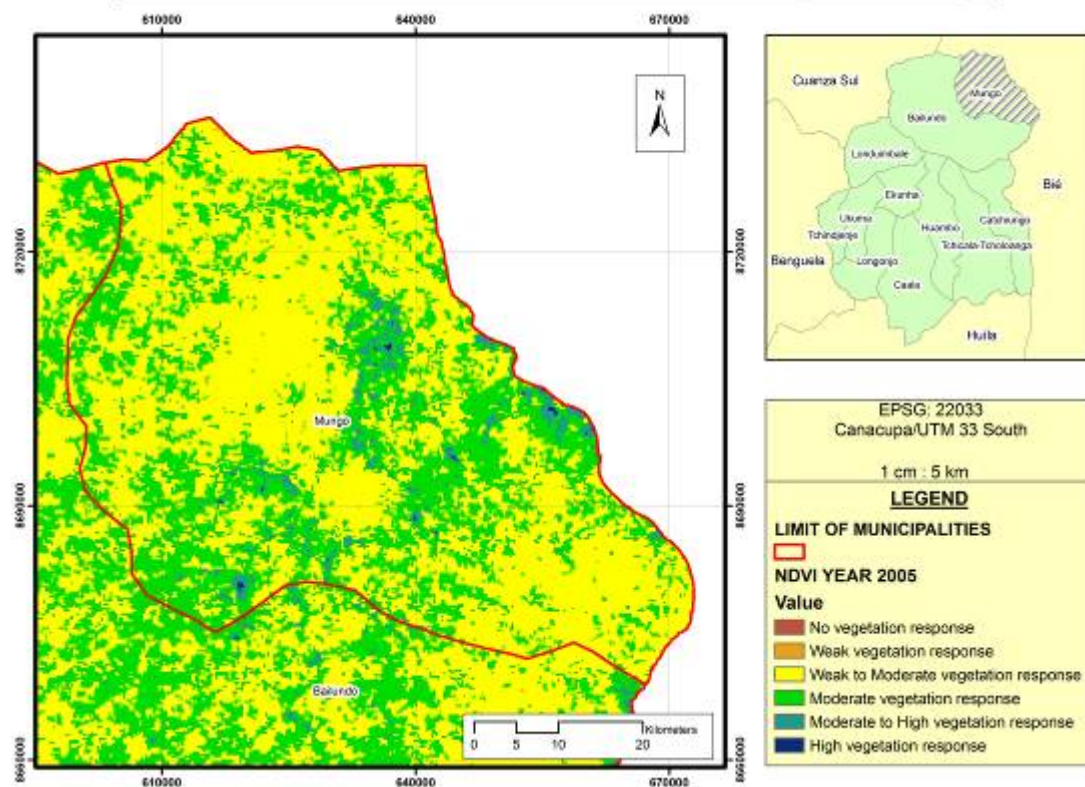
NDVI of Huambo province, municipality of Mungo.



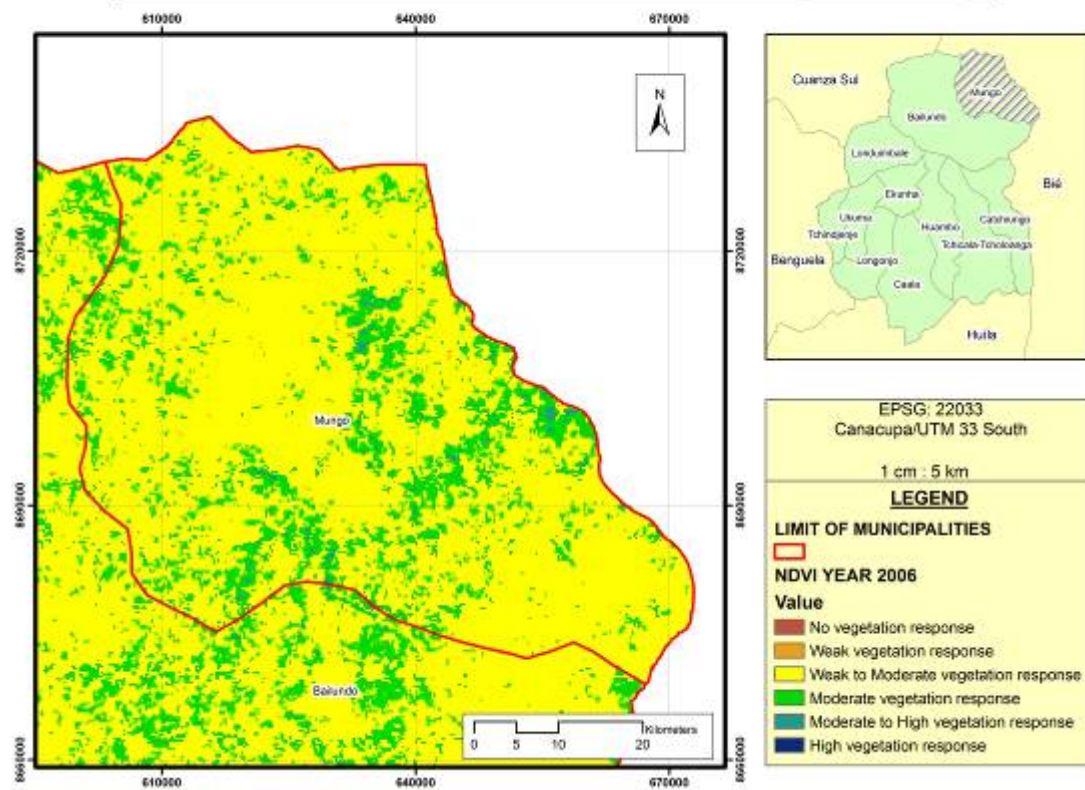
NDVI of Huambo province, municipality of Mungo.



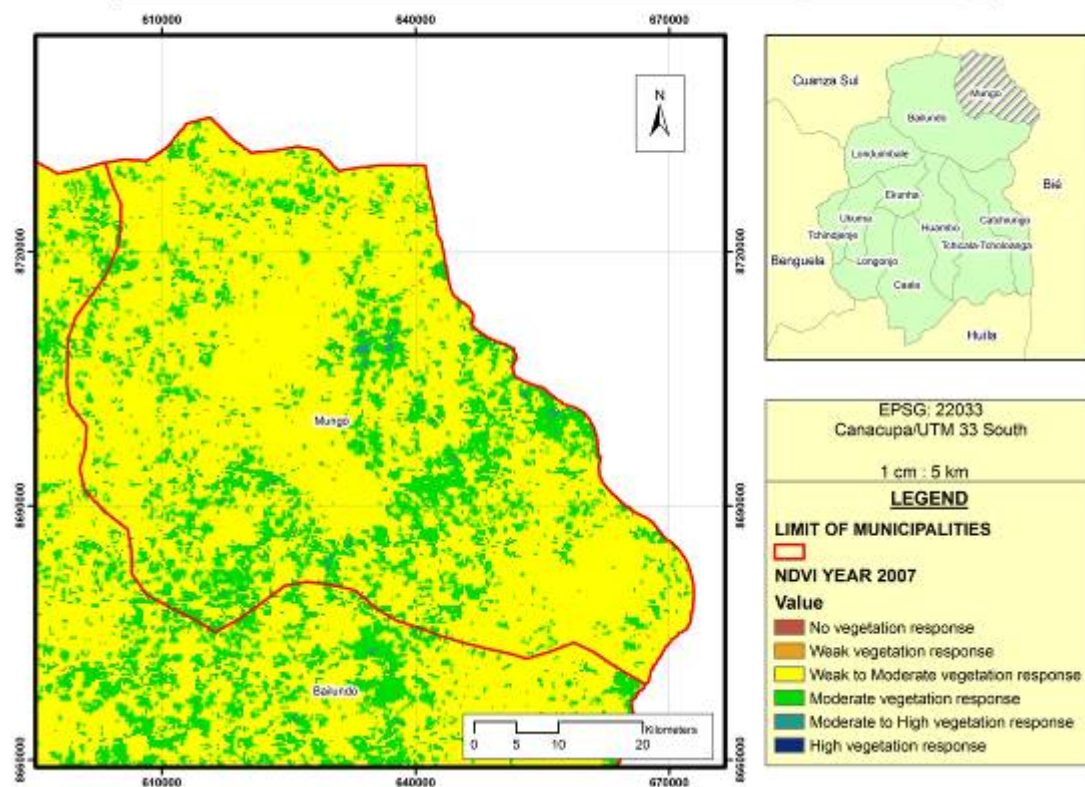
NDVI of Huambo province, municipality of Mungo.



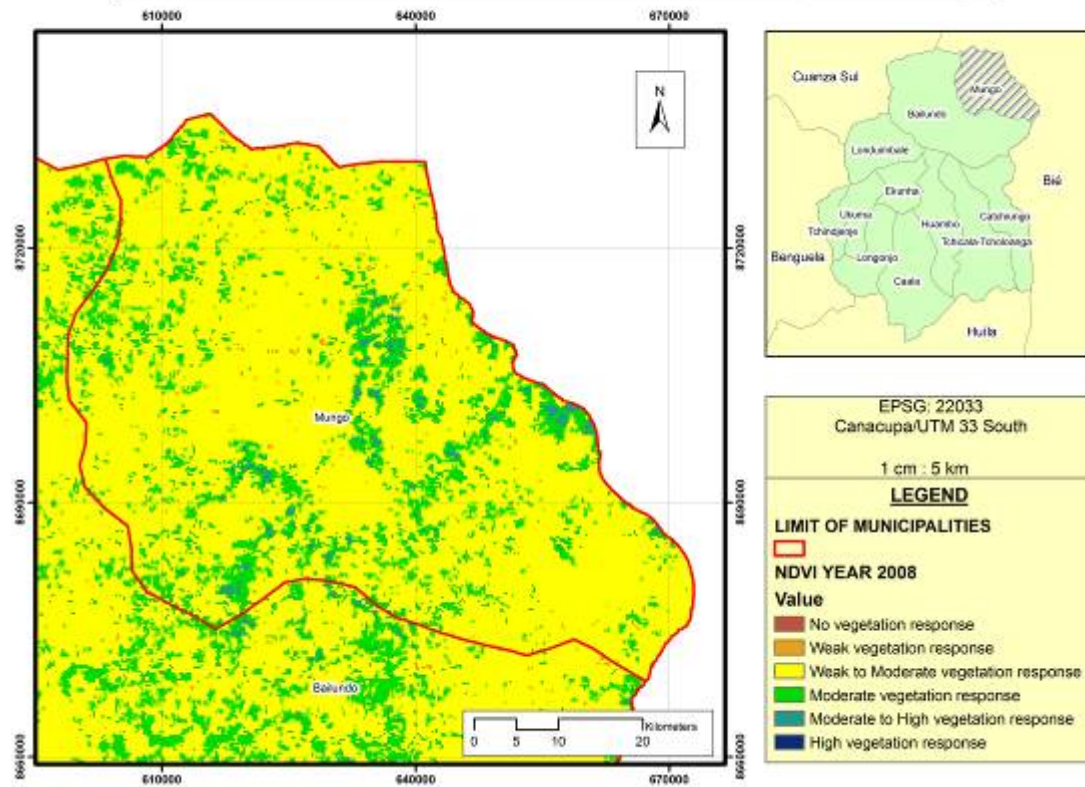
NDVI of Huambo province, municipality of Mungo.



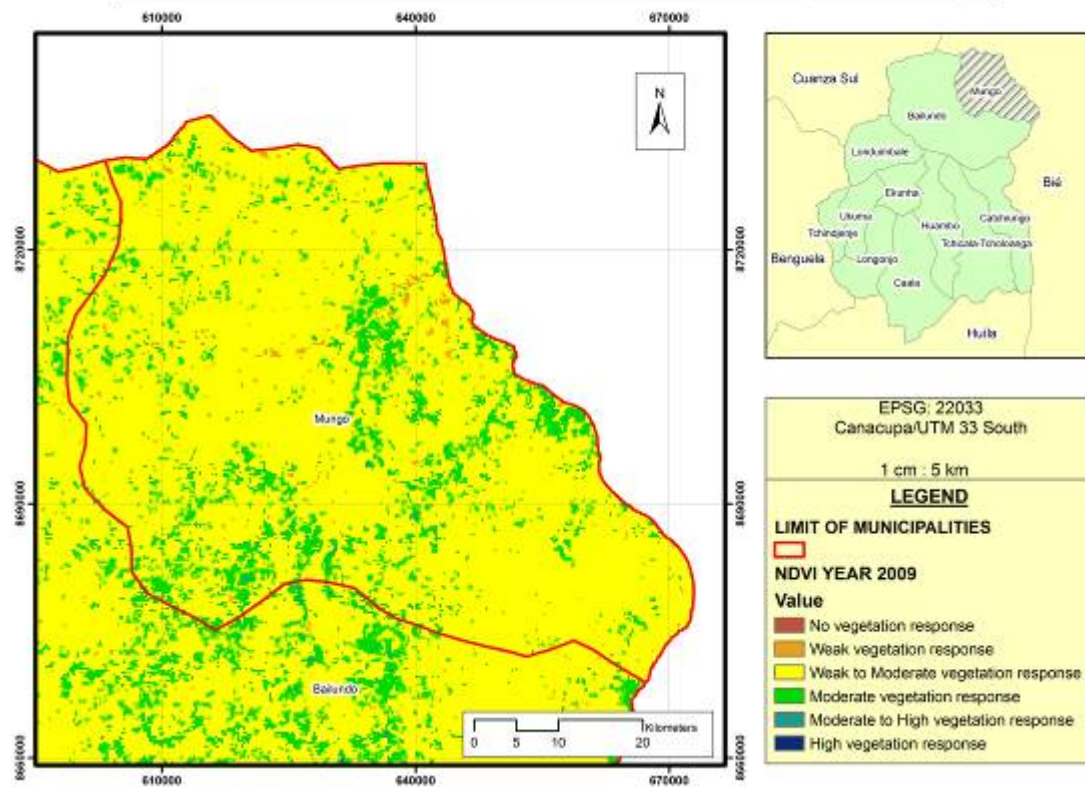
NDVI of Huambo province, municipality of Mungo.



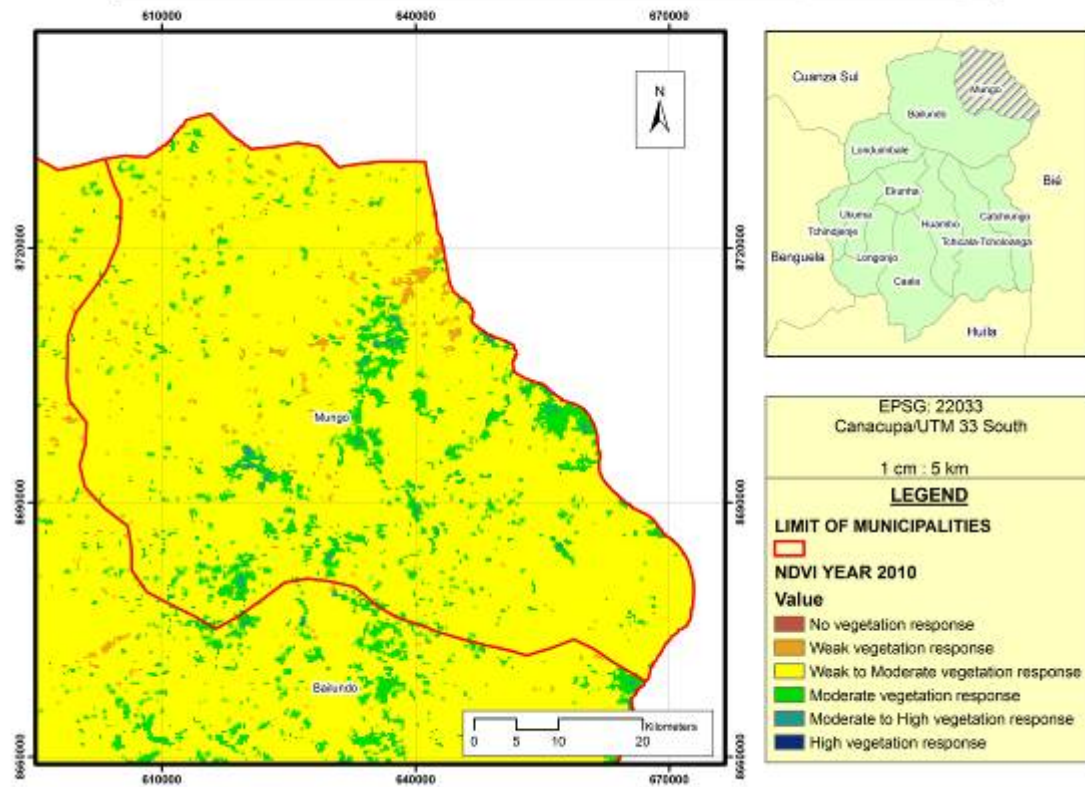
NDVI of Huambo province, municipality of Mungo.



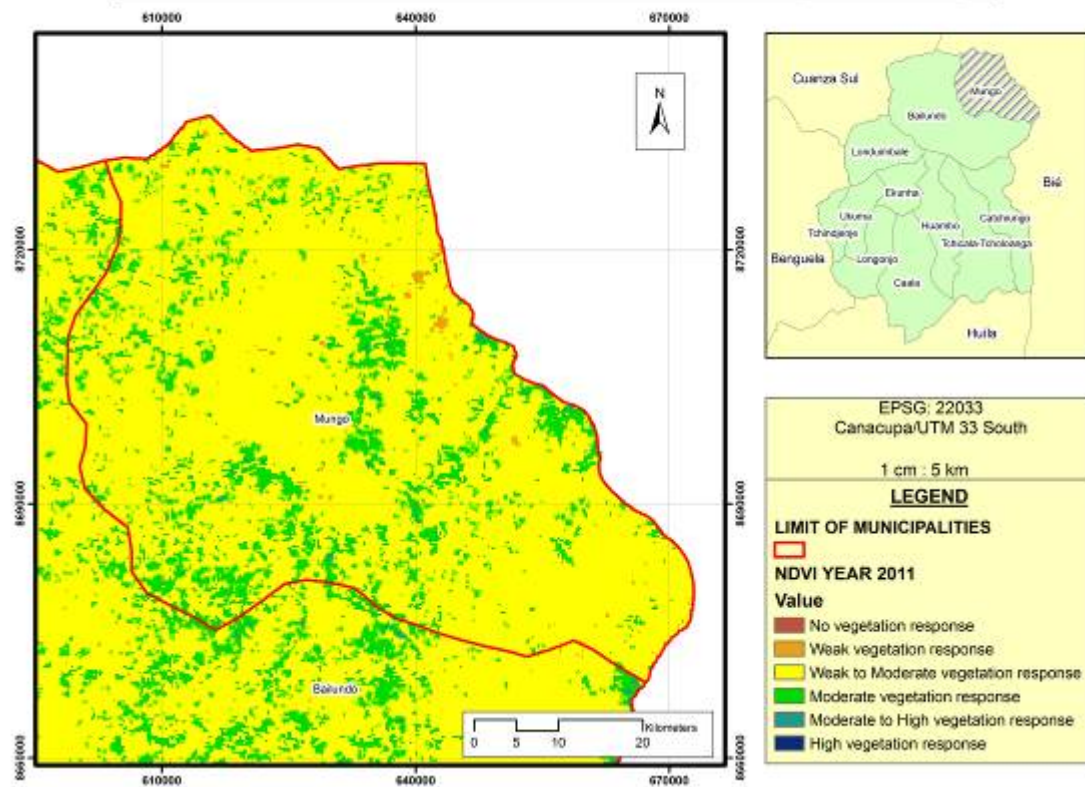
NDVI of Huambo province, municipality of Mungo.



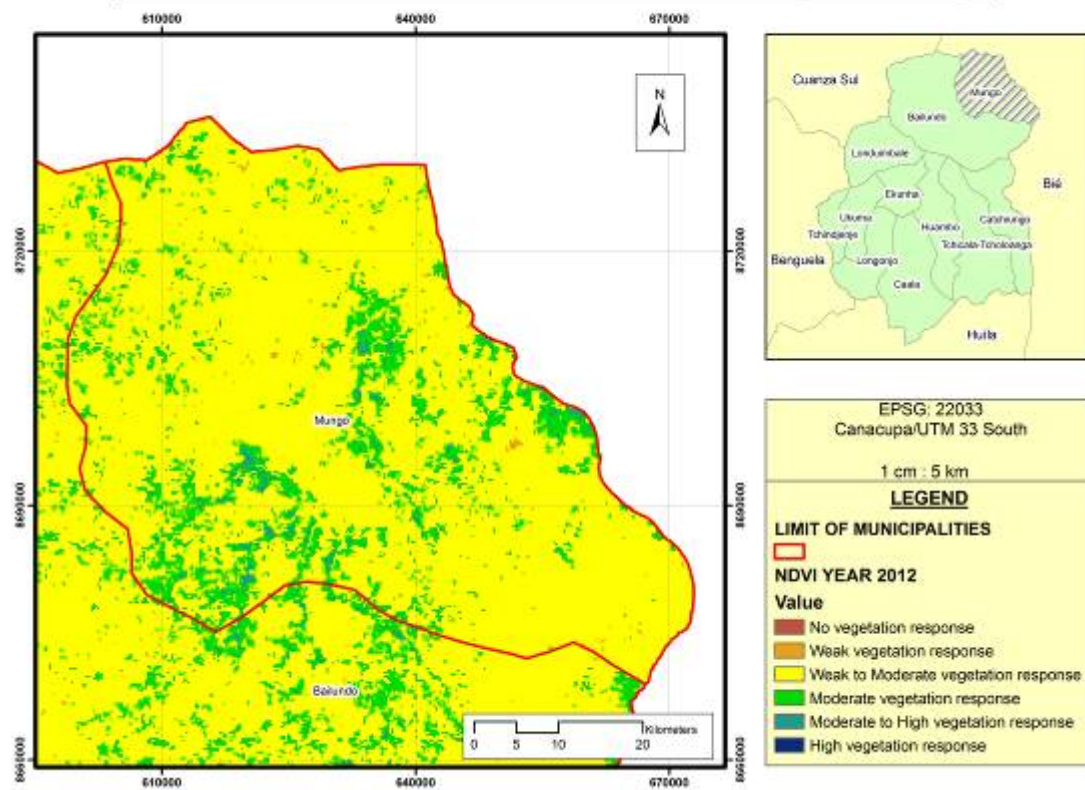
NDVI of Huambo province, municipality of Mungo.



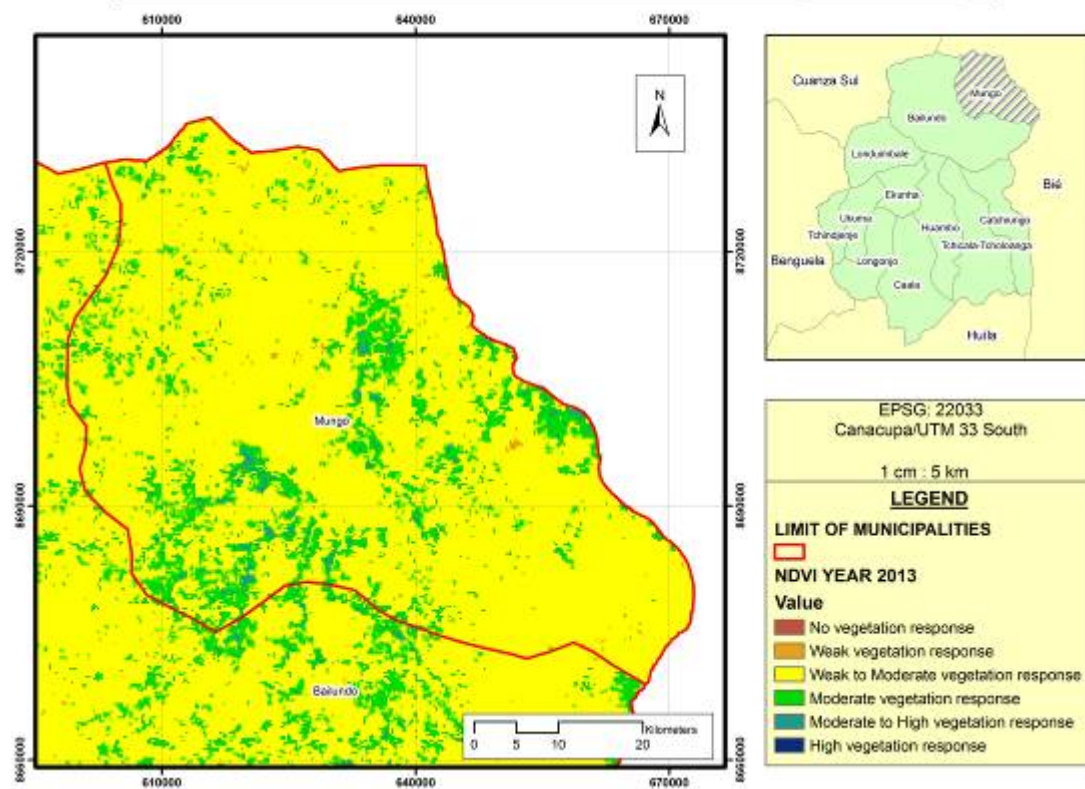
NDVI of Huambo province, municipality of Mungo.



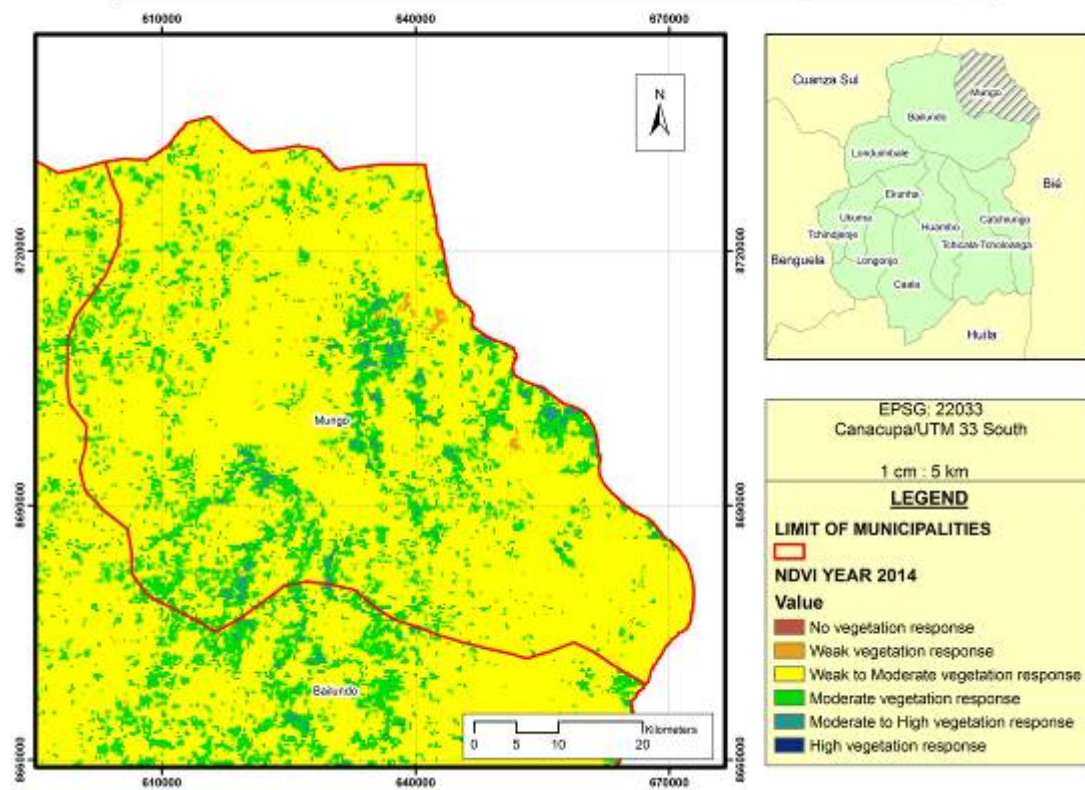
NDVI of Huambo province, municipality of Mungo.



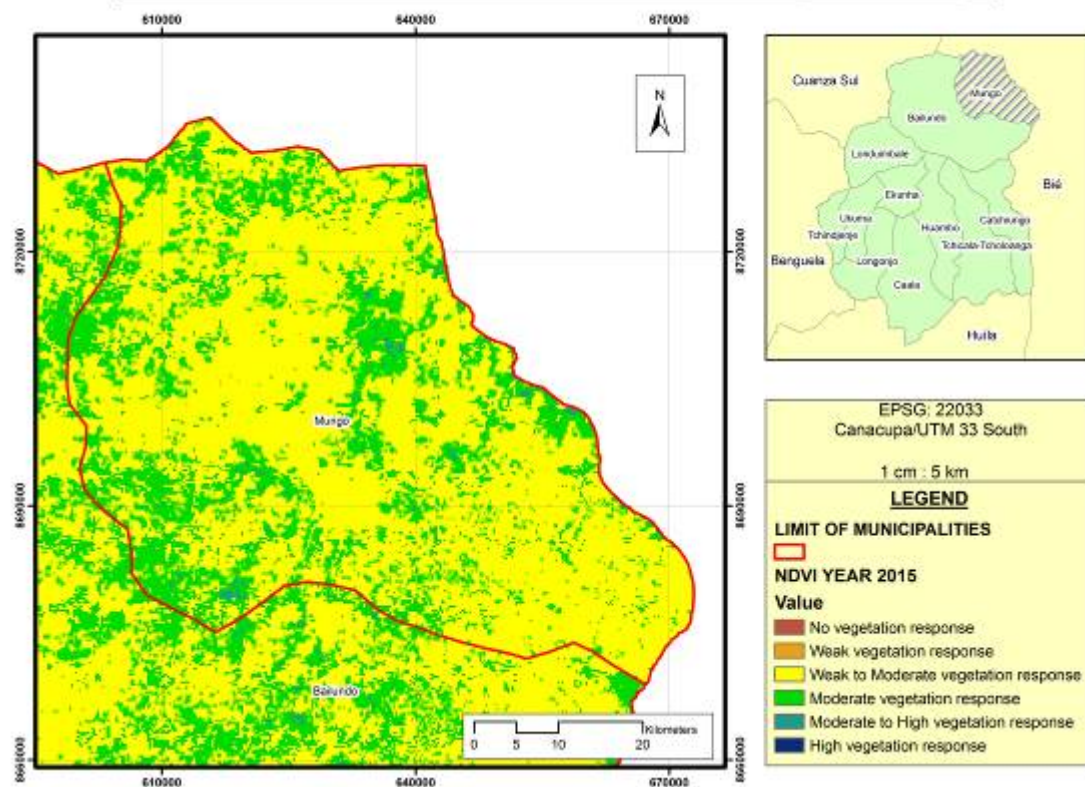
NDVI of Huambo province, municipality of Mungo.



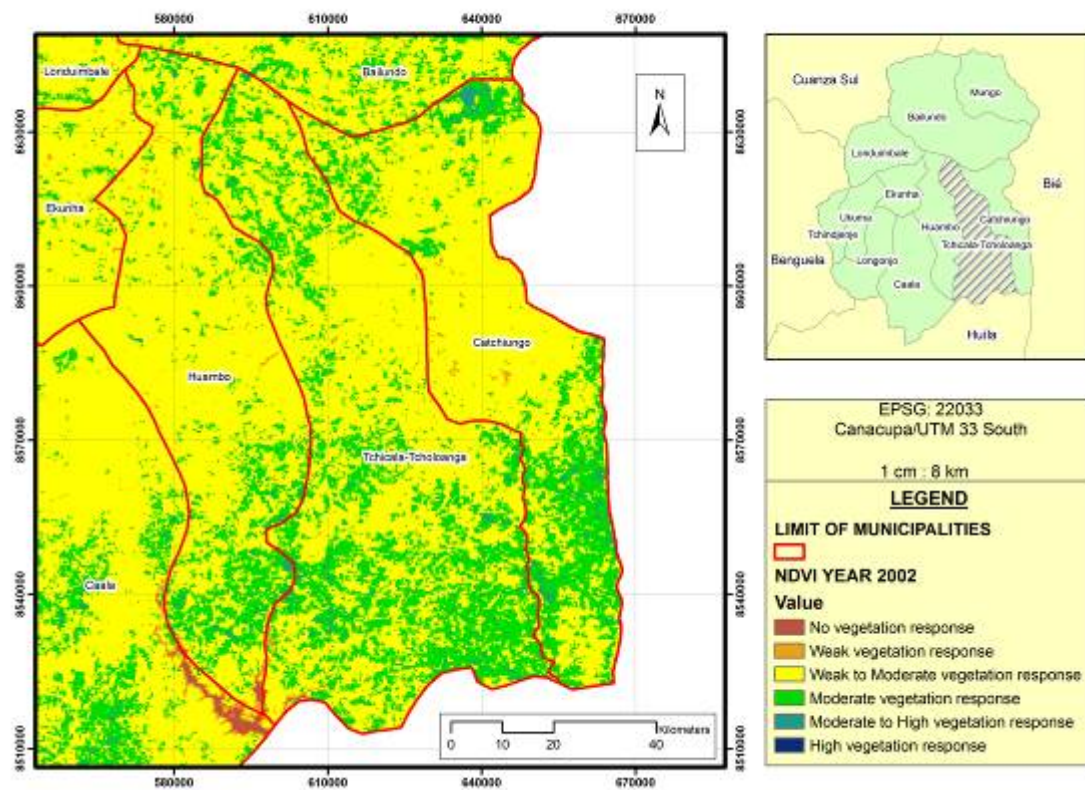
NDVI of Huambo province, municipality of Mungo.



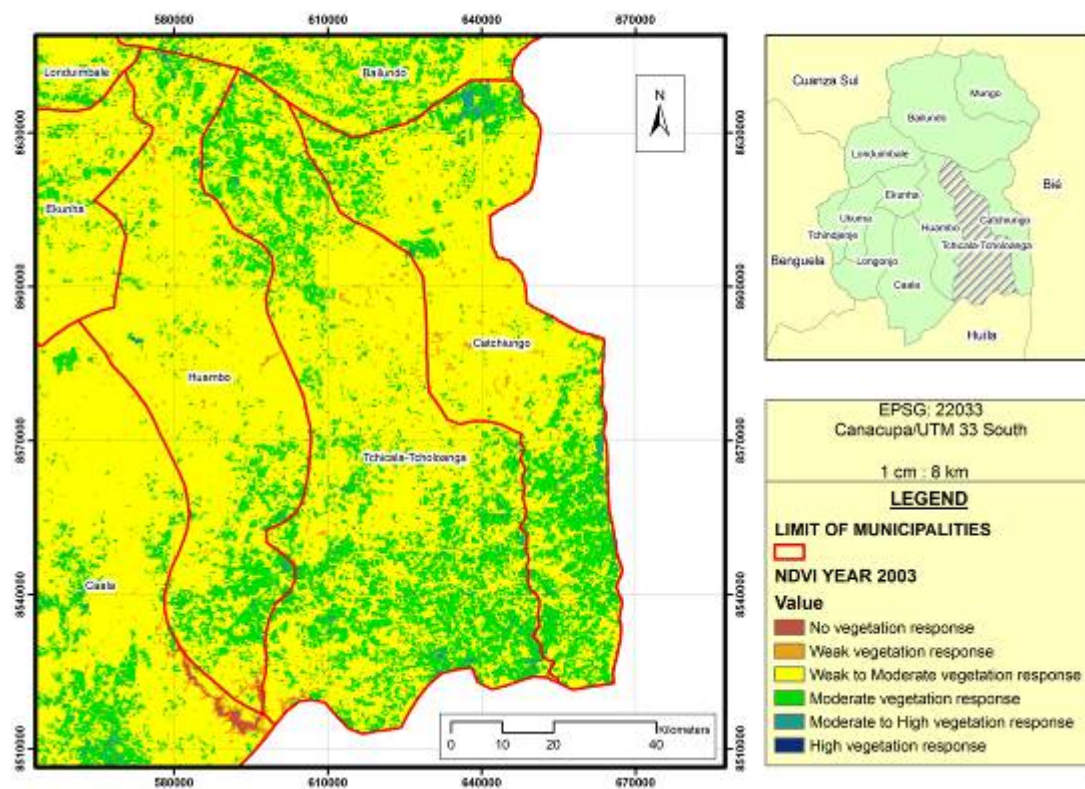
NDVI of Huambo province, municipality of Mungo.



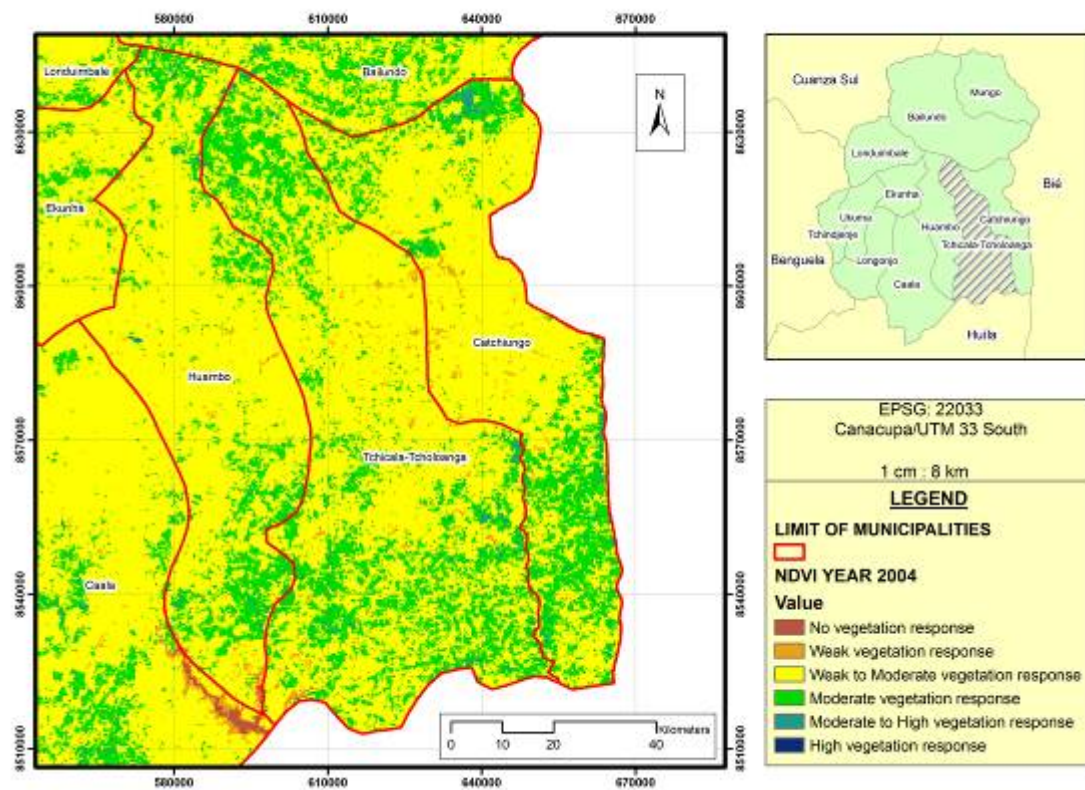
NDVI of Huambo province, municipality of Tchicala-Tcholoanga.



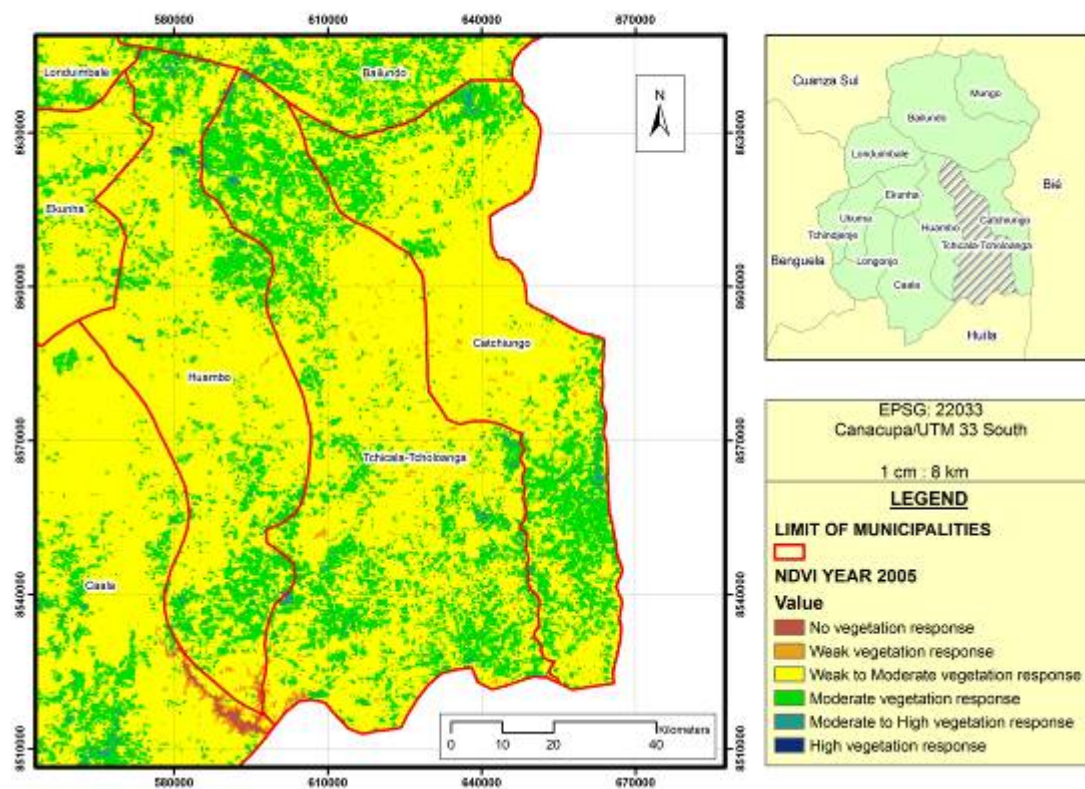
NDVI of Huambo province, municipality of Tchicala-Tcholoanga.



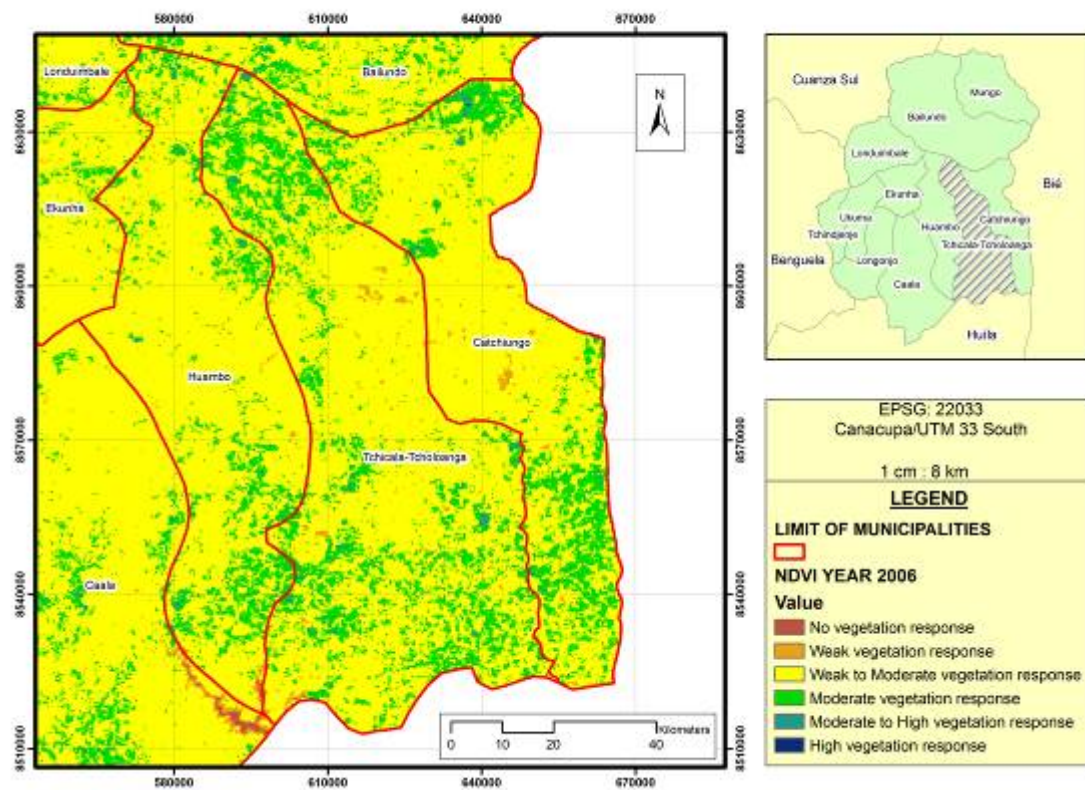
NDVI of Huambo province, municipality of Tchicala-Tcholoanga.



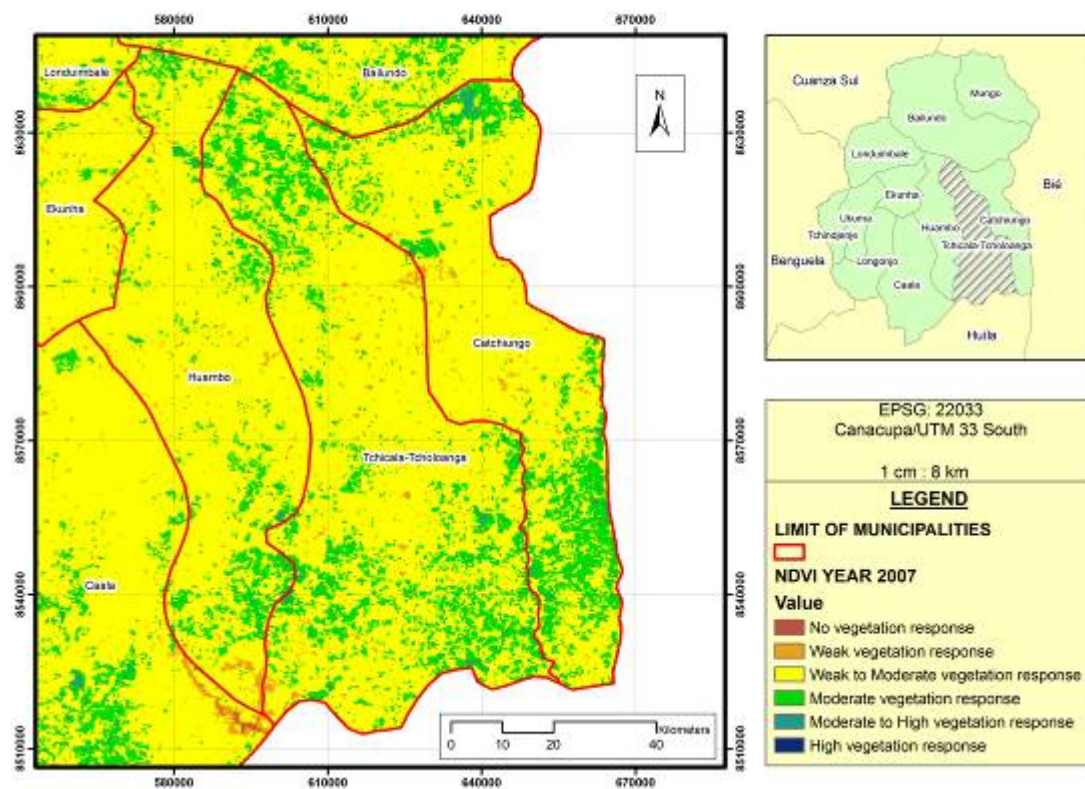
NDVI of Huambo province, municipality of Tchicala-Tcholoanga.



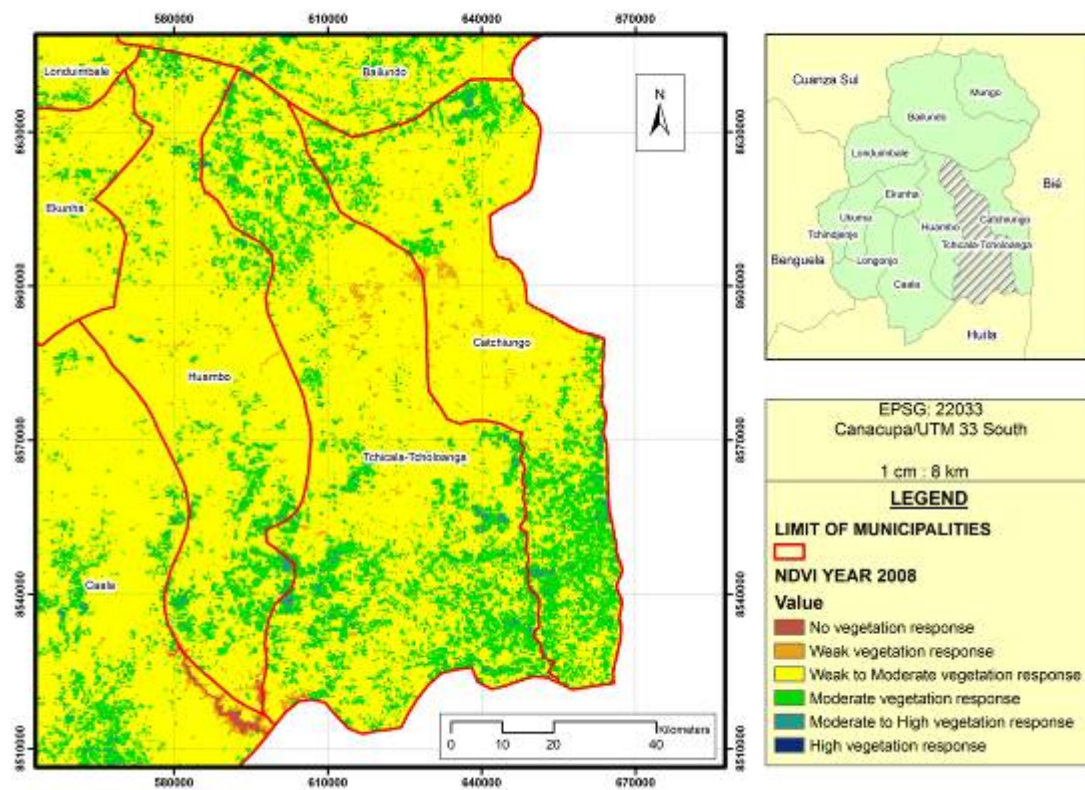
NDVI of Huambo province, municipality of Tchicala-Tcholoanga.



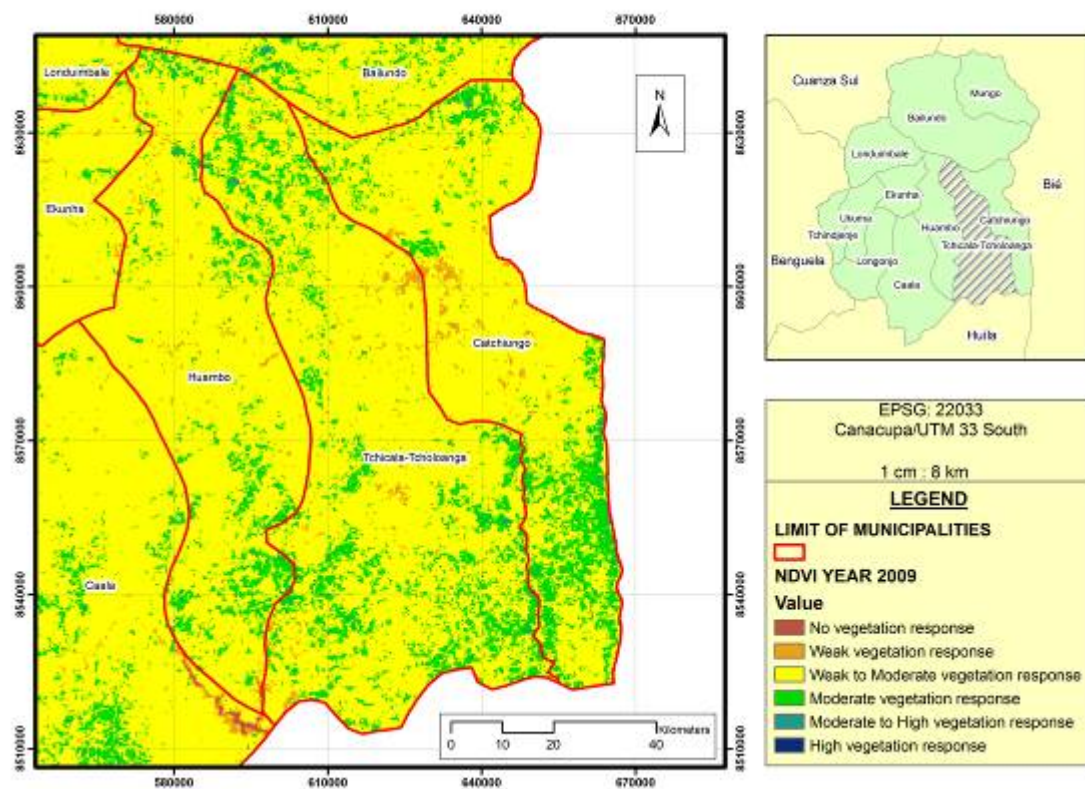
NDVI of Huambo province, municipality of Tchicala-Tcholoanga.



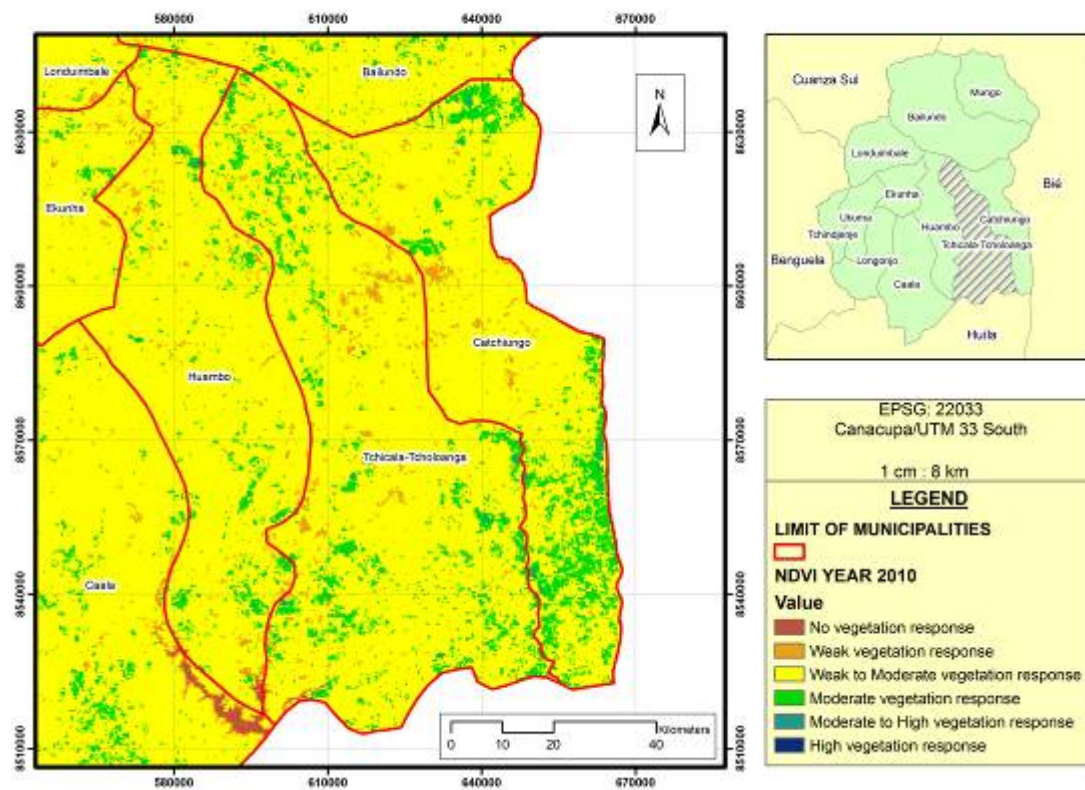
NDVI of Huambo province, municipality of Tchicala-Tcholoanga.



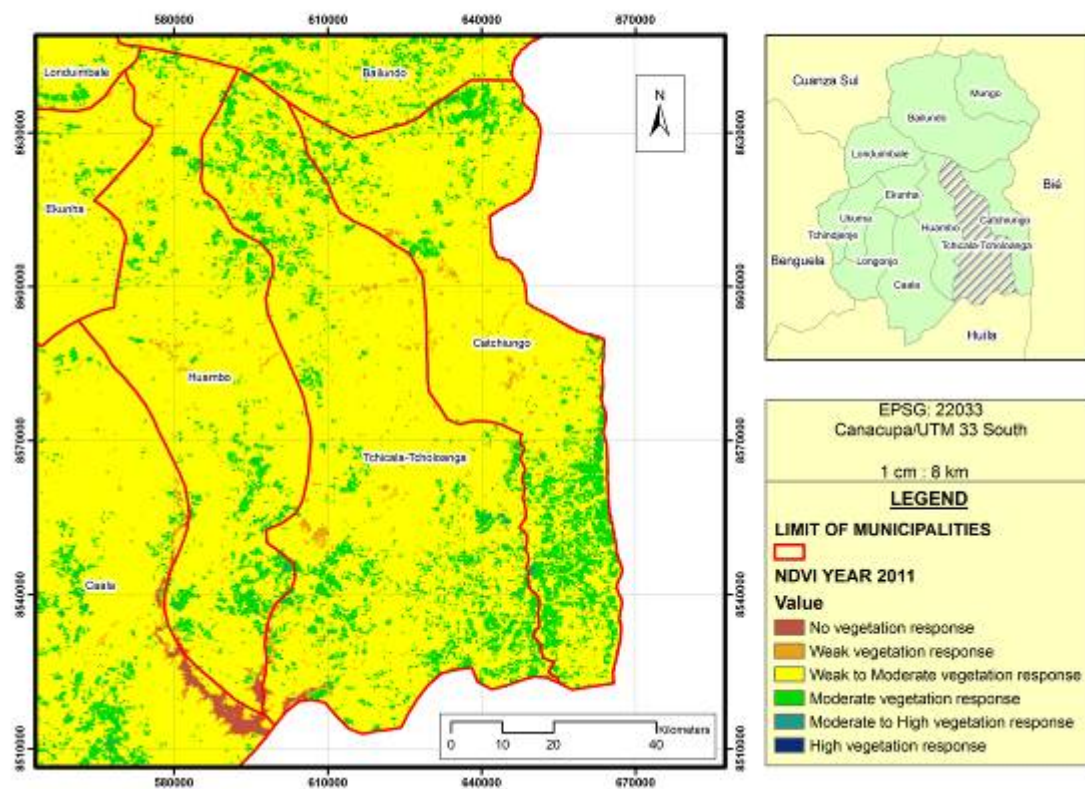
NDVI of Huambo province, municipality of Tchicala-Tcholoanga.



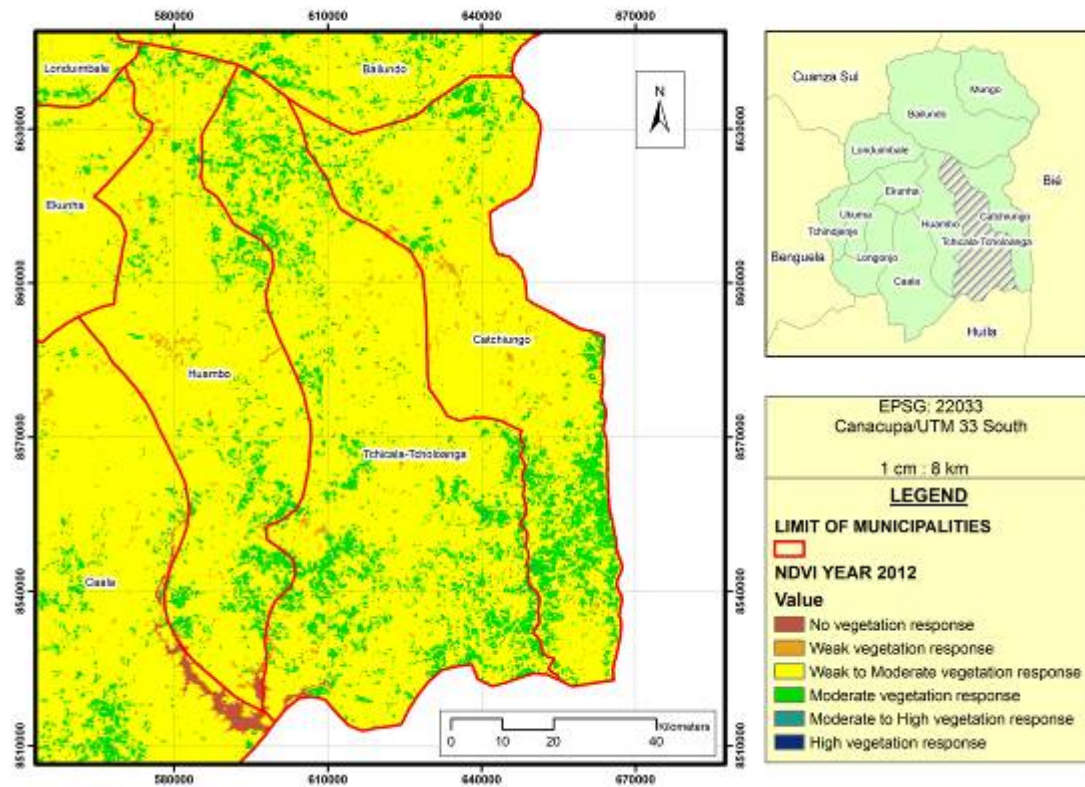
NDVI of Huambo province, municipality of Tchicala-Tcholoanga.



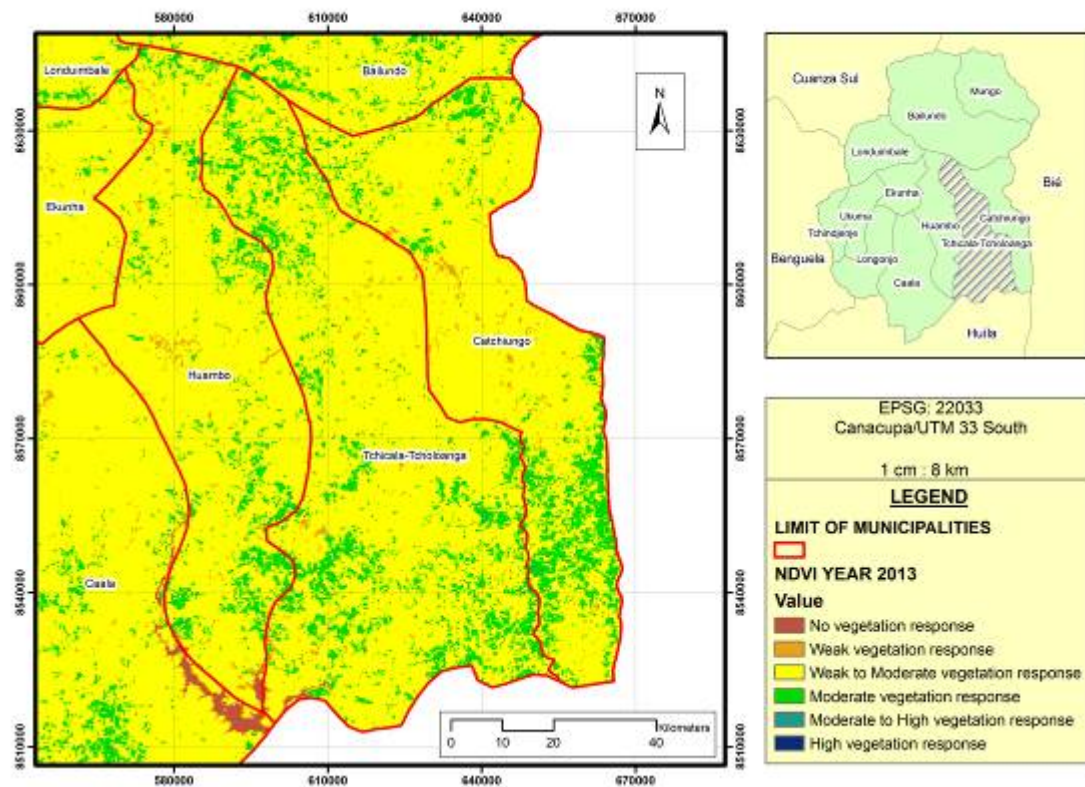
NDVI of Huambo province, municipality of Tchicala-Tcholoanga.



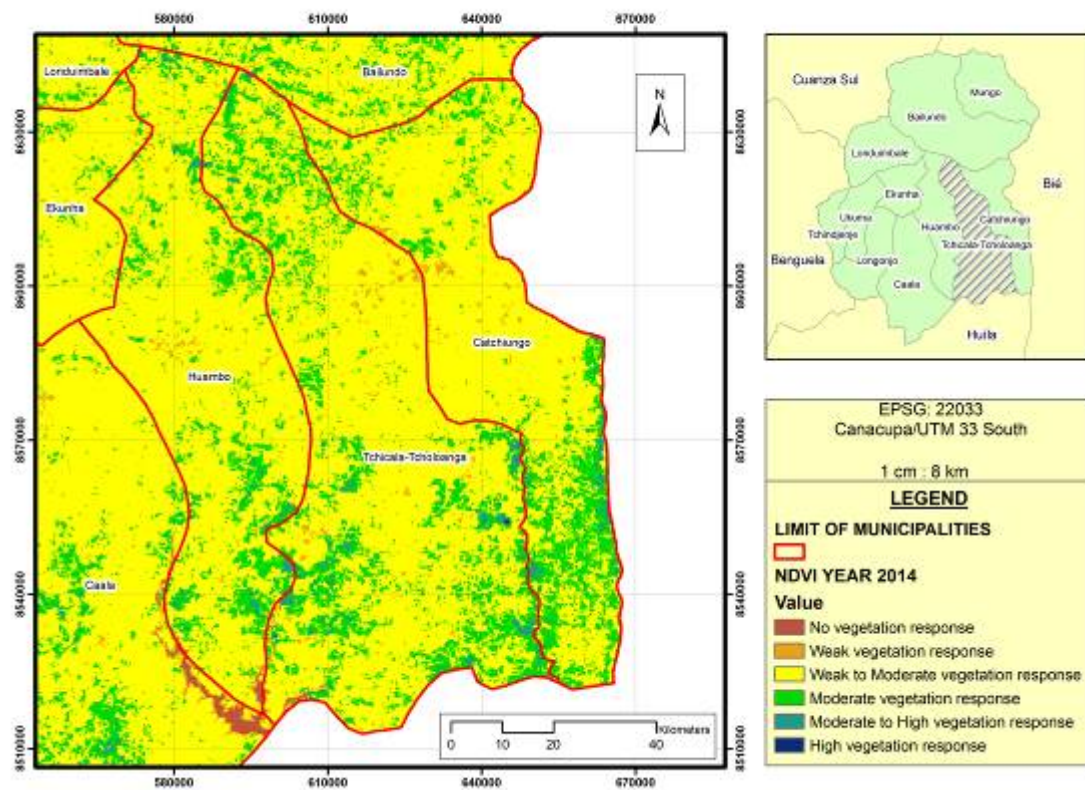
NDVI of Huambo province, municipality of Tchicala-Tcholoanga.



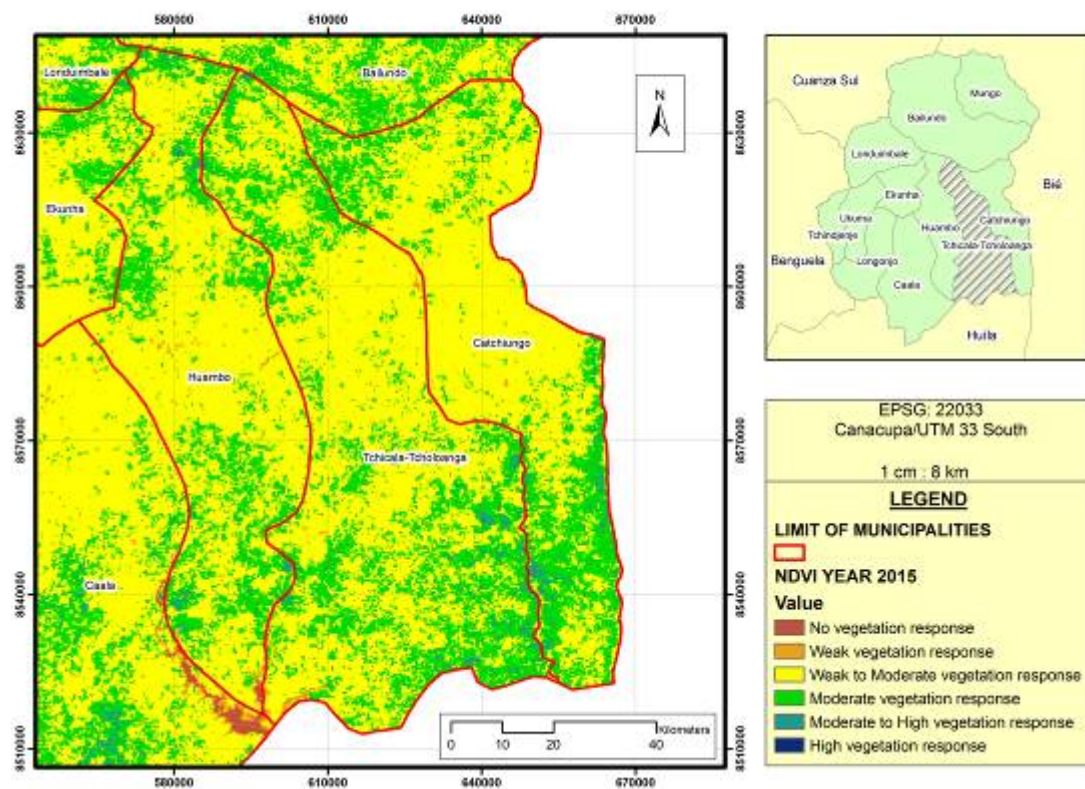
NDVI of Huambo province, municipality of Tchicala-Tcholoanga.



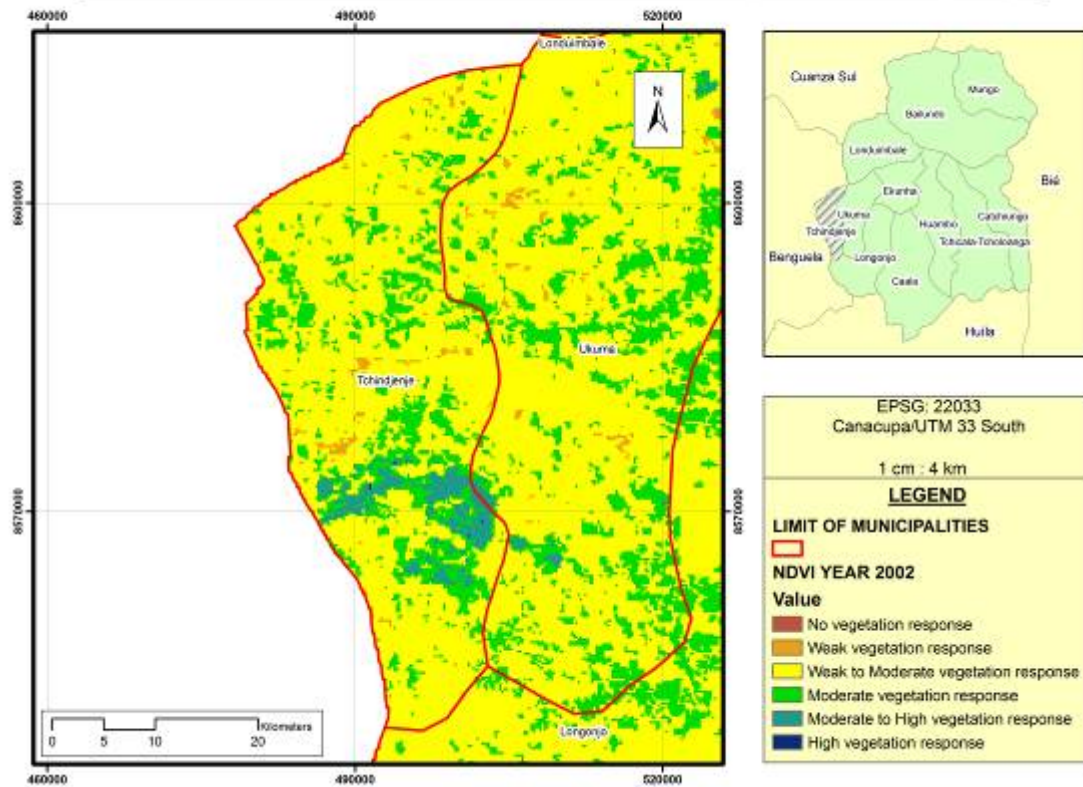
NDVI of Huambo province, municipality of Tchicala-Tcholoanga.



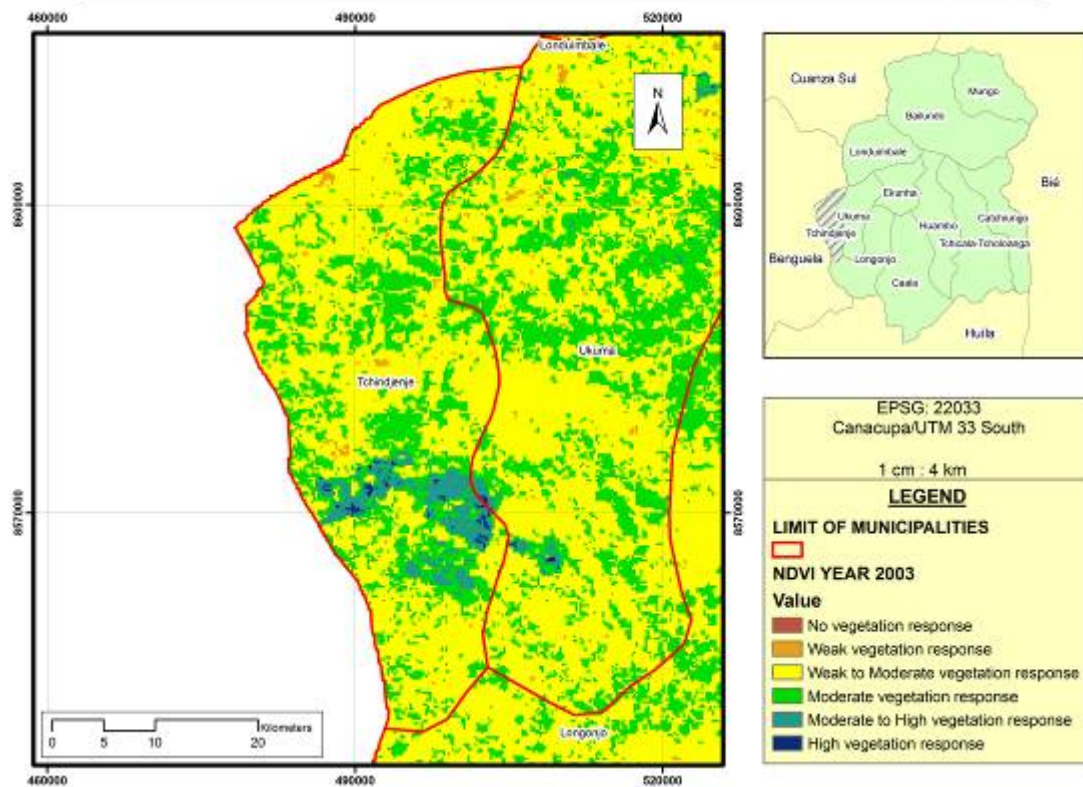
NDVI of Huambo province, municipality of Tchicala-Tcholoanga.



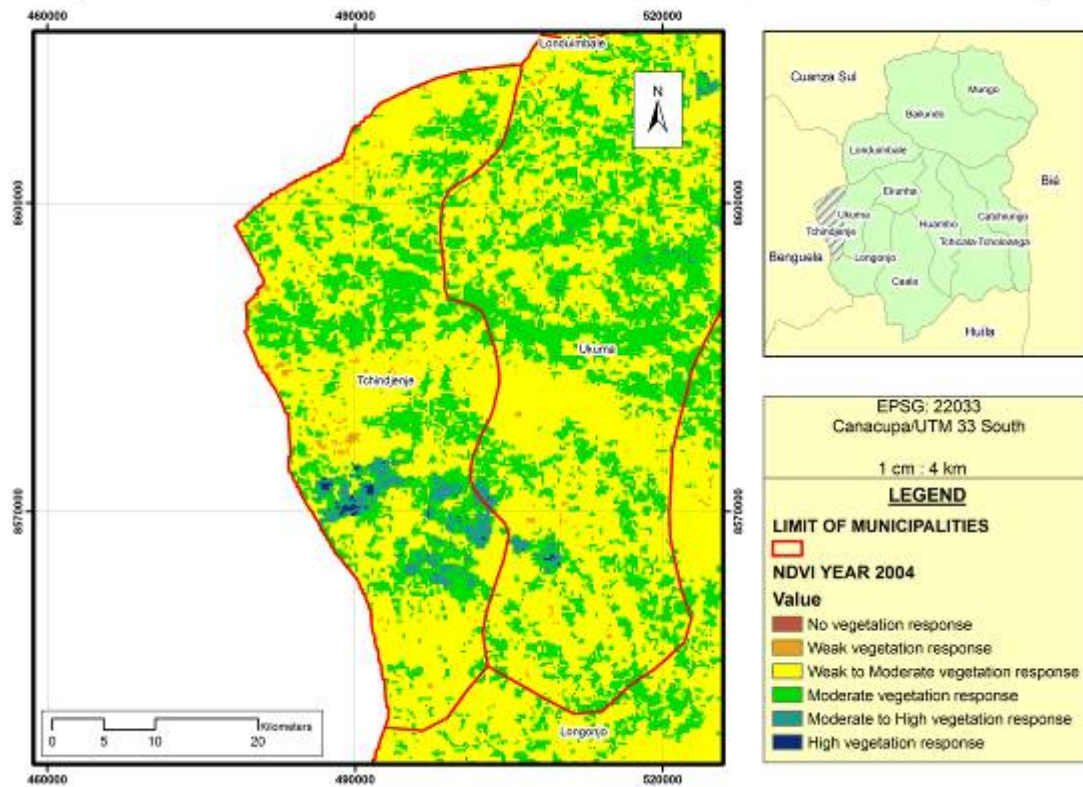
NDVI of Huambo province, municipality of Tchindjenje.



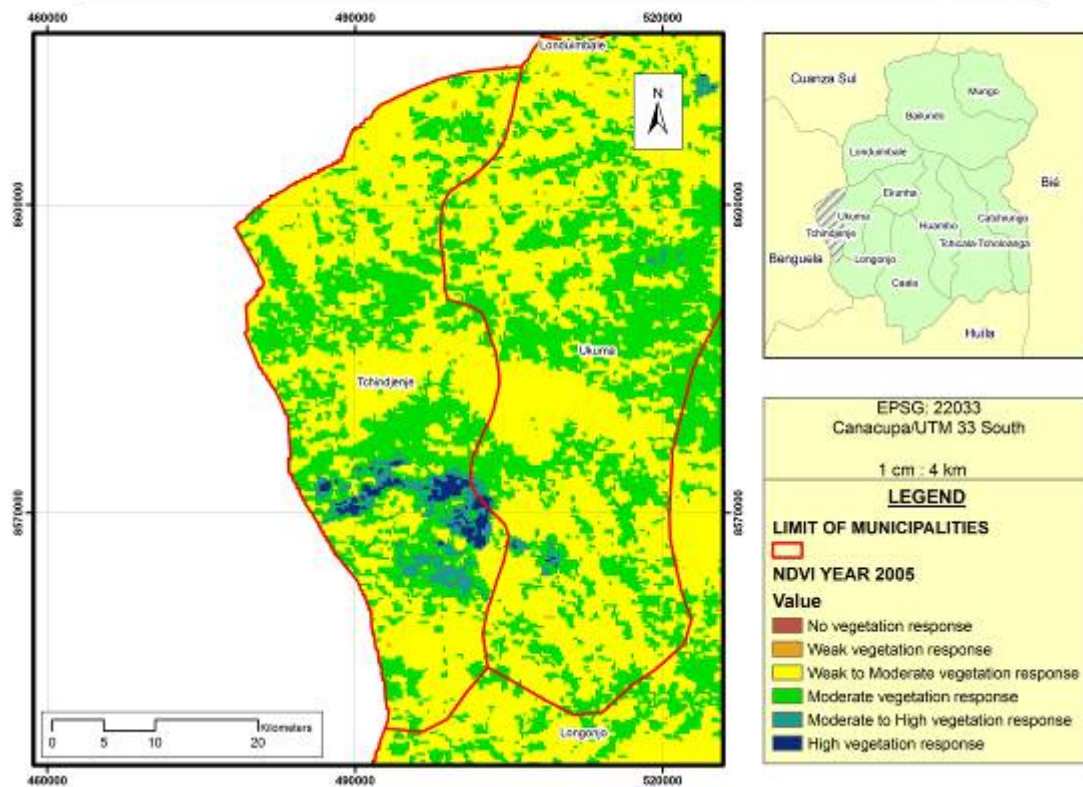
NDVI of Huambo province, municipality of Tchindjenje.



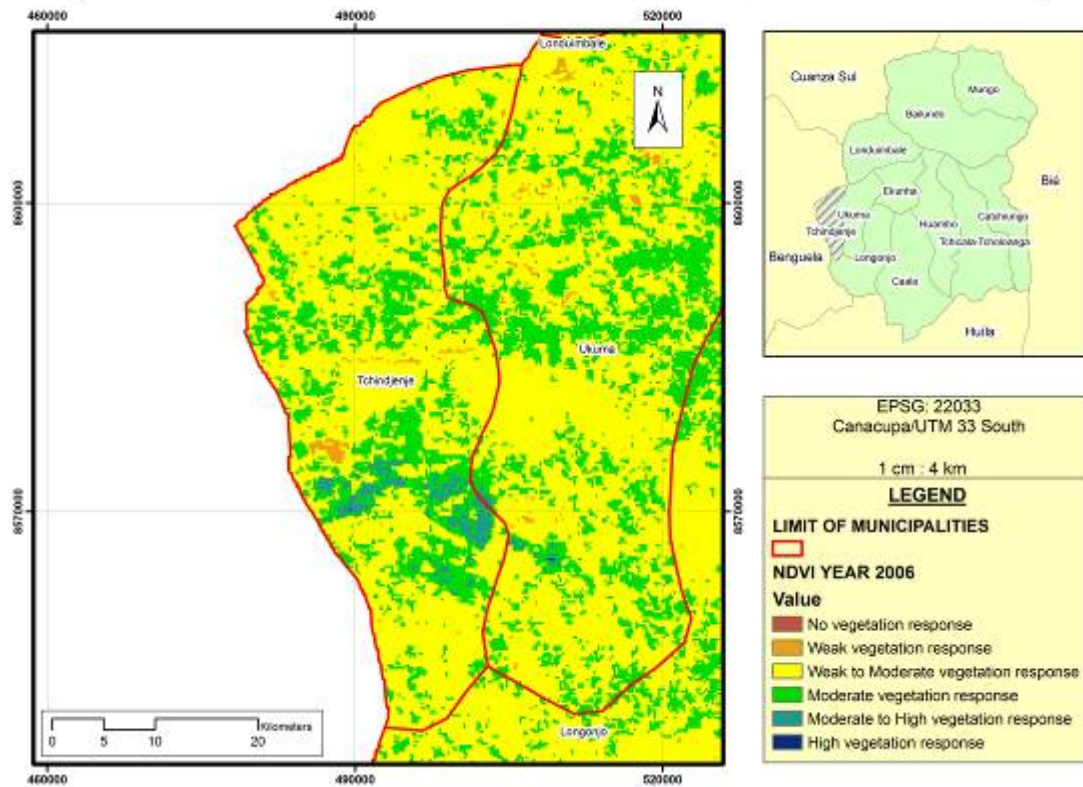
NDVI of Huambo province, municipality of Tchindjenje.



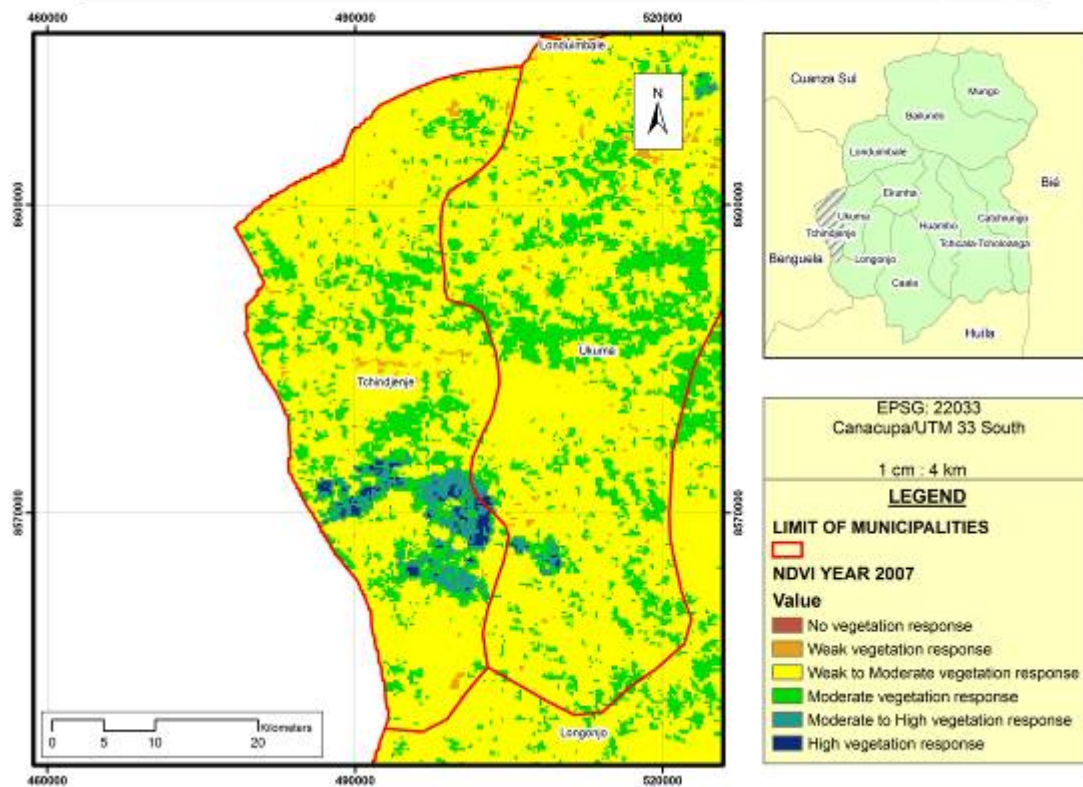
NDVI of Huambo province, municipality of Tchindjenje.



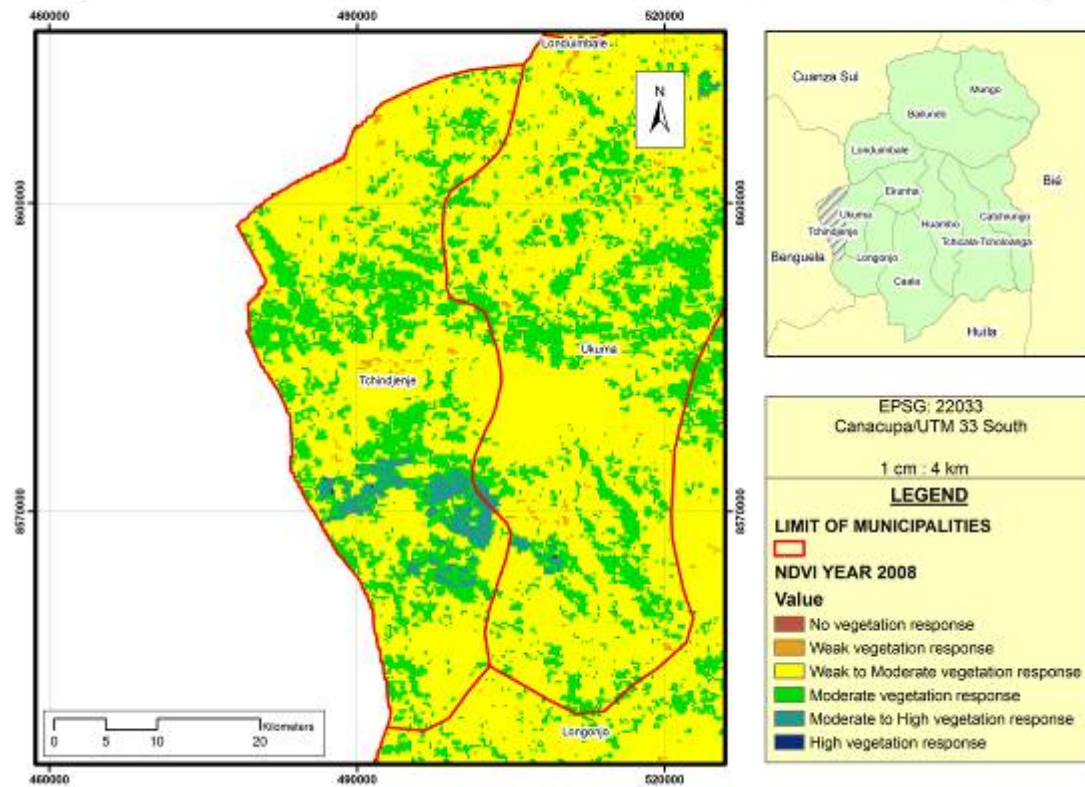
NDVI of Huambo province, municipality of Tchindjenje.



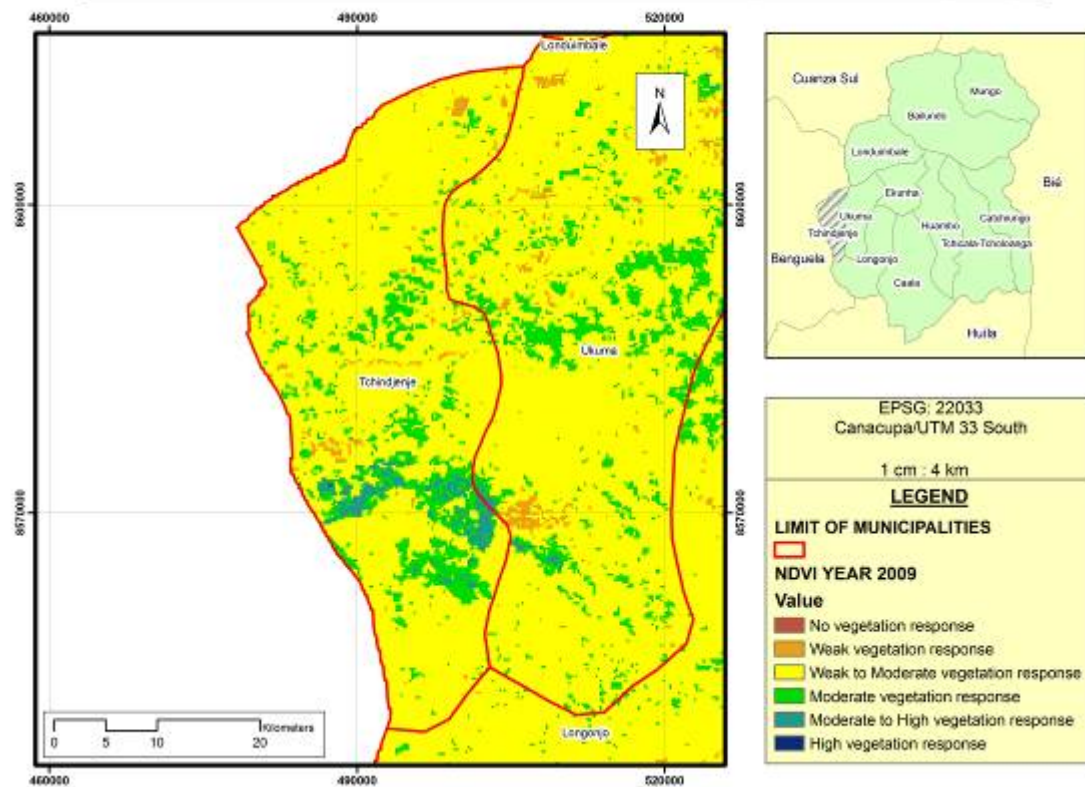
NDVI of Huambo province, municipality of Tchindjenje.



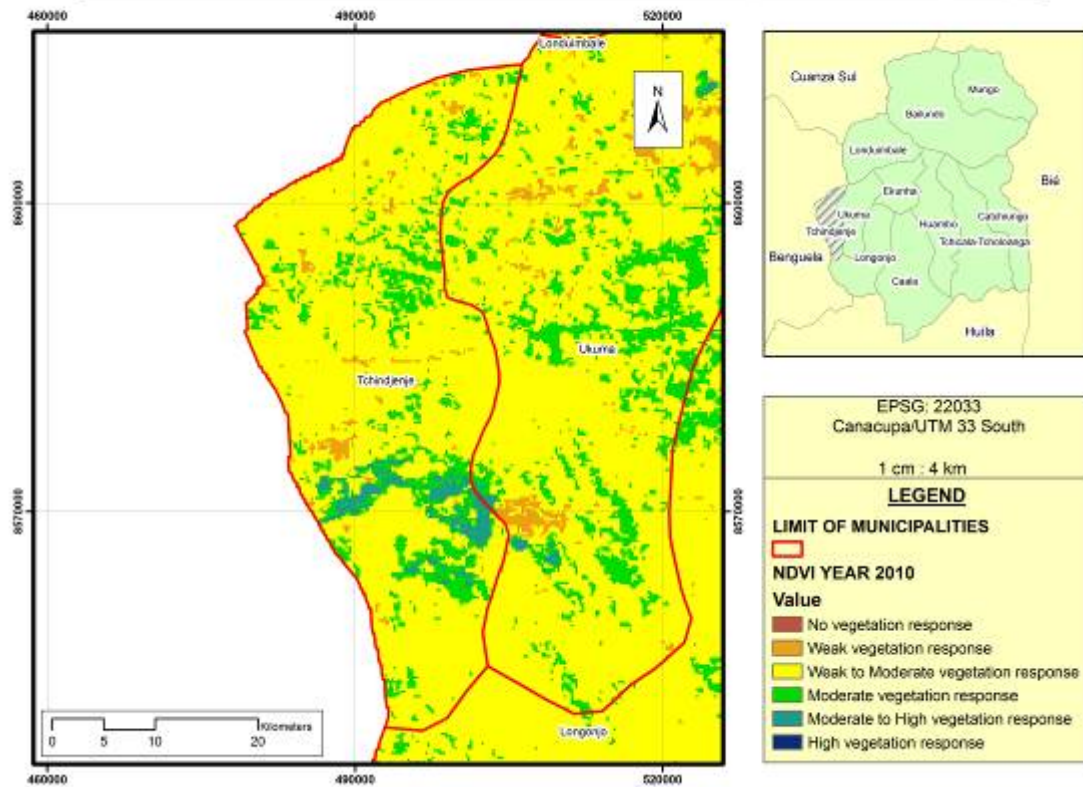
NDVI of Huambo province, municipality of Tchindjenje.



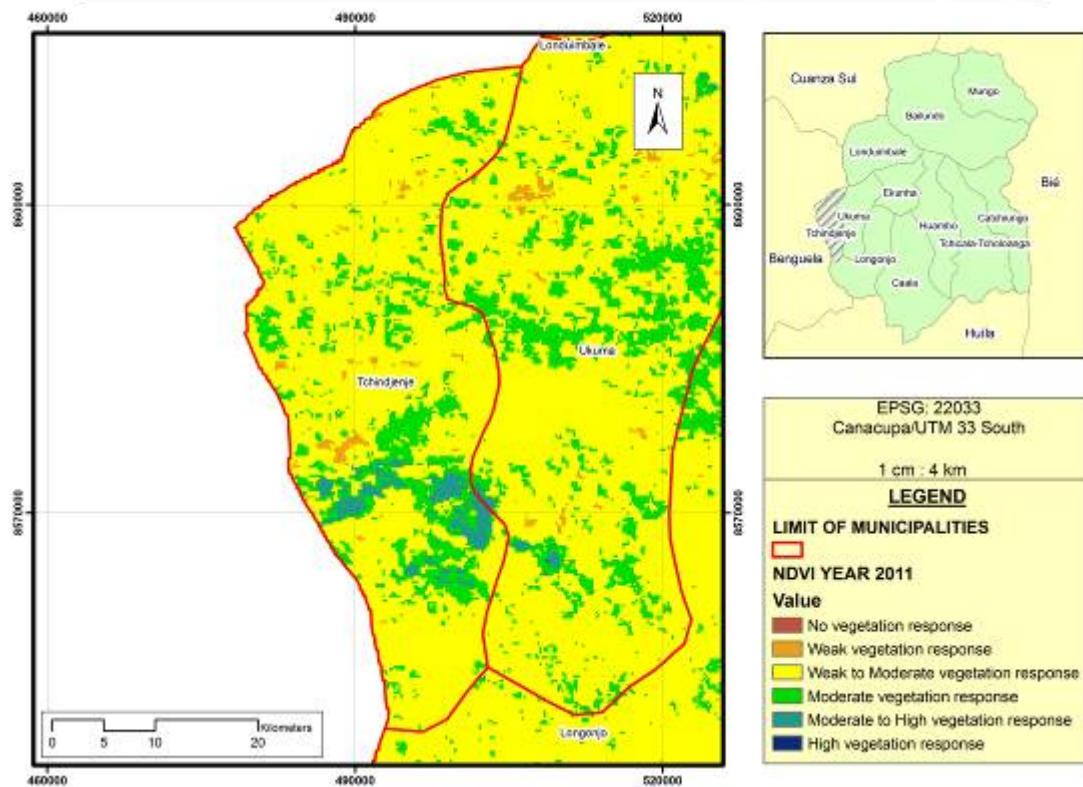
NDVI of Huambo province, municipality of Tchindjenje.



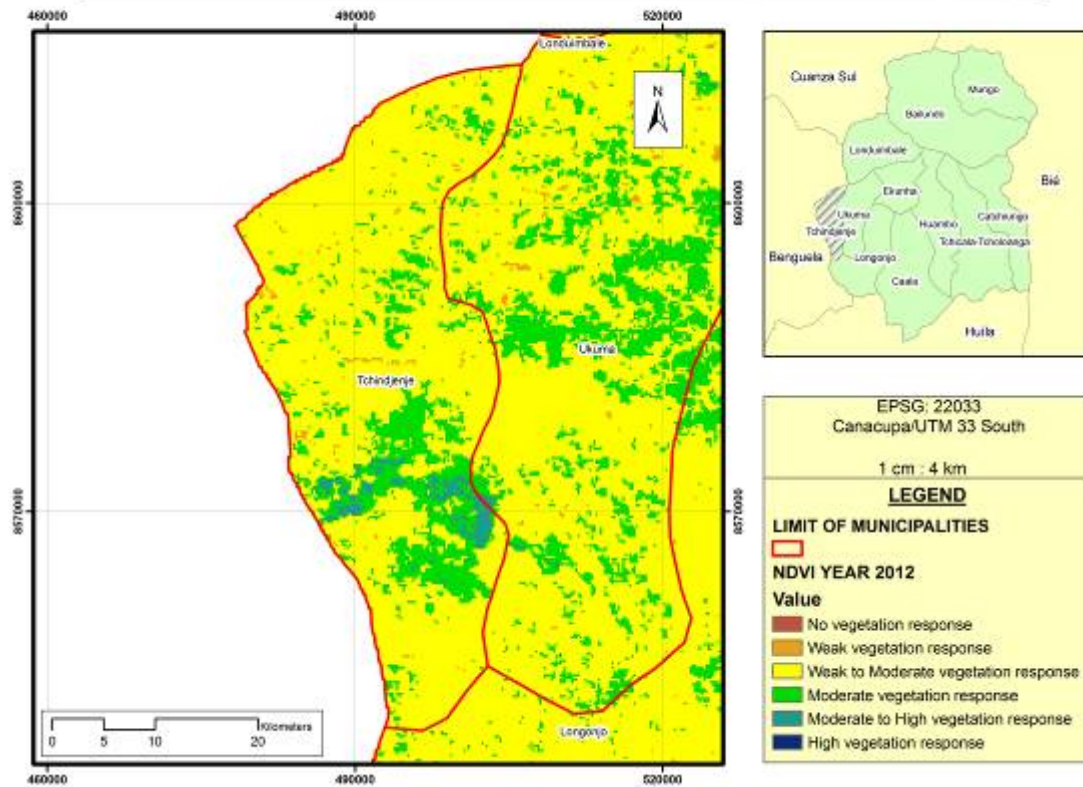
NDVI of Huambo province, municipality of Tchindjenje.



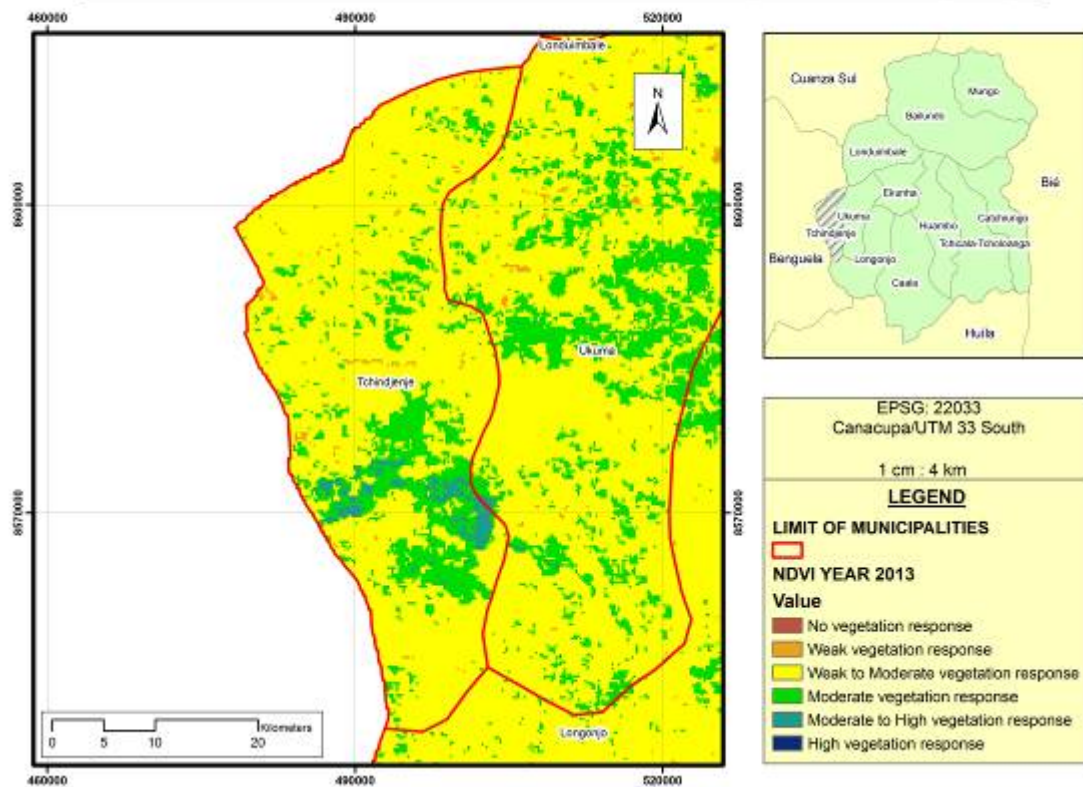
NDVI of Huambo province, municipality of Tchindjenje.



NDVI of Huambo province, municipality of Tchindjenje.

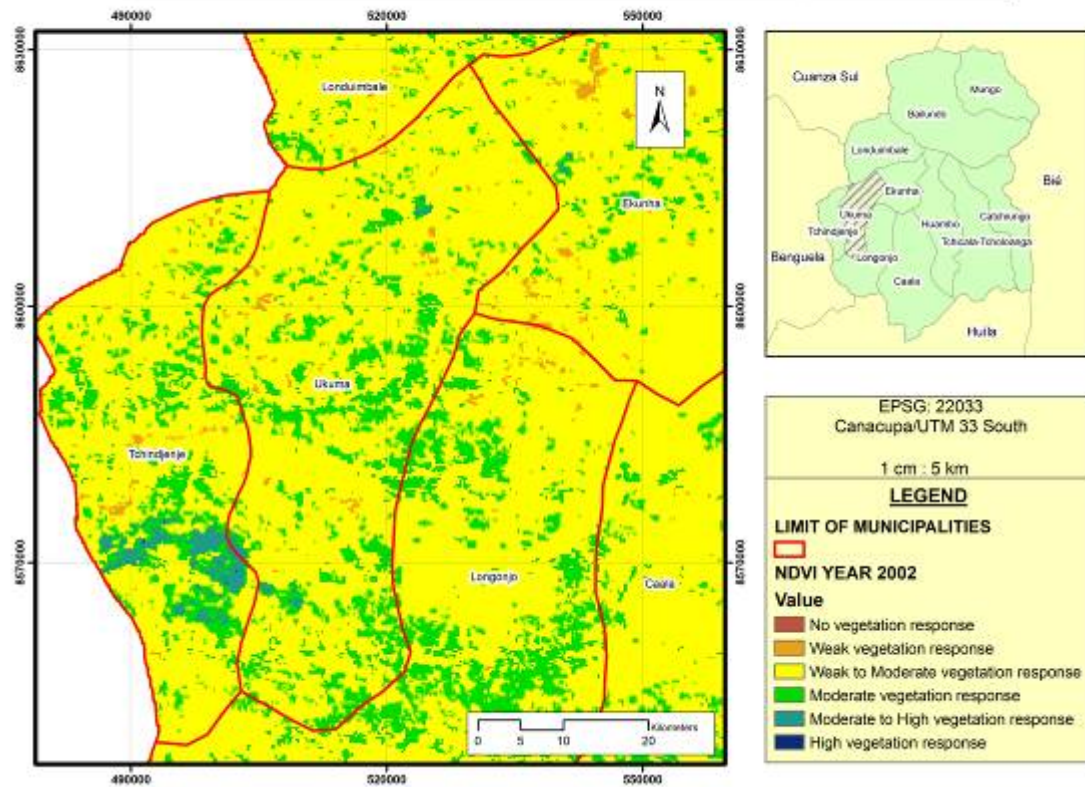


NDVI of Huambo province, municipality of Tchindjenje.

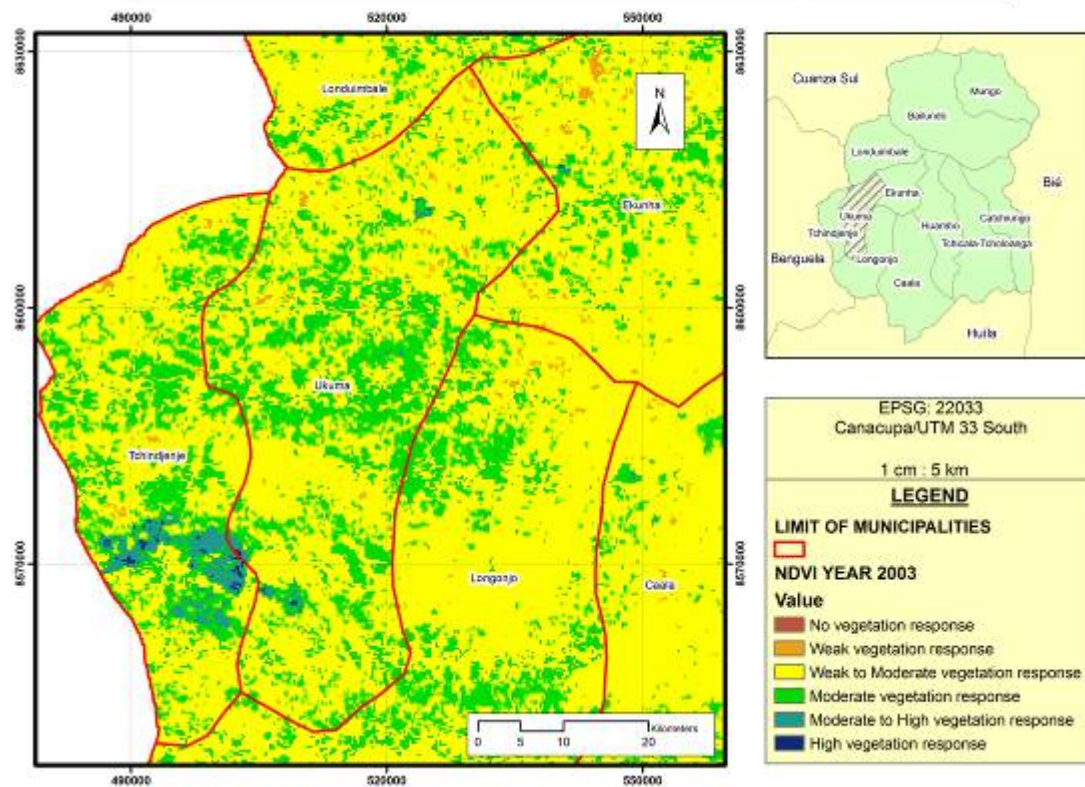




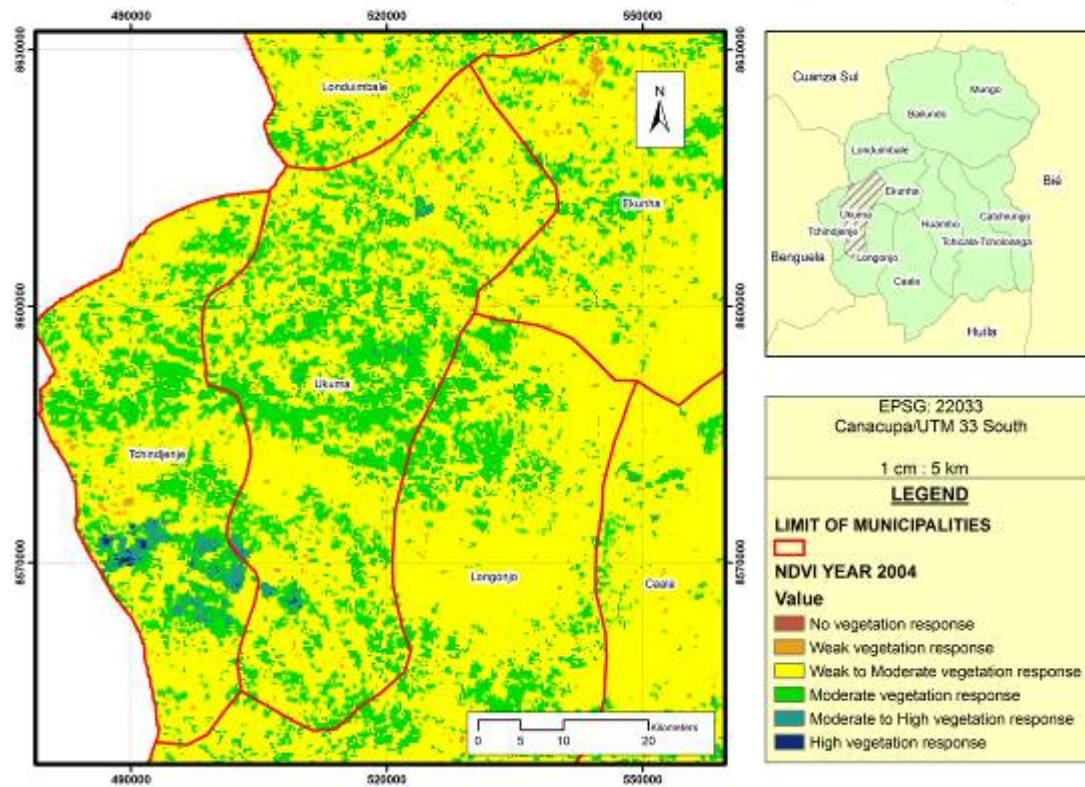
NDVI of Huambo province, municipality of Ukuma.



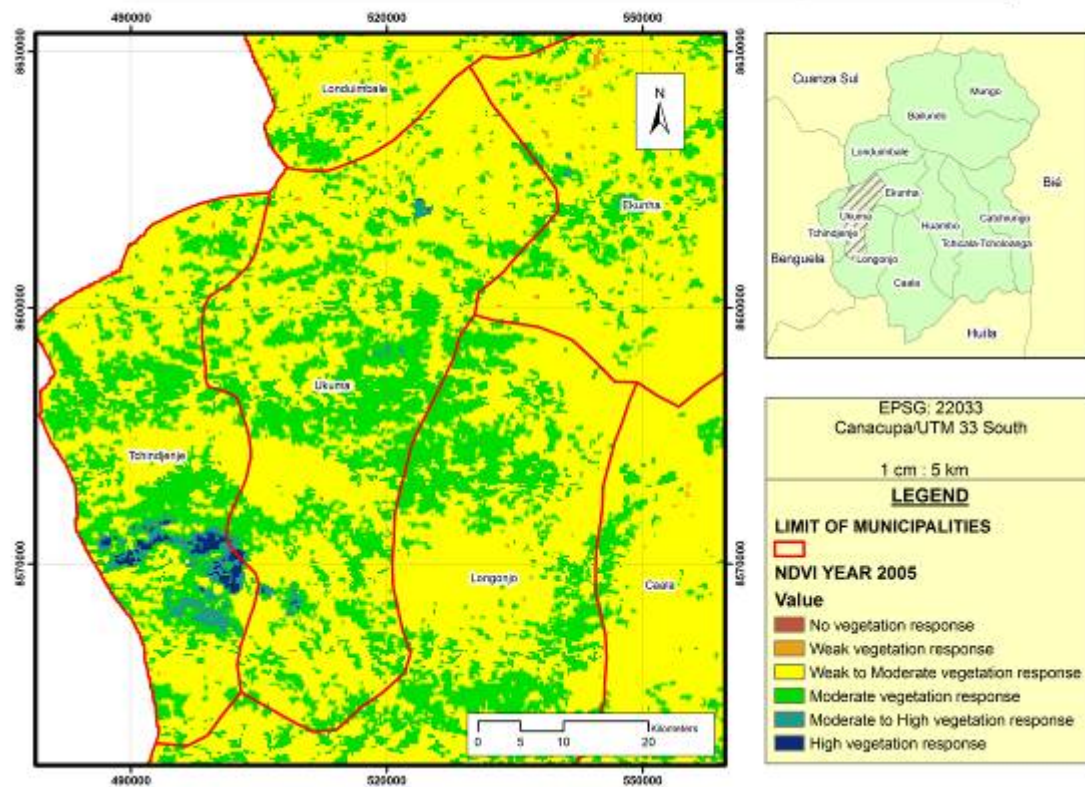
NDVI of Huambo province, municipality of Ukuma.



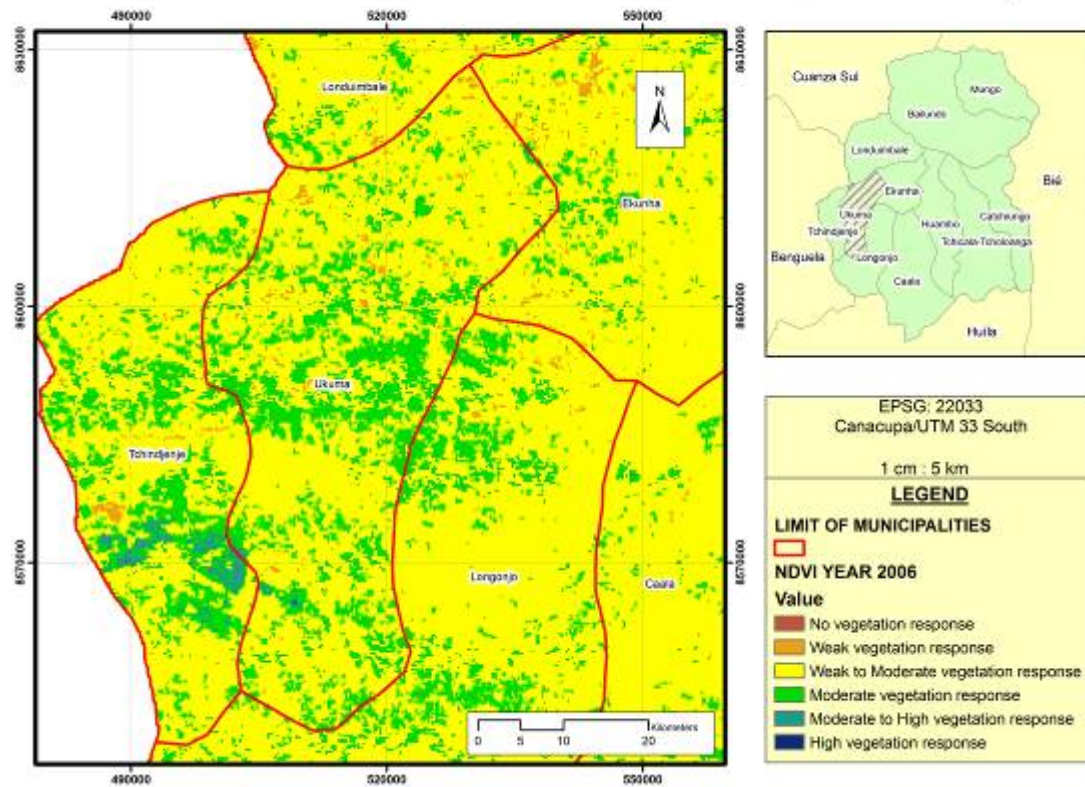
NDVI of Huambo province, municipality of Ukuma.



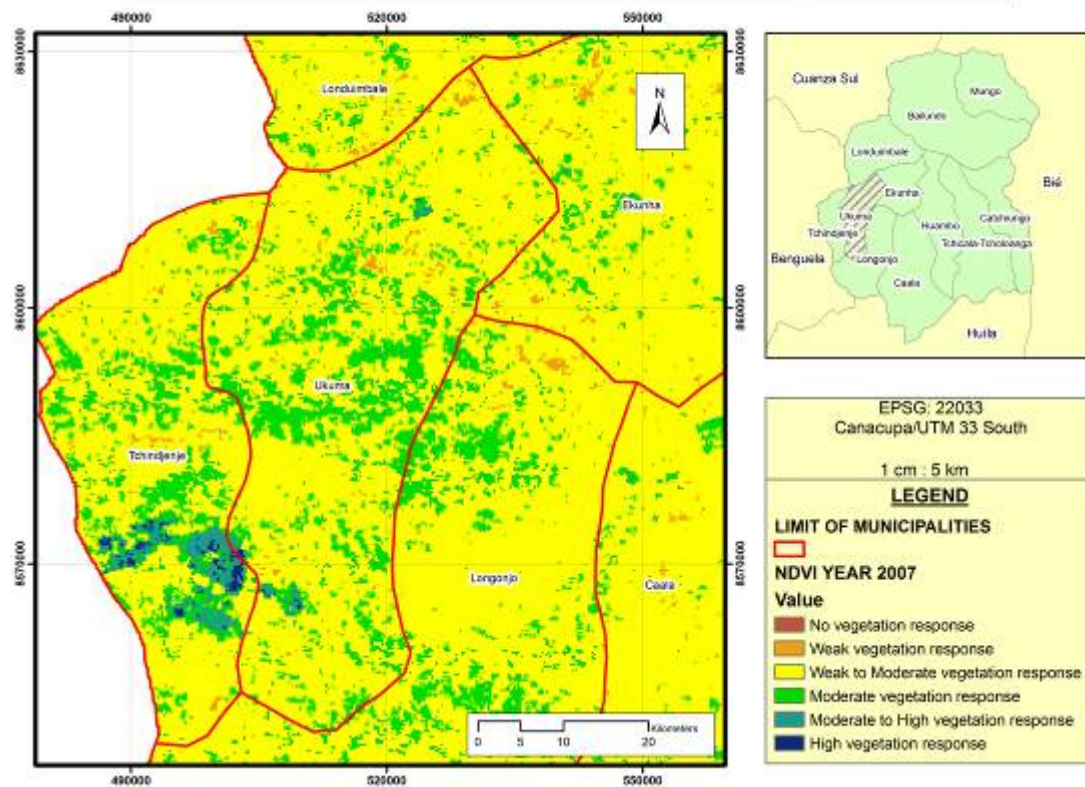
NDVI of Huambo province, municipality of Ukuma.



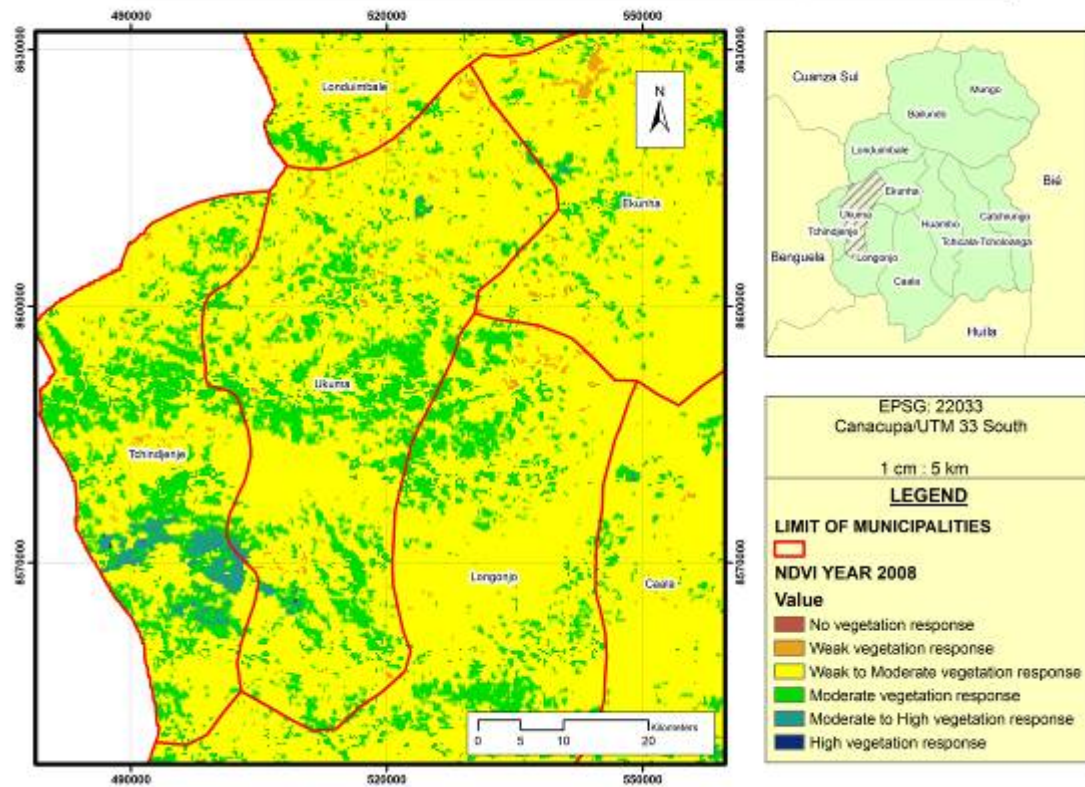
NDVI of Huambo province, municipality of Ukuma.



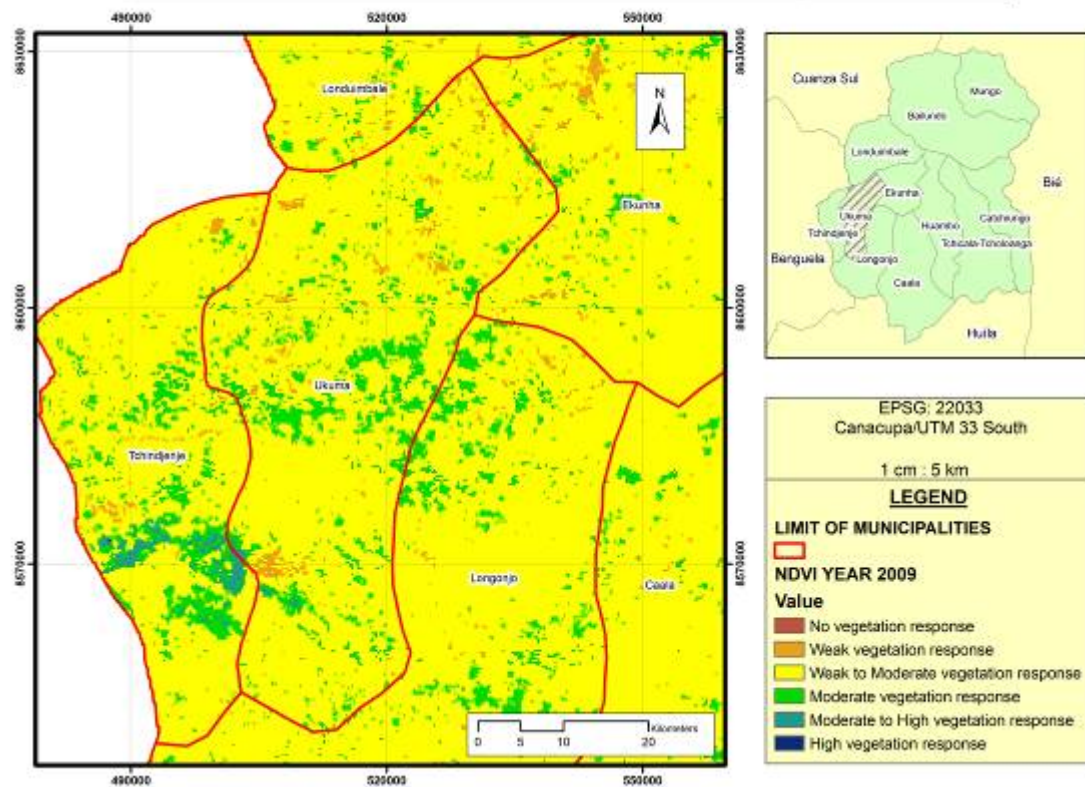
NDVI of Huambo province, municipality of Ukuma.



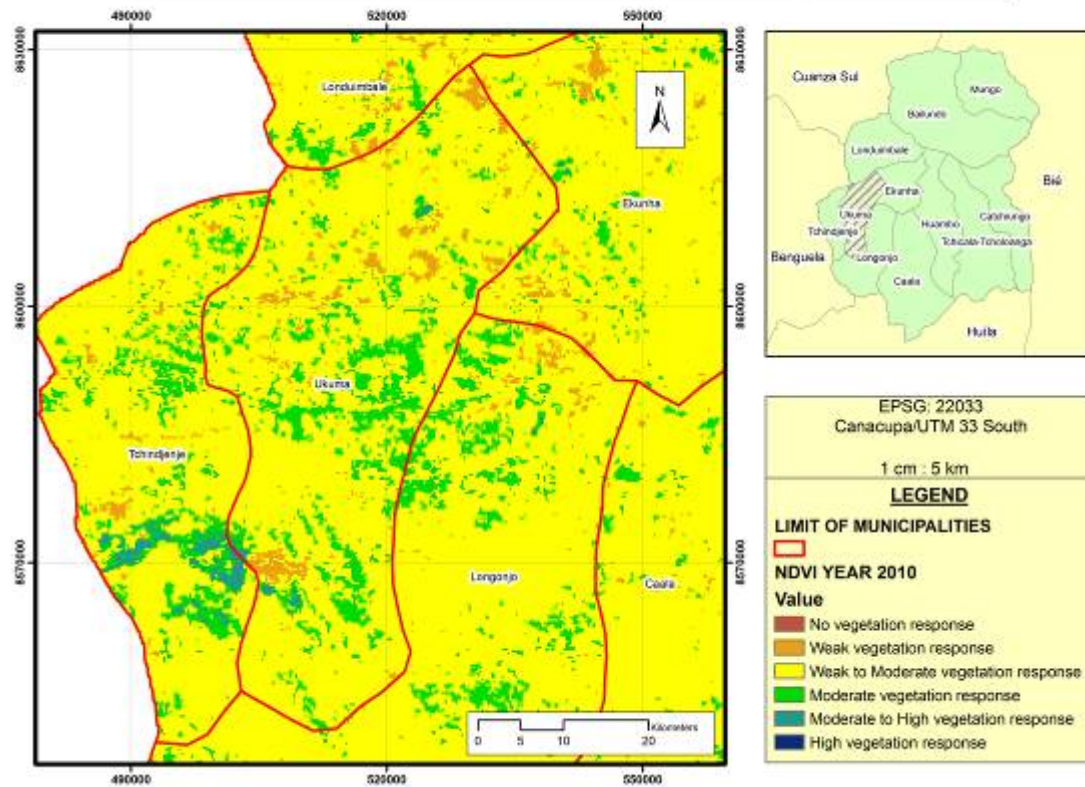
NDVI of Huambo province, municipality of Ukuma.



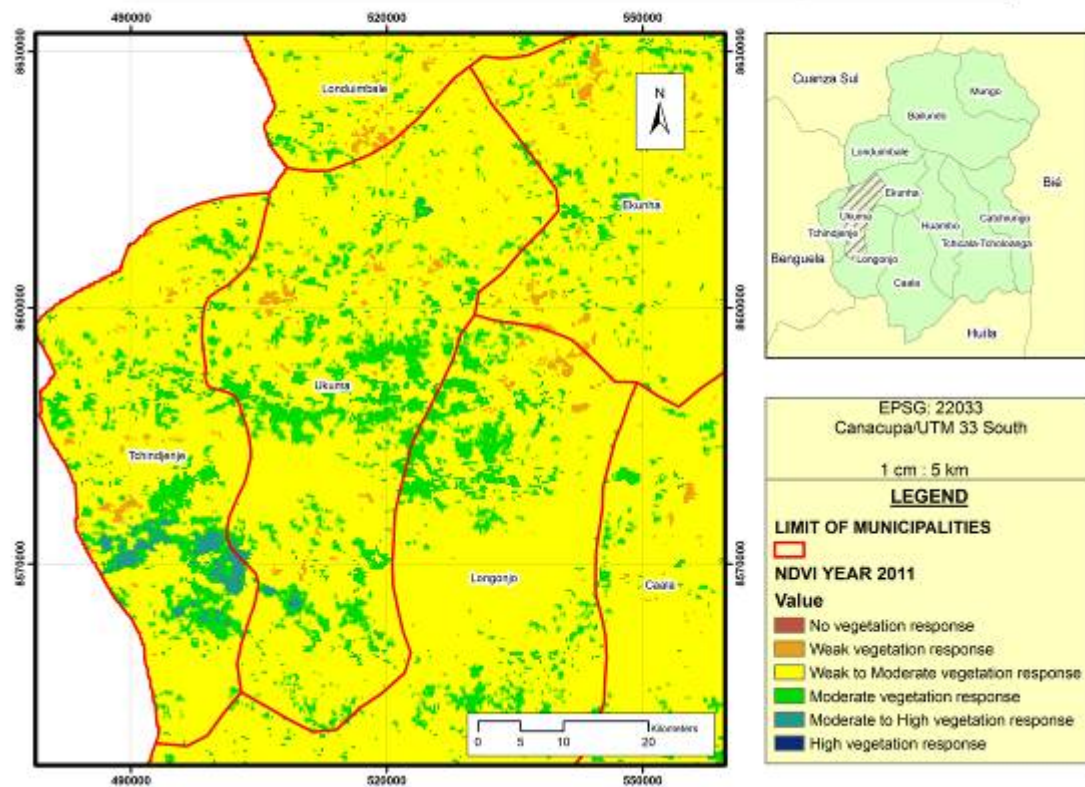
NDVI of Huambo province, municipality of Ukuma.



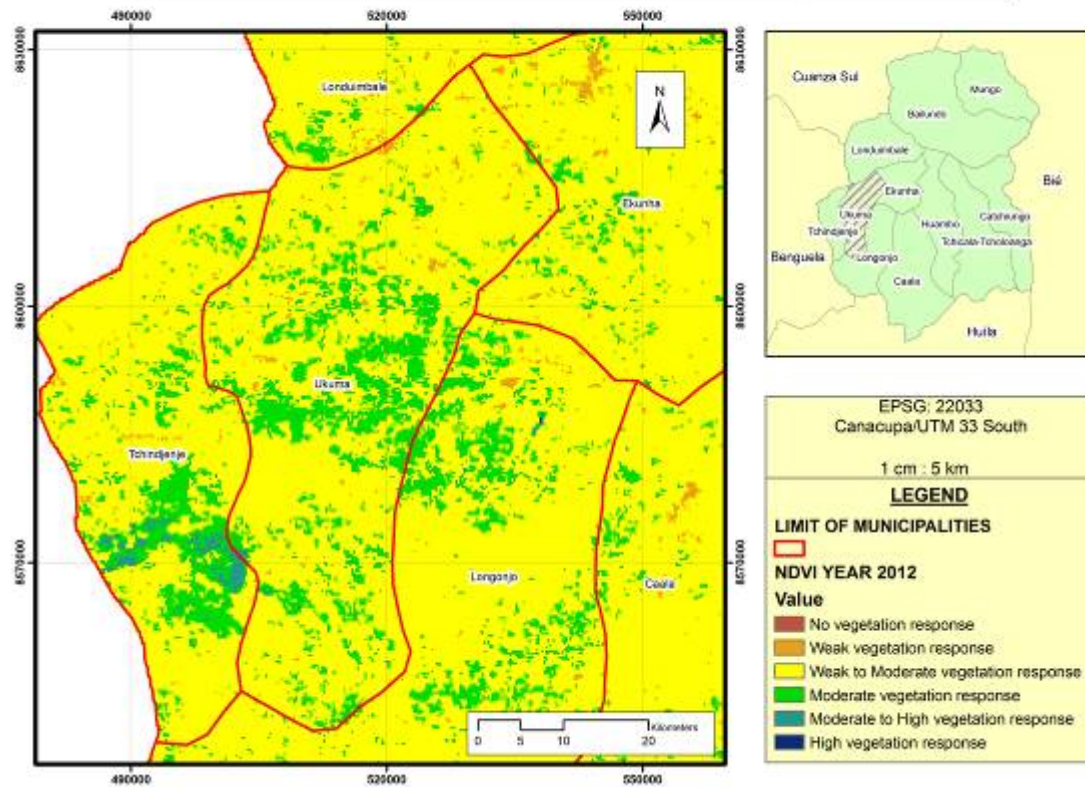
NDVI of Huambo province, municipality of Ukuma.



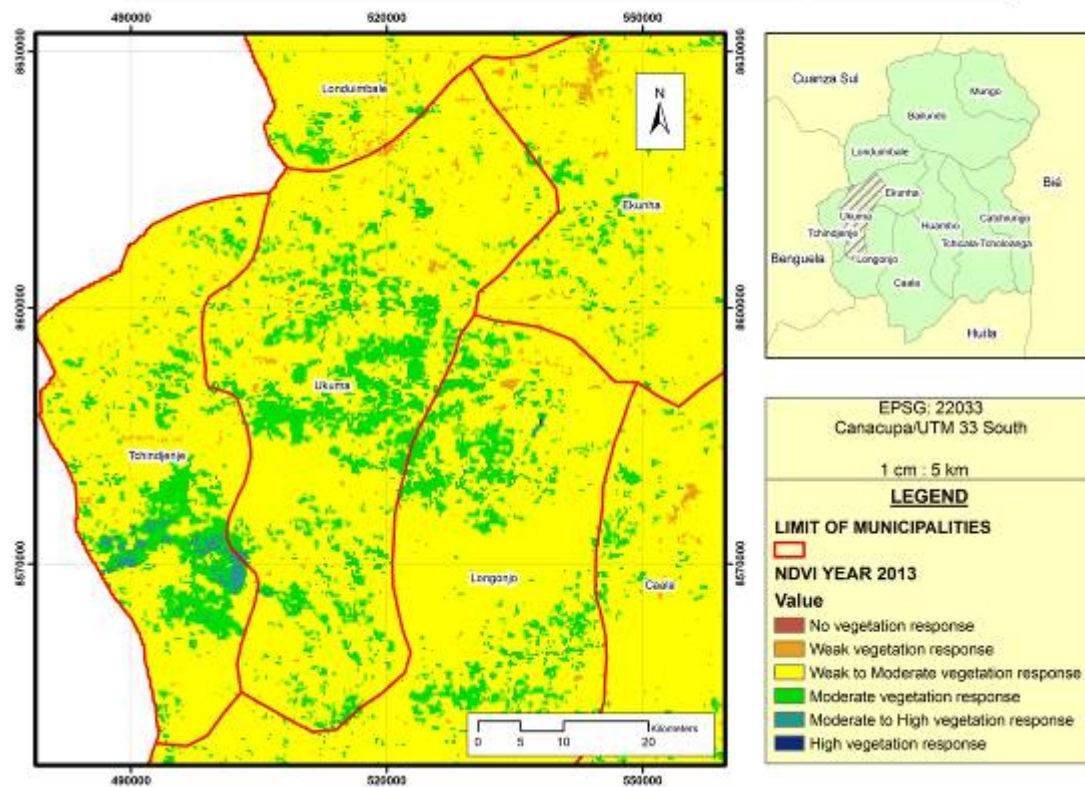
NDVI of Huambo province, municipality of Ukuma.



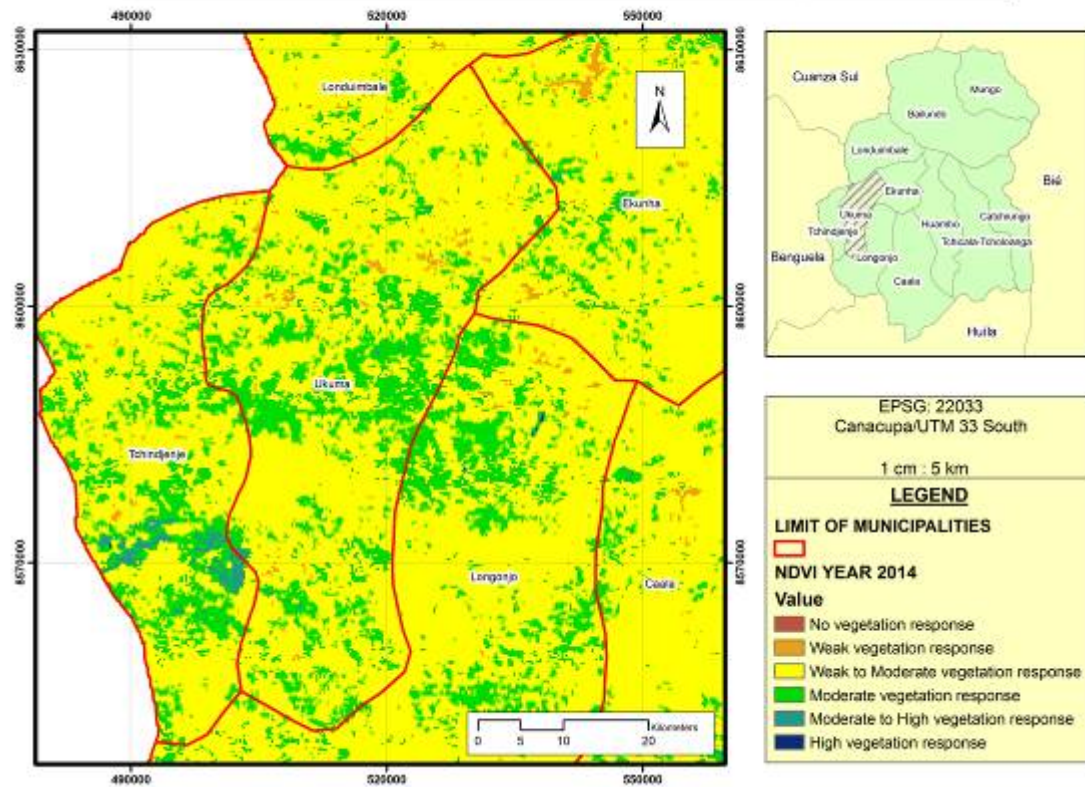
NDVI of Huambo province, municipality of Ukuma.



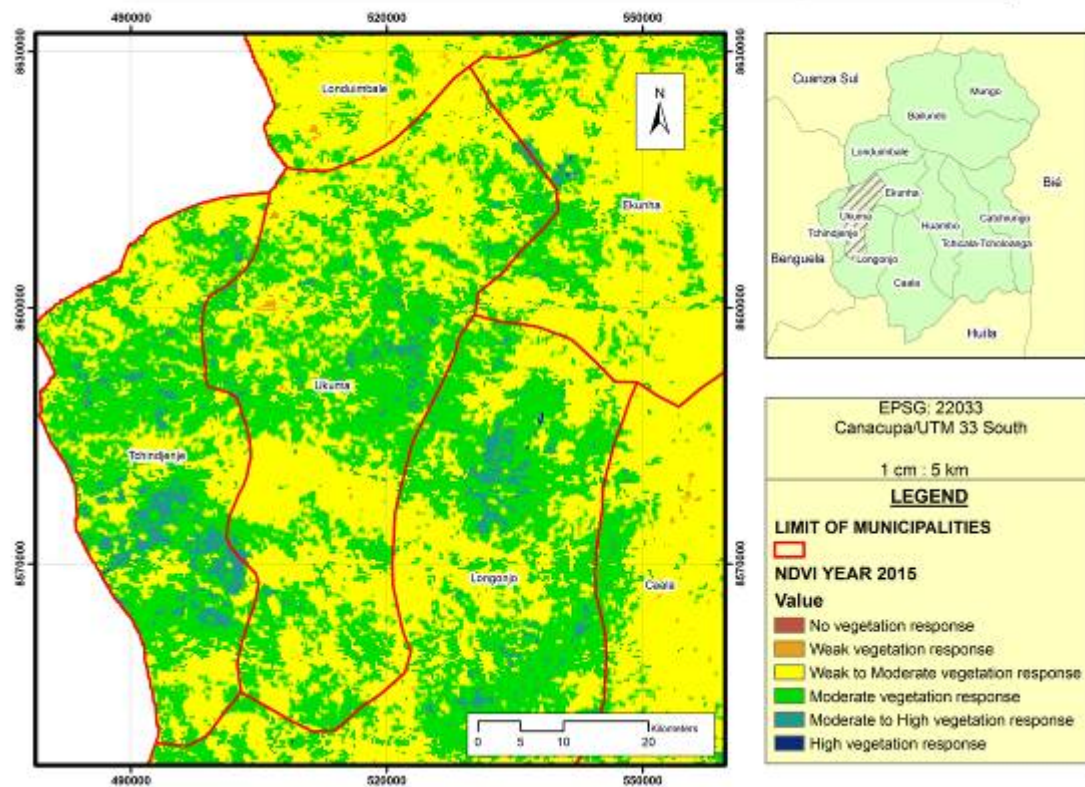
NDVI of Huambo province, municipality of Ukuma.



NDVI of Huambo province, municipality of Ukuma.

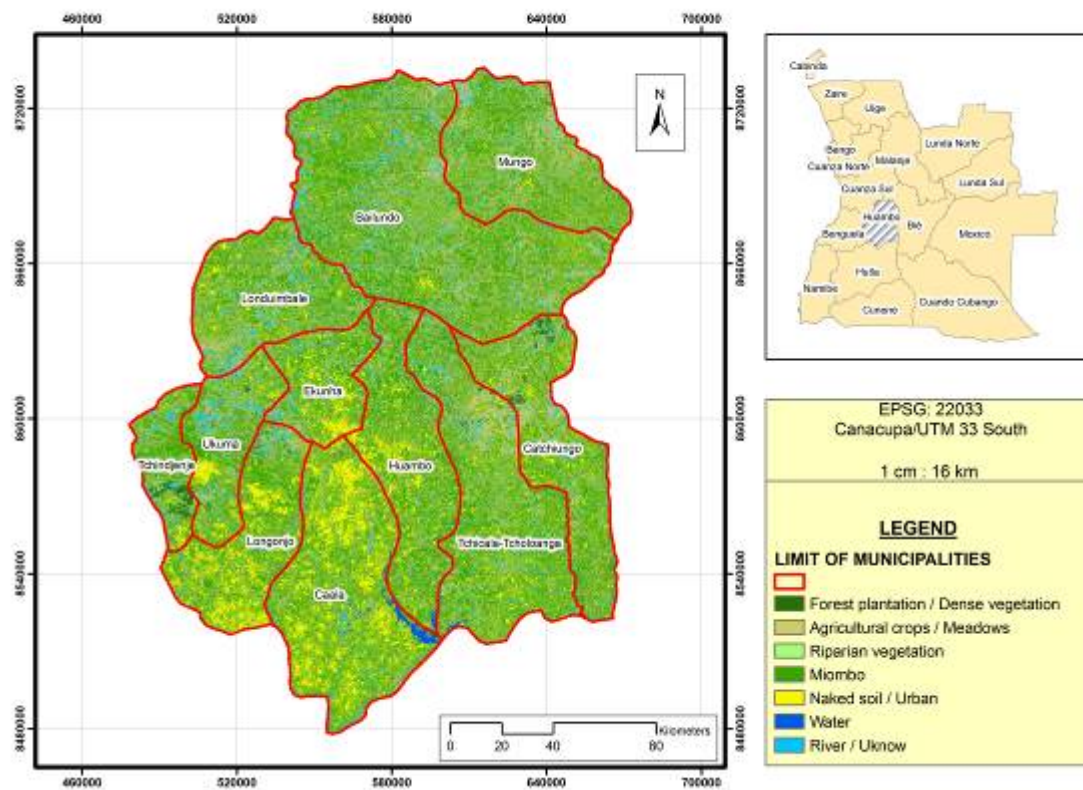


NDVI of Huambo province, municipality of Ukuma.

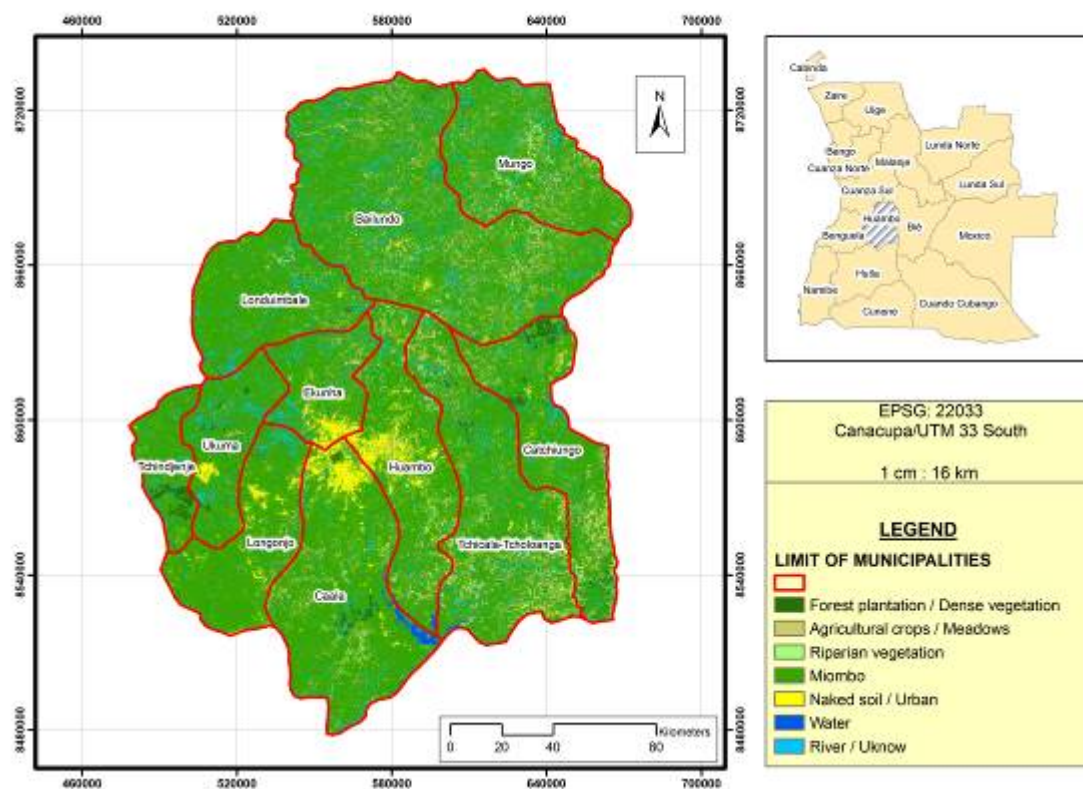


Annex IV. Land cover change 2002 and 2015

Land cover of Huambo province (2015)

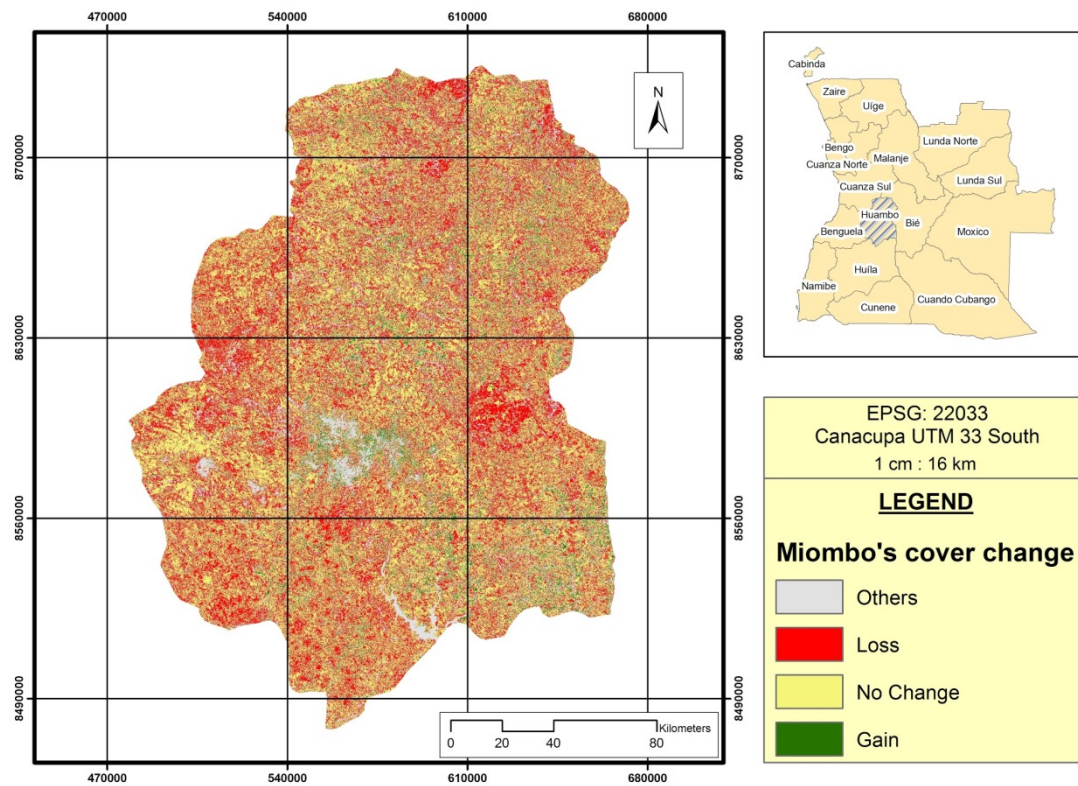


Land cover of Huambo province (2002)

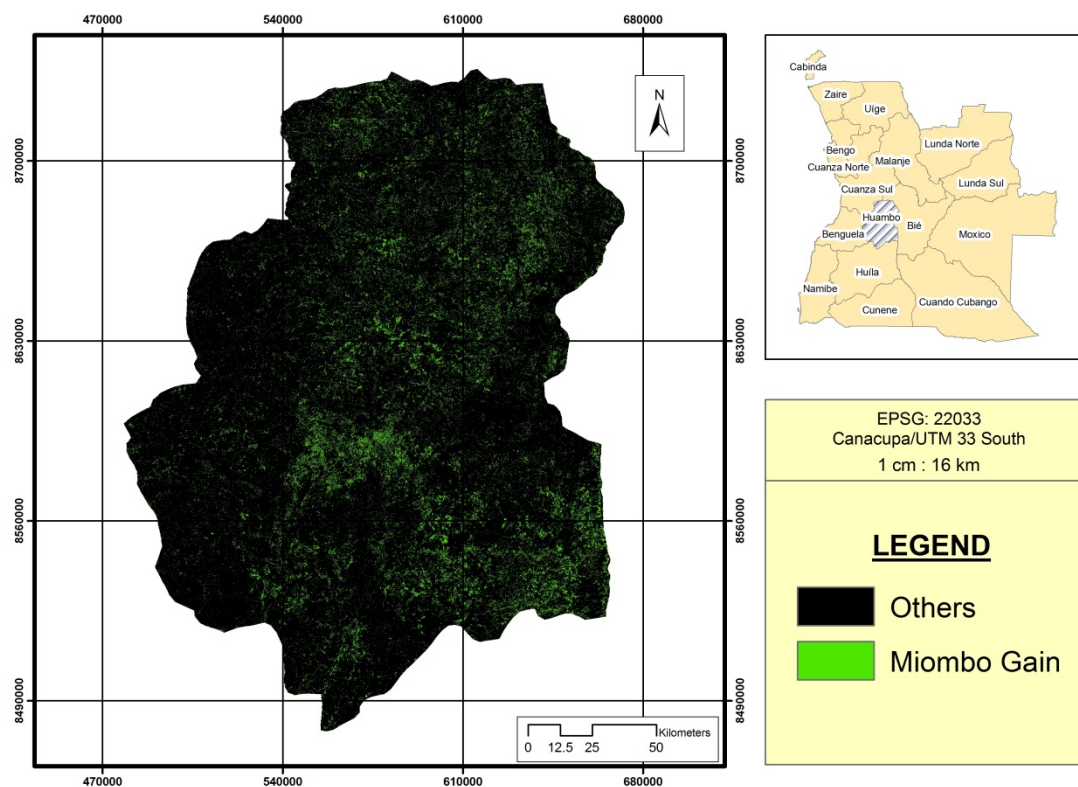


Annex V. Deforestation between 2002-2015

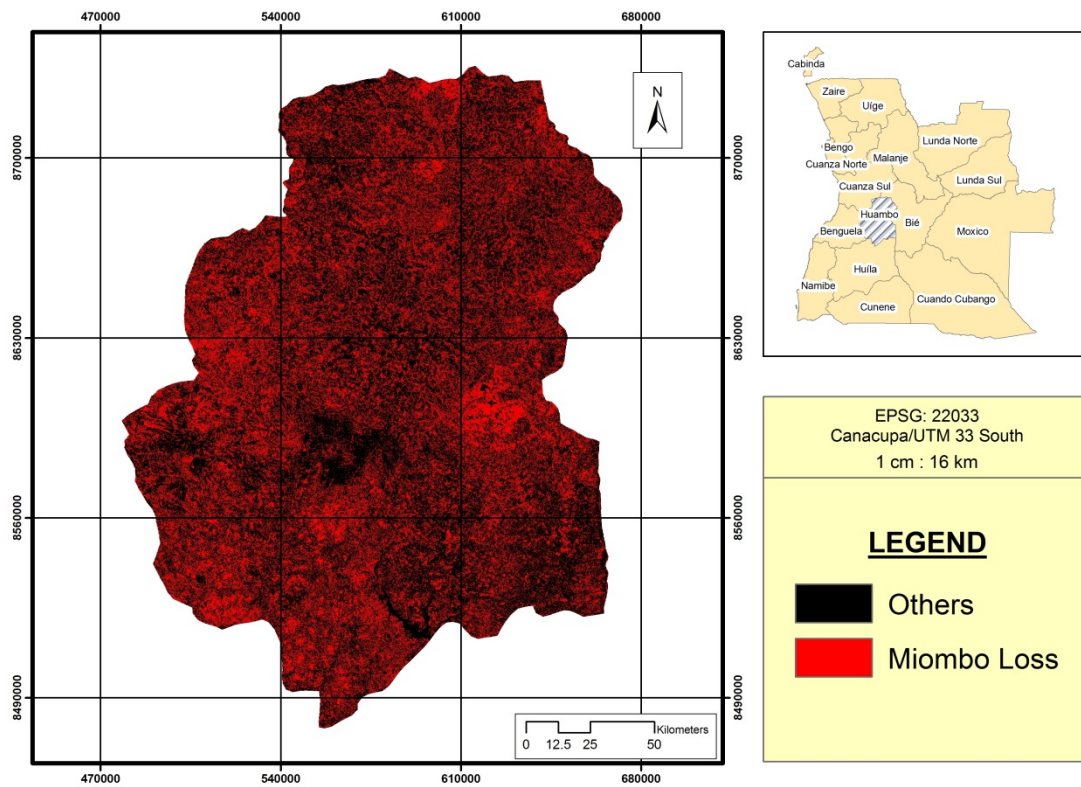
Miombo's cover change in Huambo province.



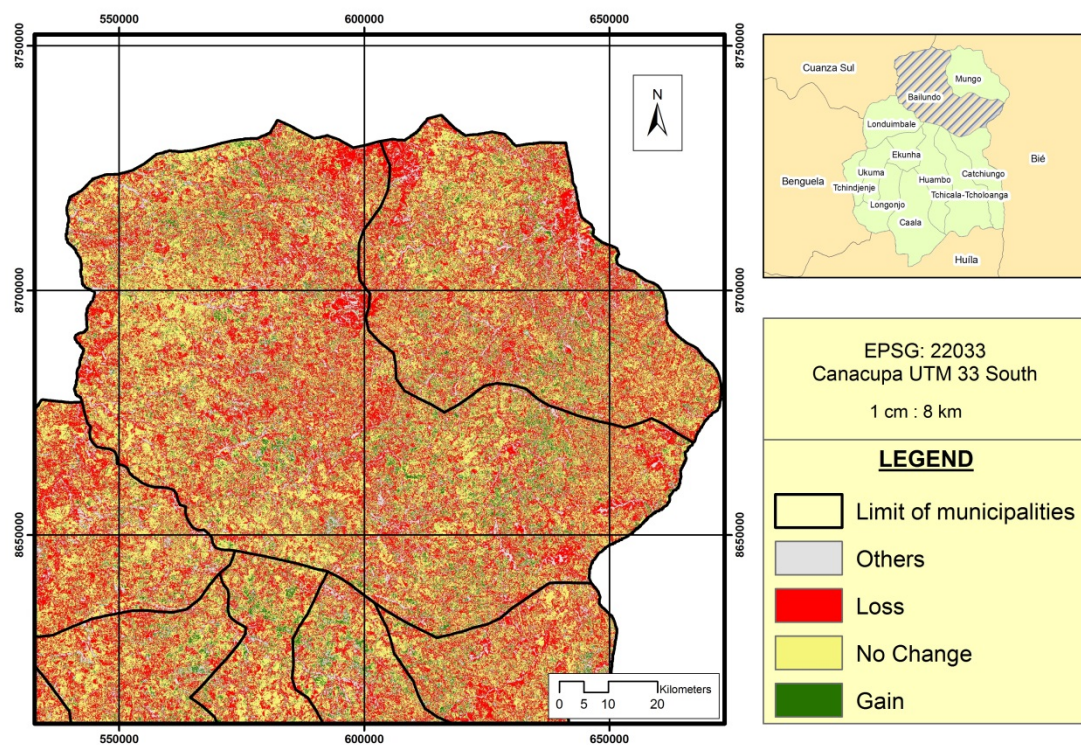
Miombo gain coverage on Huambo province (2002 - 2015)



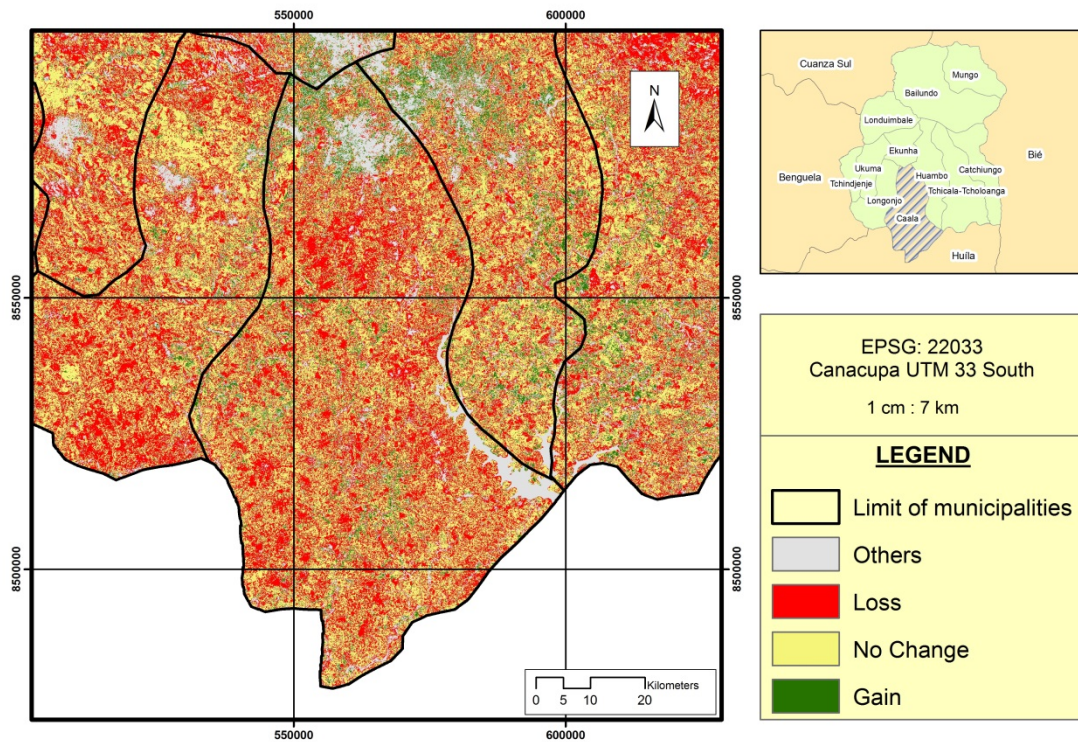
Miombo loss coverage on Huambo province (2002 - 2015)



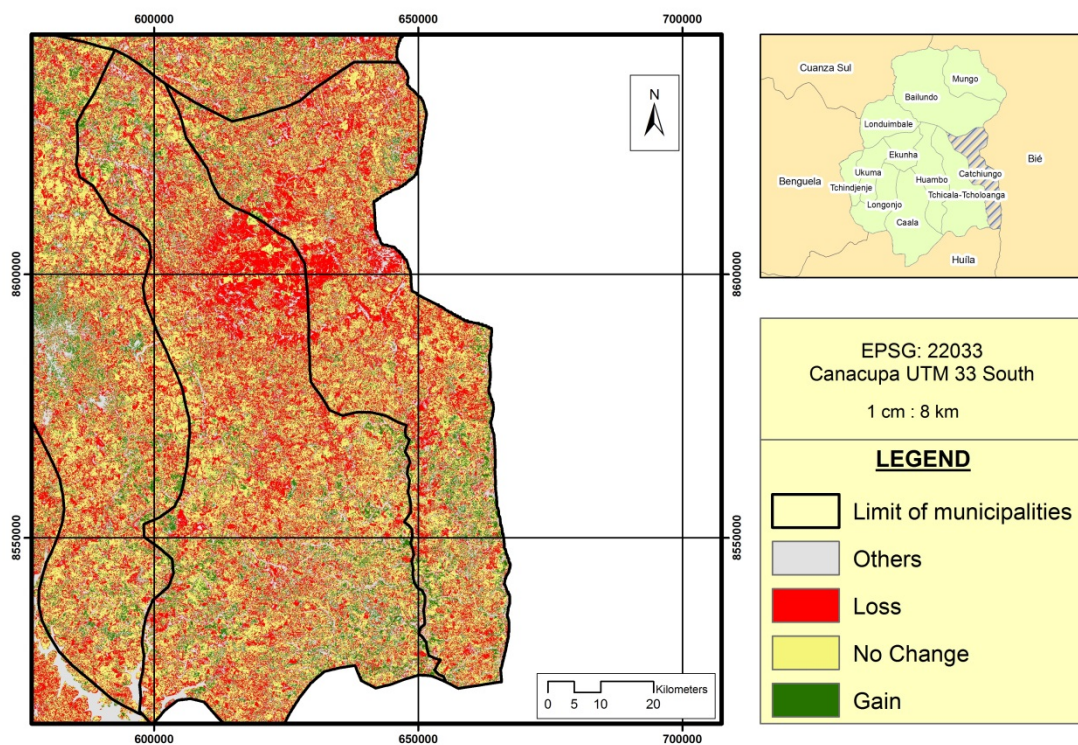
Miombo's cover change in Huambo province. Municipality of Bailundo.



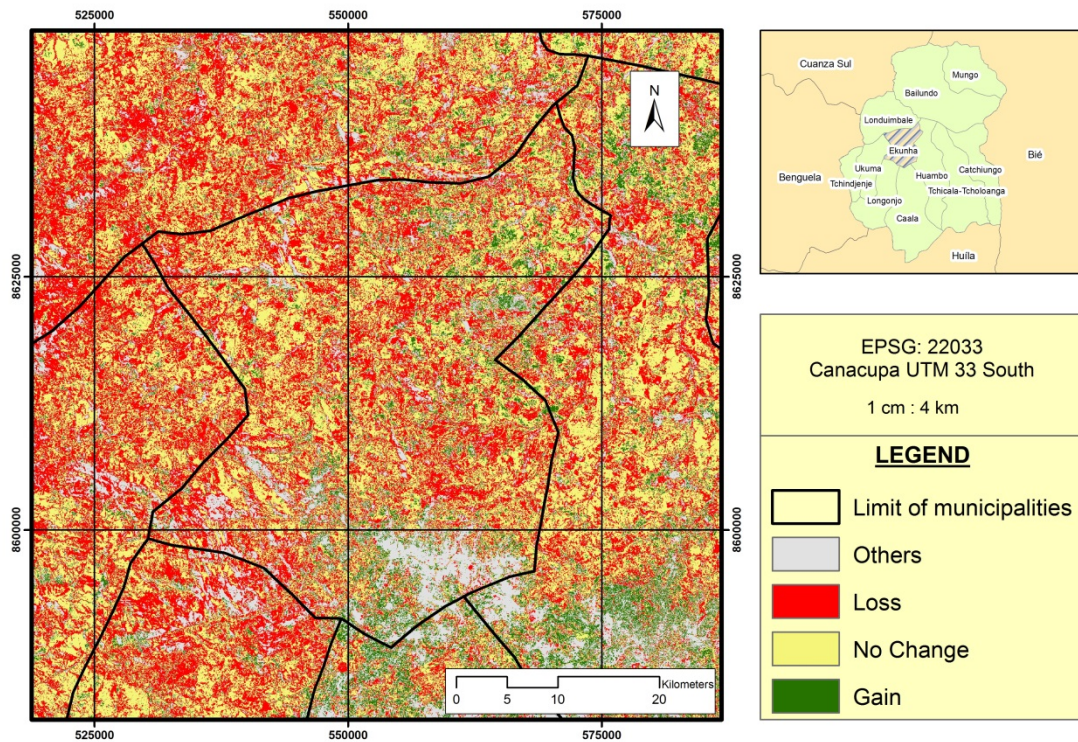
Miombo's cover change in Huambo province. **Municipality of Caala.**



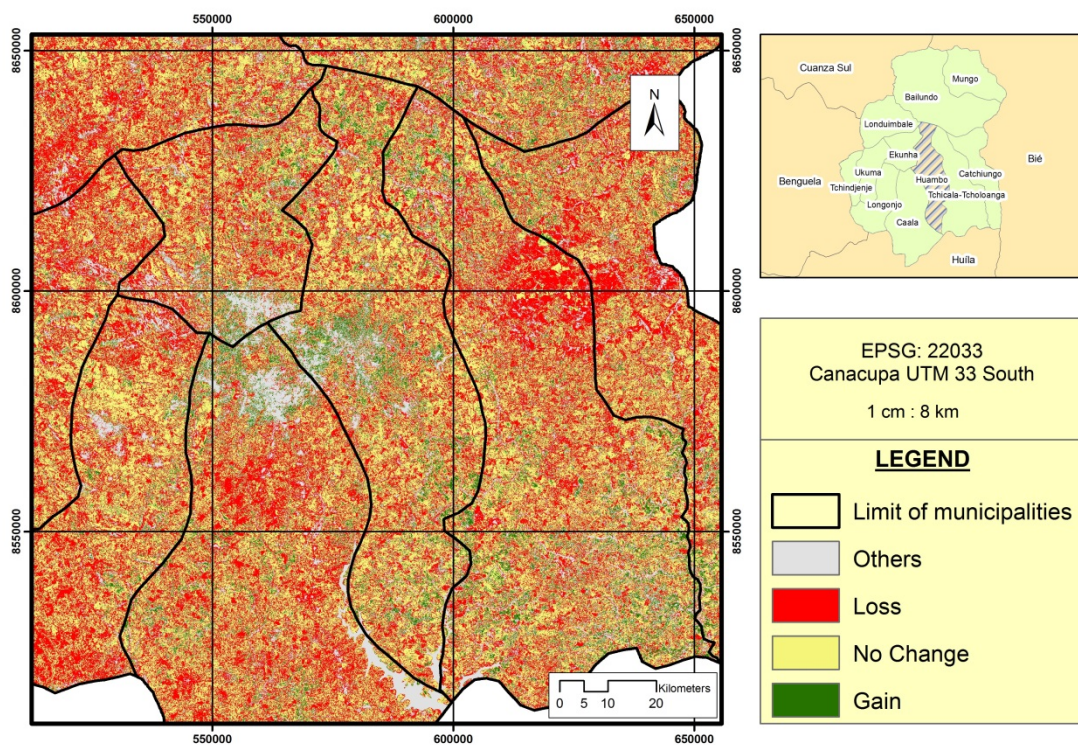
Miombo's cover change in Huambo province. **Municipality of Catchiungo.**



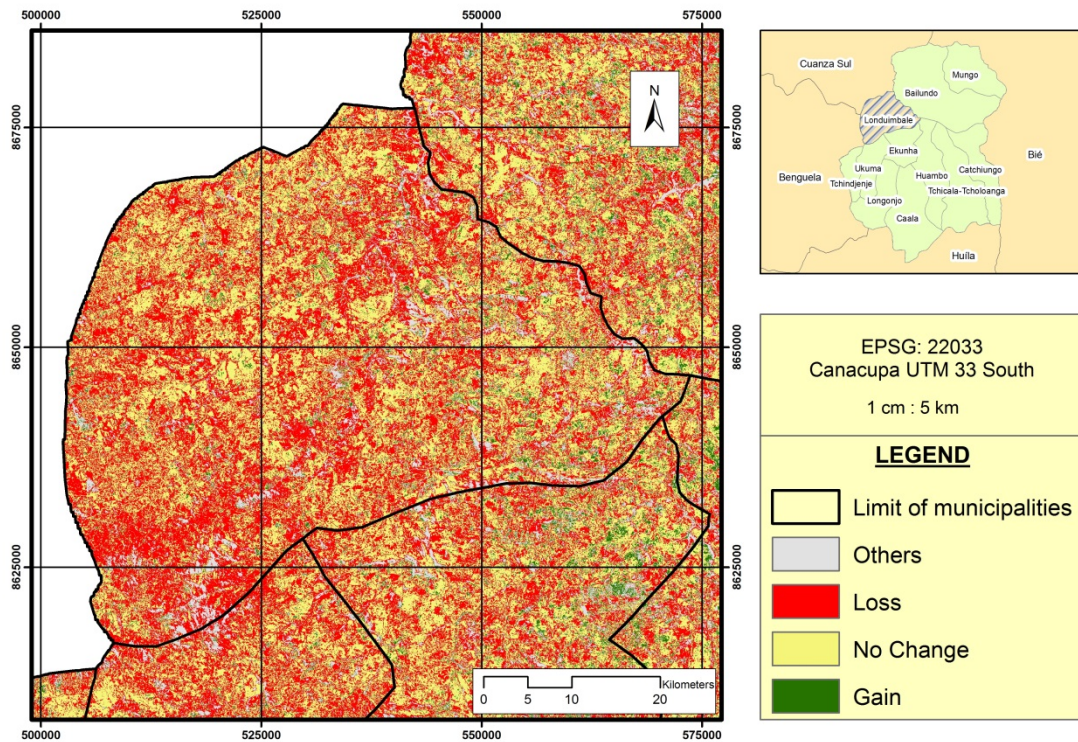
Miombo's cover change in Huambo province. **Municipality of Ekunha.**



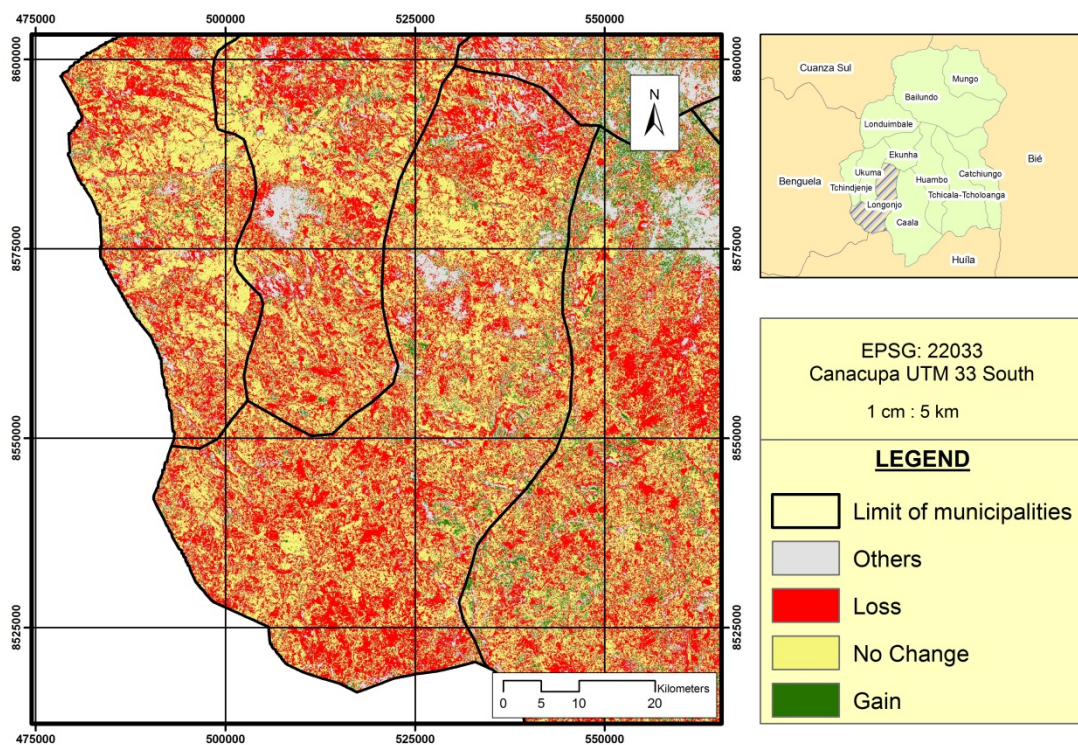
Miombo's cover change in Huambo province. **Municipality of Huambo.**



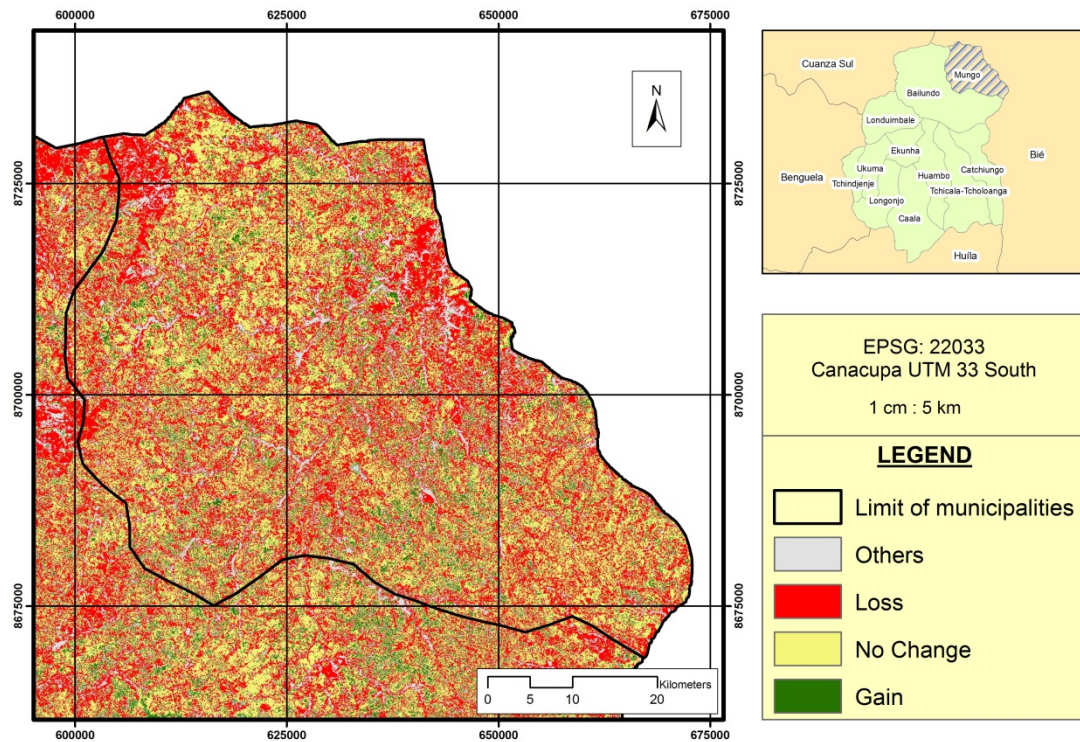
Miombo's cover change in Huambo province. **Municipality of Londuimbale.**



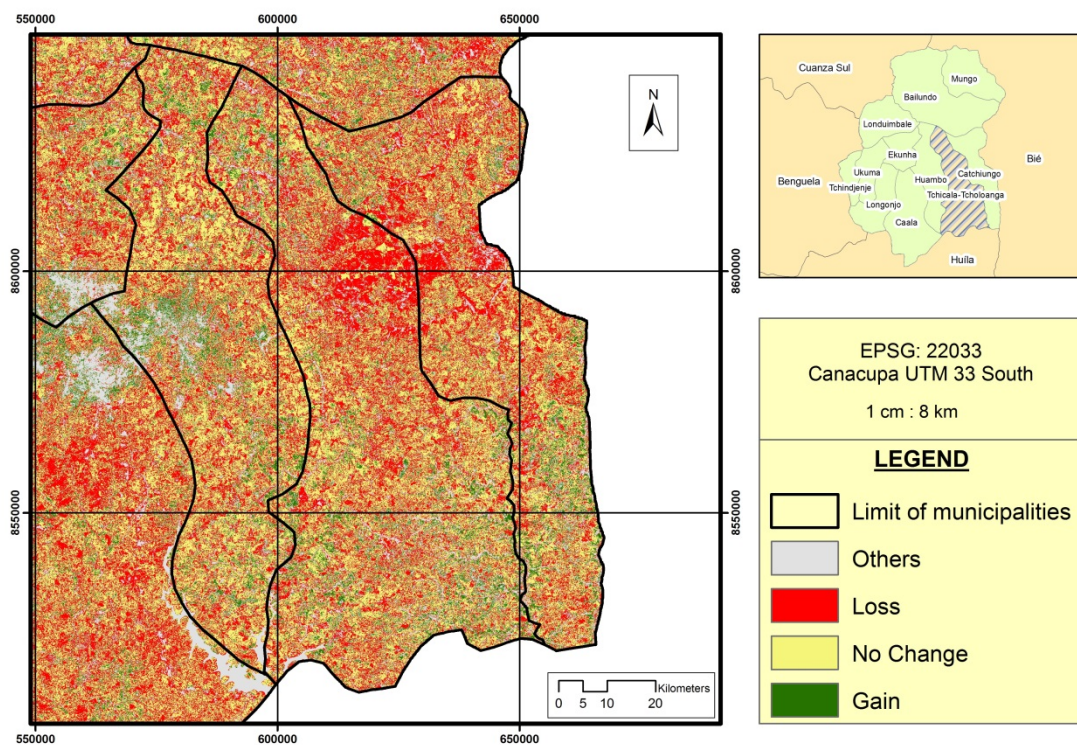
Miombo's cover change in Huambo province. **Municipality of Longonjo.**



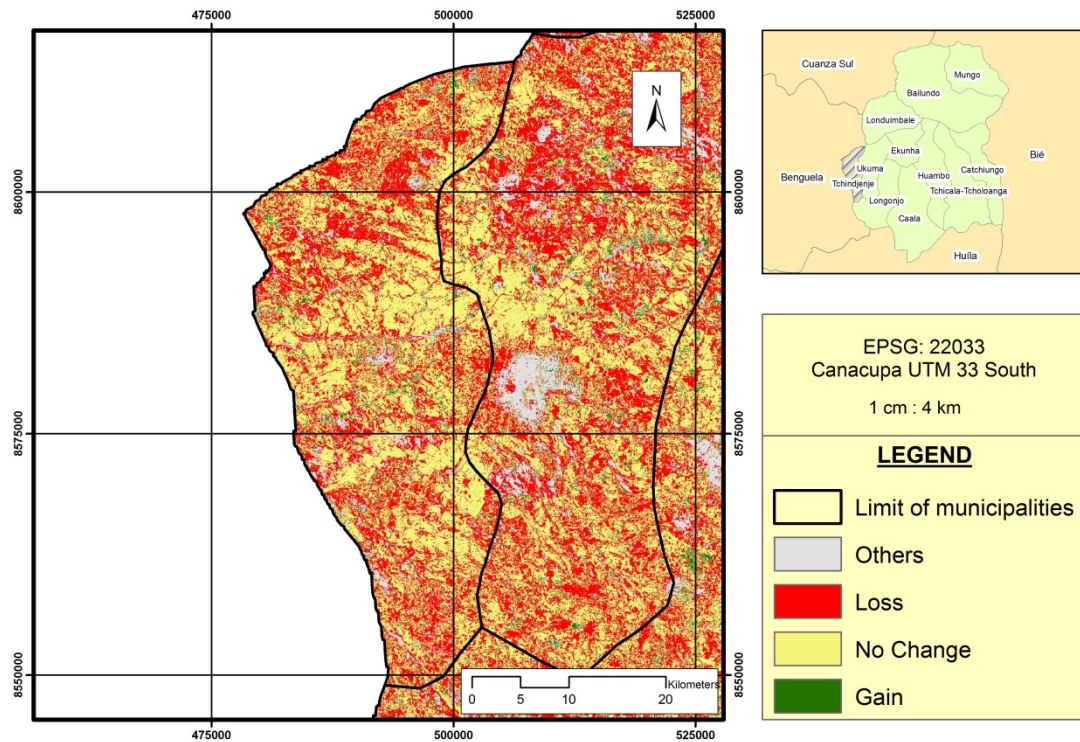
Miombo's cover change in Huambo province.
Municipality of Mungo.



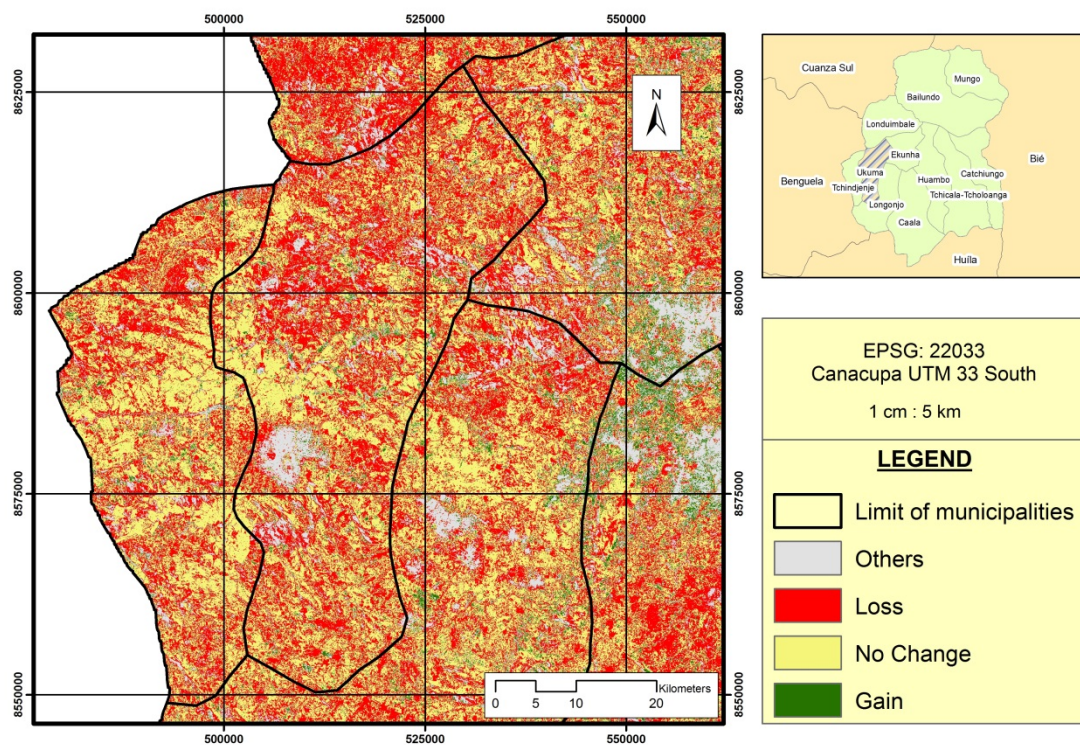
Miombo's cover change in Huambo province.
Municipality of Tchicala-Tcholoanga.



Miombo's cover change in Huambo province. **Municipality of Tchindjenje.**

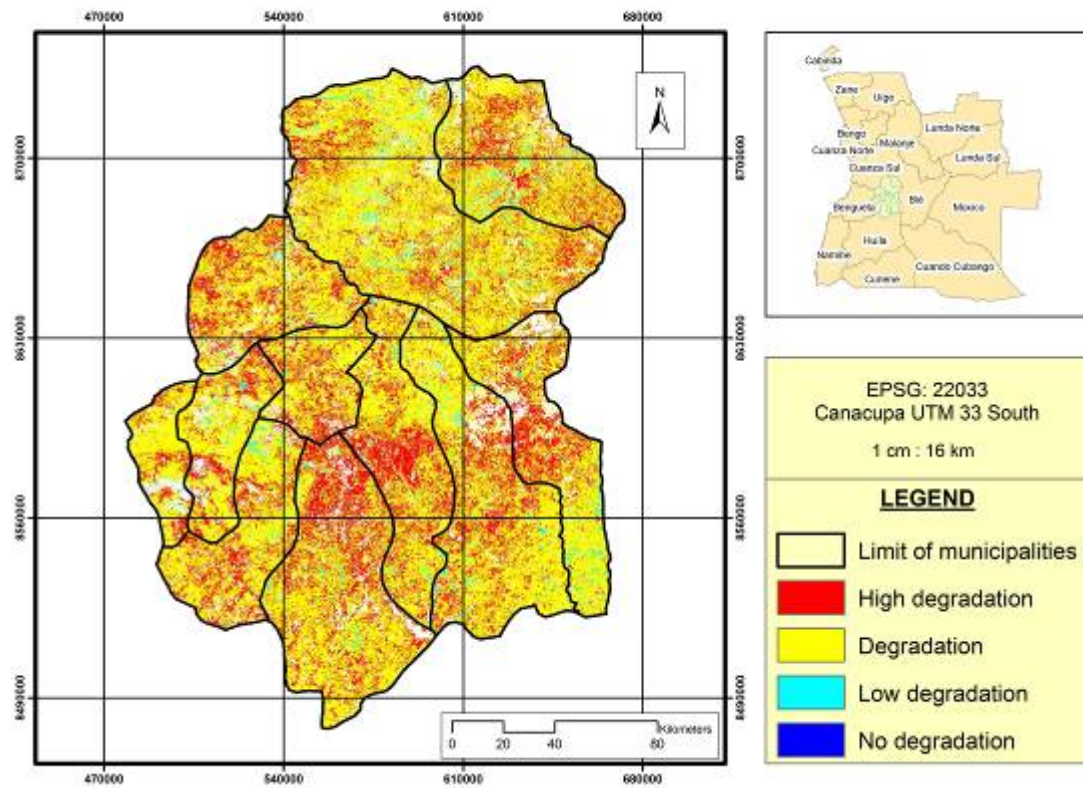


Miombo's cover change in Huambo province. **Municipality of Ukuma**

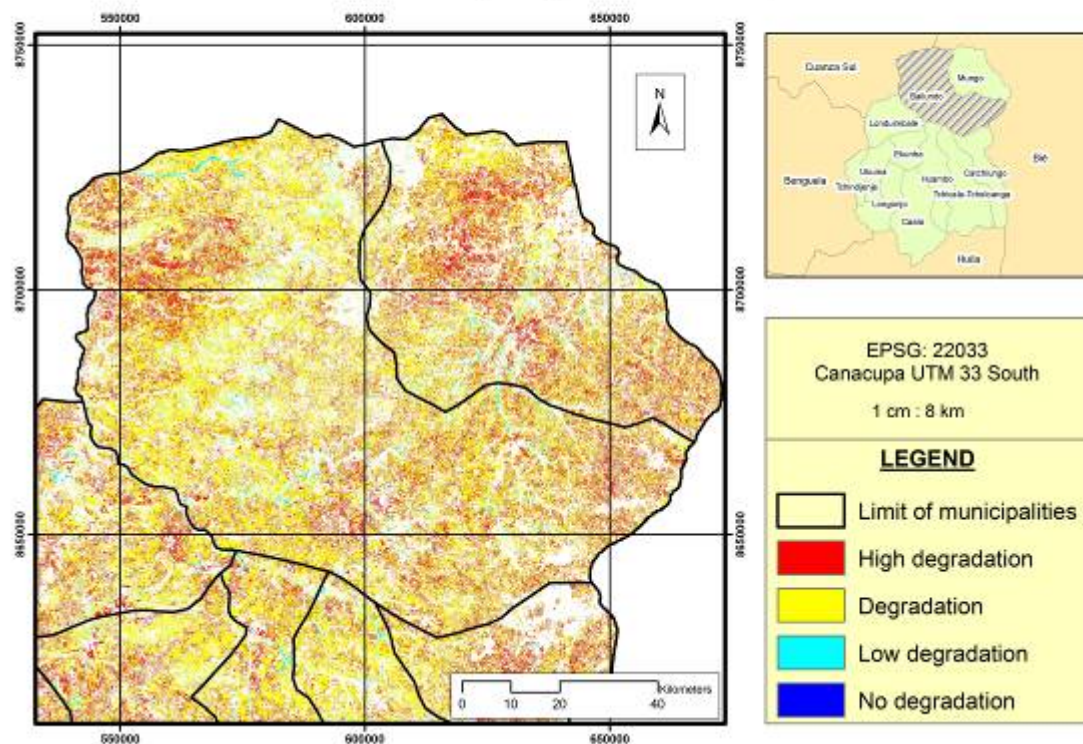


Annex VI. Degradation of miombo in 2015

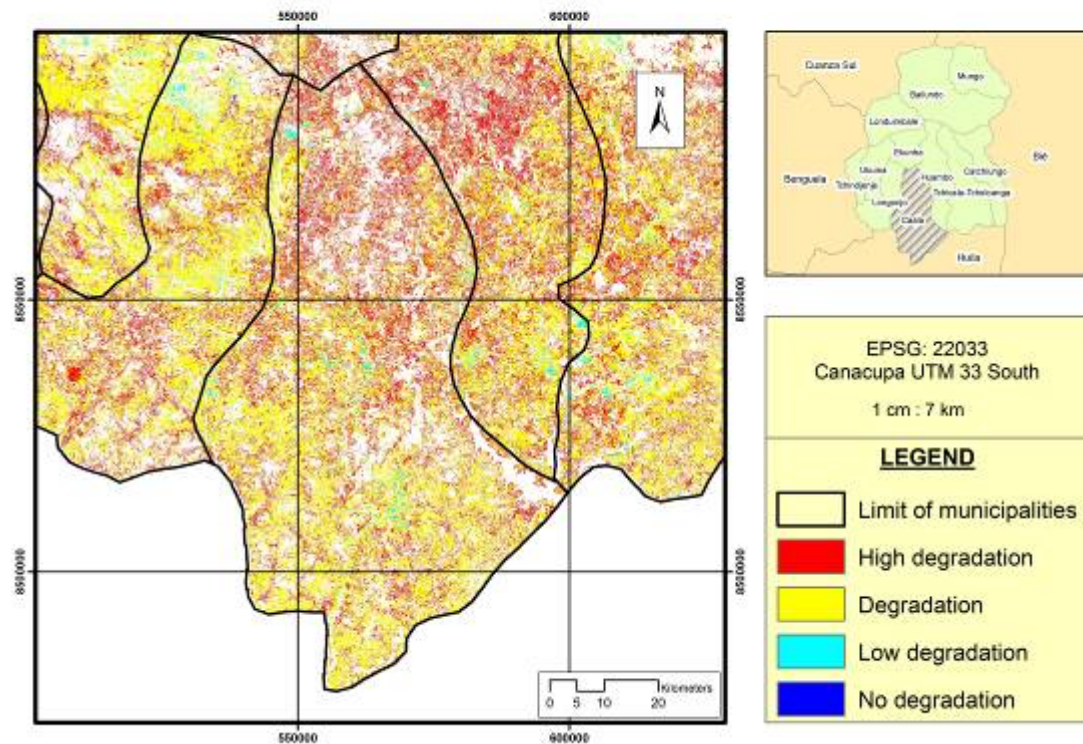
Miombo's degradation degree in Huambo province.



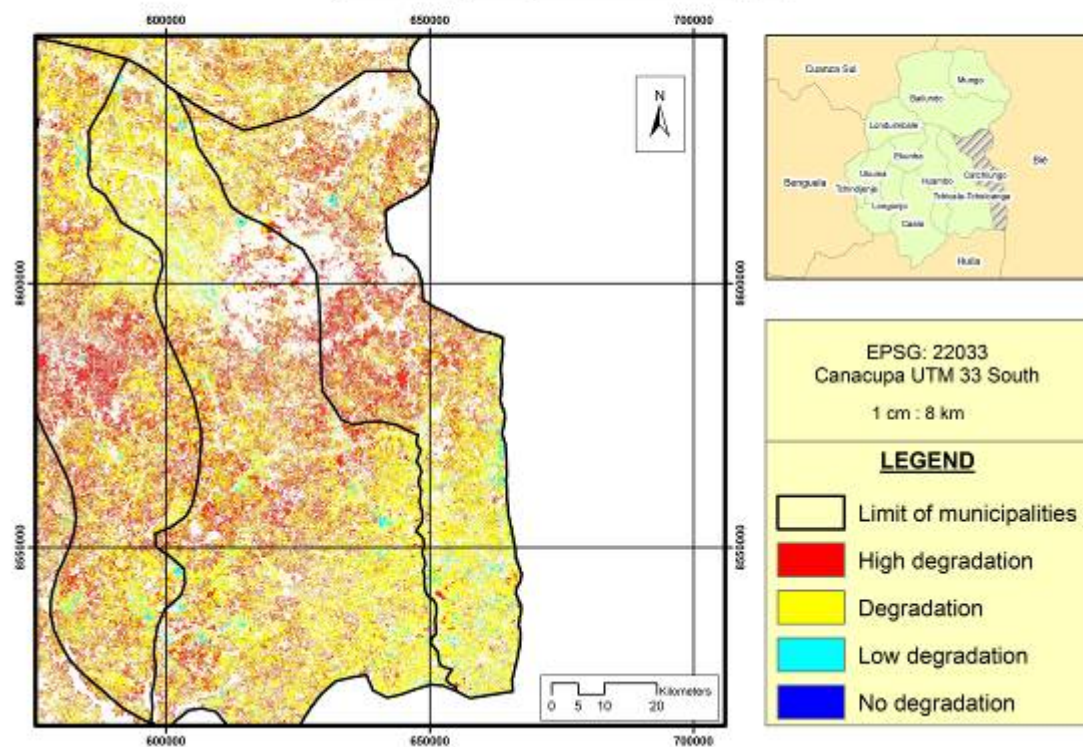
Miombo's degradation degree in Huambo province. Municipality of Bailundo.



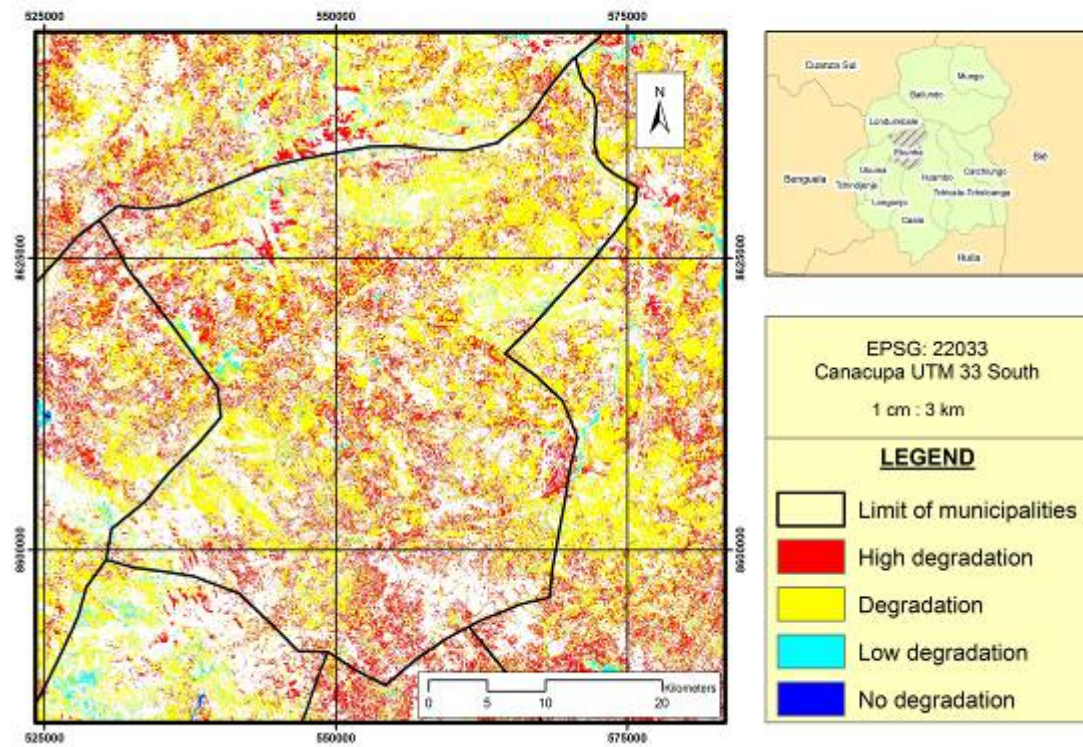
Miombo's degradation degree in Huambo province. **Municipality of Caala.**



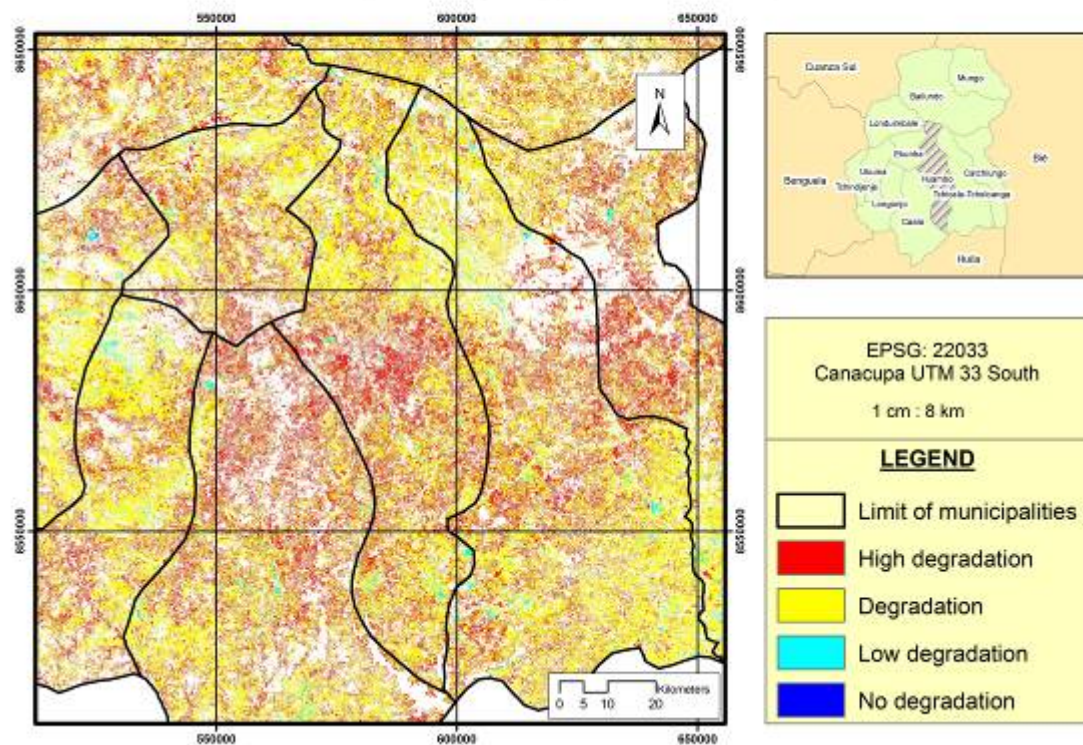
Miombo's degradation degree in Huambo province. **Municipality of Catchiungo.**



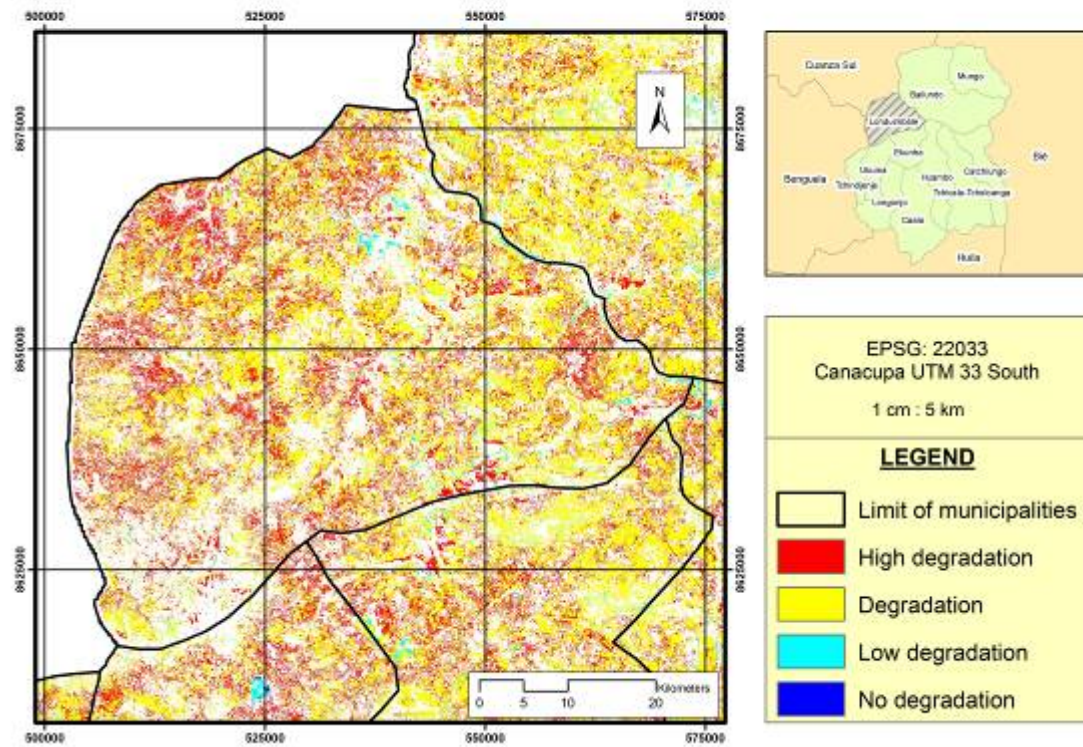
Miombo's degradation degree in Huambo province. Municipality of Ekunha.



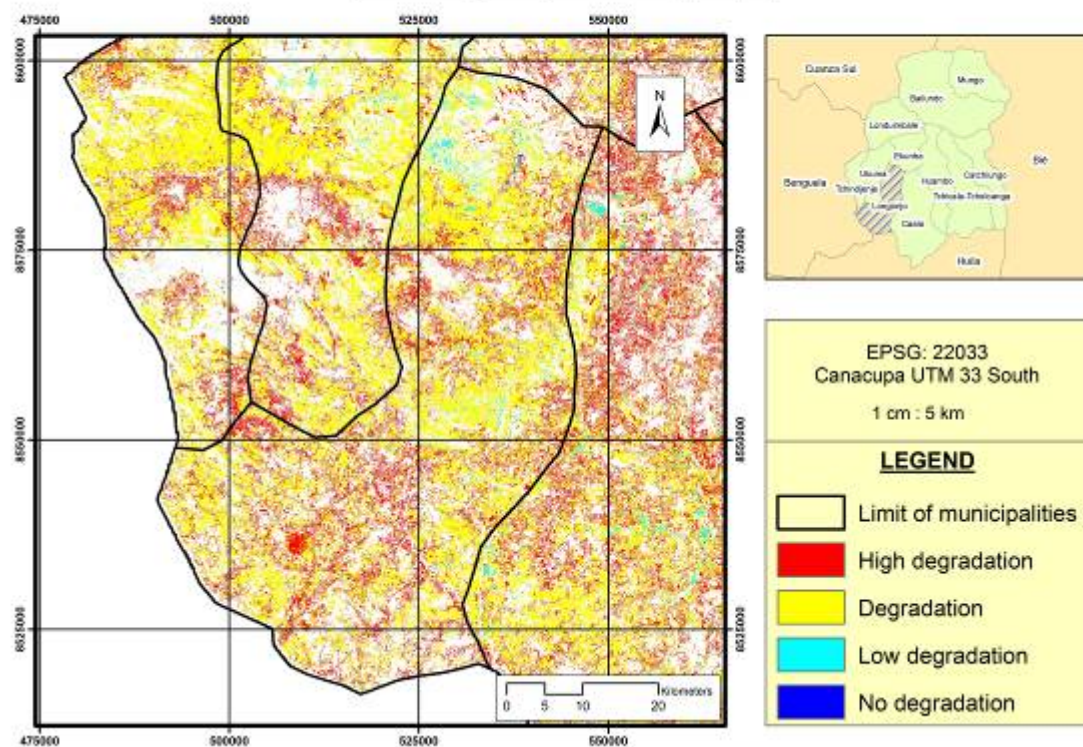
Miombo's degradation degree in Huambo province. Municipality of Huambo.



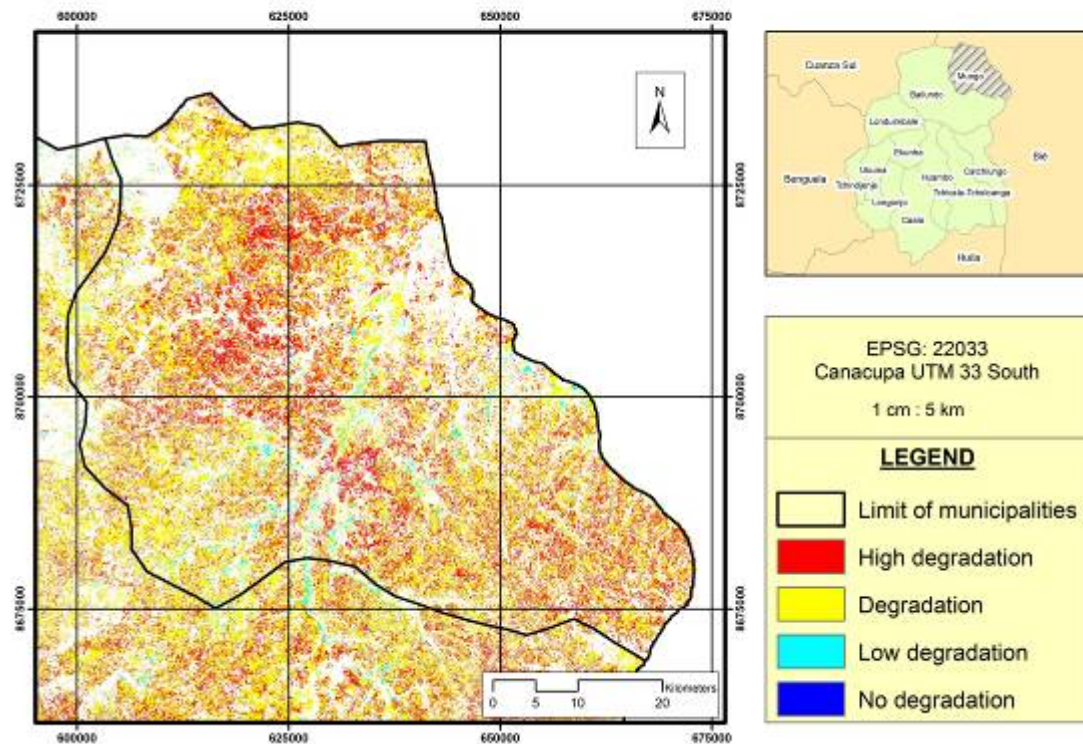
Miombo's degradation degree in Huambo province. **Municipality of Londuimbale.**



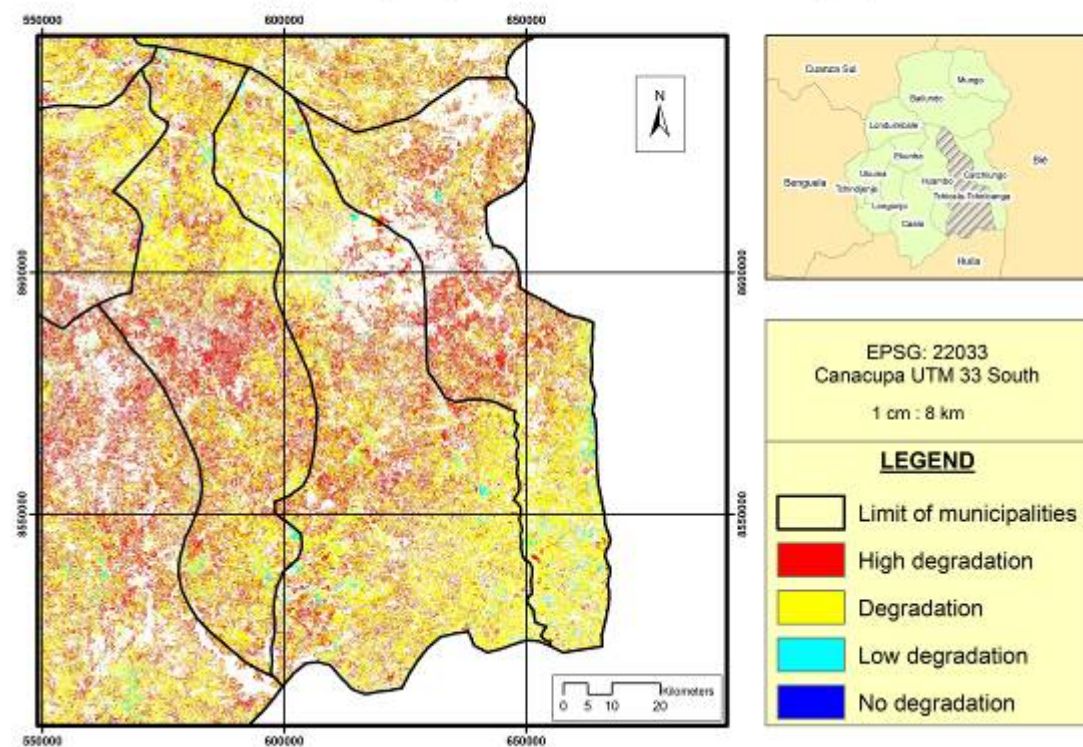
Miombo's degradation degree in Huambo province. **Municipality of Longonjo.**



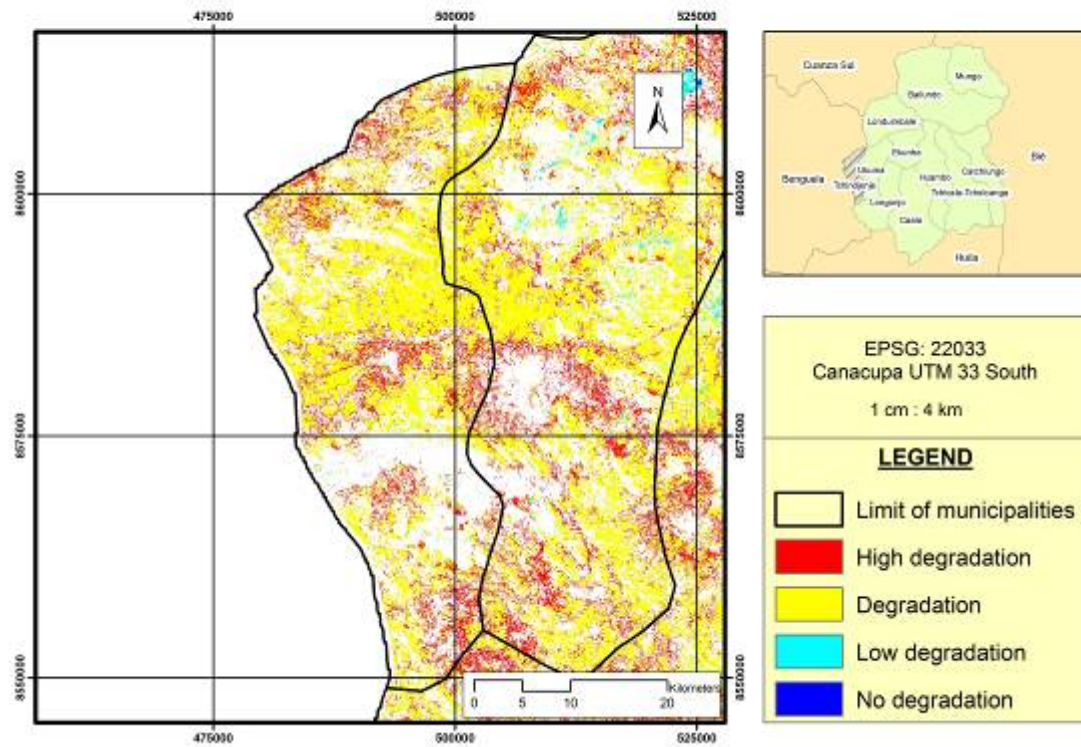
Miombo's degradation degree in Huambo province. **Municipality of Mungo.**



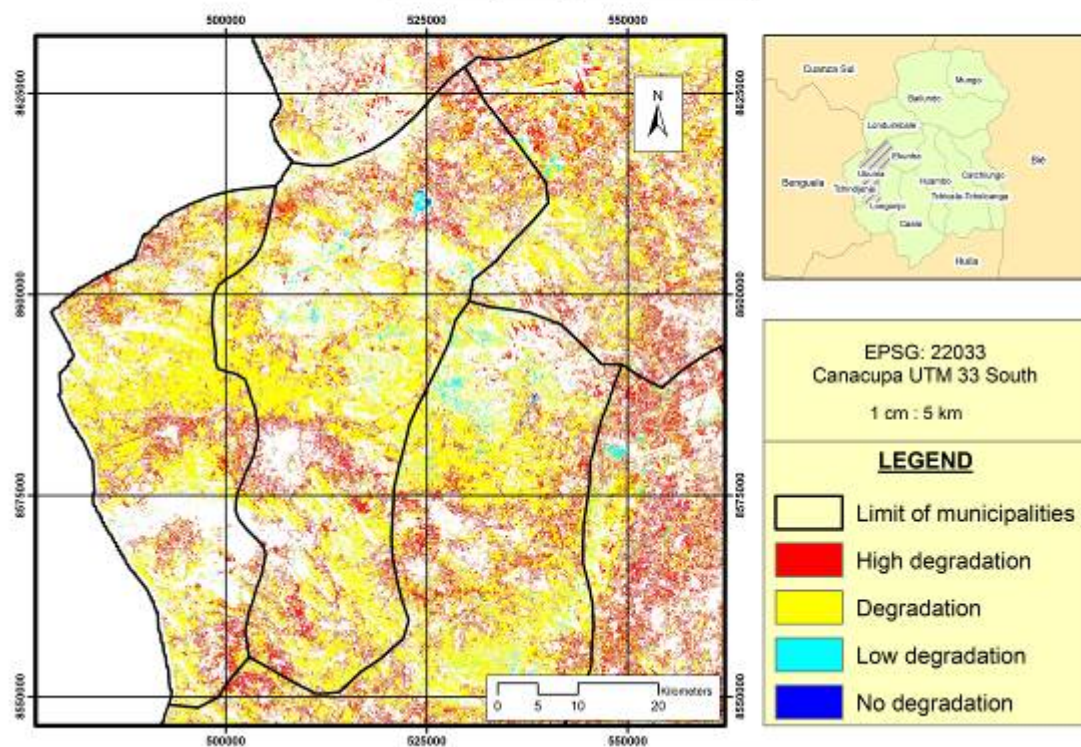
Miombo's degradation degree in Huambo province. **Municipality of Tchicala-Tcholoanga.**



Miombo's degradation degree in Huambo province. **Municipality of Tchindjenje.**



Miombo's degradation degree in Huambo province. **Municipality of Ukuma.**





TECHNICAL ASSISTANCE BY



UNIVERSIDAD DE CÓRDOBA



SPONSORED BY THE



Federal Ministry of Education and Research

